Glycopolymers and Glyconanomaterials for Biomedical and Environmental Applications

by

Yinan Wang

A thesis submitted in partial fulfillment of the requirements for the degree of

Doctor of Philosophy

in
Chemical Engineering

Department of Chemical and Materials Engineering
University of Alberta

Abstract

Protein–carbohydrate interactions are involved in a wide variety of cellular recognition processes including cell growth regulation, differentiation and adhesion, immune response, and viral or bacterial infections. Recently, utilization of carbohydrate based polymers and nanomaterials for various biomedical or environmental applications has emerged as an important topic as a result of the better understanding of the critical role of carbohydrates play in those applications.

In this thesis, a review on glycopolymer synthesis as well as the applications of the glycopolymers in biomedical and environmental applications is first presented followed by the studies on using glycopolymers modified quartz crystals microbalance with dissipation (QCM-D) to probe bacterial adhesion mediated by the carbohydrate-protein interactions. The results showed *Pseudomonas aeruginosa* (*P. aeruginosa*) PAO1 bearing galactose-specific binding lectin (PA-IL) can bind to the galactose containing glycopolymer surface stronger as compared to *Escherichia coli* (*E. coli*) K-12 (a Gram-negative bacterium with mannose-specific binding lectin) adhesion on the same surface. The presence of divalent ions, such as calcium, was also found to play an important role on bacterial adhesion events, as the ions can coordinate specific amino acid residues at the carbohydrate recognition domain and allow lectins to specifically bind the hydroxyl groups of sugars.

Temperature responsive poly(*N*-isopropylacrylamide) [P(NIPAAm)] homopolymers and copolymers (consisting of a few sugar residues) were synthesized by a one-pot reversible addition–fragmentation chain transfer (RAFT) polymerization and subsequently immobilized on QCM-D to generate biomimetic surfaces to study the two major bacterial

infection mechanisms: hydrophobic and lectin–carbohydrate interactions. Although, a greater number of *P. aeruginosa* adhered to the NIPAAm homopolymer modified surfaces at temperatures higher than the lower critical solution temperature (LCST), the bacterium–substratum bond stiffness was stronger between *P. aeruginosa* and a galactose based P(NIPAAm) surface. These observations might suggest that both hydrophobic and lectin–carbohydrate interactions contribute to bacterial adhesion on cell surfaces, while the latter plays a significant role in bacterial infections.

By exploiting the carbohydrate-protein interactions, a dual pH and glucose responsive glycopolymers modified boronic acid containing nanofiber was designed for the reversible capture and release of lectins. By immobilizing glycopolymers carrying different types of sugar residues such as glucose and galactose on the nanofiber surface, the resulting nanofibers can selectively capture lectins under alkaline conditions. On the other hand, treatment of the modified nanofibers with an acidic or glucose solution resulted in the detachment of both lectins and glycopolymers from the nanofiber surface. These functional nanofibers can therefore be easily modified and hence can be used for quick removal of selective proteins or toxins from the solution.

In conclusion, glycopolymers are ideal candidates for understanding of various biological events or materials design for various applications. Some interesting future directions for the glycopolymers based materials are also proposed at the end of this thesis.

Preface

This thesis is an original work by Yinan Wang (Y. Wang) under the supervision from Dr. Ravin Narain (R. Narain) and Dr. Yang Liu (Y. Liu).

Chapter 3 of this thesis has been published as Y. Wang, R. Narain, and Y. Liu, Study of Bacterial Adhesion on Different Glycopolymer Surfaces by Quartz Crystal Microbalance with Dissipation (QCM-D). *Langmuir* **2014**, 30, 7377-7387. I was responsible for the data collection and analysis as well as the manuscript composition. R. Narain and Y. Liu were the supervisory author and were involved with research design and manuscript composition.

Chapter 4 of this thesis has been published as Y. Wang, Y. Kotsuchibashi, Y. Liu, and R. Narain, Study of Bacterial Adhesion on Biomimetic Temperature Responsive Glycopolymer Surfaces. *ACS Appl. Mater. Interfaces* **2015**, 7, 1652-1661. I was responsible for the data collection and analysis as well as the manuscript composition. Y. Kotsuchibashi assisted with the data collection and contributed to manuscript edits. R. Narain and Y. Liu were the supervisory author and were involved with research design and manuscript composition.

Chapter 5 of this thesis has been published as Y. Wang, Y. Kotsuchibashi, K. Uto, M. Ebara, T. Aoyagi, Y. Liu, and R. Narain, pH and glucose responsive nanofibers for the reversible capture and release of lectins. *Biomater. Sci.* **2015**, 3, 152-162. I was responsible for the data collection and analysis as well as the manuscript composition. Y. Kotsuchibashi and K. Uto assisted with the data collection. M. Ebara, T. Aoyagi, Y. Liu and R. Narain were the supervisory author and were involved with research design and manuscript composition.

IN LOVEING MEMORY OF MY GRANDMOTHER

DANFEI MA (马旦飞) (1928-2015)

Acknowledgements

I would like to express my sincere thanks to my supervisors, Dr. Ravin Narain and Dr. Yang Liu, for providing me an opportunity to take this wonderful journey of exploring various topics in (Nano)Materials Science at University of Alberta. Without your constant encouragements, suggestions, and guidance, I could not have been able to achieve this degree.

I would also like to offer my sincere thanks to Dr. Takao Aoyagi (recently moved to Nihon University) and Dr. Mitsuhiro Ebara in National Institute for Materials Science (NIMS), for providing me opportunities to work with a team of excellent materials scientists/biologists. Special thanks will be credited to Dr. Young-Jin Kim and Dr. Koichiro Uto, who helped and discussed a lot with me on electrospinning and cell works, respectively, during my staying in NIMS.

Deep thanks also go to Dr. Hongbo Zeng, for your knowledge in materials science and deep discussions with me in my self-healing materials project.

Dr. Yohei Kotsuchibashi, for the helps at the beginning of my PhD program, bringing me to the new field of boronic acid derived materials, and introducing Ramen to me.

Many thanks to the previous lab members and also my good friends: Dr. Marya Ahmed, Dr. Farahnaz Lollmahomed, and Mr. Stephen Quan, and all current lab members in Dr. Narain and Dr. Liu's groups.

Thanks for my friends in Edmonton: John Ku, Tianxin Bao, Keren Jiang, Sheng Tian, Tianfu Yang, Tianbo Liu and his wife Shuning Li, Yining Wang, Hao Zheng, Hector

Cheung, Misi Zhang and her husband Pengcheng Chen. Friends in Halifax: Stacie Cao, Liang Zhou and her husband Constant Ma, Stanley Luo. Friends in Toronto: Lulu Yao, King Yeung. Friends in China: Yishi and his families and Xiaoping Liao.

Thanks financial support from the Natural Sciences and Engineering Research Council (NSERC) of Canada, the Canada Foundation for Innovation (CFI), and NIMS internship.

Thanks for all my family members. My parents for your supporting and understanding, and all the encouragements, confidences, and loves that you continuously delivered in the past 30 years.

I also want to say thank you to my fiancée, Jie Song, at the end. Thank you for your patience and understanding in the past decade. I love you.

Table of Contents

List of Schemes

List of Tables

List of Figures

List of Abbreviations

AAPBA	3-acrylamidophenylboronic acid (AAPBA)
ACVA	4,4′-azobis(4-cyanovaleric acid)
AEMA	2-aminoethyl methacrylamide hydrochloride
AFM	Atomic force microscopy
AMA	2-aminoethyl methacrylate
ARGET	Activator Regenerated by Electron Transfer
ASGPR	Asialoglycoprotein Receptor
ATRP	Atom Transfer Radical Polymerization
bpy	2,2'-Bipyridine
BSA	Bovine Serum Albumin
CRD	Carbohydrate recognition domain
CRP	Controlled Radical Polymerization
CTA	Chain Transfer Agent
CTCs	Circulating Tumor Cells
CTP	4-cyanopentanoic acid dithiobenzoate
CuAAC	Copper-Catalysed Azide-Alkyne Cycloaddition
CuBr	Copper(I) Bromide
DC-SIGN	Dendritic Cell-Specific ICAM-3 Grabbing Nonintegrin
DMF	*N*,*N*′-dimethylformamide
DMSO	Dimethyl Sulphoxide
DP	Degree of Polymerization
ECM	Extracellular Matrix
EDTA	Ethylenediamine-*N,N*,*N*′,*N*′-tetraacetic acid
E. coli	*Escherichia coli*
FITC	Fluorescein Isothiocyanate
Gal	Galactose
GAPMA	3-gluconaminopropyl methacrylamide

Glc	Glucose
GMA	Glycidyl methacrylate
GPC	Gel Permeation Chromatography
h	hour
HCl	Hydrogen Chloride
HEMA	2-hydroxyethyl methacrylate
HFIP	1,1,1,3,3,3-hexafluoro-2-propanol
HIV	Human Immunodeficiency Virus
IAZA	Iodoazomycin Arabinofuranoside
ICAR	Initiators for Continuous Activator Regeneration
k_d	Dissociation Constant
LAEMA	2-lactobionamidoethyl methacrylamide
LCST	Lower Critical Solution Temperature
LPS	Lipopolysaccharide
MBP	Mannose-specific Binding Lectins
MeOH	Methanol
M_n	Number average molecular weight
NaN_3	Sodium Azide
NCAs	N-carboxyanhydrides
NF	Nanofiber
NMP	Nitroxide-Mediated Polymerization
NMR	Nuclear Magnetic Resonance
OD	Optical Density
PA-IL	*Pseudomonas aeruginosa* lectin I
P. aeruginosa	*Pseudomonas aeruginosa*
PISA	Polymerization Induced Self-Assembly
RAFT polymerization	Reversible Addition−Fragmentation Chain-Transfer
PBS	Phosphate buffered saline
PDEGMA	Poly[di(ethylene glycol) methyl ethyl methacrylate]

PDI	Polydispersity index
PEG	Polyethylene glycol
PNIPAAm	Poly(*N*-isopropylacrylamide)
QCM	Quartz crystal microbalance
QCM-D	Quartz crystal microbalance with dissipation
RCA120	*Ricinus communis* (castor bean) Agglutinin
RDRP	Reversible-Deactivation Radical Polymerizations
ROMP	Ring-Opening Metathesis Polymerisation
ROP	Ring Opening Polymerization
SiRNA	Small interfering RNA (SiRNA)
SPAAC	Strain Promoted Azide–Alkyne Cycloadditions
SPR	Surface Plasmon Resonance
Stx-1	Shiga toxin 1
UV	Ultraviolet

List of Publications

Peer Reviewed Journals:

1. Lu, H., Wang, Y., Li, L., Kotsuchibashi, Y., Zeng, H., and Narain, R., Temperature and pH Responsive Benzoboroxole based Polymers for Flocculation and Enhanced Dewatering of Fine Particle Suspensions. *ACS Appl. Mater. Interfaces* **2015**, 7, 27176-27187.
2. Narain, R., Wang, Y., Ahmed, M., Lai, B.F., and Kizhakkedathu, J.N., Blood Components Interactions to Ionic and Non-ionic Glyconanogels. *Biomacromolecules* **2015**, 16, 2990-2997.
3. Quan, S., Wang, Y., Zhou, A., Kumar, P., and Narain, R., Galactose-based Thermosensitive Nanogels for Targeted Drug Delivery of Iodoazomycin Arabinofuranoside (IAZA) for Theranostic Management of Hypoxic Hepatocellular Carcinoma. *Biomacromolecules* **2015**, 16, 1978-1986.
4. Kotsuchibashi, Y., Ebara, M., Sato, T., Wang, Y., Lu, J., Rajender, R., Hall, D.H., Narain, R., and Aoyagi, T., Spatio-Temporal Control of Synergistic Gel Disintegration Consisting of Boroxole-and Glyco-Based Polymers via Photoinduced Proton Transfer. *J. Phys. Chem. B* **2015**, 119, 2323-2329.
5. Wang, Y., Kotsuchibashi, Y., Liu,Y., Narain, R., Study of Bacterial Adhesion on Biomimetic Temperature Responsive Glycopolymer Surfaces. *ACS Appl. Mater. Interfaces* **2015**, 7, 1652-1661.
6. Wang, Y., Uto, K., Kotsuchibashi, Y., Ebara, M., Aoyagi, T., Narain, R., pH and Glucose Responsive Nanofibers for the Reversible Capture and Release of Lectins. *Biomater. Sci.* **2015**, 3, 152-162.
7. Wang, Y., Kotsuchibashi, Y., Liu, Y., Narain, R., Temperature Responsive Hyperbranched Amine-Based Polymers for Solid-Liquid Separation. *Langmuir* **2014**, 30, 2360–2368.
8. Wang, Y., Narain, R., Liu, Y., Study of Bacterial Adhesion on Different Glycopolymer Surfaces by Quartz Crystal Microbalance with Dissipation (QCM-D). *Langmuir* **2014**, 30, 7377-7387.

9. Kotsuchibashi, Y., Wang, Y., Kim, Y.J., Ebara, M., Aoyagi, T., and Narain, R., Simple Coating with pH-Responsive Polymer-Functionalized Silica Nanoparticles of Mixed Sizes for Controlled Surface Properties. *ACS Appl. Mater. Interfaces* **2013**, 5, 10004–10010.
10. Wang, Y., Li, L., Kotsuchibashi, Y., Liu, Y., Zeng, H., and Narain, R., Underwater self-healing hydrogel based on dynamic boronate-diol covalent bond. Manuscript.

Book Chapters:

1. Wang, Y., Liu, Y., and Narain, R., Glycopolymers for Biomedical Applications. Glycopolymers: Synthesis and Applications. Smithers Rapra Technology Ltd, Shawbury, UK. 2014, pg. 97-113.
2. Wang, Y., Quan, S., Kumar, P., and Narain, R., Glyconanoparticles: Synthesis and Biomedical Applications. Glycopolymer Code. Synthesis of Glycopolymers and their Applications. RSC Polymer Chemistry Series No. 15, Cambridge, UK. 2015, pg. 196-222.

Chapter 1. General Introduction

Carbohydrates have been recognized in a wide variety of cellular recognition processes through their interaction with proteins. However, such interaction, usually with dissociation constant (k_d) values in micromolar range, is relatively weak as compared to other biomolecular interactions, such as antibody-antigen complex and biotin-avidin interaction. Glycoside cluster or multivalency effect allows molecules presenting multiple carbohydrate ligands interacting simultaneously to lectins with clustered sugar binding sites and creates a stronger binding affinity. Based on this concept, polymer chemists have synthesized glycopolymers containing multiple copies of carbohydrates attached on a polymeric backbone to create high affinity ligands. Although the concept is simple, the creation of synthetic glycopolymers with precisely controlled molecular weight and carbohydrate density to fully simulate of glycoconjugates or polysaccharides in biological system is still challenging. In the past two decades, with revolutionary developments on polymer chemistry, especially with the invention of the controlled free-radical polymerization techniques, tremendous progress has been made in the synthesis of glycopolymers and their nanomaterials for biomedical and environmental applications. However, this field is still in its infancy. The interactions of glycopolymers and biological systems, such as cells, bacteria, virus and proteins, are still unclear, and their potential applications in more advanced biomedical or environmental fields still need to be explored.

To address these issues, the chapters in this thesis focus on the synthesis and applications of glycopolymers to probe carbohydrate-protein interactions mediated bacterial adhesion and invasion in host tissues processes, as well as to develop of glycopolymers based

materials for biomedical and environmental applications. Detailed reviews on the recent progress on glycopolymer synthesis as well as their biomedical and environmental applications are provided. Two examples of using well-defined carbohydrate containing polymers and their copolymers to study bacterial adhesion and infection mechanisms are presented. In these studies, reversible addition−fragmentation chain transfer polymerization technique is applied for the polymer synthesis, providing polymers with the controlled molecular weight, structure, and molecular weight distributions. Bacterial adhesion on the resulting polymers modified surfaces is studied by QCM-D technique and the results are analyzed by "coupled resonance model". In chapter 5, well-defined glycopolymers are immobilized on electrospun boronic acid containing polymeric nanofiber surfaces through the interaction between *cis*-diols and boronic acid. The glycopolymers on the nanofiber surface allows selective lectins capture in aqueous solution, whereas the dynamic covalent bond between glycopolymer and boronic acid containing nanofibrous substrate enables lectins being released from materials surfaces in acidic or high glucose conditions. Finally, the role and relevance of glycopolymers in biomedical and environmental applications are summarized and it is concluded that, although major breakthrough has been achieved in this research, the development of more advanced glycopolymer structures can further elucidate the role of more complex multivalent carbohydrate-carbohydrate or carbohydrate-protein interactions.

Chapter 2. Glycopolymers and Their Biomedical and Environmental Applications

Chapter 2

2.1.Carbohydrate-Mediated Recognition

Carbohydrates are a large and diverse class of biomolecules that constitute of cells together with proteins, lipids and nucleic acids. For many years, the biological role of carbohydrates was considered as fuel molecules. However, this picture has been redrawn over the last 30–40 years as in living organisms, carbohydrates are found in either free or covalently linked to other structures, such as proteins and lipids, and participate in a myriad of physiological processes including cell–matrix interaction,[1] cell–cell adhesion,[2] immune defence,[3] fertilization,[4] and cancer growth and metastasis.[5] Therefore, the analysis of carbohydrate-protein interactions and the development of inhibitors or probes of these interactions are at the forefront of modern glycobiology.

At the molecular level, carbohydrate-protein interactions are governed by a combination of hydrogen bonding, van der Waals interactions and hydrophobic stacking.[6] In some cases, the presence of divalent ions, such as Ca^{2+} and Mn^{2+}, is also required, so that the specific amino acid residues at the carbohydrate recognition domain (CRD) can coordinate with these ions to specifically bind the hydroxyl groups of sugars (**Scheme 2-1**).[7] For example, the *Pseudomonas aeruginosa* lectin I (PA-IL)[8] and human asialoglycoprotein receptor (ASGPR)[9] can bind glycoproteins with galactose (Gal) terminal with high selectivity in the presence of Ca^{2+}, but with relatively low affinity ($k_d \approx 10^{-6}$ M).

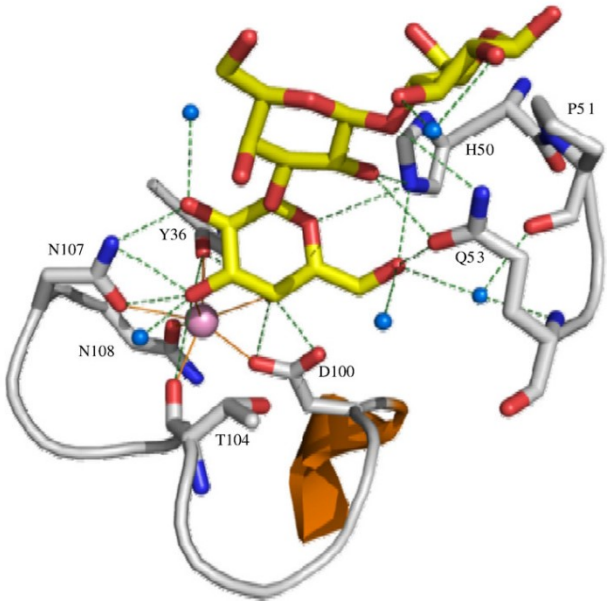

Scheme 2-1. Crystal structure of PA-IL/αGal1–3βGal1–4Glc complex. Trisaccharide is represented in yellow sticks, and calcium ion, by a pink sphere. View of the binding site with hydrogen bonds represented as green dashed lines and coordination contacts as continuous orange lines. Reprinted with permission from reference 8. Copyright 2008 Elsevier.

The carbohydrate-protein interactions affinities can however be enhanced through multivalency. Lee, in 1995, first termed these phenomena as “glycoside cluster effect”, which generally requires a lectin with clustered sugar binding sites and a multivalent ligand that can present sugars with proper orientation and spacing.[7] Since then, this theory has been extensively studied and molecular interpreted by a various possible mechanisms, including: 1) chelate effect (contacts between the multivalent ligand and multiple receptors to decrease the off-rate and increase functional affinity); 2) subsite binding (Occupying primary and secondary binding sites on a receptor); 3) steric stabilization (sterically prevents further interactions with ligands by the size of the multivalent material); 4)

receptor clustering (two-dimensional diffusion of receptors within a fluid membrane bilayer); and 5) statistical effect (a higher local concentration of ligands) (**Scheme 2-2**).[10-15]

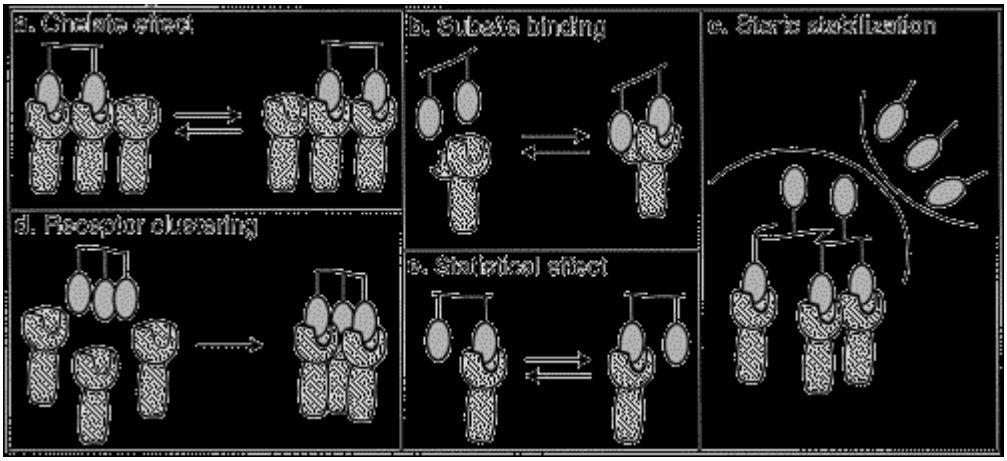

Scheme 2-2. Mechanisms of multivalent ligand binding: (a) Chelate effect; (b) Subsite binding; (c) Steric stabilization; (d) Receptor clustering; (e) Statistical effects. Reprinted with permission from reference 12. Copyright 2002 American Chemical Society.

Natural polysaccharides consisting of sugar units uniformly linked in linear chains are therefore present interesting examples for exploiting these unique properties of carbohydrate-protein interactions. However, most of polysaccharides are water insoluble even the molecules have a low molecular weight with degrees of polymerization (DP) of 20-30. The insolubility mainly resulted from their preference for partial crystallization and has limited their applications in aqueous biological system.[16] Glycopolymers, on the other hand, are synthetic polymers with pendent carbohydrates introduced either by direct polymerization of a glycomonomer or by post-polymerization modification of a preformed polymer containing of active functional groups. Compared to polysaccharides, the glycopolymers can be synthesized with designed molecular weights, architectures, or

compositions, and, therefore, being more and more attractive for developing new tools to probe carbohydrate-lectin recognitions and other biological activities.

2.2.Synthesis of Glycopolymers

The first example on preparing glycopolymers through polymerization of allyl ester of α-methylglucosides appeared as early as 1944 by Nichols and Yanovsky.[17] Soon after that, the same group described the first methacrylate glycopolymer in 1945.[18] Before the mid-90s, the glycopolymers synthesized by free radical polymerization emerged slowly as the favourite technique for developing potential tools in various biomedical fields, such as pathogen inhibitors,[19, 20] drug delivery system,[21] and biosensors.[22] During that period, the only realistic chemical routes to control the polymers architecture were ionic or metal catalyzed polymerization such as ring-opening metathesis polymerisation (ROMP).[23] However, because of the nature of the propagating species, these techniques are highly sensitive to monomer functionality, and, therefore, requiring protected species with strictly controlling over polymerization conditions.[24-26] These issues were quickly overcome by the use of ruthenium based catalysts,[27, 28] but post-polymerization removal of the heavy metal catalyst is necessary if the products are to be used for biomedical applications.

The invention of controlled radical polymerization (CRP) around 1995[29-31] allows better strategies to directly synthesize of glycopolymers with controlled molecular weight and molecular weight distribution, but also makes it possible that synthetic glycopolymers can obtain different architectures and self-assembly to nano-subjects for a myriad of applications. Soon, in 2001, Sharpless and coworkers[32] introduced the idea of “click chemistry”, which allows azide modified carbohydrates attached on polymers backbone by

interacting with an alkyne group through Huisgen dipolar cycloaddition in aqueous conditions at ambient temperature with high functional group tolerance.[33] With the development of these two powerful techniques, in the past two decades, glycopolymers prepared by either directly polymerization from unprotected glycomonomers or post-polymerization modification of reactive precursor polymers have been prepared and extensively studied in different field (**Figure 2-1**).

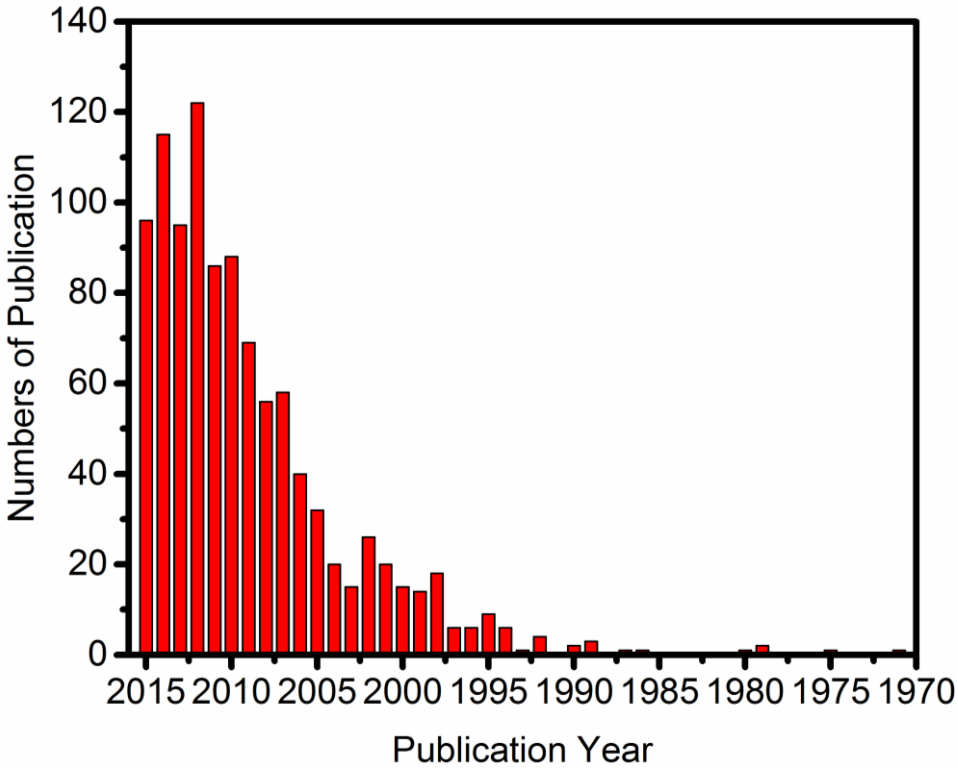

Figure 2-1. Number of publications involving glycopolymers since 1970 (SciFinder).

2.2.1. Directly Synthesis of Glycopolymers from Glycomonomers

In general, the glycomonomers for directly synthesis of glycopolymers are vinyl based molecules that connect to the spacers and carbohydrate groups through the boding units (**Scheme 2-3**). The type of vinyl groups affect parameters of the polymerization, such as

the rate of chain propagation,[34] but also influence the decision on the choice of polymerization techniques.[35] The bonding units connect the polymer backbone with the carbohydrates and affect the stability. Amide bonds are stable under most circumstances, whereas ester bonds are susceptible to hydrolysis under acid or base conditions.[36] The spacers play an important role on controlling of carbohydrate-lectin interactions. Longer spacer can enhance the flexibility of the carbohydrates and therefore ensure good binding affinities with lectins.[37]

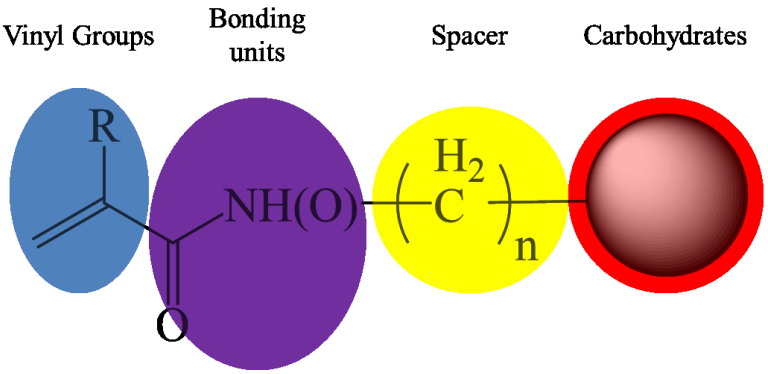

Scheme 2-3. Schematic representation of glycomonomers.

2.2.1.1.Atom Transfer Radical Polymerization (ATRP)

Although atom transfer radical polymerization (ATRP) was found to be a vital technique for the synthesis of glycopolymers, at the beginning, majority of the syntheses have involved the use of protected glycomonomers.[38-48] In 2002, Narain and Armes successfully synthesized glycomonomers via ring-opening of either glucono- or lactobiono-lactone with 2-aminoethyl methacrylate (AMA), thus removing the requirement for protecting group chemistry during the polymerization.[49] The polymerization was conducted in varying ratios of MeOH/H_2O using the common CuBr/bpy catalyst. When high MeOH/H_2O ratios were used, polymerizations showed high conversions in approximately 15 h and gave controlled

M_n and low polydispersities.[50] Reaction times could be reduced drastically on addition of water. Polymerizations in water alone reach near completion in 1 h.[50, 51] Since then, glycopolymers directly synthesized from unprotected glycomonomers bearing different carbohydrate sources, such as N-Acetylglucosamine (GlcNac),[52-54] mannose,[53] and trehalose[55] with different structures and morphologies by ATRP method started to grow.

In early 00s, ATRP method used to dominate the glycopolymers synthesis in terms of its excellent performance on controlling the polymers structure, molecular weight and molecular weight distribution. Moreover, the terminals of the ATRP glycopolymers can be modified to an azide group by either using an azide containing ATRP imitator or post-polymerization modification of the bromine group with NaN_3.[52, 56-60] For example, Finn *et. al* reported a strategy of bioconjugate a ATRP synthesized glycopolymer on an azide modified cowpea mosaic virus surface by using an dialkyne containing bridging compound through Azide-Alkyne Cycloaddition.[56] However, every technology has its limitations. For glycopolymer synthesized by ATRP, a lot of efforts need to be spent in the post-polymerization removal of the toxic transition metal complex (usually around 1,000 to 10,000 ppm during the ATRP process)[30] if the final polymers are used in biomedical or environmental fields. On the other hand, the polymerization conditions have to be carefully controlled, as synthesis of glycopolymers by ATRP in aqueous media may lead disproportionation or hydrolysis of the initiator.[61] New techniques, including initiators for continuous activator regeneration (ICAR)[62] and activator regenerated by electron transfer (ARGET) ATRPs,[63, 64] can partially solve the issues above, in which, the amount of metal catalysts can be reduced to only few, or even single digit in ppm.

2.2.1.2.Reversible Addition−Fragmentation Chain-Transfer (RAFT) Polymerization

Reversible addition−fragmentation chain-transfer (RAFT) polymerization, which was developed in 1998 by Thang and coworkers,[31] is also an important technique for the reversible-deactivation radical polymerizations (RDRP). Similar to ATRP, RAFT possesses strong abilities on controlling of the polymers synthesis in terms of molecular weight, structure, and molecular weight distributions. Therefore, these two RDRP techniques are always placed in an arguable position on which one is the most versatile and readily executable technique for RDRP. RAFT, at least with respect to monomer choice and polymerization conditions, shows great advantages over ATRP. For example, RAFT can be employed under homogenous aqueous conditions for the preparation of polymers with high degrees of hydrophilic functionality, whereas such versatility under homogenous aqueous conditions still presents some significant challenges for other common RDRP.

Operating differently from other RDRP techniques, such as nitroxide-mediated polymerization (NMP)[65] and ATRP[30] that rely on reversible termination of propagating radicals, RAFT works on the principle of degenerative chain transfer.[66] The deactivation-activation equilibrium during the RAFT process is achieved by the using of a thiocarbonylthio containing chain transfer agent (CTA), so that no net changes in radical concentration will be occurred during the activation–deactivation process. The generally accepted RAFT mechanism is outlined in **Scheme 2-4**. After the initiation of free radicals that is similar to the conventional radical polymerization, the propagating radical ($\mathbf{P}_m^{\bullet}$) adds to the thiocarbonylthio compound (**1**) to form a RAFT adduct radical (**2**). This compound is instable and may undergo a fragmentation reaction, which either yielding back the reactants or forming a dormant intermediate (**3**) and releasing an initiating leaving group

radical (R•). The leaving group radical may then re-initiates new monomers and form a new propagating radical (**P*n*•**). After the initially added CTA is consumed (i.e., completion of the "the RAFT pre-equilibrium (ii)"), the RAFT process enters its most important "main equilibrium" stage (iv). Here, by a process of rapid interchange between propagating radicals (**P*n*•** and **P*m*•**) and dormant compounds, the radicals are equally "shared" among all species that have not yet undergone termination (v). This process leads polymer chains grow to designed length with narrow molecular weight distributions.[31, 66, 67]

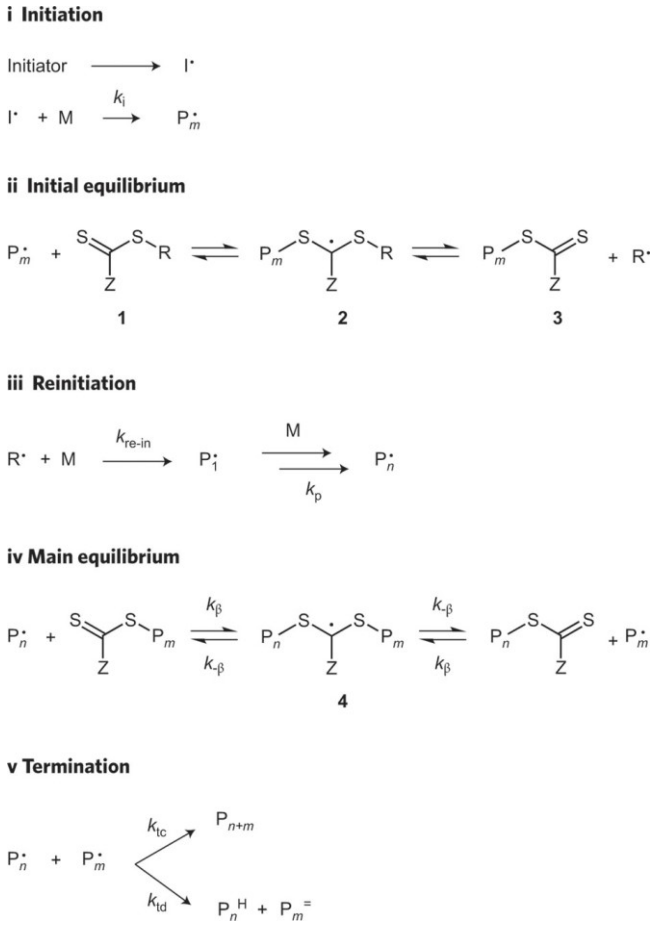

Scheme 2-4. Reversible addition–fragmentation chain transfer (RAFT) polymerization mechanism. Reprinted with permission from reference 67. Copyright 2010 Nature Publishing Group.

The key to a successful RAFT polymerization relies on the presence of a highly efficient CTA and the rapid interchange between the propagating radical chains and dormant compounds. A general structure of CTA is constituting of a free radical leaving group R, a reactive C=S double bond, and a Z group that controls the reactivity of the C=S double bond (**Scheme 2-5**). The chain transfer coefficients of RAFT polymerization are greatly affected by the species of Z groups on CTA end, and decrease in the series dithiobenzoates > trithiocarbonates ~ dithioalkanoates > dithiocarbonates (xanthates) > dithiocarbamates. Electron-withdrawing substituents on Z can enhance the activity of RAFT agents to modify the above order.[68, 69] The free radical leaving group, R, also plays a crucial role on RAFT polymerization. Usually better leaving groups require the R substitutes on CTA are more stable, electrophilic, and able to generate more bulky radicals.[70]

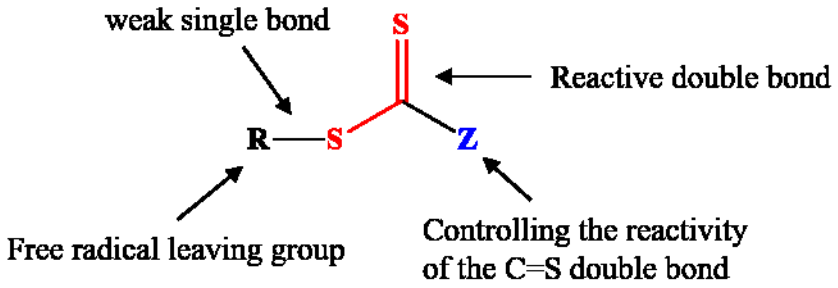

Scheme 2-5. General structure of CTA used in RAFT polymerizations.

The most attractive characters for RAFT polymerization over other RDRF techniques is its handiness. Theoretically, RAFT can be carried out under conditions that are identical to the conventional radical polymerization, with the only exception on the presence of the CTA. Therefore, it is no surprise that many of the strengths of RAFT, include wide selection on monomers,[67] polymerization solvents[31, 71-73] and temperatures,[74, 75] are actually derived from the inherent versatility of conventional radical polymerization. Importantly,

this enhanced synthetic utility does not require any metal catalysts or high polymerization temperatures (RAFT can be conducted at even -15 °C[74]), which makes RAFT as a particularly popular tool to synthesize multiple hydroxyl groups containing glycopolymers in aqueous media for many biological applications.[76]

McCormik and coworkers have worked extensively on establishing both homogeneous and heterogeneous aqueous RAFT polymerization system for the preparation of water-soluble, amphiphilic, and stimuli-responsive materials.[71-73, 77-81] Thanks for their continuous contributions on aqueous RAFT polymerization in the past decade, by employing RAFT, glycopolymer chemists now allowed to get well-defined glycopolymers in a facile manner. For example, Armes group, from which the idea of ATRP synthesis of unprotecting glycopolymer originally comes,[49-51] recently reported using a new technique called polymerization induced self-assembly (PISA) to obtain galactose containing glycopolymer nano-objects with various morphologies (**Scheme 2-6a**).[82] Compared to conventional self-assembly strategies, which only allow the glyco-block copolymers forming nano-objects in dilute solution (<1%),[83-85] the RAFT polymerization based PISA process enables well defined block copolymer form nano-objects at high concentrations.[82] Kasko and coworkers recently reported the synthesis of branched amphiphilic glycopolymer that able to self-assembly into nanoparticles.[86] The polymer is synthesized through the RAFT chain extension of a hydrophobic poly(methyl acrylate) macroCTA using a galactose containing monomer and a polymerizable CTA as branching unit. Interestingly, a higher saccharide density on the nanoparticles surface can be achieved by increasing of the carbohydrate branching units while without affecting the size and morphology of the nanoparticle. The results add another aspect of controlling design of synthetic glyconanoparticles for

improved biological activity. In Narain group, they have used RAFT polymerization in aqueous system to construct glycopolymers with different structures for drug/gene delivery purposes. For example, they have used RAFT polymerization to synthesize galactose containing cationic glycopolymers for targeting delivery of DNA or SiRNA to tumor site for cancer therapy (**Scheme 2-6b**).[87-89] By addition of *N,N′*-Methylenebisacrylamide during home/random and block RAFT co-polymerization of glycomonomer, they produced well-defined glycopolymers with hyperbranched[90, 91] and nanogel[92-94] structures, respectively. Recently, by employing the dynamic diol-boronate covalent bonding, Kotsuchibashi and Narain has reported a simple method of hydrogel formation by mixing RAFT polymerized glycopolymer and boronic ester (5-methacrylamido-1,2-benzoxaborole) containing polymer in a pH 7.4 Phosphate buffered saline (PBS).[95]

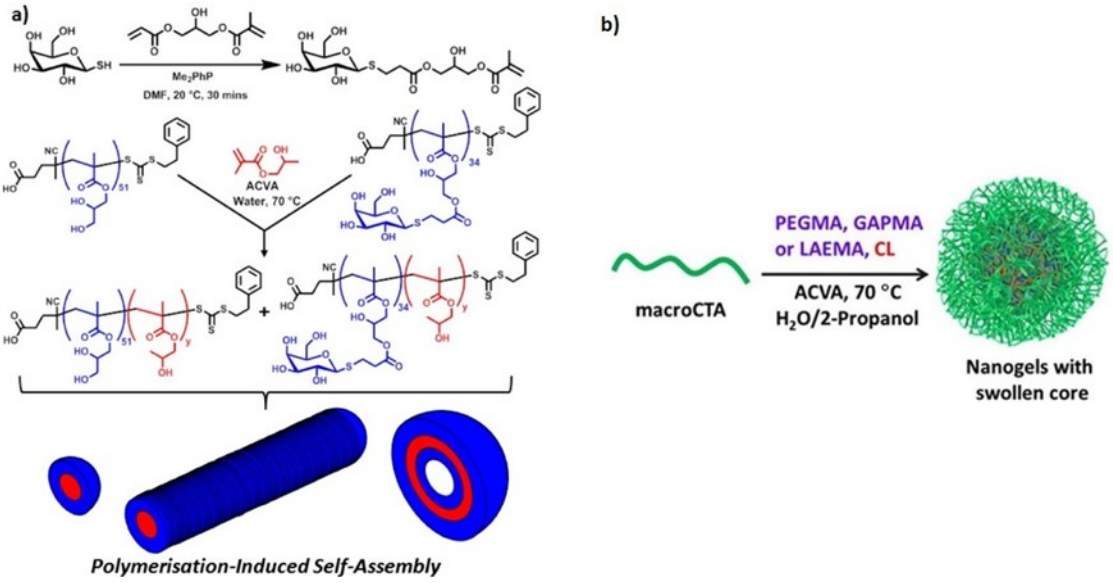

Scheme 2-6. a) Preparation of self-assembled block copolymer nano-objects (spheres, worms or vesicles) via PISA. Reprinted with permission from reference 82. Copyright 2013 American Chemical Society. b) Schematic illustration for the synthesis of

carbohydrate based nanogels. Reprinted with permission from reference 96. Copyright 2012 American Chemical Society.

Another advantage of RAFT polymerization in glycopolymer synthesis is the use of polymer terminals, where proteins, peptides, nucleic acids or functionalized nanomaterials can conjugate to glycopolymer terminals by either using these biomolecules or nanomaterials pre-modified of CTAs for RAFT polymerization or post-polymerization converted thiol terminals from the polymers dithioester or thrithioester ends. Maynard and coworkers reported examples of using pyridyl disulfide functionalized CTA to RAFT polymerize of trehalose containing glycomonomers. After conjugating thiolated proteins or nucleic acids to the glycopolymers, stabilities of those biomolecules were found increased significantly under extreme environmental stressor (e.g. lyophilization and heating at 90 °C for 1h) (**Scheme 2-7a**).[55, 59, 97] Chen and coworks synthesized glycopolymer-porphyrin conjugate as photosensitizer for targeted cancer imaging and photodynamic therapy purposes. A glucose containing glycopolymer was first synthesized by RAFT polymerization followed by converted its dithioester terminal to thiol group. Then, by employing thiol-ene "click chemistry", protoporphyrinogen was conjugated to polymer terminals and oxidized in-situ to obtain final porphyrin-glycopolymer conjugate. The materials showed enhanced binding ability toward Con A and K562 cells efficiently, and killed these cells under light irradiation (**Scheme 2-7b**).[98] No surprisingly, by converting their sulfur containing terminal compounds to the thiol ones, RAFT polymerized glycopolymers can also be easily anchored on gold nanoparticles surface by novel photochemical,[99] or conventional reduction methods[100] (**Scheme 2-7c**).

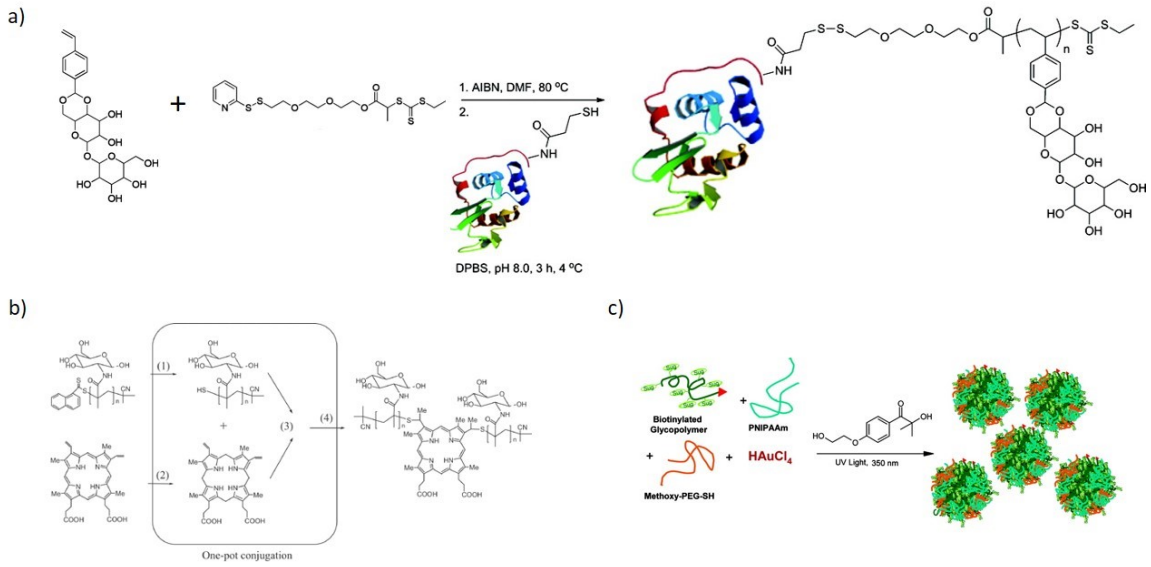

Scheme 2-7. a) Synthesis of trehalose containing thiol reactive glycopolymer by RAFT followed by conjugating to thiolated lysozyme. Reprinted with permission from reference 59. Copyright 2012 American Chemical Society. b) One-pot reaction to fabricate the Protoporphyrin-glycopolymer conjugate. Reprinted with permission from reference 98. Copyright 2014 John Wiley and Sons. c) Preparation of glycopolymer modified gold nanoparticles by photochemical method. Reprinted with permission from reference 99. Copyright 2007 American Chemical Society.

2.2.1.3.Ring Opening Polymerization (ROP) of Glycopolypeptides Synthesis

The inventions of RDRP accelerating the development of glycobiology by providing strategies on controlling synthesis of multivalent glycopolymers, but these techniques only allow researchers obtaining glycopolymers with carbohydrates attached on the non-degradable hydrocarbon backbone. In contrast, glycopolypeptides that synthesized by controlled ring opening polymerization (ROP) of amino acid N-carboxyanhydrides (NCAs) are biocompatible and biodegradable, and are much structurally closer to the naturally occurring polysaccharides or glycoconjugates due to their ability of folding into secondary,

tertiary and higher ordered structures through multiple non-covalent interactions among the amino acids.

The history of preparing glycopolypeptides from the glycosylated NCAs can be tracked back as early as 1966, when Rüde and coworkers prepared the first *O*-linked glycosylated-serine NCAs, and studied how addition of sugars to polypeptides would affect their immunological properties.[101] The preparation method are shown in **Scheme 2- 8**. However, polymerization of these NCAs can only obtain short, oligomeric products, where chain growth was likely inhibited by steric hindrance or hydrogen bonding between the sugar substituents and the NCA rings. On the other hand, the utilization of highly toxic and environmentally damaging mercury salts during the attachment of a glycosyl halide to an alcohol, known as Koenigs–Knorr reaction, may also induce potential cytotoxic problem when the final products were employing to biomedical applications.

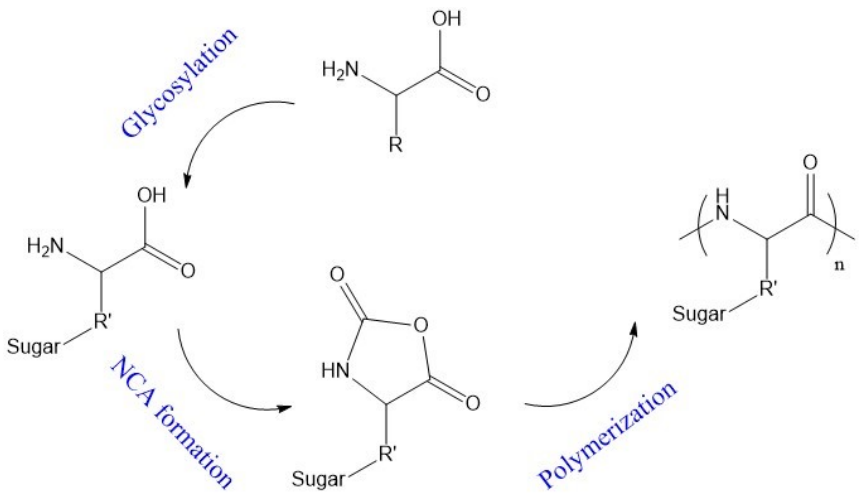

Scheme 2-8. Schematic illustration for preparation of glycopolypeptides by ring opening polymerization.

To address these issues, Cameron and coworkers improved the *O*-linked glycosylated-serine NCAs synthesis by reaction of acetobromosugars with *N*-*tert*-butoxycarbonyl-L-serine or *N*-*tert*-butoxycarbonyl-L-threonine in the presence of iodine as the Lewis acid promoter.[102] Unfortunately, after the removal of the Boc groups and converted to NCAs using triphosgene, the yield was only around 26 to 51%, which was not pure enough to allow polymerization.

Kramer and Deming reported a new route of preparing glycosylated L-lysine NCA with high purity and bearing complex functionalities (e.g. glucose, galactose or mannose) monomers.[103, 104] Different from the previously described *O*-linked conjugates, the new glycosylated L-lysine NCAs employed *C*-linked sugars and amide linkages for improved stability against de-glycosylation. Homo or block glycopolypeptides polymerized from these monomers showed high molecular weight (M_n = 160 kDa), while maintained low dispersity (PDI < 1.1) and could be readily dispersed in water after deacetylation.[105] Later, the same group has also described the preparation of glycopolypeptides with controllable secondary structure. An allyl functionalized carbohydrate was first attached to amino acid thiol by thiol-ene "click chemistry" and converted to glycosylated L-cysteine NCAs by Leuch's method via treatment with dichloro(methoxyl)methane. The conformation-switchable glycopolypeptides were then prepared by the ROP of allyl functionalized glycosylated L-cysteine NCA monomers. The resulting glycopeptides were found to be water soluble with α-helical structures in solution. Once being oxidized, the thioether linkages converted to a sulfone form, which disrupts the α-helical conformation into random coil secondary structures without loss of water solubility.[106, 107] These studies were the first examples on synthetic glycopolymers that process abilities of changing chain

conformations while reserve water-soluble in both states, and allows new capabilities for control over presentation of sugar functionality in subtly different contexts.

The main challenges on glycosylated NCAs preparation have been the multistep, as well as difficulties in obtaining the highly purified monomers for their controlled polymerization. In 2014, Schlaad's group reported a possible way of simplifying this process by *in situ* formation of glycosylated NCAs through the radical catalyzed thiol–ene reaction of allyl glycine with 1-thio-β-d-glucopyranose-2,3,4,6-tetraacetate. Despite of the high cost of the unnatural amino acid, this procedure allows the thiol–ene conjugation reactions occurring only on amino acids allyl groups without any attacks of the thiols on the NCA monomers. The as-formed glycosylated NCAs could then be polymerized directly using an amine initiator and gave glycopolypeptides with DP from 24 to 55.[108]

2.2.2. Synthesis of Glycopolymers from Post-Polymerization Modifications

A major challenge associated with synthetic glycopolymers when studying the carbohydrate-protein based multivalent interactions is precise control over the polymers molecular weight, carbohydrate density, and linker/spacer length to biomimetic their biological analogs. Directly synthesis of glycopolymers from their monomers via RDRP can partially fulfil such demands in terms of controlling polymer molecular weight, morphologies, and molecular weight distributions. Unfortunately, due to the difficulties in precise control and characterization of monomer sequencing during polymerization, these strategies are unlikely to lead sequence control of both individual monomers and multi-blocks in polymer synthesis.[37, 57, 109] Moreover, there are also some functional groups that are incompatible with RDRP methods (such as thiols, alkenes, alkynes). Considering of this, post-polymerization modification of reactive polymer precursors with carbohydrates

have demonstrated significant interest as an attractive route toward synthetic route of glycopolymers, especially with the development of "click" reactions.

2.2.2.1.Post-polymerization Modification via Click Reactions

First introduced by Sharpless and coworkers in 2001,[32] the area of post-polymerization modification of synthetic polymers with biomolecules such as carbohydrate, protein and nucleic acid has been expanded by the concept of "click chemistry".[110] Although a number of organic reactions, including thiol-ene, thiol-yne, Michael addition, pyridyl disulfide, Diels-Alder, and oxime, are accepted as the "click" reactions, copper-catalysed azide-alkyne cycloaddition (CuAAc), also known as Huisgen [3 + 2] cycloaddition, is undoubtedly the most widely used "click" reaction.[57, 110-112] CuAAC involves a reaction between an azide functionality and a terminal alkyne moiety with the presence of Cu(I) as the catalyst (**Scheme 2-9**). The beauty of CuAAC lies on simple to perform, high selectivity and conversion, mild reaction conditions, tolerant to a variety of reaction conditions, and simple purification.

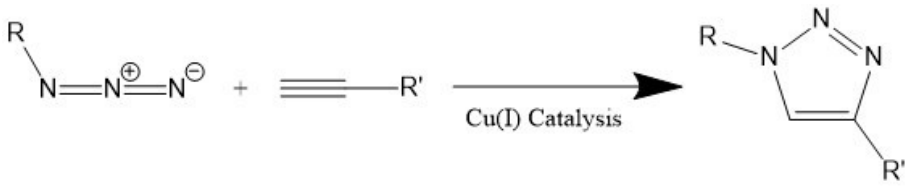

Scheme 2-9. Schematic illustration of copper-catalysed azide-alkyne cycloaddition reaction.

In the field of glycopolymer synthesis, the bulky carbohydrate pendent groups may hinder the polymerization process and, therefore, is difficult to prepare glycopolymers with precise structural control by directly polymerization from their monomers. To overcome

this shortcoming, a two-step reaction had been designed, in which small reactive functional groups are first polymerized via control radical polymerization and followed by a post-polymerization modification with carbohydrate groups by "click chemistry".[37, 113, 114] Because both ATRP and CuAAC are mediated by a Cu(I) catalyst, Haddleton and coworkers pioneered the works on combine these two reactions for the synthesis of well-defined glycopolymers.[37, 109, 115-118] For example, in one of their recent study, the authors reported a strategy for the synthesis of multi-block sequence-controlled glycopolymers by the combination of copper(0) mediated living radical polymerization with thiol–halogen, thiol–epoxy and CuAAC "click chemistry".[109] To start synthesize of the sequence controlled glycoPolymer multi-block poly(glycidyl acrylate)-*co*-(acrylic acid 3-trimethylsilanyl-prop-2-ynyl ester) were obtained by mediated living radical polymerization at ambient temperature *via* iterative monomer addition. Once the addition of thiol carbohydrate, due to the reactivity differences between thiol-halogen and thiol-epoxy as well as the presence of trimethyl silyl protected alkyne groups, glycopolymers with a defined sequence and spatial orientation are therefore obtained (**Scheme 2-10a**). Later, the same group employed a three steps tandem post-polymerisation modification developed a structural precise controlled galactose containing glycopolymer. Their route also allowed a secondary branched binding motif to be introduced onto the carbohydrate linker to dramatically increase both the affinity and the specificity (up to 20 folds) of the glycopolymers towards bacterial toxins.[119] (**Scheme 2-10b and 2-10c**).

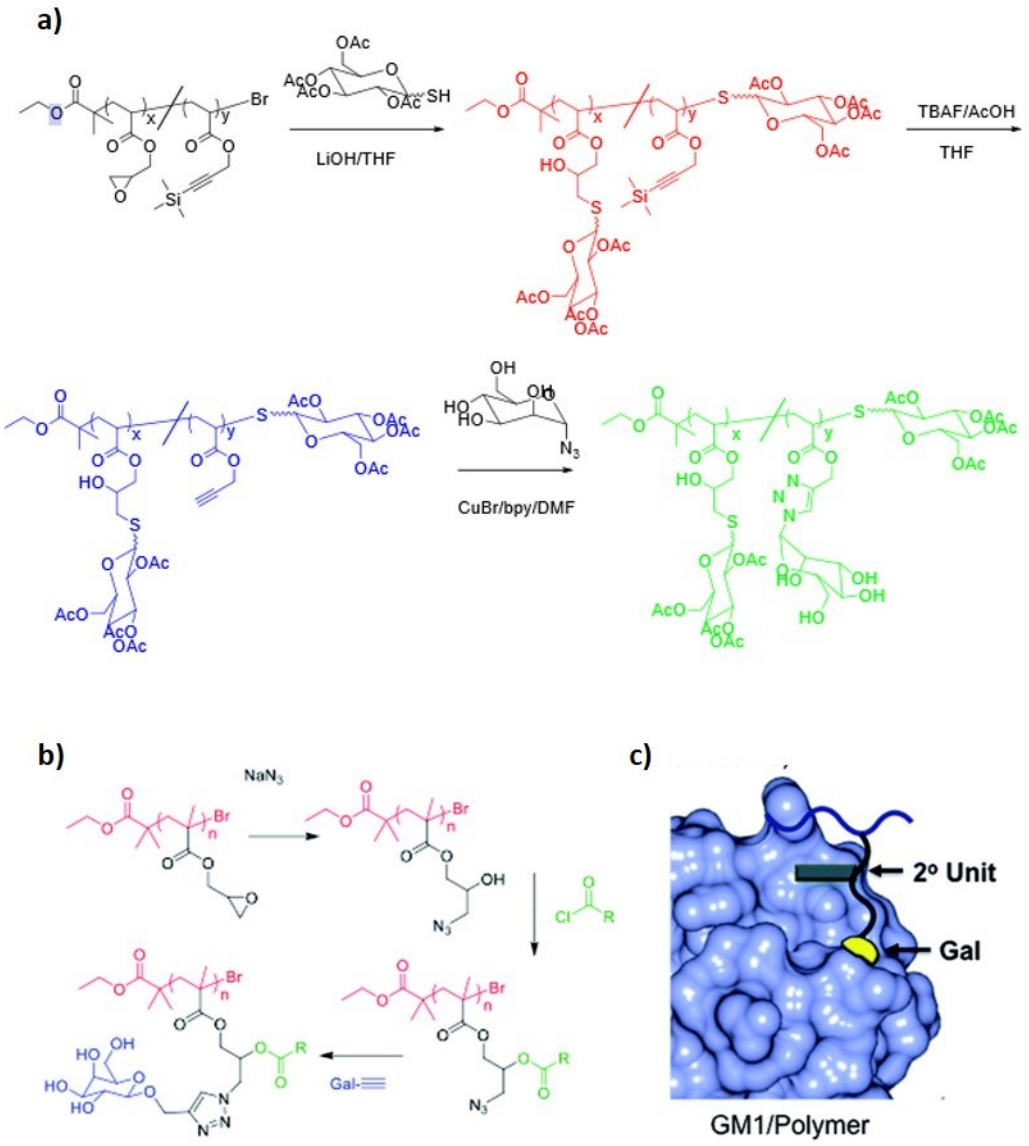

Scheme 2-10. Synthesis of multi-block glycopolymers via sequential thiol-related and CuAAC click reactions (a). Reprinted with permission from reference 109. Copyright 2014 Royal Society of Chemistry. Synthesis of glycopolymer (b) with idealized polymer-lectin interactions with enhanced affinity from the secondary binding motifs (c). Reprinted with permission from reference 119. Copyright 2014 Royal Society of Chemistry.

One of the issues related to applying glycopolymers synthesized by CuAAc post-polymerization modification in biomedical filed is the potential cytotoxicity induced from

the transition metal catalysts during the "click" reaction. Therefore, metal free "click" reactions are valuable tools for the synthesis of glycopolymers. As illustrated by Schubert and coworkers (**Scheme 2-11a**), a well-defined copolymer consisting of styrene and pentafluorostyrene was functionalized by thiol−glycoside (2,3,4,6-tetra-*O*-acetyl-1-thio-β-d-glucopyranose) under ambient conditions via a thiol−*para* fluoro "click" reaction. This nucleophilic substitution reaction was performed with high yields, with abilities to self-assembly to form glycopolymer nanoparticles.[120] Another elegant approach for obtaining well-defined glycopolymers via post-polymerization metal free "click" reaction was developed by Bertozzi group and known as strain promoted azide–alkyne cycloadditions (SPAAC) (**Scheme 2-11b**). Unfortunately, the reaction rate of the first generation SPAAC was relatively low as compared to the corresponding CuAAC reactions.[121] Later, the second[122] and third generations[123] of SPAAC has been developed by introducing electron-withdrawing groups on cyclooctyne to decrease the lowest unoccupied molecular level. The corresponding second order rate constants for the third generation of SPAAC was recorded as 31.8 M^{-1} s^{-1}, which was 30 times higher as compared to first and second generations. Glycopolymers can also be prepared by post-polymerization modification of a methyl vinyl ketone containing polymers by an addition reaction with aminooxy-terminated saccharides.[124-127] For example, Bertozzi and coworkers used a phospholipid-containing trithiocarbonate terminated CTA to RAFT polymerized a methyl vinyl ketone containing monomer. The lipid tail allows the glycopolymer anchoring on cell membrane, while the trithiocarbonate terminal is reduced to thiol group and, therefore, can conjugate with fluorophores for signalling purpose. A mucin-like glycopolymer was then obtained by reacting of the polymer's ketone pendent groups with aminooxy functionalized *N*-

acetylgalactosamine. By controlling the carbohydrate density on polymer chains, the orientation as well as the rigidity of the glycopolymers can be manipulated on live cell surfaces.[124]

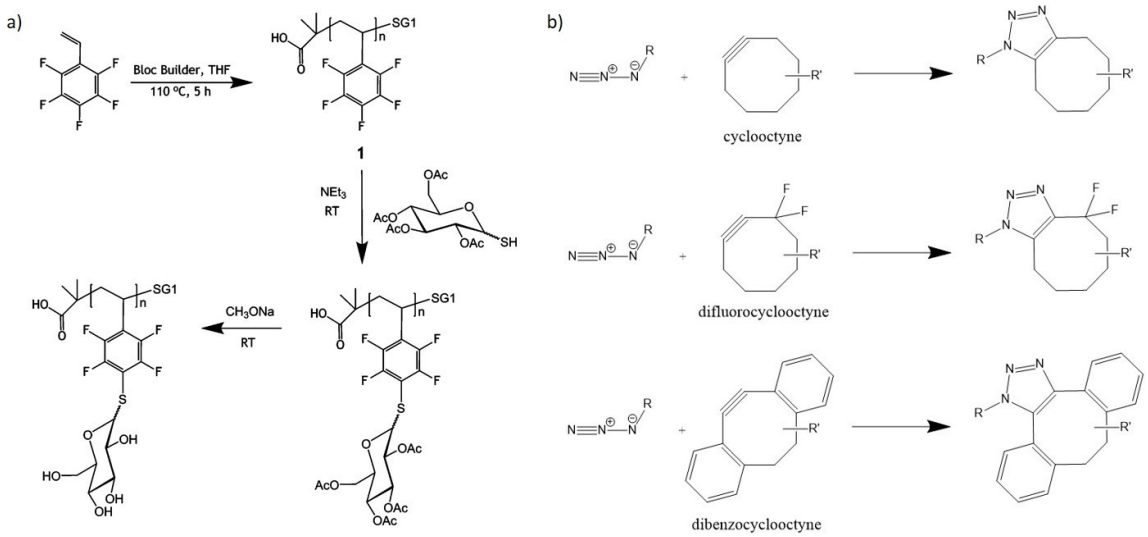

Scheme 2-11. a) glycopolymer synthesized by post-polymerization thiol−*para* fluoro "click" reaction. Reprinted with permission from reference 120. Copyright 2009 American Chemical Society. b) Copper free "click chemistry" mediated by SPAAC.

2.3.Glycopolymers for Biomedical and Environmental Applications

2.3.1. Glycopolymers for Biomedical Applications

2.3.1.1.Pathogen Inhibitor

As mentioned in the section 2.1, the multivalency of glycopolymers amplifies the molecular interactions with lectins, bacteria, viruses, and cells by the "glycoside cluster effect", these materials have great potentials to be used as inhibitors to block pathogens infection to host cells.[15] For example, the benefits of using multivalent glycopolymers to inhibit bacterial toxins were shown by Lee's group in 2001, in which the inhibition of Shiga

toxin 1 (Stx-1) was enhanced at least 5000 times with glycopolymer based inhibitor as compared to the monosaccharides.[128] However, the development of glycopolymer based pathogen inhibitors is still a challenging because the binding sites on CRD are usually shallow, and the inhibition efficiency of glycopolymers may be affected by the density of the carbohydrate ligands.[11, 37, 126, 129, 130] Kiick and coworkers has investigated using glycopolymers as cholera toxin inhibitor in detail. They found the best inhibition should be achieved when the spacing between polymers carbohydrate ligands matches with the CRD distances on toxins (ca. 3.5 nm).[129] At high ligand density, the spacing between carbohydrates becomes smaller, and a decrease in the toxin inhibitory effect could be explained by the steric hindrance between the unbound ligands (**Scheme 2-12**). Based on this finding, Gibson and coworkers reported an example of employing tandem post-polymerization modification to precise control of carbohydrate ligand densities as well as spacer lengths on glycopolymer for bacterial toxin inhibition.[37] Their study shows, for a glycopolymer with long spacer length and 100% ligand density, a good inhibition is recalled, which can be explained by full penetration of the ligand to the binding site and high rates of statistical rebinding, respectively. In contrast, at a ligand density lower than 10%, a good inhibition is also observed, which is due to the lower steric hindrance and a better fit to the binding sites. Between these values, the inhibitory efficiency decreases.

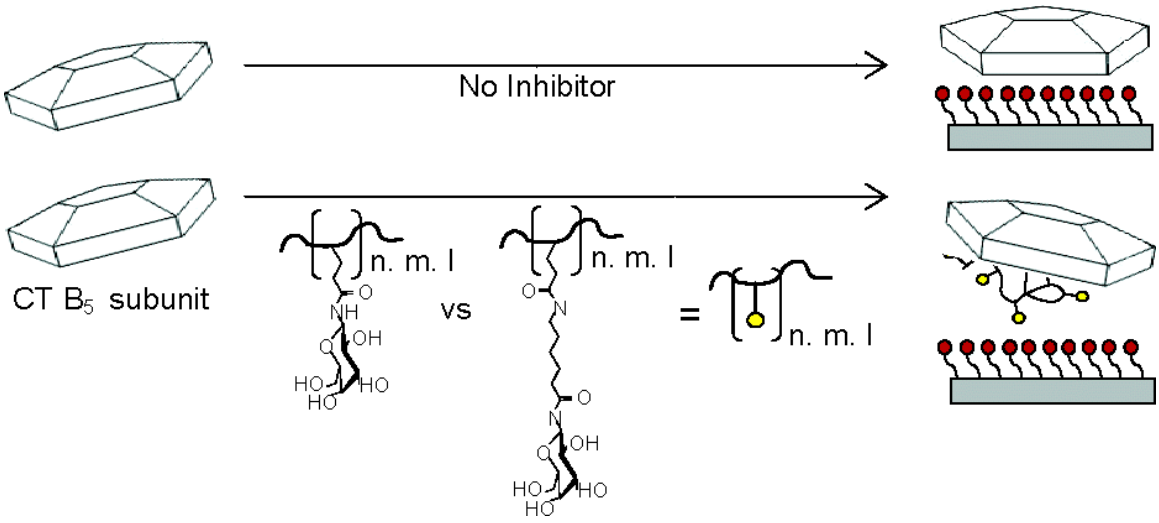

Scheme 2-12. Glycopolymer with different spacer lengths and carbohydrate densities for cholera toxin B_5 subunit inhibition. Reprinted with permission from reference 129. Copyright 2006 American Chemical Society.

The applications of glycopolymers on inhibition of virus have also been reported. The influenza viruses infect host cells by interacting with sialyl oligosaccharides on the cell surface. Strategies on using glycopolymers bearing sialic acid groups to inhibit various types of influenza viruses infections have been reported by blocking hemagglutination from binding to viral hemagglutinin.[19, 131-134] Dendritic cell-specific ICAM-3 grabbing nonintegrin (DC-SIGN) is a C-type lectin present mainly on the immature dendritic cells surface, and is responsible for the binding and uptake of a multitude of pathogens, such as human immunodeficiency,[135] ebola,[136] and hepatitis C viruses[137] via oligomannose-dependent interactions. Applying of glycopolymers as human immunodeficiency virus (HIV) inhibitors have also been reported by many research groups.[117, 138-140] For example, Haddleton and coworkers showed that novel multiblock mannose and glucose containing sequence controlled glycopolymers (**Scheme 2-13**) can inhibit HIV infections by binding

with the DC-SIGN presented macrophages and dendritic cells (**Table 2-1**).[141] Although the impact of the glycopolymer's sugar sequence or density on HIV inhibition requires further studies, the inhibition of DC-SIGN binding to the HIV envelope glycoprotein gp120 in the presence of nanomolar concentrations of this polymer showed huge potential as compared to the glycopolymers with randomly distributed α-mannoside and β-galactoside reported from their pervious works.[117]

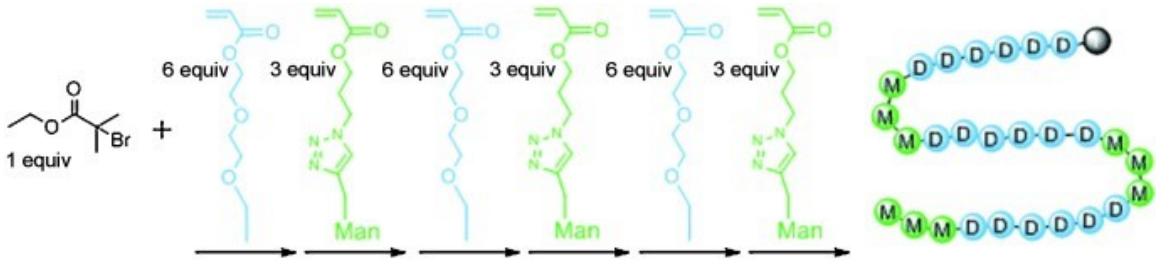

Scheme 2-13. Sequence controlled mannose and glucose containing glycopolymers synthesized by ATRP. Reprinted with permission from reference 141. Copyright 2013 John Wiley and Sons.

Table 2-1. Binding kinetics and inhibition concentration of glycopolymers. Reprinted with permission from reference 141. Copyright 2013 John Wiley and Sons.

Code	Sequence	DC-SIGN binding			
		k_{on}	k_{off}	K_D	IC_{50}
		$[M^{-1}\ s^{-1}]$	$[s^{-1}]$[a]	[nM][b]	[nM]
gp120	gp120	7.3×10^{5}	7.8×10^{-5}	0.11	11
C1	$ManMA_{58}$	2.9×10^{5}	2.0×10^{-4}	0.66	230
S1	$ManA_{23}$	8.0×10^{4}	3.1×10^{-5}	0.39	153
S2	$ManA_{13}$-*b*-$OEGA_2$	3.6×10^{4}	7.6×10^{-5}	2.2	380
S3	$ManA_9$-*r*-$DEGEEA_{18}$	3.9×10^{3}	2.6×10^{-5}	6.6	>1000
S4	$ManA_9$-*s*-$DEGEEA_{18}$	4.7×10^{3}	6.7×10^{-5}	14	>1000
S5	$GluA_6$-*s*-$ManA_4$-*s*-$FucA_4$	4.0×10^{3}	6.2×10^{-5}	15	>1000
S6	$GluA_4$-*s*-$ManA_4$-*s*-$GluA_4$	9.7×10^{3}	9.7×10^{-5}	34	n/a

[a] k_{off} values are close to the limit of the SPR detection, so probably reflect upper limits of such values. [b] For the same reason as in [a], K_D values probably also represent the upper limits of such values. *b*=block, *r*=random, and *s*=sequence controlled.

2.3.1.2.Improving the Biocompatibility of Materials

Implantable medical devices are increasingly important in the practice of modern medicine. Unfortunately, lots of the devices suffer from adverse reactions, including inflammation, fibrosis, thrombosis and infection, when applied in vivo. The implant-associated protein adsorption and conformational changes have been shown to promote immune reactions.[142] Engineering of the materials surface property, such as physical and chemical characteristics, can improve the implants biocompatibility by reducing protein adsorption and cell interactions from the materials surfaces. For example, hydrophilic poly(ethylene glycol) (PEG),[143, 144] and zwitterionic poly(sulfobetaine methacrylate) (PSBMA)[143-145] and poly(2-Methacryloyloxyethyl phosphorylcholine) (PMPC),[144, 146] have been extensively used on modification of a material surface and reduce the biofouling by improving the materials surface hydrophilicity.

Glycopolymers, which carrying multiple carbohydrate repeating units, are structural similar to biological cell surface and can also be used to improve a material surface hydrophilicity. Therefore, these materials have also been reported in the purpose of improving the biocompatibility of biomaterials. For example, carbon nanotubes and graphene are classes of carbon materials that received tons of research interests as biomaterials due to their unique physicochemical properties.[147, 148] However, their low solubility, in aqueous system as well as high cytotoxicity always limit their applications in biomedical fields.[149, 150] It was found, by modifying these materials surfaces with glycopolymers, the materials biocompatibility can be significantly improved.[151] For example, Bertozzi and coworkers noticed improved affinities between cells and carbon nanotube, and that covalently or non-covalently immobilized glycopolymers on the surface

can reduce the materials cytotoxicity significantly.[152, 153] Kizhakkedathu and coworkers evaluated the hemocompatibility of glycopolymer modified biomimetic surfaces and concluded that the increased cell viability could be due to the reduction of cell-materials interactions at glycopolymer modified nanomaterials surfaces.[92, 154]

2.3.1.3.Control Cell Function

In a typical inflammatory response, leukocytes are recruited to a site of injury or infection, which involves multiple steps including: leukocytes roll across the endothelium, adhere to the endothelium wall, and migrate into the inflamed tissue.[155] A key mediator of leukocyte migration process is L-selectin, which is cell surface lectin and interacts with glycoproteins displayed on the endothelium of blood vessels.[156] The physiological L-selectin ligands have been identified as highly glycosylated mucin-like glycoprotein which capped with sialyl Lewis x epitopes.[157] Kiessling and coworkers discovered, a sialyl Lewis x derived glycopolymer not only binds to L-selectin but also facilitates its downregulation [158] After treatment of lymphocytes with the glycoPolymer L-selectin expression was observed dramatic decrease on cell surface while increase as their soluble form, indicating the ligand binding triggered the proteolytic release of L-selectin. Their finding suggested that clustering of L-selectin leads to a signal transduction cascade that results in L-selectin releasing. Thus, glycopolymers can be potentially used as macro drug that can promote lymphocytes generate a soluble form of the L-selectin to inhibit cell surface interactions. In their other study, Kiessling and coworkers explored the roles of glycopolymers play in B cell signalling cascade. A hapten containing glycopolymer is found only interact with the B cell antigen receptor and activates B cell signalling. In contrast, when a copolymer

bearing both hapten and ligand for inhibitory co-receptor CD22 interacts with B cell, an attenuation on B cell activation and suppression of immunity is observed (**Scheme 2-14**).[159]

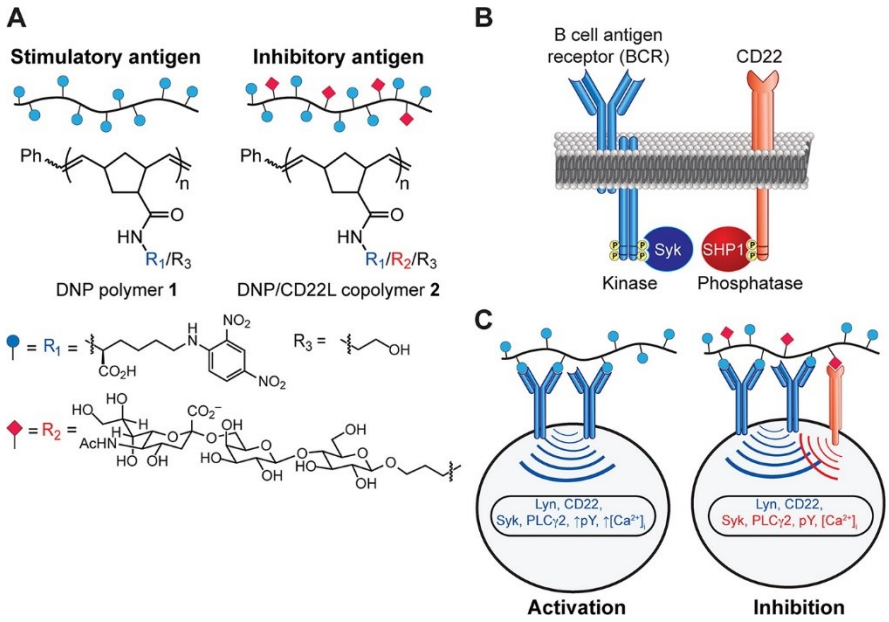

Scheme 2-14. Synthetic antigens used to modulate B cell antigen receptor (BCR) signaling. (A) Structures of the synthetic antigens. Homopolymer **1** displays the dinitrophenyl (DNP, R_1, blue) group. The inhibitory antigen copolymer **2** displays both DNP groups and the CD22 ligand (R_2, red). (B) Targets of the polymers include the DNP-specific BCR and the inhibitory lectin CD22. (C) Engagement of the BCR by polymer **1** results in the activation of multiple signaling components. Activation of many of these components is inhibited in copolymer **2**-treated cells. Reprinted with permission from reference 159. Copyright 2014 American Chemical Society.

Bertozzi and coworkers recently modified live cell surfaces by mucin mimetic glycopolymers and glycopolypeptides with lipid insertion domains and studied the role of cellular glycocalyx on cell singling, growth and differentiation (**Figure 2-2a**).[127, 160] It was found the glycoprotein mimetics could promote tumor aggregation by regulating integrin

adhesion on extracellular matrix (ECM). Kinetic rates of integrin-ECM interactions showed a strong correlation to the length of mucin mimetics presented on cell membranes (**Figure 2-2b**). Large glycoprotein mimetics reduced the overall rate of integrin bond formation, but significantly promoted clustering of integrins into focal adhesion (**Figure 2-2c**). Glycoprotein mimetics were also found to facilitate metastasis by promote focal adhesion signalling and enhance tumor cell growth and survival on soft substrates (**Figure 2-2 d and e**).

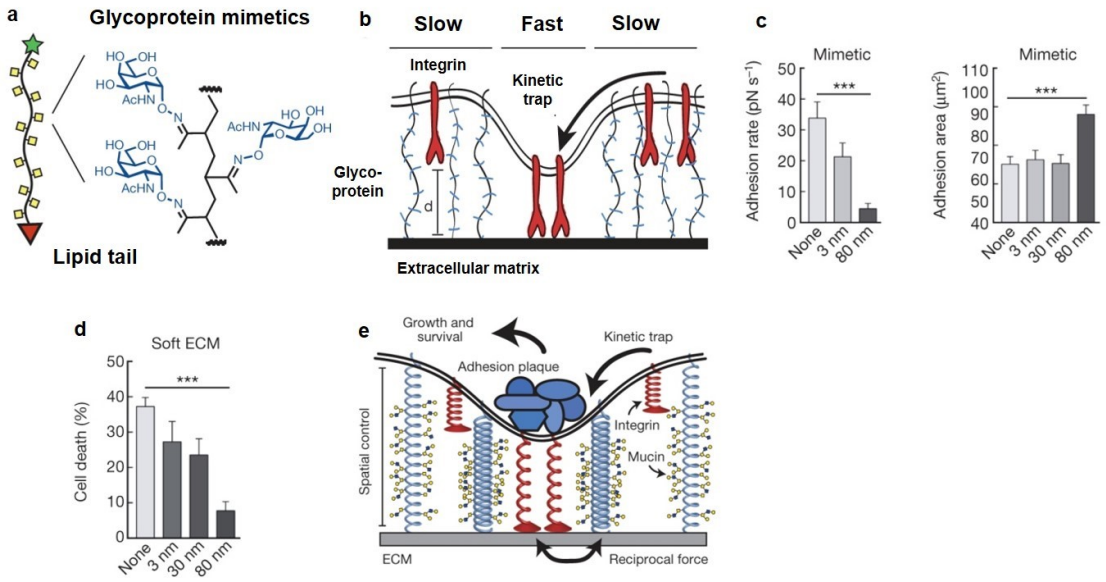

Figure 2-2. Schematic illustration of glycoprotein mimetics with lipid insertion domain (a) and glycocalyx-mediated integrin clustering (b). Shorter distances between integrin–ligand pairs result in faster kinetic rates of binding. (c) Rate of integrin–ECM adhesion and total adhesion complex area per cell measured in glycopolymer modified non-malignant mammary epithelial cells. (d) Cell death in control non-malignant mammary epithelial cells and those with incorporated glycomimetics quantified 24 h after plating on a soft (140 Pa) fibronectin-conjugated hydrogel substrate. (e) Schematic illustration of biophysical

regulation of integrin-dependent growth and survival by bulky glycoproteins. Adapt with permission from reference 127. Copyright 2014 Nature Publishing Group.

2.3.1.4.Biosensor and bioimaging

The carbohydrates molecular recognition ability can also be used as a biosensor. By amplifying the binding signal through multivalency, a glycopolymer decorated sensor should is a promising alternative to antibodies for use in biosensing and diagnosis.[161, 162] Techniques such as surface plasmon resonance (SPR),[163] quartz crystal microbalance (QCM),[164] nuclear magnetic resonance (NMR),[165] capillary electrophoresis,[166] fluorescence spectroscopy,[167] and atomic force microscopy (AFM)[168] have been reported to investigate carbohydrate-protein interactions. Among those technique, label-free SPR and QCM are the most widely used as they do not require prelabelling of carbohydrates or proteins on sensor surface and can therefore reduce "pseudobinding"[169] Most glycopolymer based biosensors require immobilization of the polymers on a solid surface by covalent immobilization,[170] physical adsorption,[171] and bioaffinity-based interactions.[172]

Due to the well-known carbohydrate-protein interaction, pathogen detection is an important application of glycopolymer based biosensors. For example, Nishida and coworkers reported a polyanionic glycopolymer based biosensor with relatively high sensitivity (10 ng/mL) to Shiga toxin detection by SPR[173, 174] and QCM.[175] Russell and coworkers designed glycopolymer-gold nanoparticles based materials that can colorimetrically detect of cholera toxin[176] and human influenza viruses (**Scheme 2-15**).[177] In their studies, glycopolymer decorated gold nanoparticles with diameters of 16 nm was red in solution due to the intense surface plasmon adsorption band at 524 nm. However,

after the addition of toxin or virus to the solution, the nanoparticles started to aggregate in less than 10 min and the solution turned to a deep purple color due to the red shifts of the surface plasmon adsorption band. This simple bioassay showed good selectivity for metal ions, anions and proteins, and could discriminate between human and avian influenza viruses.

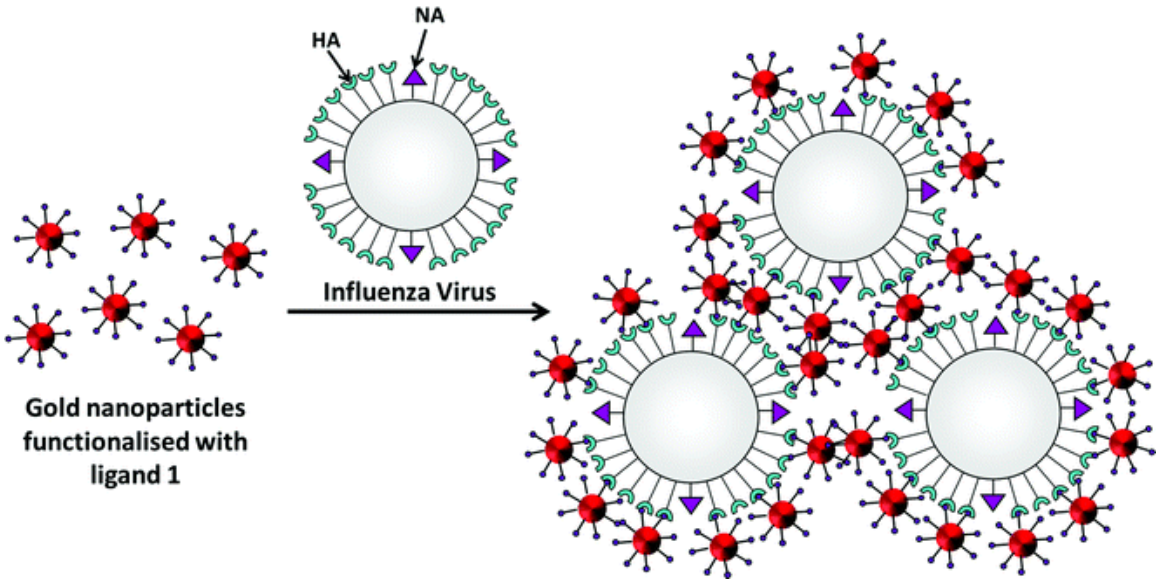

Scheme 2-15. Aggregation of the glycopolymer coated gold nanoparticles in the presence of the influenza virus. Reprinted with permission from reference 177. Copyright 2013 Royal Society of Chemistry.

Although QCM readily detects interactions between glycopolymers and small objectives, such as toxins or viruses, bacterial adhesion on glycopolymers modified QCM substrates have rarely been reported due to the damping effect of large bacterial cells.[178] However, using quartz crystal microbalance with dissipation (QCM-D), Narain group has recently reported studies on studying bacteria-carbohydrate interactions on glycopolymer modified QCM-D surfaces.[179, 180] Compared to *Escherichia coli (E. coli)* k-12 strain brings mannose

specific binding lectin, larger amount of *Pseudomonas aeruginosa* (*P. aeruginosa)* PAO1 can adhere on galactose containing glycopolymer modified QCM-D sensor surface and result stronger contact point stiffness due to the interaction between PA-IL and glycopolymer. The adhesion of *P. aeruginosa* PAO1 to the glycopolymers is also found to be highly dependent on the presence of calcium ions due to the specific C-type lectin interactions of PA-IL.[179] Furthermore, by incorporating of thermally responsive poly(*N*-isopropylacrylamide) (PNIPAAm) moieties to the galactose containing glycoPolymer they were able to generate a biomimetic QCM-D surface to probe bacterial adhesion on host cell surface (**Scheme 2-16**). Two major bacterial infection mechanisms, hydrophobic or lectin–carbohydrate interactions were studied accordingly. Compared to bacterial adhesion on PNIPAAm homopolymer surface, the event occurred on the galactose containing thermally responsive surface at 37 °C showed higher bond stiffness might suggest the lectin–carbohydrate interaction play a significant role in bacterial infections.[180]

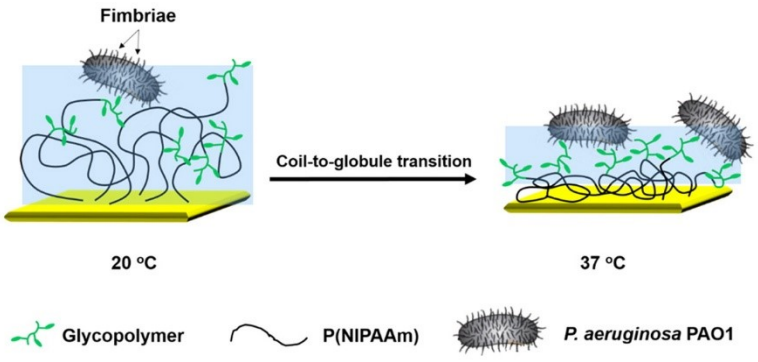

Scheme 2-16. Study of bacterial adhesion on temperature responsive glycopolymer modified biomimetic QCM-D surface. Reprinted with permission from reference 180. Copyright 2015 American Chemical Society.

Recently, Leisner and coworkers also reported a label-free, cantilever microarray based sensor for discrimination of *E. coli* strains.[181] Mannose and galactose containing glycopolymers were immobilized on gold coated cantilever array and set as specific target and nonspecific references, respectively. In the static mode, the type I pili containing *E. coli* strain ORN178 can specifically bound to the mannose surface via the binding protein FimH and induce differences in surface stresses, which led to cantilever deflections.

Quantum dots are nanosized fluorescent semiconductors. Compared to the conventional organic dyes and fluorescent proteins, quantum dots possess unique optical and electronic properties as the bioimaging materials. The incorporation of glycopolymers to quantum dots not only improve the materials solubility and biocompatibility but also allow the materials used as probe for various diseases. For example, a glycopolymer decorated quantum dots can be used to target and imaging the tumor sites due to the overexpressed lectins on cancerous cells.[182-184] Seeberger and coworkers used glycopolymers modified quantum dots to achieve in vivo liver imaging. Compared to the mannose and galactosamine containing glycopolymer modified nanomaterials, only the one with galactose containing glycopolymer decoration can be selectively taken up by hepatocellular carcinoma HepG2 cells, which is mediated by an interaction between galactose and the overexpressed ASGPR on the cell surface. Glycopolymers modified magnetic nanoparticles have also been reported to be used as contrast agents for noninvasive and label free in vivo magnetic resonance imaging.[185-187] For example, Hyaluronic acid modified magnetic nanoparticles have been used for in vivo imaging of macrophages,[188] reactive oxygen species,[189] CD-44 overexpressing breast cancer[190] and livers in cirrhotic mice.[191]

2.3.1.5.Drug/Gene Delivery

The interactions of carbohydrates with specific cells, such as galactose–hepatocyte, mannose-macrophage, and glucose-cancer, are well known. Multivalent glycopolymers with precise controlled molecular weight, structure, and carbohydrate densities are ideal candidates as drug/gene delivery vectors due to their low cytotoxic[91, 92] and high uptake to the specific cell lines.[87, 93] Additionally, for glyco-block copolymers consisting of hydrophobic segment, the linear copolymers are able to self-assembly to nanoparticles, which allows encapsulation of hydrophobic medicines, such as doxorubicin, in the nanoparticle core,[192] and enhance drug/gene delivery to the tumor site through the enhanced permeability and retention (EPR) effect.[193] For example, Li and coworkers reported the synthesis of a galactose containing glyco-block copolymer and self-assembly with doxorubicin to nanoparticles with average size of 100 nm. The multivalent galactose containing glycopolymer shell allows targeting of HepG2 cells via the interaction with ASGPR and release of the doxorubicin due to the reductive endocellular condition (**Scheme 2-17**).[194] The Armes group has prepared self-assembled glycopolymers nano-subjects with various morphologies, including wormlike, spherical micelles and vesicles. Those materials show high affinity with galectin on cell surface, and are able to intracellular delivery drugs to Human Dermal Fibroblasts cells.[82]

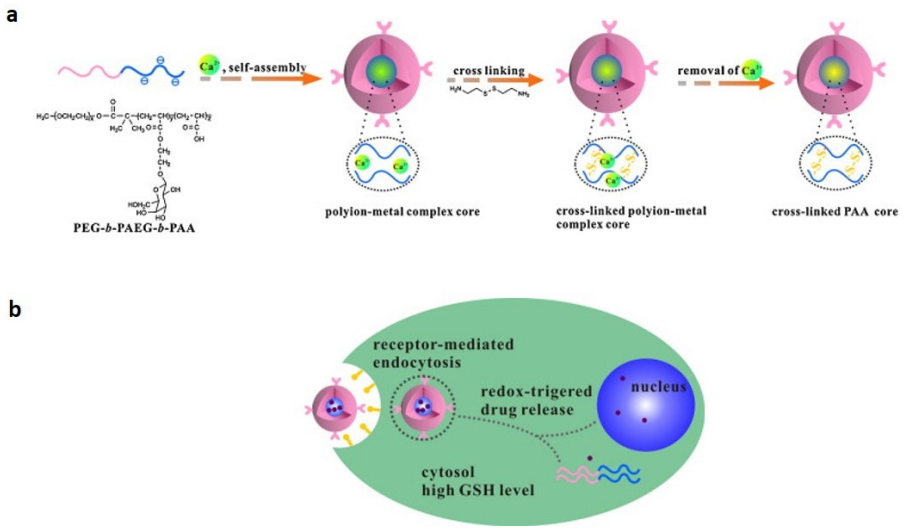

Scheme 2-17. Preparation of glycopolymer nanoparticles by self-assembly (a) used for target delivery of doxorubicin to HepG2 cells (b). Adapt with permission from reference 194. Copyright 2013 Elsevier.

Glycopolymers with stimulus responsiveness have also been reported for sophisticated drug delivery systems. The most well-known method is the utilization of thermos-responsive polymer such as PNIPAAm[95, 195, 196] or poly[di(ethylene glycol) methyl ethyl methacrylate] (PDEGMA).[93] For example, Narain group has synthesized galactose containing glycopolymer nanogels with different size and charge distributions to facilitate the targeted delivery of iodoazomycin arabinofuranoside (IAZA) to HepG2 cells via ASGPR mediated uptake (**Scheme 2-18a**). The thermally responsive nature allowed the drug encapsulated in nanogels. The glycopolymer nanogel delivery system demonstrated a loading capacity of IAZA up to 0.6 mM with stable, non-burst release of the drug over 10 h. IAZA in encapsulated form showed a superior radio-sensitization of hypoxic cells with sensitizer enhancement ratio from IAZA alone, 1.33, to 1.62.[93] By copolymerization with amino[197] or carboxylic acid[198] containing monomers or incorporation of disulfide bond,[199]

glycopolymers can also be used as drug delivery system that response to pH changes or redox environment. These classes of materials are particularly useful for targeting and control release of drug to tumors, which usually show an acidic pH[200] and redox environment.[201] Glucose responsive drug carriers have also been reported for insulin delivery for diabetes patients (**Scheme 2-18b**). The glycopolymers, which bearing multiple copies of carbohydrate, can interact with phenylboronic acids or their derives and form nanoparticles[202] or hydrogels.[95, 203] In the presence of high glucose concentration, the nanoparticles or hydrogels are dissociated due to the competition reaction between glucose and boronates, and release of the encapsulated insulin.[95]

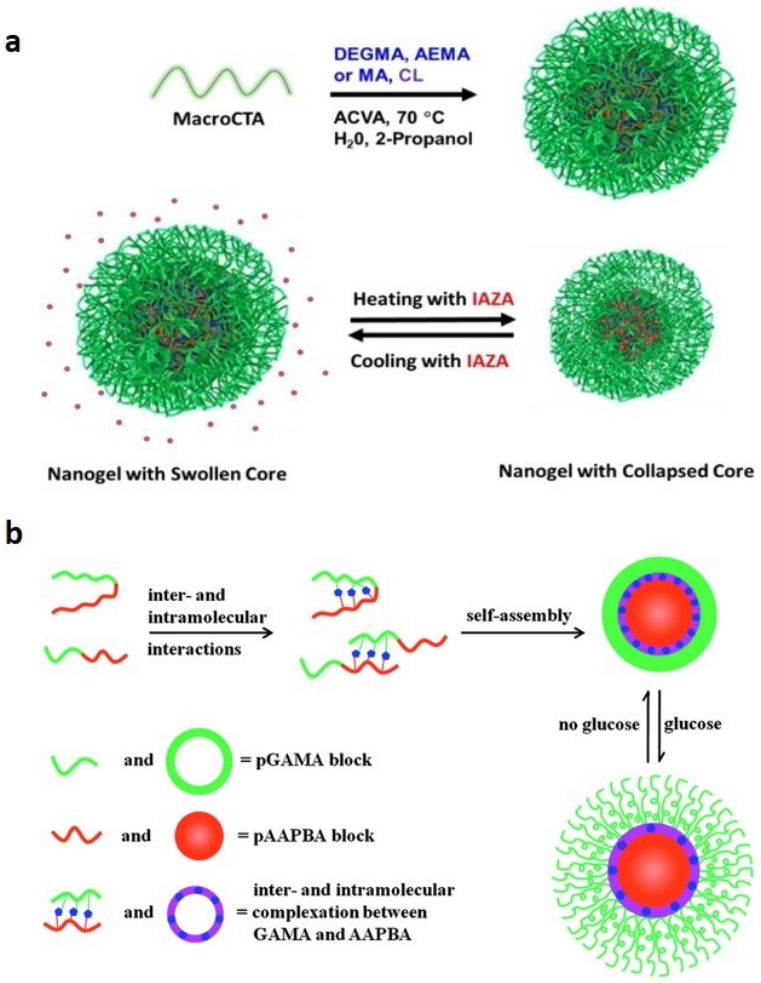

Scheme 2-18. (a) galactose containg glycopolymer nanogel for targeting delivery of radioactive iodoazomycin arabinofuranoside (IAZA) to HepG2 cells. Reprint with permission from reference 93. Copyright 2015 American Chemical Society. (b) Self-assembly of boronic acid and glucose containing glycopolymer to nanoparticles and used for control release of insulin. Reprint with permission from reference 202. Copyright 2014 Royal Society of Chemistry.

Glycopolymers are usually copolymerized or modified cationic polymers and used as non-viral vectors for gene delivery. The multivalent glycopolymers are used for active targeting of tumor sites,[93] but also reducing the cytotoxicity of the cationic moieties in the copolymers,[172] which are normally used to conjugate with negatively charged DNA or small interfering RNA (SiRNA). Narain group have extensively studied on delivery of DNA of SiRNA to different cancerous cell lines by various cationic glycopolymer carriers (e.g. linear[87-89] and hyperbranched[91] polymers, nanoparticles,[204, 205] carbon nanotubes,[206] and polymer nanogels[96, 207]). Recently, Reineke and coworkers also reported on delivering of gene/therapeutics to glioblastoma and cardiomyoblaster cell lines by unitization of the trehalose[208-211] or glucose[212] containing glycopolymer carriers.

2.3.1.6.Cell and Protein Isolation

Glycopolymers show strong affinities to receptors that overexpress on cancer cell surfaces, such as ASFPR in HepG2[89] and CD44 in breast cancer,[213] which can potentially be used to isolate tumor cells from health tissues.[214, 215] Aoyagi and coworkers prepared a thermally responsive glycopolymer modified surface that could separate HepG2 from NIH 3T3 cell line.[214] In their study, at a temperature over the polymer's lower critical solution temperature (LCST), the polymer layer on material surface collapsed and exposed

galactoses to surface to capture HepG2 cells. When temperature was reduced to 25 °C, the polymer brushes on the material surface became hydrophilic and released captured HepG2 cells. By immobilization of poly(*N*-*p*-vynylbenzyl-4-*O*-*b*-D-galactopyranosyl-D-glyconamide) with E-cadherin-IgG Fc to a surface, Akaike and coworkers introduced a strategy of isolation of hepatocytes from mouse embryonic stem cells.[215] In a galactose containing glycopolymer modified microfluidic assay, Di Fabrizio and coworkers successfully separated galactin-3 expressed tumor cells (HCT-116, MCF-7 and EPH-4) from healthy cells and demonstrated that the materials could be used for tumor cell isolation or for the capture of circulating tumor cells.[216, 217]

Affinity membrane chromatography can be used to achieve protein separation and purification from various complex aqueous samples such as human blood or river water. Miura and coworkers employed a mannose containing glycopolymer modified QCM surface to selectively separate of concanavalin A (ConA) from a ConA/bovine serum albumin (BSA) mixture.[218] Xu and coworkers reported examples on using different strategies to post-electrospun modification (such as chemical coupling,[219] click chemistry,[220] and UV grafting[221]) of carbohydrates to electrospun polymer nanofibrous mats for selective capturing of ConA from ConA/BSA mixture. The nanofibers showed excellent performance on lectin capture due to their large surface area, high porosity and good specificity for lectin binding. Very recently, Narain and coworkers have reported a dual pH and glucose responsive boronic acid containing nanofibrous material for the reversible capture and release of lectins (**Scheme 2-19**).[222] By surface modification of those nanofibers with galactose or glucose containing glycopolymers, the nanofibers could be used to selectively capture of Jacalin and ConA, respectively at pH 7.4. The nanofiber

surface and be regenerated to the pristine one by treating with acidic or high concentration of glucose solutions. These glycopolymers functionalized nanofibers can therefore be easily modified and hence can be potentially used for quick removal of selective proteins or toxins from aqueous solutions.

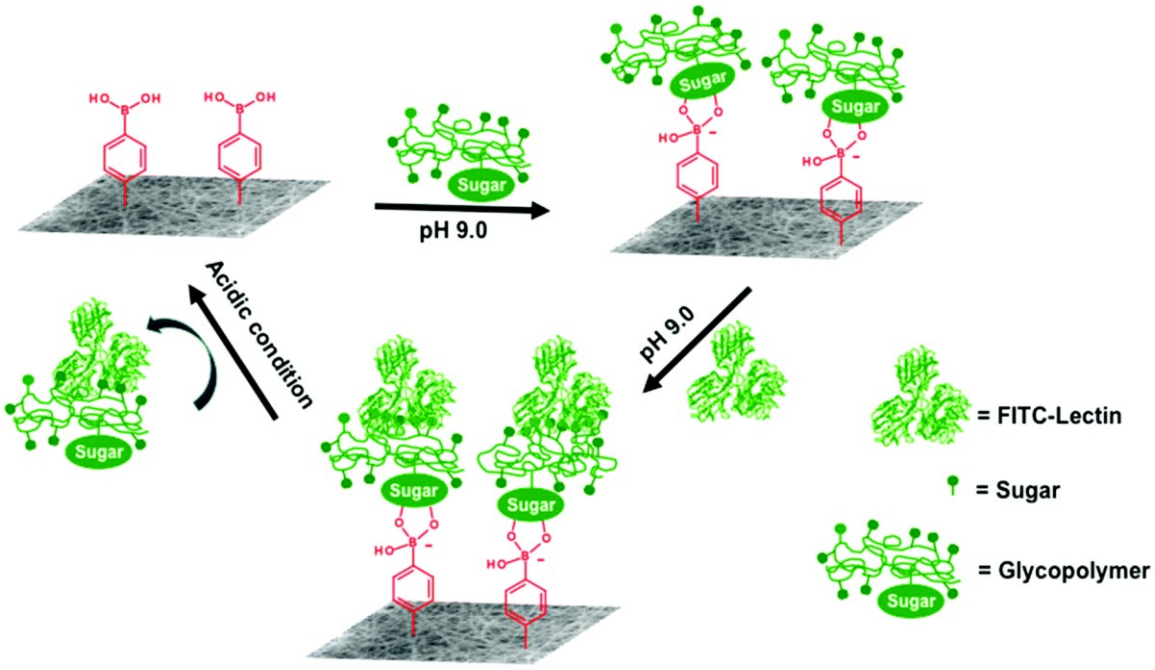

Scheme 2-19. Reversible capture and release of lectin on photo-crosslinked glycopolymers modified boronic acid containing polymer nanofiber surface. Reprint with permission from reference 222. Copyright 2015 Royal Society of Chemistry.

2.3.1.7.Cryopreservation and Protein Stabilizer

The cryopreservation of cells, tissue and organs is fundamental to modern biotechnology, transplantation medicine and chemical biology. A popular approach for cryopreservation process, known as vitrification, is adding organic solvent (such as dimethyl sulphoxide (DMSO) or glycerol) to cell suspension and cooled rapidly to promote the formation of the glassy (ice crystal free) water.[223] However, during the devitrification process, serval

problems associated with cell damages, which include intrinsic cytotoxicity from the organic solvents,[224] mechanical damage due to the ice growth,[225] and extracellular osmotic shock,[226] suggest new technology is urgently for modern cryopreservation. Inspired by nature that arctic fishes produce a series of antifreeze glycoproteins that allow them surviving in polar oceans where the surface temperature is below - 2 °C, synthetic glycopolymers[227] or glycopolypeptides[227-229] have been reported for the development of new cryopreservation technique, or, more particularly, reducing ice crystal growth during thawing (**Scheme 2-20**). For example, Gibson and Cameron compared the ice recrystallization inhibition from synthetic vinyl based glycoPolymer glycopolypeptides, and carboxylic acid and amine containing polymers.[227] They concluded hydroxyl group is essential for the ice recrystallization inhibition, while the glycopolymers show a strong molecular weight dependence on the abilities of antifreeze, with the higher molecular polymers being more active. Although the ice recrystallization inhibition abilities from the synthetic glycopolymers are lower as compared to polyvinyl alcohol,[230] the authors were confident that more active glycopolymer based antifreeze agents can be created by using the wealth of the well-established controlled polymerization techniques.

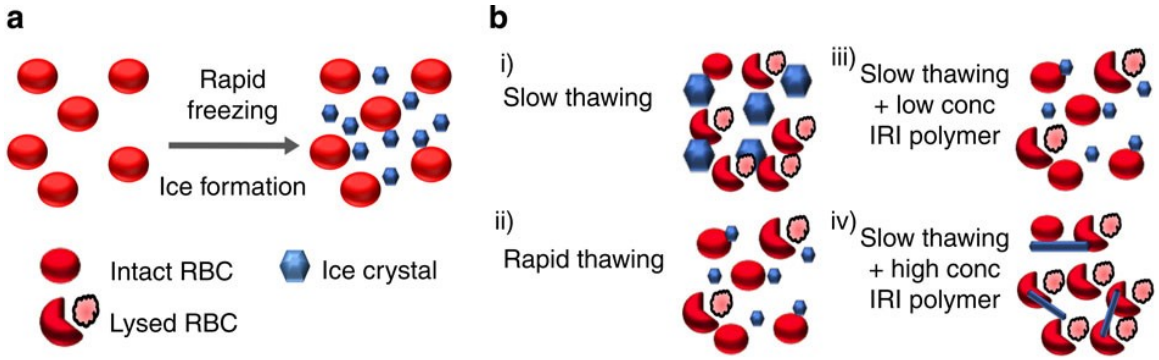

Scheme 2-20. Proposed mechanisms of cryoprotection or cell damage. (**a**) Initial rapid freezing step to produce large numbers of very small ice crystals. (**b**) Cell lysis outcomes associated with different thawing rates, the presence or absence of glycopolymer based ice recrystallization inhibition active additives. Reprint with permission from reference 230. Copyright 2014 Nature Publishing Group.

Proteins or polypeptides are widely applied as laboratory reagents or therapeutics for many different diseases. However, the instability of proteins during storage or transport increases costs and reduces effectiveness of protein drugs. Maynard group recently reported a series of studies of stabilization of proteins towards heat, acidic, and lyophilization stresses by conjugating proteins on RAFT polymerized trehalose containing glycopolymers.[55, 59, 97, 231] They proposed several mechanisms for protein stabilization by glycopolymers including: vitrification, water replacement, water entrapment, and non-ionic surfactant effect.[55, 59] Among them, the non-ionic surfactant effect may play a significant important role on protein stabilization, as the non-ionic surfactants are known as excipients and are proposed to stabilize proteins by preventing proteins from adsorbing onto hydrophobic surfaces and directly interacting with hydrophobic residues of proteins.

2.3.2. Glycopolymers for Environmental Applications

Membrane filtration techniques, such as microfiltration, ultrafiltration, nanofiltration, and reverse osmosis, have been extensively used in water treatment. However, the natural disadvantages of common membrane materials are hydrophobic, which always associate with (bio)fouling during the operation and, therefore, shortening the materials service life. One of the popular strategies for solving this problem is modifying the membrane surfaces with hydrophilic polymers, such as zwitterionic polymers[145] or hydrophilic polymers

bearing abundant hydroxyl groups.[232] Glycopolymers, which carry multiple hydroxyls containing carbohydrate as the pendent groups, are also considered as a good candidate for modifying membrane surface's hydrophilicity and generate a non-fouling surface. For example, Wei *et al.* applied photo-induced graft polymerization of a glucose containing glycomonomer to a polypropylene microporous membrane to meet such requirement.[233] The surface modification was characterized by Fourier transform infrared spectroscopy and X-ray photoelectron spectroscopy. Water contact angle on the modified membrane decreased with the increase of the grafting chain length, and showed a minimum value of 43.2 degree, approximately 51.8 degree lower than that of the pristine membrane. The pure water fluxes for the modified membranes increased systematically with the increase of the grafting chain length. After continuous operation in the membrane for about 70 h, the glycopolymer modified membranes showed 9.97% lower reduction on pure water flux with 15.23% lower flux recovery after water cleaning as compared to those for the unmodified membranes. The excellent antifouling properties on the glycopolymer modified membrane surface can be explained by a highly hydrated polymer layer grafted on the membranes surface prevented foulants from contacting membrane surface directly. The foulants deposited on the glycopolymer layer could be removed easily by water washing due to the reversible fouling characteristics.

Recently, glycopolymers modified polysulfone membrane for boron removal was reported by Zhang and coworkers.[234] By applying surface initiated ATRP, the polysulfone membrane was first modified by poly(glycidyl methacrylate), followed by epoxy ring-opening reaction with N-methyl-d-glucamine. The resulted membrane showed more hydrophilic surfaces, more open porous structures, higher permeation flux and better anti-

fouling properties as compared to the polysulfone pristine membrane. Moreover, the glycopolymer modified membrane showed boron uptake of 0.193 mmol/g within half an hour of contact in 300 mg/L boron solution.

A low dose of the waterborne pathogen can be infectious and cause illness in host. Although most of them can be removed from water by filtration, their interaction with filter media as well as desorption during backwash process are largely unknown. Studying of pathogen adsorption/desorption coefficiency on filter media by directly using live pathogens at bench or pilot scales may cause risks to public health. To address this issue, glycoprotein modified microspheres are usually employed as pathogen surrogates.[235, 236] However, glycoprotein is expensive and instable during storage and transportation. Synthetic glycopolymers, on the other hand, are cheap and can be used as an alternative strategy for surface modification of microspheres to get the pathogen surrogates. Although, so far, there has no report on using glycopolymer modified microspheres as pathogen surrogates, therefore these types of materials possess great research potentials in environmental engineering area.

2.4.Conclusions and Future Perspectives

In this chapter, the history and recent studies on the synthesis of glycopolymers and their applications in biomedical and environmental engineering have been reviewed and summarized. Although the synthetic glycopolymers have achieved great success in terms of well control over molecular weight, structures, and carbohydrate sequence, huge efforts are still required for the development of more sophisticated techniques on glycopolymers synthesis. This is because glycopolymers synthesized by reversible-deactivation radical

polymerization are non-degradable, which may lead side effects if they are planned for long-term in vivo applications, while the biodegradable glycopolypeptides obtained by ring opening polymerization are always subject to the low yield and hard to purify.

The application of synthetic glycopolymers in cellular signal transduction and protein/cell stabilization has emerged as a relatively new area in glycobiology. However, the detailed mechanisms behind such applications are largely unclear. Most of the time, glycopolymers are only tested in vitro to study their potential applications as nanomedicines, in vivo studies of such materials for biomedical applications, such as gene and drug delivery, are remain challenges, because the carbohydrates on polymer pendant groups can also interact with plasma proteins during blood circulating. Reports on the applications of glycopolymers in environmental engineering are very limited, and most of them only emphasized on using their hydrophilic natures to enhance the membranes' anti-fouling properties. More complex glycopolymers based materials that involve in carbohydrate-protein interactions should be designed for environmental applications.

2.5.References

1. L. L. Kiessling, J. E. Gestwicki and L. E. Strong, *Curr. Opin. Chem. Biol.* , 2000, **4**, 696-703.

2. A. E. Smith and A. Helenius, *Science*, 2004, **304**, 237-242.

3. Uffe Holmskov, Steffen Thiel and J. C. Jensenius, *Annu. Rev. Immunol.*, 2003, **21**, 547-578.

4. E. Töpfer-Petersen, *Hum. Reprod. Update*, 1999, **5**, 314-329.

5. K. Ohtsubo and J. D. Marth, *Cell*, 2006, **126**, 855-867.

6. D. R. Bundle and N. M. Young, *Curr. Opin. Struct. Biol.* , 1992, **2**, 666-673.

7. Y. C. Lee and R. T. Lee, *Acc. Chem. Res.* 1995, **28**, 321-327.

8. B. Blanchard, A. Nurisso, E. Hollville, C. Tétaud, J. Wiels, M. Pokorná, M. Wimmerová, A. Varrot and A. Imberty, *J. Mol. Biol.* , 2008, **383**, 837-853.

9. M. Meier, M. D. Bider, V. N. Malashkevich, M. Spiess and P. Burkhard, *J. Mol. Biol.* , 2000, **300**, 857-865.

10. C. R. Bertozzi, Kiessling and L. L., *Science*, 2001, **291**, 2357-2364.

11. C. W. Cairo, J. E. Gestwicki, M. Kanai and L. L. Kiessling, *J. Am. Chem. Soc.* 2002, **124**, 1615-1619.

12. J. E. Gestwicki, C. W. Cairo, L. E. Strong, K. A. Oetjen and L. L. Kiessling, *J. Am. Chem. Soc.* 2002, **124**, 14922-14933.

13. S. M. Dimick, S. C. Powell, S. A. McMahon, D. N. Moothoo, J. H. Naismith and E. J. Toone, *J. Am. Chem. Soc.* 1999, **121**, 10286-10296.

14. J. J. Lundquist and E. J. Toone, *Chem. Rev.* 2002, **102**, 555-578.

15. M. Mammen, S.-K. Choi and G. M. Whitesides, *Angew. Chem. Int. Ed.* 1998, **37**, 2754-2794.

16. W. Roy L, in *Carbohydrates in Solution*, AMERICAN CHEMICAL SOCIETY, 1973, vol. 117, pp. 242-255.

17. P. L. Nichols and E. Yanovsky, *J. Am. Chem. Soc.* 1944, **66**, 1625-1627.

18. R. H. Treadway and E. Yanovsky, *J. Am. Chem. Soc.* 1945, **67**, 1038-1039.

19. S.-K. Choi, M. Mammen and G. M. Whitesides, *J. Am. Chem. Soc.* 1997, **119**, 4103-4111.

20. E. J. Gordon, L. E. Strong and L. L. Kiessling, *Bioorganic & Medicinal Chemistry*, 1998, **6**, 1293-1299.

21. R. Roy, *Curr. Opin. Struct. Biol.* , 1996, **6**, 692-702.

22. K. Matsuoka and S.-I. Nishimura, *Macromolecules*, 1995, **28**, 2961-2968.

23. G. Descotes, J. Ramza, J.-M. Basset and S. Pagano, *Tetrahedron Lett.* , 1994, **35**, 7379-7382.

24. M. Minoda, K. Yamaoka, K. Yamada, A. Takaragi and T. Miyamoto, *Macromolecular Symposia*, 1995, **99**, 169-177.

25. K. Yamada, K. Yamaoka, M. Minoda and T. Miyamoto, *J. Polym. Sci., Part A: Polym. Chem.* 1997, **35**, 255-261.

26. S. Loykulnant, M. Hayashi and A. Hirao, *Macromolecules*, 1998, **31**, 9121-9126.

27. C. Fraser and R. H. Grubbs, *Macromolecules*, 1995, **28**, 7248-7255.

28. K. H. Mortell, M. Gingras and L. L. Kiessling, *J. Am. Chem. Soc.* 1994, **116**, 12053-12054.

29. M. Kato, M. Kamigaito, M. Sawamoto and T. Higashimura, *Macromolecules*, 1995, **28**, 1721-1723.

30. J.-S. Wang and K. Matyjaszewski, *J. Am. Chem. Soc.* 1995, **117**, 5614-5615.

31. J. Chiefari, Y. K. Chong, F. Ercole, J. Krstina, J. Jeffery, T. P. T. Le, R. T. A. Mayadunne, G. F. Meijs, C. L. Moad, G. Moad, E. Rizzardo and S. H. Thang, *Macromolecules*, 1998, **31**, 5559-5562.

32. H. C. Kolb, M. G. Finn and K. B. Sharpless, *Angew. Chem. Int. Ed.* 2001, **40**, 2004-2021.

33. F. Pérez-Balderas, M. Ortega-Muñoz, J. Morales-Sanfrutos, F. Hernández-Mateo, F. G. Calvo-Flores, J. A. Calvo-Asín, J. Isac-García and F. Santoyo-González, *Org. Lett.* 2003, **5**, 1951-1954.

34. M. Buback, A. Feldermann, C. Barner-Kowollik and I. Lacík, *Macromolecules*, 2001, **34**, 5439-5448.

35. G. Odian, *Principle of Polymerization*, 4th edn., Wiley, New York, 2004.

36. C. A. G. N. Montalbetti and V. Falque, *Tetrahedron*, 2005, **61**, 10827-10852.

37. S.-J. Richards, M. W. Jones, M. Hunaban, D. M. Haddleton and M. I. Gibson, *Angew. Chem. Int. Ed.* 2012, **51**, 7812-7816.

38. M. Ejaz, K. Ohno, Y. Tsujii and T. Fukuda, *Macromolecules*, 2000, **33**, 2870-2874.

39. Y.-Z. Liang, Z.-C. Li, G.-Q. Chen and F.-M. Li, *Polym. Int.* 1999, **48**, 739-742.

40. Z.-C. Li, Y.-Z. Liang and F.-M. Li, *Chem. Commun.* 1999, 1557-1558.

41. J.-Q. Meng, F.-S. Du, Y.-S. Liu and Z.-C. Li, *J. Polym. Sci., Part A: Polym. Chem.* 2005, **43**, 752-762.

42. C.-M. Dong, X.-L. Sun, K. M. Faucher, R. P. Apkarian and E. L. Chaikof, *Biomacromolecules*, 2004, **5**, 224-231.

43. V. Ladmiral, L. Monaghan, G. Mantovani and D. M. Haddleton, *Polymer* 2005, **46**, 8536-8545.

44. L.-C. You, F.-Z. Lu, Z.-C. Li, W. Zhang and F.-M. Li, *Macromolecules*, 2003, **36**, 1-4.

45. S. Muthukrishnan, D. P. Erhard, H. Mori and A. H. E. Müller, *Macromolecules*, 2006, **39**, 2743-2750.

46. S. Muthukrishnan, G. Jutz, X. André, H. Mori and A. H. E. Müller, *Macromolecules*, 2005, **38**, 9-18.

47. S. Muthukrishnan, H. Mori and A. H. E. Müller, *Macromolecules*, 2005, **38**, 3108-3119.

48. Y.-M. Chen and G. Wulff, *Macromol. Rapid Commun.* 2002, **23**, 59-63.

49. R. Narain and S. P. Armes, *Chem. Commun.* 2002, 2776-2777.

50. R. Narain and S. P. Armes, *Biomacromolecules*, 2003, **4**, 1746-1758.

51. R. Narain and S. P. Armes, *Macromolecules*, 2003, **36**, 4675-4678.

52. R. M. Broyer, G. M. Quaker and H. D. Maynard, *J. Am. Chem. Soc.* 2008, **130**, 1041-1047.

53. Y. Pan, C. Ma, W. Tong, C. Fan, Q. Zhang, W. Zhang, F. Tian, B. Peng, W. Qin and X. Qian, *Anal. Chem.* 2015, **87**, 656-662.

54. J. Lazar, H. Park, R. R. Rosencrantz, A. Böker, L. Elling and U. Schnakenberg, *Macromol. Rapid Commun.* 2015, **36**, 1472-1478.

55. J. Lee, E.-W. Lin, U. Y. Lau, J. L. Hedrick, E. Bat and H. D. Maynard, *Biomacromolecules*, 2013, **14**, 2561-2569.

56. S. S. Gupta, K. S. Raja, E. Kaltgrad, E. Strable and M. G. Finn, *Chem. Commun.* 2005, 4315-4317.

57. S. Slavin, J. Burns, D. M. Haddleton and C. R. Becer, *Eur. Polym. J.* 2011, **47**, 435-446.

58. K. L. Heredia and H. D. Maynard, *Org. Biomol. Chem.* 2007, **5**, 45-53.

59. R. J. Mancini, J. Lee and H. D. Maynard, *J. Am. Chem. Soc.* 2012, **134**, 8474-8479.

60. V. Vázquez-Dorbatt and H. D. Maynard, *Biomacromolecules*, 2006, **7**, 2297-2302.

61. N. V. Tsarevsky, T. Pintauer and K. Matyjaszewski, *Macromolecules*, 2004, **37**, 9768-9778.

62. K. Matyjaszewski, W. Jakubowski, K. Min, W. Tang, J. Huang, W. A. Braunecker and N. V. Tsarevsky, *Proc. Natl. Acad. Sci.* 2006, **103**, 15309-15314.

63. W. Jakubowski and K. Matyjaszewski, *Angew. Chem. Int. Ed.* 2006, **45**, 4482-4486.

64. W. Jakubowski, K. Min and K. Matyjaszewski, *Macromolecules*, 2006, **39**, 39-45.

65. V. Sciannamea, R. Jérôme and C. Detrembleur, *Chem. Rev.* 2008, **108**, 1104-1126.

66. M. R. Hill, R. N. Carmean and B. S. Sumerlin, *Macromolecules*, 2015, **48**, 5459-5469.

67. M. Semsarilar and S. Perrier, *Nat. Chem.* 2010, **2**, 811-820.

68. J. Chiefari, R. T. A. Mayadunne, C. L. Moad, G. Moad, E. Rizzardo, A. Postma and S. H. Thang, *Macromolecules*, 2003, **36**, 2273-2283.

69. S. J. Stace, G. Moad, C. M. Fellows and D. J. Keddie, *Polym. Chem.* 2015, **6**, 7119-7126.

70. Y. K. Chong, J. Krstina, T. P. T. Le, G. Moad, A. Postma, E. Rizzardo and S. H. Thang, *Macromolecules*, 2003, **36**, 2256-2272.

71. C. L. McCormick and A. B. Lowe, *Acc. Chem. Res.* 2004, **37**, 312-325.

72. D. B. Thomas, A. J. Convertine, R. D. Hester, A. B. Lowe and C. L. McCormick, *Macromolecules*, 2004, **37**, 1735-1741.

73. A. B. Lowe and C. L. McCormick, *Prog. Polym. Sci.* 2007, **32**, 283-351.

74. X.-L. Sun, W.-D. He, J. Li, L.-Y. Li, B.-Y. Zhang and T.-T. Pan, *J. Polym. Sci., Part A: Polym. Chem.* 2009, **47**, 6863-6872.

75. X.-L. Sun, W.-D. He, T.-T. Pan, Z.-L. Ding and Y.-J. Zhang, *Polymer* 2010, **51**, 110-114.

76. Y. K. Chong, T. P. T. Le, G. Moad, E. Rizzardo and S. H. Thang, *Macromolecules*, 1999, **32**, 2071-2074.

77. Y. Mitsukami, M. S. Donovan, A. B. Lowe and C. L. McCormick, *Macromolecules*, 2001, **34**, 2248-2256.

78. Y. Li, B. S. Lokitz and C. L. McCormick, *Macromolecules*, 2006, **39**, 81-89.

79. Y. Li, B. S. Lokitz, S. P. Armes and C. L. McCormick, *Macromolecules*, 2006, **39**, 2726-2728.

80. A. B. Lowe, B. S. Sumerlin, M. S. Donovan and C. L. McCormick, *J. Am. Chem. Soc.* 2002, **124**, 11562-11563.

81. A. J. Convertine, B. S. Lokitz, Y. Vasileva, L. J. Myrick, C. W. Scales, A. B. Lowe and C. L. McCormick, *Macromolecules*, 2006, **39**, 1724-1730.

82. V. Ladmiral, M. Semsarilar, I. Canton and S. P. Armes, *J. Am. Chem. Soc.* 2013, **135**, 13574-13581.

83. X. Li and G. Chen, *Polym. Chem.* 2015, **6**, 1417-1430.

84. Y. Kotsuchibashi, M. Ebara, A. S. Hoffman, R. Narain and T. Aoyagi, *Polym. Chem.* 2015, **6**, 1693-1697.

85. Q. Zhang, P. Wilson, A. Anastasaki, R. McHale and D. M. Haddleton, *ACS Macro Letters* 2014, **3**, 491-495.

86. W. T. Liau, C. Bonduelle, M. Brochet, S. Lecommandoux and A. M. Kasko, *Biomacromolecules*, 2015, **16**, 284-294.

87. M. Ahmed and R. Narain, *Biomaterials* 2013, **34**, 4368-4376.

88. M. Ahmed, M. Jawanda, K. Ishihara and R. Narain, *Biomaterials* 2012, **33**, 7858-7870.

89. M. Ahmed and R. Narain, *Biomaterials* 2011, **32**, 5279-5290.

90. M. Ahmed and R. Narain, *Biomaterials* 2012, **33**, 3990-4001.

91. M. Ahmed, B. F. L. Lai, J. N. Kizhakkedathu and R. Narain, *Bioconjugate Chem.* 2012, **23**, 1050-1058.

92. R. Narain, Y. Wang, M. Ahmed, B. F. L. Lai and J. N. Kizhakkedathu, *Biomacromolecules*, 2015, **16**, 2990-2997.

93. S. Quan, Y. Wang, A. Zhou, P. Kumar and R. Narain, *Biomacromolecules*, 2015, **16**, 1978-1986.

94. M. Ahmed, P. Wattanaarsakit and R. Narain, *Polym. Chem.* 2013, **4**, 3829-3836.

95. Y. Kotsuchibashi, R. V. C. Agustin, J.-Y. Lu, D. G. Hall and R. Narain, *ACS Macro Letters* 2013, **2**, 260-264.

96. M. Ahmed and R. Narain, *Mol. Pharm.* 2012, **9**, 3160-3170.

97. E. Bat, J. Lee, U. Y. Lau and H. D. Maynard, *Nat. Commun.* 2015, **6**.

98. J. Lu, W. Zhang, L. Yuan, W. Ma, X. Li, W. Lu, Y. Zhao and G. Chen, Macromol. Biosci. 2014, **14**, 340-346.

99. R. Narain, A. Housni, G. Gody, P. Boullanger, M.-T. Charreyre and T. Delair, *Langmuir* 2007, **23**, 12835-12841.

100. S. G. Spain, L. Albertin and N. R. Cameron, *Chem. Commun.* 2006, 4198-4200.

101. E. Rüde, O. Westphal, E. Hurwitz, S. Fuchs and M. Sela, *Immunochemistry*, 1966, **3**, 137-151.

102. M. I. Gibson, G. J. Hunt and N. R. Cameron, *Org. Biomol. Chem.* 2007, **5**, 2756-2757.

103. J. R. Kramer and T. J. Deming, *J. Am. Chem. Soc.* 2010, **132**, 15068-15071.

104. J. R. Kramer and T. J. Deming, *Biomacromolecules*, 2010, **11**, 3668-3672.

105. J. R. Kramer, A. R. Rodriguez, U.-J. Choe, D. T. Kamei and T. J. Deming, *Soft Matter* 2013, **9**, 3389-3395.

106. J. R. Kramer and T. J. Deming, *J. Am. Chem. Soc.* 2012, **134**, 4112-4115.

107. J. R. Kramer and T. J. Deming, *J. Am. Chem. Soc.* 2014, **136**, 5547-5550.

108. K.-S. Krannig, A. Doriti and H. Schlaad, *Macromolecules*, 2014, **47**, 2536-2539.

109. Q. Zhang, A. Anastasaki, G.-Z. Li, A. J. Haddleton, P. Wilson and D. M. Haddleton, *Polym. Chem.* 2014, **5**, 3876-3883.

110. J. E. Moses and A. D. Moorhouse, *Chem. Soc. Rev.* 2007, **36**, 1249-1262.

111. R. K. Iha, K. L. Wooley, A. M. Nyström, D. J. Burke, M. J. Kade and C. J. Hawker, *Chem. Rev.* 2009, **109**, 5620-5686.

112. S. Hotha and S. Kashyap, *J. Org. Chem.* 2006, **71**, 364-367.

113. C. R. Becer, *Macromol. Rapid Commun.* 2012, **33**, 742-752.

114. Y. Miura, Y. Hoshino and H. Seto, *Chem. Rev.* 2015.

115. V. Ladmiral, G. Mantovani, G. J. Clarkson, S. Cauet, J. L. Irwin and D. M. Haddleton, *J. Am. Chem. Soc.* 2006, **128**, 4823-4830.

116. G. Chen, L. Tao, G. Mantovani, J. Geng, D. Nyström and D. M. Haddleton, *Macromolecules*, 2007, **40**, 7513-7520.

117. C. R. Becer, M. I. Gibson, J. Geng, R. Ilyas, R. Wallis, D. A. Mitchell and D. M. Haddleton, *J. Am. Chem. Soc.* 2010, **132**, 15130-15132.

118. A. Anastasaki, V. Nikolaou, G. Nurumbetov, P. Wilson, K. Kempe, J. F. Quinn, T. P. Davis, M. R. Whittaker and D. M. Haddleton, *Chem. Rev.* 2015.

119. M. W. Jones, L. Otten, S. J. Richards, R. Lowery, D. J. Phillips, D. M. Haddleton and M. I. Gibson, *Chemical Science*, 2014, **5**, 1611-1616.

120. C. R. Becer, K. Babiuch, D. Pilz, S. Hornig, T. Heinze, M. Gottschaldt and U. S. Schubert, *Macromolecules*, 2009, **42**, 2387-2394.

121. J. M. Baskin, J. A. Prescher, S. T. Laughlin, N. J. Agard, P. V. Chang, I. A. Miller, A. Lo, J. A. Codelli and C. R. Bertozzi, *Proc. Natl. Acad. Sci.* 2007, **104**, 16793-16797.

122. J. A. Codelli, J. M. Baskin, N. J. Agard and C. R. Bertozzi, *J. Am. Chem. Soc.* 2008, **130**, 11486-11493.

123. E. M. Sletten and C. R. Bertozzi, *Org. Lett.* 2008, **10**, 3097-3099.

124. K. Godula, M. L. Umbel, D. Rabuka, Z. Botyanszki, C. R. Bertozzi and R. Parthasarathy, *J. Am. Chem. Soc.* 2009, **131**, 10263-10268.

125. K. Godula and C. R. Bertozzi, *J. Am. Chem. Soc.* 2010, **132**, 9963-9965.

126. K. Godula and C. R. Bertozzi, *J. Am. Chem. Soc.* 2012, **134**, 15732-15742.

127. M. J. Paszek, C. C. DuFort, O. Rossier, R. Bainer, J. K. Mouw, K. Godula, J. E. Hudak, J. N. Lakins, A. C. Wijekoon, L. Cassereau, M. G. Rubashkin, M. J. Magbanua, K. S. Thorn, M. W. Davidson, H. S. Rugo, J. W. Park, D. A. Hammer, G. Giannone, C. R. Bertozzi and V. M. Weaver, *Nature*, 2014, **advance online publication**.

128. J. M. Gargano, T. Ngo, J. Y. Kim, D. W. K. Acheson and W. J. Lees, *J. Am. Chem. Soc.* 2001, **123**, 12909-12910.

129. B. D. Polizzotti and K. L. Kiick, *Biomacromolecules*, 2005, **7**, 483-490.

130. K. Lin and A. M. Kasko, *Biomacromolecules*, 2012, **14**, 350-357.

131. A. Spaltenstein and G. M. Whitesides, *J. Am. Chem. Soc.* 1991, **113**, 686-687.

132. R. Roy, F. O. Andersson, G. Harms, S. Kelm and R. Schauer, *Angewandte Chemie International Edition in English*, 1992, **31**, 1478-1481.

133. M. Ogata, K. I. P. J. Hidari, W. Kozaki, T. Murata, J. Hiratake, E. Y. Park, T. Suzuki and T. Usui, *Biomacromolecules*, 2009, **10**, 1894-1903.

134. T. Tanaka, H. Ishitani, Y. Miura, K. Oishi, T. Takahashi, T. Suzuki, S.-i. Shoda and Y. Kimura, *ACS Macro Letters* 2014, **3**, 1074-1078.

135. T. B. H. Geijtenbeek, D. S. Kwon, R. Torensma, S. J. van Vliet, G. C. F. van Duijnhoven, J. Middel, I. L. M. H. A. Cornelissen, H. S. L. M. Nottet, V. N. KewalRamani, D. R. Littman, C. G. Figdor and Y. van Kooyk, *Cell*, 2000, **100**, 587-597.

136. C. P. Alvarez, F. Lasala, J. Carrillo, O. Muñiz, A. L. Corbí and R. Delgado, *Journal of Virology*, 2002, **76**, 6841-6844.

137. I. S. Ludwig, A. N. Lekkerkerker, E. Depla, F. Bosman, R. J. P. Musters, S. Depraetere, Y. van Kooyk and T. B. H. Geijtenbeek, *Journal of Virology*, 2004, **78**, 8322-8332.

138. N. Varga, I. Sutkeviciute, R. Ribeiro-Viana, A. Berzi, R. Ramdasi, A. Daghetti, G. Vettoretti, A. Amara, M. Clerici, J. Rojo, F. Fieschi and A. Bernardi, *Biomaterials* 2014, **35**, 4175-4184.

139. X. Wu, L. Su, G. Chen and M. Jiang, *Macromolecules*, 2015, **48**, 3705-3712.

140. D. Appelhans, B. Klajnert-Maculewicz, A. Janaszewska, J. Lazniewska and B. Voit, *Chem. Soc. Rev.* 2015, **44**, 3968-3996.

141. Q. Zhang, J. Collins, A. Anastasaki, R. Wallis, D. A. Mitchell, C. R. Becer and D. M. Haddleton, *Angew. Chem. Int. Ed.* 2013, **52**, 4435-4439.

142. P. Thevenot, W. Hu and L. Tang, *Curr. Top. Med. Chem.* , 2008, **8**, 270-280.

143. C. Leng, H.-C. Hung, S. Sun, D. Wang, Y. Li, S. Jiang and Z. Chen, *ACS Appl. Mat. Interfaces* 2015, **7**, 16881-16888.

144. S. Chen, L. Li, C. Zhao and J. Zheng, *Polymer* 2010, **51**, 5283-5293.

145. G. Cheng, Z. Zhang, S. Chen, J. D. Bryers and S. Jiang, *Biomaterials* 2007, **28**, 4192-4199.

146. M. Ukawa, H. Akita, T. Masuda, Y. Hayashi, T. Konno, K. Ishihara and H. Harashima, *Biomaterials* 2010, **31**, 6355-6362.

147. N. Saito, Y. Usui, K. Aoki, N. Narita, M. Shimizu, K. Hara, N. Ogiwara, K. Nakamura, N. Ishigaki, H. Kato, S. Taruta and M. Endo, *Chem. Soc. Rev.* 2009, **38**, 1897-1903.

148. B. C. Thompson, E. Murray and G. G. Wallace, *Adv. Mater.* 2015, n/a-n/a.

149. G. Jia, H. Wang, L. Yan, X. Wang, R. Pei, T. Yan, Y. Zhao and X. Guo, *Environ. Sci. Technol.* 2005, **39**, 1378-1383.

150. A. Magrez, S. Kasas, V. Salicio, N. Pasquier, J. W. Seo, M. Celio, S. Catsicas, B. Schwaller and L. Forró, *Nano Lett.* 2006, **6**, 1121-1125.

151. Y. Chen, A. Star and S. Vidal, *Chem. Soc. Rev.* 2013, **42**, 4532-4542.

152. X. Chen, U. C. Tam, J. L. Czlapinski, G. S. Lee, D. Rabuka, A. Zettl and C. R. Bertozzi, *J. Am. Chem. Soc.* 2006, **128**, 6292-6293.

153. P. Wu, X. Chen, N. Hu, U. C. Tam, O. Blixt, A. Zettl and C. R. Bertozzi, *Angew. Chem., Int. Ed.* 2008, **47**, 5022-5025.

154. K. Yu, B. F. L. Lai and J. N. Kizhakkedathu, *Advanced Healthcare Materials*, 2012, **1**, 199-213.

155. R. A. Worthylake and K. Burridge, *Curr. Opin. Cell Biol.* , 2001, **13**, 569-577.

156. S. D. Rosen, *The American Journal of Pathology*, 1999, **155**, 1013-1020.

157. S. D. Rosen, *Annu. Rev. Immunol.*, 2004, **22**, 129-156.

158. P. Mowery, Z.-Q. Yang, E. J. Gordon, O. Dwir, A. G. Spencer, R. Alon and L. L. Kiessling, *Chemistry & Biology*, 2004, **11**, 725-732.

159. A. H. Courtney, N. R. Bennett, D. B. Zwick, J. Hudon and L. L. Kiessling, *ACS Chem. Biol.* , 2014, **9**, 202-210.

160. J. R. Kramer, B. Onoa, C. Bustamante and C. R. Bertozzi, *Proc. Natl. Acad. Sci.* 2015, **112**, 12574-12579.

161. M. Malmqvist, *Nature*, 1993, **361**, 186-187.

162. I. H. El-Sayed, X. Huang and M. A. El-Sayed, *Nano Lett.* 2005, **5**, 829-834.

163. X. Liu, Q. Zhang, Y. Tu, W. Zhao and H. Gai, *Anal. Chem.* 2013, **85**, 11851-11857.

164. Y. Zhang, S. Luo, Y. Tang, L. Yu, K.-Y. Hou, J.-P. Cheng, X. Zeng and P. G. Wang, *Anal. Chem.* 2006, **78**, 2001-2008.

165. M. Mayer and B. Meyer, *J. Am. Chem. Soc.* 2001, **123**, 6108-6117.

166. R. Kuhn, R. Frei and M. Christen, *Anal. Biochem.* 1994, **218**, 131-135.

167. Y. C. Lee, *J. Biochem. (Tokyo, Jpn.)*, 1997, **121**, 818-825.

168. T. V. Ratto, K. C. Langry, R. E. Rudd, R. L. Balhorn, M. J. Allen and M. W. McElfresh, *Biophys. J.*, 2004, **86**, 2430-2437.

169. X. Zeng, C. S. Andrade, M. L. Oliveira and X.-L. Sun, *Anal. BioAnal. Chem.* 2012, **402**, 3161-3176.

170. S. Slavin, A. H. Soeriyadi, L. Voorhaar, M. R. Whittaker, C. R. Becer, C. Boyer, T. P. Davis and D. M. Haddleton, *Soft Matter* 2012, **8**, 118-128.

171. Y. Chen, H. Vedala, G. P. Kotchey, A. Audfray, S. Cecioni, A. Imberty, S. Vidal and A. Star, *ACS Nano* 2011, **6**, 760-770.

172. X. Jiang, M. Ahmed, Z. Deng and R. Narain, *Bioconjugate Chem.* 2009, **20**, 994-1001.

173. H. Uzawa, H. Ito, P. Neri, H. Mori and Y. Nishida, *ChemBioChem*, 2007, **8**, 2117-2124.

174. T. Nagatsuka, H. Uzawa, K. Sato, S. Kondo, M. Izumi, K. Yokoyama, I. Ohsawa, Y. Seto, P. Neri, H. Mori, Y. Nishida, M. Saito and E. Tamiya, *ACS Appl. Mater. Interfaces* 2013, **5**, 4173-4180.

175. H. Uzawa, S. Kamiya, N. Minoura, H. Dohi, Y. Nishida, K. Taguchi, S.-i. Yokoyama, H. Mori, T. Shimizu and K. Kobayashi, *Biomacromolecules*, 2002, **3**, 411-414.

176. C. L. Schofield, R. A. Field and D. A. Russell, *Anal. Chem.* 2007, **79**, 1356-1361.

177. M. J. Marin, A. Rashid, M. Rejzek, S. A. Fairhurst, S. A. Wharton, S. R. Martin, J. W. McCauley, T. Wileman, R. A. Field and D. A. Russell, *Org. Biomol. Chem.*, 2013, **11**, 7101-7107.

178. Z. Shen, M. Huang, C. Xiao, Y. Zhang, X. Zeng and P. G. Wang, *Anal. Chem.* 2007, **79**, 2312-2319.

179. Y. Wang, R. Narain and Y. Liu, *Langmuir* 2014, **30**, 7377-7387.

180. Y. Wang, Y. Kotsuchibashi, Y. Liu and R. Narain, *ACS Appl. Mat. Interfaces* 2015, **7**, 1652-1661.

181. A. Mader, K. Gruber, R. Castelli, B. A. Hermann, P. H. Seeberger, J. O. Rädler and M. Leisner, *Nano Lett.* 2011, **12**, 420-423.

182. X. Gao, Y. Cui, R. M. Levenson, L. W. K. Chung and S. Nie, *Nat. Biotech.* 2004, **22**, 969-976.

183. R. Kikkeri, B. Lepenies, A. Adibekian, P. Laurino and P. H. Seeberger, *J. Am. Chem. Soc.* 2009, **131**, 2110-2112.

184. C.-T. Chen, Y. S. Munot, S. B. Salunke, Y.-C. Wang, R.-K. Lin, C.-C. Lin, C.-C. Chen and Y. H. Liu, *Adv. Funct. Mater.*, 2008, **18**, 527-540.

185. L. Yang, X.-H. Peng, Y. A. Wang, X. Wang, Z. Cao, C. Ni, P. Karna, X. Zhang, W. C. Wood, X. Gao, S. Nie and H. Mao, *Clinical Cancer Research*, 2009, **15**, 4722-4732.

186. S. I. van Kasteren, S. J. Campbell, S. Serres, D. C. Anthony, N. R. Sibson and B. G. Davis, *Proceedings of the National Academy of Sciences*, 2009, **106**, 18-23.

187. M. K. Yu, Y. Y. Jeong, J. Park, S. Park, J. W. Kim, J. J. Min, K. Kim and S. Jon, *Angew. Chem., Int. Ed.* 2008, **47**, 5362-5365.

188. M. Kamat, K. El-Boubbou, D. C. Zhu, T. Lansdell, X. Lu, W. Li and X. Huang, *Bioconjugate Chem.* 2010, **21**, 2128-2135.

189. H. Hyun, K. Lee, K. H. Min, P. Jeon, K. Kim, S. Y. Jeong, I. C. Kwon, T. G. Park and M. Lee, *J. Controlled Release*, 2013, **170**, 352-357.

190. K. Y. Choi, K. H. Min, H. Y. Yoon, K. Kim, J. H. Park, I. C. Kwon, K. Choi and S. Y. Jeong, *Biomaterials* 2011, **32**, 1880-1889.

191. K. S. Kim, W. Hur, S.-J. Park, S. W. Hong, J. E. Choi, E. J. Goh, S. K. Yoon and S. K. Hahn, *ACS Nano* 2010, **4**, 3005-3014.

192. S. Mura, J. Nicolas and P. Couvreur, *Nat. Mater.* , 2013, **12**, 991-1003.

193. K. Cho, X. Wang, S. Nie, Z. Chen and D. M. Shin, *Clin. Cancer Res.*, 2008, **14**, 1310-1316.

194. Y. Wang, X. Zhang, P. Yu and C. Li, *Int. J. Pharm.* , 2013, **441**, 170-180.

195. Y. Kotsuchibashi, M. Ebara, N. Idota, R. Narain and T. Aoyagi, *Polym. Chem.* 2012, **3**, 1150-1157.

196. G. Chen, S. Amajjahe and M. H. Stenzel, *Chem. Commun.* 2009, 1198-1200.

197. L. Liu, J. Zhang, W. Lv, Y. Luo and X. Wang, *J. Polym. Sci., Part A: Polym. Chem.* 2010, **48**, 3350-3361.

198. M. Mahkam, *Drug Delivery*, 2007, **14**, 147-153.

199. S. Vandewalle, S. Wallyn, S. Chattopadhyay, C. R. Becer and F. Du Prez, *Eur. Polym. J.* 2015, **69**, 490-498.

200. I. F. Tannock and D. Rotin, *Cancer Res.*, 1989, **49**, 4373-4384.

201. A. Acharya, I. Das, D. Chandhok and T. Saha, *Oxidative Medicine and Cellular Longevity*, 2010, **3**, 23-34.

202. Q. Guo, Z. Wu, X. Zhang, L. Sun and C. Li, *Soft Matter* 2014, **10**, 911-920.

203. E. Audebeau, E. K. Oikonomou, S. Norvez and I. Iliopoulos, *Polym. Chem.* 2014, **5**, 2273-2281.

204. M. Ahmed, Z. Deng and R. Narain, *ACS Appl. Mater. Interfaces* 2009, **1**, 1980-1987.

205. J.-T. Chen, M. Ahmed, Q. Liu and R. Narain, *Journal of Biomedical Materials Research Part A*, 2012, **100A**, 2342-2347.

206. M. Ahmed, X. Jiang, Z. Deng and R. Narain, *Bioconjugate Chem.* 2009, **20**, 2017-2022.

207. R. Sunasee, P. Wattanaarsakit, M. Ahmed, F. B. Lollmahomed and R. Narain, *Bioconjugate Chem.* 2012, **23**, 1925-1933.

208. L. Xue, N. P. Ingle and T. M. Reineke, *Biomacromolecules*, 2013.

209. A. Sizovs, L. Xue, Z. P. Tolstyka, N. P. Ingle, Y. Wu, M. Cortez and T. M. Reineke, *J. Am. Chem. Soc.* 2013, **135**, 15417-15424.

210. L. Xue, N. P. Ingle and T. M. Reineke, *Biomacromolecules*, 2013, **14**, 3903-3915.

211. K. Anderson, A. Sizovs, M. Cortez, C. Waldron, D. M. Haddleton and T. M. Reineke, *Biomacromolecules*, 2012, **13**, 2229-2239.

212. M. Tranter, Y. Liu, S. He, J. Gulick, X. Ren, J. Robbins, W. K. Jones and T. M. Reineke, *Mol. Ther.* 2012, **20**, 601-608.

213. E.-K. Lim, H.-O. Kim, E. Jang, J. Park, K. Lee, J.-S. Suh, Y.-M. Huh and S. Haam, *Biomaterials* 2011, **32**, 7941-7950.

214. I. Naokazu, E. Mitsuhiro, K. Yohei, N. Ravin and A. Takao, *Science and Technology of Advanced Materials*, 2012, **13**, 064206.

215. Q. Meng, A. Haque, B. Hexig and T. Akaike, *Biomaterials* 2012, **33**, 1414-1427.

216. G. Simone, N. Malara, V. Trunzo, G. Perozziello, P. Neuzil, M. Francardi, L. Roveda, M. Renne, U. Prati, V. Mollace, A. Manz and E. Di Fabrizio, *Small*, 2013, **9**, 2152-2161.

217. G. Simone, N. Malara, V. Trunzo, M. Renne, G. Perozziello, E. Di Fabrizio and A. Manz, *Mol. BioSyst.* 2014, **10**, 258-265.

218. H. Seto, Y. Ogata, T. Murakami, Y. Hoshino and Y. Miura, *ACS Appl. Mater. Interfaces* 2011, **4**, 411-417.

219. A.-F. Che, X.-J. Huang and Z.-K. Xu, *J. Membr. Sci.* 2011, **366**, 272-277.

220. Y.-C. Qian, N. Ren, X.-J. Huang, C. Chen, A.-G. Yu and Z.-K. Xu, *Macromol. Chem. Phys.* 2013, **214**, 1852-1858.

221. X.-Y. Ye, X.-J. Huang and Z.-K. Xu, *Colloids and Surfaces B: Biointerfaces* 2014, **115**, 340-348.

222. Y. Wang, Y. Kotsuchibashi, K. Uto, M. Ebara, T. Aoyagi, Y. Liu and R. Narain, *Biomater. Sci.* 2015, **3**, 152-162.

223. A. Fowler and M. Toner, *Ann. N.Y. Acad. Sci.* 2006, **1066**, 119-135.

224. G. M. Fahy, J. Saur and R. J. Williams, *Cryobiol.* 1990, **27**, 492-510.

225. J. A. Raymond, P. Wilson and A. L. DeVries, *Proc. Natl. Acad. Sci.* 1989, **86**, 881-885.

226. D. Gao and J. K. Critser, *ILAR Journal*, 2000, **41**, 187-196.

227. M. I. Gibson, C. A. Barker, S. G. Spain, L. Albertin and N. R. Cameron, *Biomacromolecules*, 2009, **10**, 328-333.

228. L. Corcilius, G. Santhakumar, R. S. Stone, C. J. Capicciotti, S. Joseph, J. M. Matthews, R. N. Ben and R. J. Payne, *Bioorganic & Medicinal Chemistry*, 2013, **21**, 3569-3581.

229. B. L. Wilkinson, R. S. Stone, C. J. Capicciotti, M. Thaysen-Andersen, J. M. Matthews, N. H. Packer, R. N. Ben and R. J. Payne, *Angew. Chem. Int. Ed.* 2012, **51**, 3606-3610.

230. R. C. Deller, M. Vatish, D. A. Mitchell and M. I. Gibson, *Nat. Commun.* 2014, **5**.

231. E. M. Pelegri-O'Day, E.-W. Lin and H. D. Maynard, *J. Am. Chem. Soc.* 2014, **136**, 14323-14332.

232. W. Yandi, S. Mieszkin, P. Martin-Tanchereau, M. E. Callow, J. A. Callow, L. Tyson, B. Liedberg and T. Ederth, *ACS Appl. Mat. Interfaces* 2014, **6**, 11448-11458.

233. J.-S. Gu, H.-Y. Yu, L. Huang, Z.-Q. Tang, W. Li, J. Zhou, M.-G. Yan and X.-W. Wei, *J. Membr. Sci.* 2009, **326**, 145-152.

234. Q. Shi, J.-Q. Meng, R.-S. Xu, X.-L. Du and Y.-F. Zhang, *J. Membr. Sci.* 2013, **444**, 50-59.

235. X. Dai and R. M. Hozalski, *Environ. Sci. Tech.* 2003, **37**, 1037-1042.

236. L. Pang, U. Nowostawska, L. Weaver, G. Hoffman, A. Karmacharya, A. Skinner and N. Karki, *Environ. Sci. Tech.* 2012, **46**, 11779-11787.

Chapter 3. Study of Bacterial Adhesion on Different Glycopolymer Surfaces by Quartz Crystal Microbalance with Dissipation

The content of this chapter was published in *Langmuir* **2014**, 30, 7377-7387

3.1.Introduction

Bacterial initial adhesion to a solid surface is important because it is the first step in biofilm formation which impacts both industry [1, 2] and public health.[3, 4] Exemplifying the former, formation of biofilms in pipelines causes clogging and corrosion[1] and in watercraft reduces vessel speed, which affects many different forms of life after other marine organisms attach themselves on a biofilm-covered hull surface.[2] Alternatively, key public health issues include bacterial adhesion on biomedical implants, believed to be one of the main factors for biomaterial-centered infections.[3]

Generally, two major bacteria–substratum interactions are widely discussed these years, namely, nonspecific interactions including electrostatic forces and hydrophobic interactions and specific interactions such as carbohydrate–protein interactions.[3, 5, 6] The nonspecific interactions have been widely analyzed in terms of the hydrophobicity and charges of the solid surface,[7-9] the macromolecules on bacteria (e.g., lipopolysaccharide (LPS)),[10] and the effects of solution chemistry (such as pH[11] and ionic strength[12]). In some other studies,[13-15] DLVO theory (the combined effect of van der Waals and double-layer forces) and the extended DLVO (XDLVO) theory were also established in order to qualitatively and quantitatively evaluate the adhesion of bacteria on surfaces. In contrast, the specific bacteria–substratum interactions usually occur between carbohydrates and lectins on the tips of Gram-negative bacterial fimbriae.[5, 16] Different bacterial strains possess different lectins that can specifically interact with various carbohydrates. For example, *Escherichia coli* can bind to mannose on epithelial cells to cause urinary tract infections,[17, 18] while wild-type *Pseudomonas aeruginosa* PAO1 infects the respiratory

tract by using their D-galactose specific PA-IL (lectin A) or L-fructose specific PA-IIL (lectin B).[19]

Although various methods including biochemical tests,[20] microscopy, immunosensing,[21, 22] and quartz crystal microbalance with dissipation (QCM-D)[23-25] have been developed to study the mechanisms of bacterial adhesion, only a few studies have focused on comparing bacterial adhesion on different surfaces in terms of specific and nonspecific interactions.[26, 27] Therefore, the aim in this study was to compare the different interactions during bacterial adhesion to a surface through use of the rapid and highly sensitive QCM-D technique.

Previous studies that have examined the specific carbohydrate–protein interactions in bacterial adhesion by QCM-D showed certain disadvantages, such as the complicated procedures for immobilizing carbohydrates on the QCM-D sensor surface and its weak sensitivity to bacteria–substratum interactions.[24, 28, 29] In this study, gold-coated QCM-D sensor surfaces were easily modified with well-defined glycopolymers (poly(2-lactobionamidoethyl methacrylamide) (PLAEMA)) and cationic polymers (poly(2-aminoethyl methacrylamide hydrochloride (PAEMA))[30, 31] using their dithioester groups at the end of the polymer chains.[32] More importantly, using glycopolymers with multiple carbohydrates on backbones (e.g., PLAEMA) to study carbohydrate–lectin interactions, stronger bacteria–substratum interactions are anticipated to be observed due to the "glycoside cluster effect".[33, 34] To the best of our knowledge, this is the first report of using glycopolymers to study specific bacteria–substratum interactions by the QCM-D technique.

3.2.Materials and Methods

3.2.1. Materials

All chemicals were purchased from Sigma-Aldrich Chemicals (Oakville, ON, Canada), and organic solvents were from Caledon Laboratories Ltd. (Georgetown, ON, Canada). The chain transfer agent, 4-cyanopentanoic acid dithiobenzoate (CTP), and monomers were synthesized as previously described (the monomers NMR spectra are shown in Appendix).[30, 31, 35, 36] The structures are shown in **Scheme 3-1**.

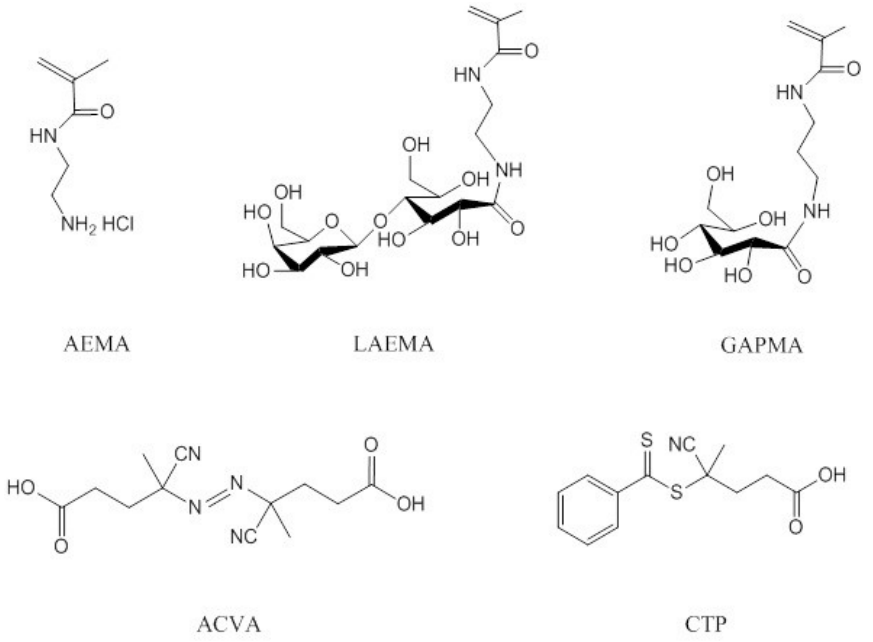

Scheme 3-1. Chemical structures of the monomers, ACVA and CTP.

3.2.2. Methods

^{1}H NMR spectra of the monomers and polymers were recorded on a Varian 500 MHz spectrometer using D_2O as the solvent. The number-average molecular weight (M_n) and polydispersity (M_w/M_n) were determined using Pullulan standards (M_w = 5900–788 000 g mol^{-1}) at room temperature and a Viscotek model 250 dual detector

(refractometer/viscometer in aqueous eluents (0.5 M sodium acetate and 0.5 M acetic acid) with a flow rate of 1.0 mL/min. The interactions of lectin and bacteria with polymers were studied by QCM-D (Q-Sense, Sweden, E4 chamber) on gold-coated sensor chips (frequency, 4.95 MHz 50 kHz; cut, AT; diameter, 14 mm; thickness, 0.3 mm; surface roughness, <3 nm (RMS); electrode layer, 10–300 nm). The bacterial adhesion to the sensor's surface was visualized by fluorescence microscopy (Microscope Axio Imager.M2, Carl Zeiss, Germany) with a wide-field fluorescence microscope excitation light source (X-cite 120Q, Lumen Dynamic, ON, Canada).

3.2.2.1.RAFT Polymerization of LAEMA

RAFT polymerization was chosen to produce the well-defined glycopolymers.[31, 36] For a typical homopolymerization, 2-lactobionamidoethyl methacrylamide (LAEMA) (1 g, 2 mmol) was dissolved in 6 mL of distilled water in a 10 mL Schlenk tube with 1 mL of CTP (16 mg, 0. 057 mmol) and 4,4′-azobis(4-cyanovaleric acid) (ACVA) (8 mg, 0.032 mmol) DMF stock solution. The tube was then sealed and degassed by purging it with nitrogen for 30 min. Polymerization was conducted in an oil bath (70 ^{o}C) for 24 h and followed by precipitation in acetone and subsequent washing with methanol to remove the monomers and residual RAFT agents. Conversion of the polymerization was determined by Varian 500 ^{1}H NMR using D_2O. The polymer's molecular weight and polydispersity were determined by aqueous GPC (Viscotek GPC system) at room temperature with a flow rate of 1.0 mL/min.

3.2.2.2.RAFT Copolymerization of LAEMA with AEMA

Copolymerization was performed at 70 °C employing ACVA and CTP as the radical initiator and chain transfer agent, respectively. In a 10 mL Schlenk tube, LAEMA (0.5 g,

1.07 mmol) and AEMA (0.5 g, 3.02 mmol) were dissolved in 7 mL of double-distilled deionized water before addition of CTP (16 mg, 0.057 mmol) and ACVA (8 mg, 0.032 mmol) *N,N'*-dimethylformamide (DMF) stock solution (1 mL). After degassing under nitrogen atmosphere for 30 min, the flask was placed in a preheated oil bath for 24 h. After precipitation in acetone, the polymer was extensively washed with methanol to remove any residual monomers and then dried under vacuum (**Scheme 3-2**). Conversion and composition of the copolymer were determined by Varian 500 ^{1}H NMR in D_2O. The polymer molecular weight and molecular weight distributions were determined by aqueous GPC (Viscotek GPC system) at room temperature with a flow rate of 1.0 mL/min.[30]

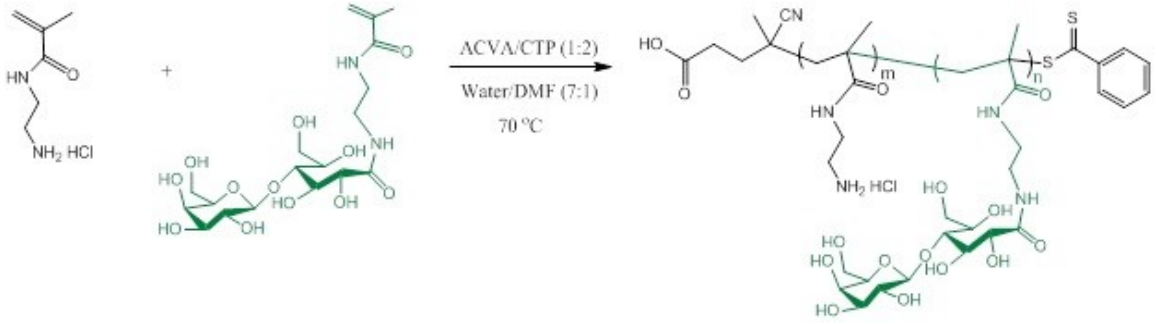

Scheme 3-2. RAFT synthesis of P(LAEMA-co-AEMA).

3.2.2.3.Bacterial Cultivation

The stored bacterial strains (*P. aeruginosa* PAO1 and *E. coli* K-12) were streaked onto a Luria-Bertani (LB) agar plate and incubated at 37 °C overnight. A single colony was transferred into 5 mL of LB broth and grown overnight in a shaker incubator at 200 rpm and 37 °C. Stationary-phase bacterial cells were harvested by centrifugation at 4000 g and 4 °C for 5 min. After decanting the supernatant, the pellets were resuspended in 10 mM NaCl or 10 mM $CaCl_2$ solution. The centrifugation and resuspension procedure was repeated at least twice to remove traces of growth media and suspended extracellular

polymeric substances from the solution.[37] The final bacterial concentration was adjusted to 10^7 cells/mL by the optical density (OD).

3.2.2.4.Studying the Lectin–Polymer Interactions by QCM-D

QCM-D (Q-Sense, Sweden, E4 chamber) was applied in real time to study the interactions between lectin and gold-coated sensor chips (frequency, 4.95 MHz 50 kHz; cut, AT; diameter, 14 mm; thickness, 0.3 mm; surface roughness, <3 nm (RMS); electrode layer, 10–300 nm) that had been modified by the polymers. Modification was initiated by pumping 1 mg/mL of polymer salt solutions (10 mM NaCl or 10 mM $CaCl_2$ solution rather than a buffer) into the sensor chambers at a flow rate of 50 μL/min until no further changes in frequency were detected by the QCM-D (which indicates that polymer adsorption on the sensor surface was complete). Subsequently, the salt solutions were pumped (0.15 mL/min) into the sensor chambers to remove any polymers weakly bound to the sensor surface. A 10 μg/mL amount of lectin salt solution was then pumped into the sensor chamber at a flow rate of 50 μL/min, and immediately thereafter the sensor chips were stabilized again. After the weakly bounded lectins were removed by washing the sensor with salt solutions (0.15 mL/min), 10 mg/mL of ethylenediamine-*N,N,N′,N′*-tetraacetic acid (EDTA) aqueous solution was pumped into the sensors (0.15 mL/min) to form complexes with calcium salts to dissociate the adsorbed lectins from the glycopolymer layer. The adsorption–desorption cycles of lectins from the glycopolymer layers were repeated three times.

3.2.2.5.Studying the Bacteria–Polymer Interactions by QCM-D

In order to study the interactions between bacteria and polymers by QCM-D, the gold sensor chips were modified by polymers by injecting 1 mg/mL of a polymer salt solution (10 mM NaCl or 10 mM $CaCl_2$ solution rather than a buffer) at a flow rate of 50 μL/min.

Once the polymer adsorption on the sensor surface was complete (the resonant frequencies no longer changed), test media (10 mM NaCl solution or 10 mM $CaCl_2$) were injected at a flow rate of 0.15 mL/min to remove any weakly bound polymers. Then bacterial suspension (10^7 cells/mL, determined by the optical density (OD)) was injected at a flow rate of 50 μL/min until the sensors' resonant frequencies remained stable. Bacterial suspensions from the QCM-D outlet were collected during different experiment periods (0, 1, 2, and 4 h) and the bacterial numbers were counted on LB-agar plate. At the end of the experiment, the bacteria adhered on QCM-D sensor chips were stained by SYTO 9 and propidium iodide (PI) to identify the live and dead bacterial cells, respectively. ImageJ was used to reduce the background intensity in the fluorescent images and count the live bacteria stained by SYTO 9 (at least 3 images were taken and 3 different fields were counted). The numbers of cells were then normalized with the image area and given total cell numbers in cells/cm^2. All measurements were performed in duplicate with separately cultured bacteria.

QCM-D data was analyzed by the coupled resonance model. To do this, the bandwidth values (Γ) were first calculated from $\Gamma = Df/2$ (where D is the dissipation shifts measured by QCM-D and f is the frequency at each overtone (i.e., 5, 15, 25, 35, 45, and 55 MHz at the fundamental frequency, 3rd, 5th, 7th, 9th, and 11th overtone, respectively)). The shifts in frequency (Δf) and bandwidth ($\Delta\Gamma$) were then normalized to the number of bacterial per unit area N_b (bacteria/cm^2), which was determined from images captured from the center of the QCM-D sensor surface by fluorescent microscope (Microscope Axio Imager.M2, Carl Zeiss, Germany), and analyzed by the small-loading approximation. The small-loading approximation is the essential concept of QCM-D analysis, which includes the

well-known formalism of QCM data analysis for planar layer systems (i.e., Sauerbrey equation). The relationship between normalized frequency and bandwidth shifts ($\Delta f/N_b$ and $\Delta\Gamma/N_b$) can be given as

$$\frac{\Delta f^*}{N_b} = \frac{\Delta f + i\Delta\Gamma}{N_b} = \frac{f_F}{\pi Z_q} f_{osc} \frac{m\omega(k + i\omega\zeta)}{m\omega^2 - (k + i\omega\zeta)} \qquad \textbf{(1)}$$

in which f_F is the fundamental frequency (5 MHz), Z_q is the acoustic impedance of AT-cut quartz crystal (8.8×10^6 kg/m^2/s), k is the spring constant, and f_{osc} is the oscillator strength ($0 < f_{osc} < 1$). When bacterial cells interact with the sensor surface strongly ($k \gg m\omega^2$, $\Delta f^* = N_b((-2f_F)/(Z_q))f_{osc}\Delta m$) they can move together with the resonator and are termed as inertial loading in the Sauerbrey sense ($\Delta m = (-C\Delta f)/n$). On the other hand, for weak elastic bonding ($k \ll m\omega^2$), the frequency shift is positive and the equation can be rewritten as ($\Delta f^* = N_b((f_F)/(\pi Z_q))f_{osc}(k/\omega)$, describing elastic loading.

By further developing **equation 1** into **equation 2** one can find that $\Delta\Gamma = \mathrm{Im}(\Delta f^*)$ versus $\Delta f = \mathrm{Re}(\Delta f^*)$ (Im, image part; Re, real part) could be plotted into circles in polar diagrams and the radius is proportional to the adhesive bond stiffness k

$$2R \approx \frac{\Delta\Gamma(\omega = \omega_b)}{N_b} \approx \frac{f_F}{\pi Z_q} f_{osc} \frac{m\omega_b(\omega_b^2 + i\omega_b\gamma)}{i\omega_b\gamma} \approx \frac{f_F}{\pi Z_q} \frac{k}{\gamma} \qquad \textbf{(2)}$$

where γ is the introduced damping rate, as the ratio of the drag coefficient (ξ) and the mass of the particle (m), with the dimension of frequency.[38-41] The radius of the circles in polar diagrams by bacterial adhesion on different surfaces and test media was then calculated in MATLAB by the Taubin method.

Another parameter to compare the results from bacterial adhesion on different surfaces is the frequency of zero crossing, f_{ZC}, which is obtained when Δf changes sign from being negative to being positive[39] (note in some cases that the f_{ZC} values locate outside the range of the observable frequencies (from 5 to 55 MHz in this study); they might be determined by extrapolation). The relationship between f_{ZC} and bond stiffness can be presented as

$$f_{zc} = \frac{1}{2\pi}\omega_{b,eff} = \frac{1}{2\pi}\sqrt{\frac{k_{eff}}{m}} \qquad \textbf{(3)}$$

and when the effective mass, m, remains constant during the experiments, the increase of f_{ZC} indicates an increase in bond stiffness.

3.3.Results and Discussions

3.3.1. Adsorption Behavior of Synthesized Polymers on QCM-D Sensor Surface

A range of glycopolymers was synthesized via the reversible addition–fragmentation chain transfer (RAFT) process. Detailed information on the synthesized polymers is shown in **Table 3-1**.

Table 3-1. Molecular Weights, Conversions, and PDI of Polymers Synthesized by RAFT.

Polymer Compositions	**Conversion (%)**	M_n **(GPC, g/mol)**	M_w/M_n
$PGAPMA_{39}$	100	12 490	1.33
$PLAEMA_{28}$	97	13 338	1.30
$PAEMA_{83}$	98.5	13 783	1.27
$P(LAEMA_{15}$-*st*-$AEMA_{45})$	82	14 787	1.38

The polymers obtained have relatively narrow molecular weight distributions. The compositions of the statistical copolymers were determined by ^{1}H NMR (**Figure 3-S1 in Appendix**). QCM-D technique has been extensively used in the study of polymers and

their subsequent interactions.[32, 42, 43] In this work, the RAFT-synthesized polymers were first immobilized on the gold-coated sensor chips of the QCM-D for the study of bacterial adhesion. PEG-SH was also immobilized on the sensor surface and used as a negative control. The synthesized polymers were found to interact well with the QCM-D sensor chips, so no prior reduction of the dithioester into thiol was carried out. Sensor surfaces were treated by PAEMA (cationic polymer), PLAEMA (glycopolymer with galactose pendent groups), P(LAEMA-*st*-AEMA), or PGAPMA (glycopolymer with glucose pendent groups) to study the different bacterial adhesion mechanisms (e.g., electrostatic interactions, lectin–carbohydrate conjugation, and nonspecific interactions). The PEG-SH-modified sensor chip was set as the negative control, as the hydrophilic PEG brushes on surface are well known in preventing adhesion of proteins/cells on materials surface due to hydrophilicity, high mobility, and great steric hindrance effect.[9]

The frequency and thickness shifts (which were calculated by the Voigt viscoelastic model built in the QTools software (Goteborg, Sweden)) on the sensor surface after immobilization of the polymers are shown in **Figure 3-1a and 1b**, respectively. Among the different groups, the PEG-SH-treated sensor exhibited the largest frequency and thickness changes. This observation suggested that the grafting density of the flexible PEG-SH was much higher on the sensor surface as compared to the RAFT polymers, which are more rigid and bulky.[32] While comparing the frequency and thickness shifts among the different RAFT polymers, the positively charged PAEMA showed the smallest negative frequency shift possibly due to poor interaction of these polymers to the sensor surface. The low grafting density of these polymers on the gold surface can also be due to electrostatic repulsion between the chains.

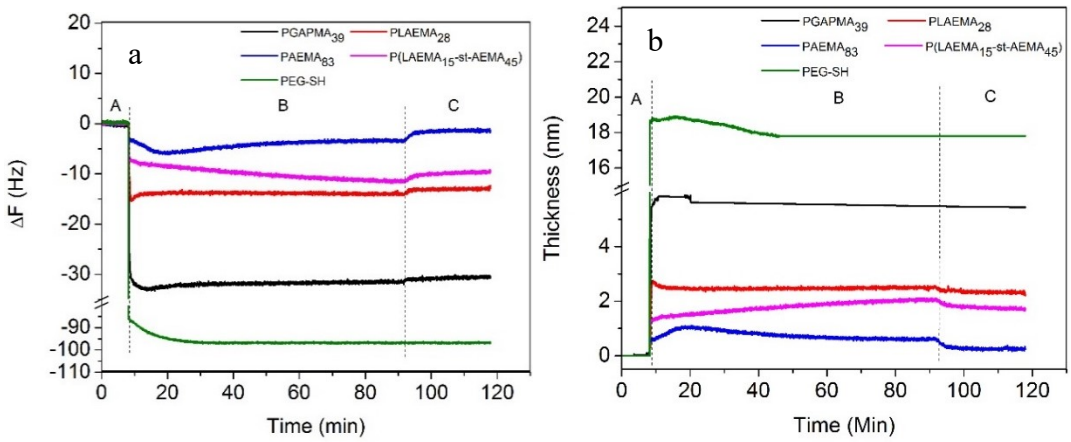

Figure 3-1. Frequency (a) and thickness (b) changes after polymer adsorbed on gold-coated QCM-D sensor chips. (A) Stabilization of the sensor chip by test media. (B) Injection of polymer solutions to QCM-D sensor. (C) Purging test media to sensors to remove any unbound polymers.

3.3.2. Polymer–Lectin Interactions

The interactions between lectin and the immobilized polymers were then studied by QCM-D (**Figure 3-2a and 2b**). Lectin from *Ricinus communis* (castor bean) Agglutinin (RCA120), a lectin known to specifically interact to galactose,[44] was injected over the polymer-modified QCM-D sensor surface. In **Figure 3-2a**, the stage that appeared during the first injection of lectin (at a period between D and E) might be due to the air entrapped in the tubes. After the frequency shifts have be stabilized, salt solution was injected. The shifts of dissipation and frequency agreed with the conventional Sauerbrey relation between mass and frequency shifts. As expected, a large negative frequency shift was recorded after injection of RCA_{120} on the PLAEMA-treated sensor surface. This large response was probably due to the specific interactions of the lectin (10 μg/mL) with dense galactose residues on the sensor surface (red line in **Figure 3-2**).[33, 45] Interestingly, in the case of the positively charged PAEMA-treated sensor surface, a negative frequency shift

could also be observed when RCA_{120} was injected (blue line in **Figure 3-2a**). This nonspecific interaction could be due to the electrostatic interaction between the positively charged polymer chains and the negatively charged RCA_{120}, as the pH of RCA_{120} in the presence of $CaCl_2$ is higher than its isoelectric point (7.5–7.9).[46] Furthermore, PGAPMA- (blackline in **Figure 3-2**) and PEG-SH-treated (purple line in **Figure 3-2**) sensor surfaces showed no frequency shifts when RCA_{120} was injected. This result is expected as PEG is well known to prevent protein adsorption[9] and the PGAPMA has no specific galactose residues to interact with RCA_{120}.[47]

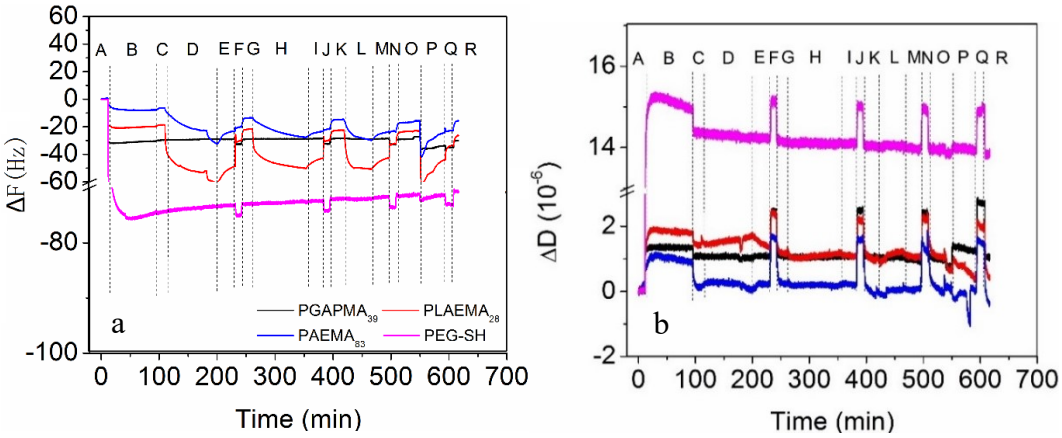

Figure 3-2. Shifts on frequency (a) and dissipation (b) for lectin (RCA_{120}) interaction on different polymer-treated sensor surfaces at the 7th overtone (n = 7). (A, C, E, G, I, K, M, O, R) Stabilizing the sensor chips by test media (10 mM $CaCl_2$). (B) Injecting of polymer solutions to sensor surface. (D, H, L, P) Injecting 10 μg/mL of RCA_{120} $CaCl_2$ solution to sensor surface. (F, J, N, Q) Washing the sensors by 10 mg/mL EDTA aqueous solution.

To confirm that the RCA_{120} interacts with the polymers and not with the sensor surface, EDTA aqueous solution (10 mg/mL) was injected after the lectin treatment. Due to complexation of EDTA to calcium ions, the RCA_{120} lectin[48] was released from the PLAEMA surface and the frequency shifts were found to revert back to the same level as

the polymer-treated sensor surface. A negative frequency shift could again be recorded if RCA_{120} was injected to the PLAEMA sensor surface. Interestingly, in the case of PAEMA-treated sensor surface, lectin was also found to be removed from the sensor surface when it was washed with EDTA.

3.3.3. Study of Bacteria–Polymer Interactions

Subsequently, *P. aeruginosa* PAO1 (a Gram-negative bacterium with galactose specific binding lectin (PA-IL)) and *E. coli* K-12 (a Gram-negative bacterium with mannose specific binding lectin) were then used as model bacteria to study bacterial adhesion mechanisms on different glycopolymer-treated sensor surfaces. A schematic representation of the specific interactions of bacteria to glycopolymers immobilized on QCM-D surface is shown in **Scheme 3-3**.

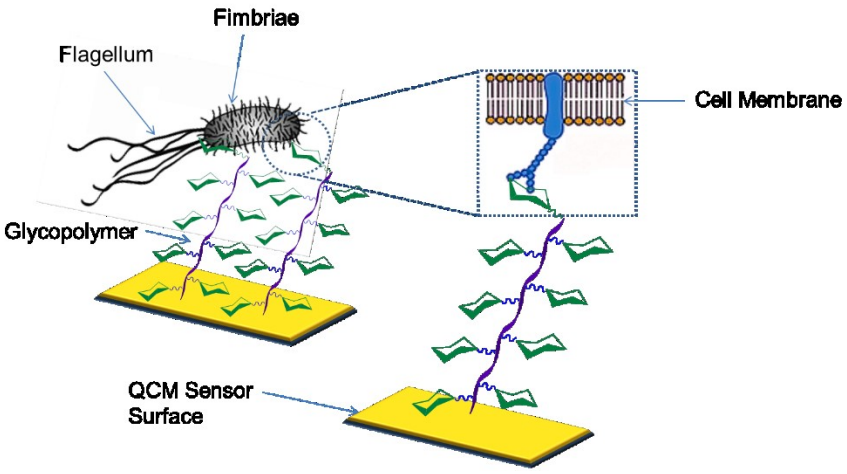

Scheme 3-3. Schematic Representation of the Specific Interactions of Bacteria to Glycopolymers Immobilized on QCM-D Surface.

3.3.3.1.P. aeruginosa PAO1 Adhesion on Different Polymer Surfaces in Different Test Media

The shifts in frequency and dissipation and polar diagrams for *P. aeruginosa* PAO1 adhering on different polymer-treated QCM-D sensors in calcium chloride (10 mM) and sodium chloride (10 mM) are shown in **Figures 3-3, 3-S5 in Appendix, and 3-4,** respectively. The shifts were found to be dependent on the surface treatments as well as the type of test media. The slight positive resonant frequency and negative dissipation shifts observed for the PEG-SH-treated sensor upon *P. aeruginosa* PAO1 injection in either test medium indicated their low adhesion to the surface (**see Figures 3-3i and 3-S5j in Appendix**), which can be attributed to removal of the physically adsorbed PEG from the polymer film.

In 10 mM $CaCl_2$, *P. aeruginosa* PAO1 adhesion on synthetic polymer-coated QCM-D surfaces showed positive frequency shifts at the end of the tests (except on the 1st overtones on PLAEMA, P(LAEMA-*st*-AEMA), and PAEMA surfaces) **(Figure 3-3**). Therefore, from **equation 1** these results indicated *P. aeruginosa* PAO1 interact with PGAPMA by weakly elastic loading, whereas their interactions with PLAEMA, P(LAEMA-*st*-AEMA), and PAEMA are mediated by both inertial and elastic loading. Apparently, the weak elastic loading of *P. aeruginosa* PAO1 on PGAPMA surface can be explained due to the lack of ligand–receptor interaction between the glucose and the bacterial lectins (the two lectins, PA-IL and PA-IIL, on *P. aeruginosa* PAO1 membrane can only specifically interact to galactose galactose[19, 49] and fructose,[50] respectively). The frequency shifts observed from *P. aeruginosa* PAO1 adhesion on PLAEMA, P(LAEMA-*st*-AEMA), and PAEMA surfaces agreed with previous reports from Olsson et al., in which negative frequency shifts were

observed for streptavidin-coated microparticles interacting with biotinylated surface[39] or staphylococcus aureus adhesion on fibronectin surface.[51]

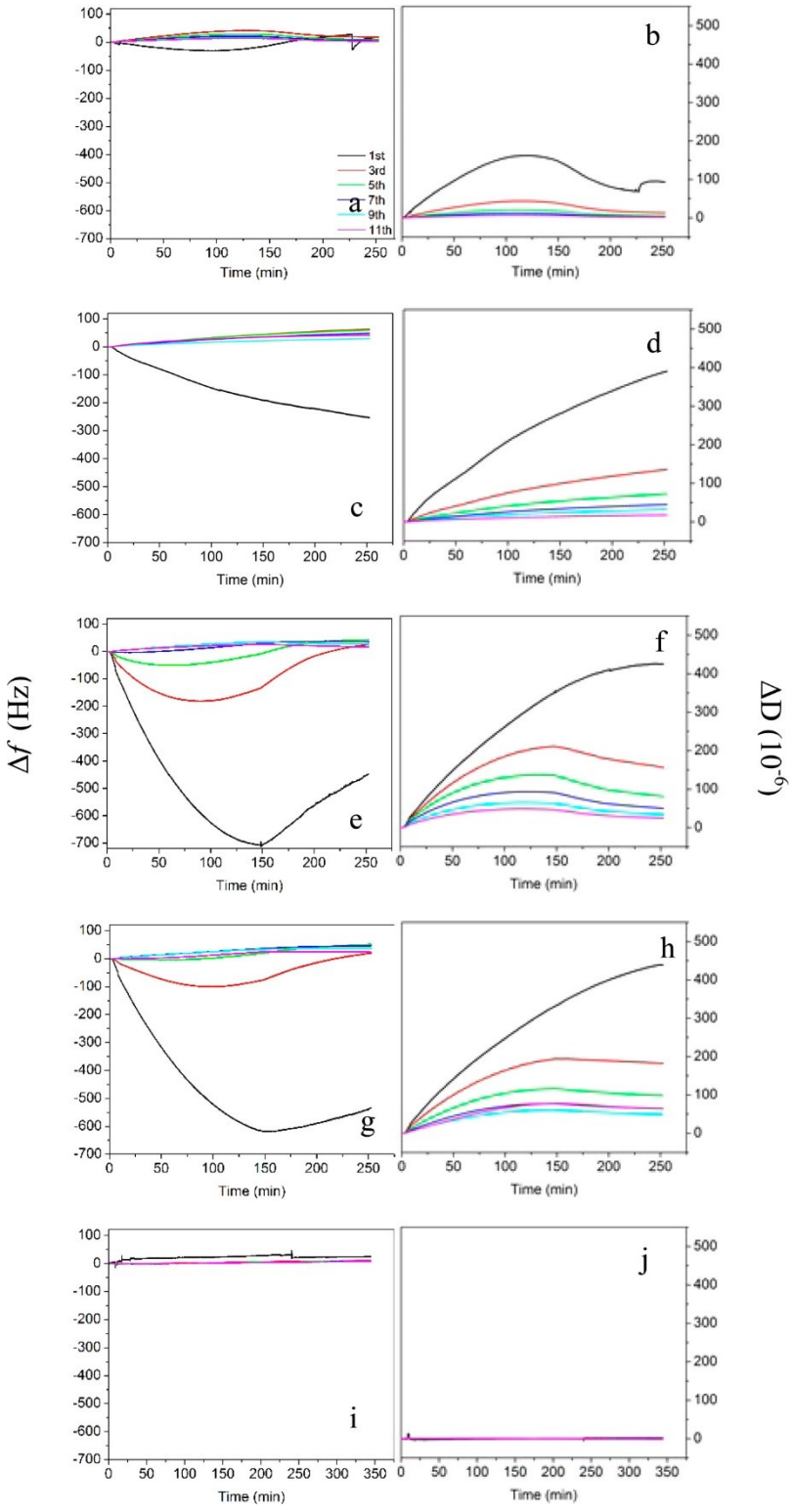

Figure 3-3. Frequency (a, c, e, g, i) and dissipation (b, d, f, h, j) shifts of *P. aeruginosa* PAO1 adhesion on different polymers-treated QCM-D sensor surface (in 10 mM $CaCl_2$). (a, b) PGAPMA (Glc). (c, d) PLAEMA (Gal). (e, f) PAEMA (cationic). (g, h) P(LAEMA-*st*-AEMA) (Gal/cationic). (i, j) PEG-SH.

Moreover, in this study, interesting nonlinear frequency shifts were first recorded when *P. aeruginosa* PAO1 interacted with the cationic polymers surface (**Figure 3-3e and 3g**). On the basis of the plate counting and fluorescence image results (**Figures 3-S7 and 2-S8 in Appendix**, respectively), the cationic polymer-modified sensor surface was revealed to be noncytotoxic, and this may be due to water release from the bacterium–substratum interfaces when the cationic polymers are collapsed under the stronger ionic strength condition[39, 52] (the ionic strength in 10 mM $CaCl_2$ is 3 times higher than that of 10 mM NaCl). In addition, the collapse of polymer under strong ionic strength conditions resulted in stiffer surfaces, which could explain the enhanced bacterial adhesion in **Figures 3-S2 and 3-S4 in Appendix.**[53]

When 10 mM NaCl solution was used as the test medium, only small negative frequency shifts could be observed for *P. aeruginosa* PAO1 adhering on PLAEMA and PGAPMA surfaces (**Figure 3-S5a and 3-S5c in Appendix**). These results can be explained by the blocking of the lectin–carbohydrate pathway when the Ca^{2+}-dependent PA-IL on *P. aeruginosa* PAO1 membrane was "deactivated" to interact with PLAEMA surface in NaCl[19] (**Figure 3-3c versus Figure 3-S5c in Appendix**). Interestingly, although the bacterium–PGAPMA interaction was not regulated by the ligand–receptor interaction, the sign changed in frequency shifts for bacterial adhesion on PGAPMA surfaces in different test media (**Figure 3-3a versus Figure 3-S5a in Appendix**) showed the same trends as

that on PLAEMA surface (**Figure 3-3c versus Figure 3-S5c in Appendix**). These observations might be explained by DLVO theory.[39] The bacterial adhesion on PGAPMA surface is balanced between attractive Lifshitz van der Waals forces and electrostatic repulsion. When $CaCl_2$ was replaced by NaCl, the reduction of electrostatic repulsion[54] makes bacteria interact with the polymer layer easier and makes them closer to the surface to decrease the contact area.[39, 40, 51] Eventually the bacteria–substratum interactions were turned from weak elastic loading to inertia loading. The nonlinear frequency shifts can again be observed for bacterial adhesion on cationic polymers surfaces in 10 mM NaCl (**Figure 3-S5e and 3-S5g in Appendix**). However, the frequency shifts scales were much smaller than the same tests performed in 10 mM $CaCl_2$ (**Figure 3-3e and 3-3g**). This is due to the fact that the cationic polymers are more swollen in the lower ionic strength condition (10 mM NaCl solution),[39, 52] and less water was released from the bacterium–substratum interfaces.

To obtain quantitative information on bacterial adhering on surfaces with different polymer coatings, next, the polar diagrams were plotted based on the coupled resonance model and the radius and f_{ZC} values were compared. It was found that in 10 mM $CaCl_2$ the strongest bacterium–substratum interaction with the highest contact point stiffness could be found on the PLAEMA-modified sensor surface, as evidenced by the f_{ZC} value (between 5 and 15 MHz) and radius of the circle in the polar diagram (R_{PD} = 210.56 μHz cm^2) (**Figure 3-4a**). Since multiple galactose groups are located on PLAEMA backbones,[36, 55] this interaction is most likely mediated by PA-IL on the *P. aeruginosa* PAO1 fimbriae tip[19, 49] and galactose on the sensor surface. In contrast, for *P. aeruginosa* PAO1 adhesion on PGAPMA in 10 mM $CaCl_2$, the smaller f_{ZC} value (below 5 MHz) and failure of simulating

the polar diagram (**Figure 3-4a**) suggested a weak bacteria–substratum interaction due to the lack of galactose functional groups to interact with bacterial cells. Interestingly, the radii of the circles in the polar diagram were reduced to 101.13 and 114.31 μHz cm^2 for *P. aeruginosa* PAO1 adhesion on cationic PAEMA and P(LAEMA-st-AEMA) surface, respectively, which contradict with the fact that the electrostatic interaction is stronger than the hydrogen bonding, van der Waals force, and hydrophobic interaction-mediated carbohydrate–protein interactions.[56] However, in the "coupling resonance model" the bacterium-substratum interaction is described by a paralleled dashpot (viscous part) and spring (elastic part),[39, 40] and the one with a smaller value always dominates the bacterium–substratum interaction. Therefore, in the case of *P. aeruginosa* PAO1 adhesion on cationic polymer surface, the smaller viscous part in the viscoelastic interaction was shown as the dominate factor for the overall contact point stiffness.

In 10 mM NaCl, the frequency shifts for *P. aeruginosa* PAO1 adhesion on all RAFT polymer surfaces changed to the negative direction, which is probably due to the change of the distance between bacteria and substratum when the bacterial appendage length was changed in different media.[40] However, it seems counterintuitive that when the lectin–carbohydrate pathway was blocked in 10 mM NaCl, *P. aeruginosa* PAO1 adhesion on PLAEMA was pure inertial loading, whereas weaker elastic loading was observed when the pathway was in the activated state in 10 mM $CaCl_2$. Probably, these observations can be explained as in NaCl the contact areas between bacteria and polymers were increased as *P. aeruginosa* PAO1 may be deformed and "sink" into polymer layers.[51]

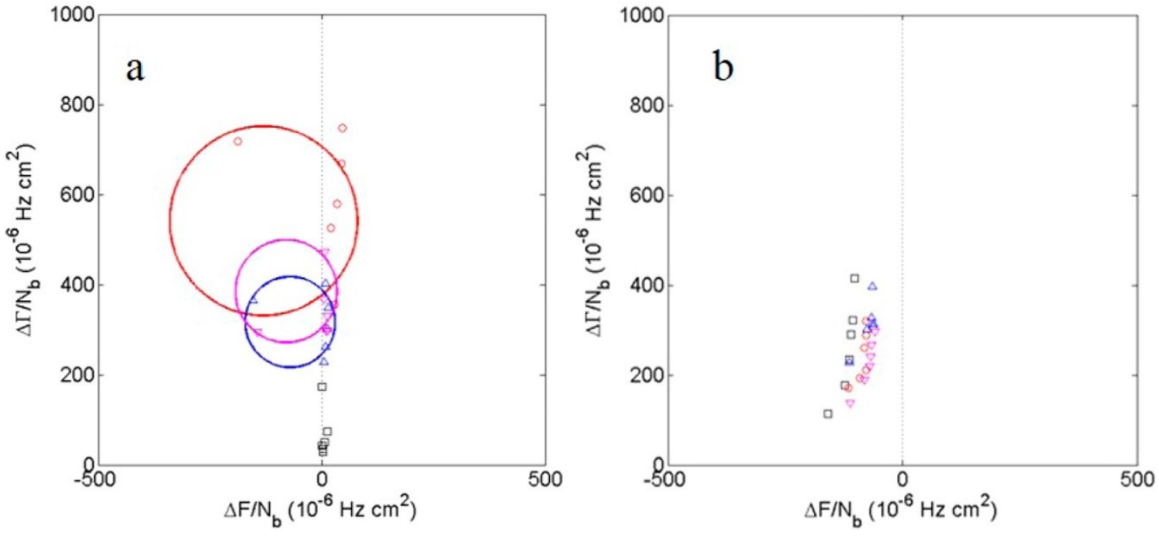

Figure 3-4. Polar diagrams for *P. aeruginosa* PAO1 adhesion on different polymers surfaces ((□) PGAPMA (Glc), (○) PLAEMA (Gal), (△) PAEMA (cationic), (▽) P(LAEMA-*st*-AEMA) (cationic/gal)) in different test media ((a) 10 mM $CaCl_2$, (b) 10 mM NaCl).

3.3.3.2.E. coli K-12 Adhesion on Different Polymer Surfaces in Different Test Media

Next, *E. coli* K-12, which has mannose-specific binding lectins (MBP) located at the tip of bacterial fimbriae,[16, 57, 58] adhesion on different polymer surfaces in each test medium was studied by QCM-D to further illustrate the role of cellular lectin in bacterial adhesion. The shifts in frequency and dissipation and the polar diagrams for *E. coli* K-12 adhesion on different QCM-D sensors surfaces in different test media are shown in **Figures 3-5, 3-S6 in Appendix, and 3-6,** respectively, and found significantly to be smaller than those values collected from *P. aeruginosa* PAO1 adhesion tests (**Figures 3-5 and 3-S6 in Appendix vs Figures 3-3 and 3-S5 in Appendix**). The slight positive resonant frequency and negative dissipation shifts observed for the PEG-SH-treated sensor upon *E. coli* K-12 injection in

either test medium again can be explained as removal of the physically adsorbed PEG from the polymer film (see **Figures 3-5i and 3-S6j in Appendix**).

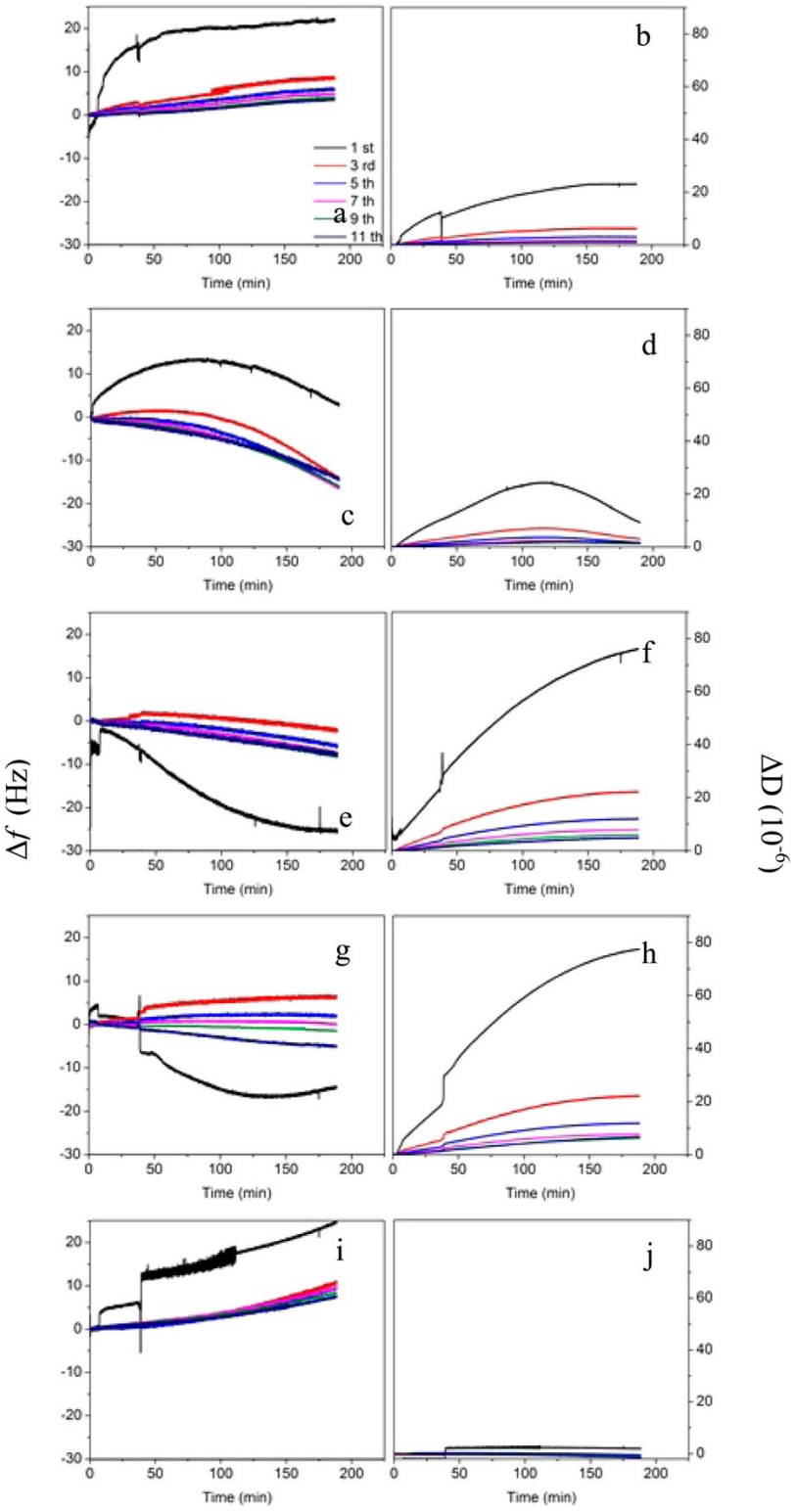

Figure 3-5. Frequency (a, c, e, g, i) and dissipation (b, d, f, h, j) shifts of *E. coli* K-12 adhesion on different polymer-treated QCM-D sensor surfaces (in 10 mM $CaCl_2$): (a, b) PGAPMA (Glc), (c, d) PLAEMA (Gal), (e, f) PAEMA (cationic), (g, h) P(LAEMA-st-AEMA) (cationic/gal), (i, j) PEG-SH.

Comparing the adhesion results of the two bacterial strains on the RAFT polymers surfaces, *E. coli* K-12 always showed smaller shifts in frequency and dissipation (**Figures 3-3 and 3-S5 in Appendix, vs Figures 3-5 and 3-S6 in Appendix**) and radii in polar diagrams in either test medium (**Figure 3-4 vs Figure 3-6**). These observations can be explained by the smaller contact area and higher bacterium–substratum repulsive force due to more negative charges presented on *E. coli* K-12 surface.[59] The significantly smaller contact point stiffness (**Figure 3-6a**) for *E. coli* K-12 adhesion on PLAEMA surface in $CaCl_2$ can be clearly explained by the lack of galactose binding lectins on the bacteria surface.[16, 24] The nonlinear frequency shifts observed for *E. coli* K-12 adhesion on PLAEMA surface in 10 mM $CaCl_2$ (**Figure 3-5c**) might indicate twostages bacterial adhesion on the polymer surface. In the first stage, it is possible that bacteria were attached to the sensor surface via weak elastic loading and showed positive frequency shifts (first 100 min in **Figure 3-5c**). However, as bacterial adhesion on the polymer surface goes into the irreversible attachment stage, the bacteria start to "spread" on the polymer layers. The resulted larger contact area and smaller bacteria–substratum interface distance could possibly alter the initial weakly elastic loading to stronger inertia loading and hence resulting in negative frequency shifts. In the case of *E. coli* K-12 adhesion on PGAPMA surface in 10 mM $CaCl_2$, the results were similar to *P. aeruginosa* PAO1 adhesion under the same conditions (f_{ZC} lower than 5 MHz and failure to generate circles in the polar diagram) (**Figures 3-6a and 3-4a**). The positive

frequency shifts (**Figures 3-3a and 3-5a**) indicated that, in the absence of lectins that could specifically interact to the glucose groups, both *P. aeruginosa* PAO1 and *E. coli* K-12 showed weak elastic loading on the PGAPMA layer.

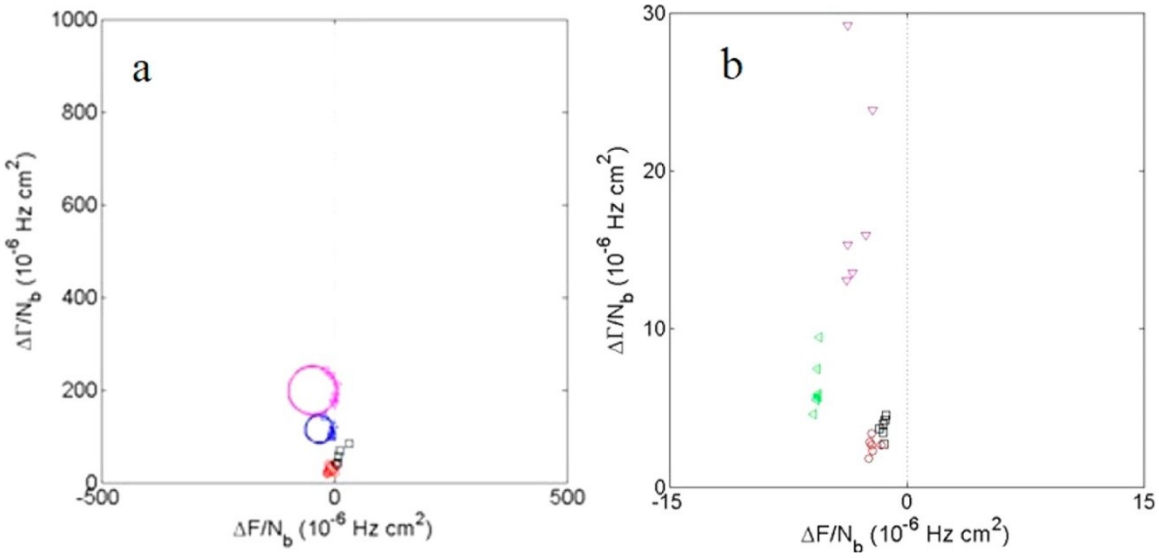

Figure 3-6. Polar diagrams for *E. coli* K-12 adhesion on different polymer surfaces ((□) PGAPMA (Glc), (○) PLAEMA (Gal), (△) PAEMA (cationic), (▽) P(LAEMA-*st*-AEMA) (cationic/gal)) in different test media ((a) 10 mM $CaCl_2$, (b) 10 mM NaCl).

For *E. coli* K-12 adhesion on cationic polymers in either test media, since the bacterial surface is more negatively charged,[59] the negative frequency shifts can be clearly explained by stronger inertia loading between bacteria and substrate (**Figures 3-5e, 3-5g, 3-S6e in Appendix, and 3-S6g in Appendix**). Moreover, as compared to the frequency and dissipation shifts for *P. aeruginosa* PAO1 adhesion on cationic polymers surfaces (**Figures 3-3 and 3-S5 in Appendix**), *E. coli* K-12 adhesion on the same surfaces resulted in smaller frequency and dissipation shifts and lower contact point stiffness. The changes on frequency and dissipation shifts can be explained by removal of water at the bacterium–

substratum interface, and hence, this may cause less viscous shear and friction at the liquid gap.[60] On the other hand, since the viscous part in the *E. coli* K-12 adhesion on cationic polymers surfaces was reduced, the overall contact bond stiffness was reduced as well, and hence, a smaller radius (**Figure 3-6a**) was observed for *E. coli* K-12 adhesion as compared to *P. aeruginosa* PAO1 adhesion under the same condition (**Figure 3-4a**).

3.4.Conclusions

Well-defined glycopolymers carrying galactose residues as pendant groups were successfully synthesized by the RAFT process and subsequently immobilized on the QCM-D sensor surface. Interactions between the polymers and the bacteria (*P. aeruginosa* PAO1 and *E. coli* K-12) were studied by QCM-D in different test media (10 mM NaCl versus 10 mM $CaCl_2$). The results showed, compared to *P. aeruginosa* PAO1 and *E. coli* K-12 (absence of galactose binding lectin) adhesion on galactose-containing glycopolymer surface (PLAEMA) in 10 mM NaCl and 10 mM $CaCl_2$, respectively, that a significantly higher contact point stiffness was observed when *P. aeruginosa* PAO1 adhesion on PLAEMA surface in 10 mM $CaCl_2$. Because of the calcium-dependent nature of the galactose binding lectin (PA-IL) at *P. aeruginosa* PAO1 fimbriae tip, these results indicate the lectins on the bacterial membrane were involved in adhesion to the glycopolymers, and such interaction was found to be strong and highly dependent on the presence of calcium ions.

3.5. References

1. T. Juhna, D. Birzniece, S. Larsson, D. Zulenkovs, A. Sharipo, N. F. Azevedo, F. Ménard-Szczebara, S. Castagnet, C. Féliers and C. W. Keevil, *Appl. Environ. Microbiol.* 2007, **73**, 7456-7464.

2. N. J. Shikuma and M. G. Hadfield, *Biofouling* 2009, **26**, 39-46.

3. A. G. Gristina, *Science*, 1987, **237**, 1588-1595.

4. V. Zijnge, M. B. M. van Leeuwen, J. E. Degener, F. Abbas, T. Thurnheer, R. Gmür and H. J. M. Harmsen, *PLoS ONE* 2010, **5**, e9321.

5. H. J. Busscher and A. H. Weerkamp, *FEMS Microbiol. Lett.* 1987, **46**, 165-173.

6. M. C. van Loosdrecht, J. Lyklema, W. Norde, G. Schraa and A. J. Zehnder, *Appl. Environ. Microbiol.* 1987, **53**, 1893-1897.

7. É. Kiss, J. Samu, A. Tóth and I. Bertóti, *Langmuir* 1996, **12**, 1651-1657.

8. Y. Sakagami, H. Yokoyama, H. Nishimura, Y. Ose and T. Tashima, *Appl. Environ. Microbiol.* 1989, **55**, 2036-2040.

9. D. Kiaei, A. S. Hoffman, T. A. Horbett and K. R. Lew, *J. Biomed. Mater. Res.* 1995, **29**, 729-739.

10. W. P. Johnson and B. E. Logan, *Water Res.* 1996, **30**, 923-931.

11. G. Smit, M. H. Straver, B. J. Lugtenberg and J. W. Kijne, *Appl. Environ. Microbiol.* 1992, **58**, 3709-3714.

12. T. A. Camesano and B. E. Logan, *Environ. Sci. Technol.* 1998, **32**, 1699-1708.

13. M. C. M. Van Loosdrecht, W. Norde and A. J. B. Zehnder, *J. Biomater. Appl.* 1990, **5**, 91-106.

14. N. P. Boks, W. Norde, H. C. van der Mei and H. J. Busscher, *Microbiology*, 2008, **154**, 3122-3133.

15. S. Bayoudh, A. Othmane, L. Mora and H. Ben Ouada, *Colloids Surf. B* 2009, **73**, 1-9.

16. N. Sharon, *FEBS Lett.* 1987, **217**, 145-157.

17. X.-Q. Mu and E. Bullitt, *Proc. Natl. Acad. Sci.* 2006, **103**, 9861-9866.

18. S. J. Hultgren, F. Lindberg, G. Magnusson, J. Kihlberg, J. M. Tennent and S. Normark, *Proc. Natl. Acad. Sci.* 1989, **86**, 4357-4361.

19. G. Cioci, E. P. Mitchell, C. Gautier, M. Wimmerová, D. Sudakevitz, S. Pérez, N. Gilboa-Garber and A. Imberty, *FEBS Lett.* 2003, **555**, 297-301.

20. N. Laurent, J. Voglmeir and S. L. Flitsch, *Chem. Commun.* 2008, **37**, 4400-4412.

21. X.-L. Su and Y. Li, *Biosens. Bioelectron.* 2005, **21**, 840-848.

22. Y.-T. Tseng, H.-Y. Chang and C.-C. Huang, *Chem. Commun.* 2012, **48**, 8712-8714.

23. C. Poitras and N. Tufenkji, *Biosens. Bioelectron.* 2009, **24**, 2137-2142.

24. Z. Shen, M. Huang, C. Xiao, Y. Zhang, X. Zeng and P. G. Wang, *Anal. Chem.* 2007, **79**, 2312-2319.

25. A. L. J. Olsson, H. C. van der Mei, H. J. Busscher and P. K. Sharma, *Langmuir* 2009, **25**, 1627-1632.

26. H. J. Busscher, W. Norde and H. C. van der Mei, *Appl. Environ. Microbiol.* 2008, **74**, 2559-2564.

27. H. C. van der Mei, M. Rustema-Abbing, J. de Vries and H. J. Busscher, *Appl. Environ. Microbiol.* 2008, **74**, 5511-5515.

28. Y. Gou, S.-J. Richards, D. M. Haddleton and M. I. Gibson, *Polym. Chem.* 2012, **3**, 1634-1640.

29. M. Huang, Z. Shen, Y. Zhang, X. Zeng and P. G. Wang, *Bioorg. Med. Chem. Lett.* 2007, **17**, 5379-5383.

30. Z. Deng, M. Ahmed and R. Narain, *J. Polym. Sci., Part A: Polym. Chem.* 2009, **47**, 614-627.

31. Z. Deng, H. Bouchékif, K. Babooram, A. Housni, N. Choytun and R. Narain, *J. Polym. Sci., Part A: Polym. Chem.* 2008, **46**, 4984-4996.

32. S. Slavin, A. H. Soeriyadi, L. Voorhaar, M. R. Whittaker, C. R. Becer, C. Boyer, T. P. Davis and D. M. Haddleton, *Soft Matter* 2011, **8**, 118-128.

33. Y. C. Lee and R. T. Lee, *Acc. Chem. Res.* 1995, **28**, 321-327.

34. S. M. Dimick, S. C. Powell, S. A. McMahon, D. N. Moothoo, J. H. Naismith and E. J. Toone, *J. Am. Chem. Soc.* 1999, **121**, 10286-10296.

35. M. Benaglia, E. Rizzardo, A. Alberti and M. and Guerra, *Macromolecules*, 2005, **38**, 3129-3140.

36. Z. Deng, S. Li, X. Jiang and R. Narain, *Macromolecules*, 2009, **42**, 6393-6405.

37. X. Sun, C. Danumah, Y. Liu and Y. Boluk, *Chem. Eng. J.* 2012, **198-199**, 476-481.

38. A. L. J. Olsson, H. C. van der Mei, H. J. Busscher and P. K. Sharma, *Langmuir* 2010, **26**, 11113-11117.

39. A. L. J. Olsson, H. C. van der Mei, D. Johannsmann, H. J. Busscher and P. K. Sharma, *Anal. Chem.* 2012, **84**, 4504-4512.

40. A. L. J. Olsson, N. Arun, J. S. Kanger, H. J. Busscher, I. E. Ivanov, T. A. Camesano, Y. Chen, D. Johannsmann, H. C. van der Mei and P. K. Sharma, *Soft Matter* 2012, **8**, 9870-9876.

41. I. Reviakine, D. Johannsmann and R. P. Richter, *Anal. Chem.* 2011, **83**, 8838-8848.

42. J. C. Munro and C. W. Frank, *Polymer* 2003, **44**, 6335-6344.

43. S.-F. Chou, W.-L. Hsu, J.-M. Hwang and C.-Y. Chen, *Anal. Chim. Acta* 2002, **453**, 181-189.

44. H. Lis and N. Sharon, *Lectins*, Springer, 2007.

45. J. J. Lundquist and E. J. Toone, *Chem. Rev.* 2002, **102**, 555-578.

46. R. Karamanska, B. Mukhopadhyay, D. A. Russell and R. A. Field, *Chem. Commun.* 2005, 3334-3336.

47. M. Ahmed, B. F. L. Lai, J. N. Kizhakkedathu and R. Narain, *Bioconjugate Chem.* 2012, **23**, 1050-1058.

48. I. van Die, S. J. van Vliet, A. K. Nyame, R. D. Cummings, C. M. C. Bank, B. Appelmelk, T. B. H. Geijtenbeek and Y. van Kooyk, *Glycobiology*, 2003, **13**, 471-478.

49. S. P. Diggle, R. E. Stacey, C. Dodd, M. Cámara, P. Williams and K. Winzer, *Environ. Microbiol.* 2006, **8**, 1095-1104.

50. D. Tielker, S. Hacker, R. Loris, M. Strathmann, J. Wingender, S. Wilhelm, F. Rosenau and K.-E. Jaeger, *Microbiology*, 2005, **151**, 1313-1323.

51. A. L. J. Olsson, P. K. Sharma, H. C. van der Mei and H. J. Busscher, *Appl. Environ. Microbiol.* 2012, **78**, 99-102.

52. J. J. I. Ramos, I. Llarena and S. E. Moya, *J. Polym. Sci., Part A: Polym. Chem.* 2011, **49**, 2346-2352.

53. J. A. Lichter, M. T. Thompson, M. Delgadillo, T. Nishikawa, M. F. Rubner and K. J. Van Vliet, *Biomacromolecules*, 2008, **9**, 1571-1578.

54. McLaughl.Sg, G. Szabo and G. Eisenman, *J. Gen. Physiol.* 1971, **58**, 667-&.

55. M. Ahmed and R. Narain, *Biomaterials* 2011, **32**, 5279-5290.

56. D. R. Bundle and N. M. Young, *Curr. Opin. Struct. Biol.* , 1992, **2**, 666-673.

57. N. Kawasaki, T. Kawasaki and I. Yamashina, *J. Biochem.* 1989, **106**, 483-489.

58. Z. Barshavit, R. Goldman, I. Ofek, N. Sharon and D. Mirelman, *Infection and Immunity*, 1980, **29**, 417-424.

59. B. Li and B. E. Logan, *Colloids Surf. B* 2004, **36**, 81-90.

60. I. M. Marcus, M. Herzberg, S. L. Walker and V. Freger, *Langmuir* 2012, **28**, 6396-6402.

Chapter 4. Study of Bacterial Adhesion on Biomimetic Temperature Responsive Glycopolymer Surfaces

The content of this chapter was published in *ACS Appl. Mater. Interfaces* **2015**, 7, 1652-1661.

4.1. Introduction

Pseudomonas aeruginosa is a rod shaped Gram-negative bacteria about 1–3 μm in length. Although common in the environment, it rarely causes disease in healthy humans. *P. aeruginosa* is usually linked to human disease, such as bacteremia in severe burn victims, chronic lung infection in cystic fibrosis (CF) patients, and acute ulcerative keratitis in soft contact lenses users.[1-3] Exotoxins and endotoxins released by *P. aeruginosa* can be life-threatening because they continue to damage host tissues even after the bacteria have been killed by antibiotics.[1] Bacterial adhesion to tissue surfaces is the initial step in *P. aeruginosa* infection.[4-6]

Adhesion of *P. aeruginosa* to mammalian cell surfaces is believed to be regulated by hydrophobic,[7-15] lectin–carbohydrate,[5, 16-19] or antigen–antibody interactions.[3, 20-22] Although all these interactions have been extensively studied individually to understand the mechanisms of microbial based pathogen infection,[7, 16, 19, 22-24] only a few reports described bacterium–cell interactions in *P. aeruginosa* infection.[8, 10, 13] The glycoproteins presented on mammalian cell membranes have a certain degree of hydrophobicity[25] that can attract and interact with bacterial lectins.[16, 26] Thus, bacterial adhesion to host tissues is regulated by both hydrophobic and lectin–carbohydrate interactions.

The hydrophobic and lectin–carbohydrate interactions on a quartz crystal microbalance with dissipation (QCM-D) have been compared. Compared to other sensing techniques (e.g., surface plasmon resonance (SPR),[27] surface forces apparatus (SFA),[22] mass spectrometry (MS),[28] and atomic force microscopy (AFM)[29]), the QCM-D with flow modules can simulate the physiological conditions and provides a dynamic view on

bacterial adhesion to a surface. Moreover, this technique provides the ability to probe the changes in softness (energy dissipation) and enables a better understanding on the bacterial adhesion process.[24, 30, 31] In the present study, the QCM-D sensor surface was therefore coated with three different types of polymers, namely, glyco-homopolymers, NIPAAm homoPolymer and their corresponding diblock copolymers (containing only a small amount of pendant carbohydrate residues). The diblock copolymers were synthesized by a one-pot reversible addition–fragmentation chain transfer (RAFT) polymerization[32] and directly immobilized on gold-coated QCM-D sensors.[24, 33] By comparing *P. aeruginosa* PAO1 adhesion on different thermally responsive surfaces at different temperatures (20 and 37 °C), it was found that the lectin–carbohydrate interactions played a prominent role in bacterial adhesion besides hydrophobicity of the surfaces.

4.2. Materials and Methods

4.2.1. Materials

Chemicals were purchased from Sigma-Aldrich Chemicals (Oakville, ON, Canada), and organic solvents were from Caledon Laboratories Ltd. (Georgetown, ON, Canada). The chain transfer agent 4-cyanopentanoic acid dithiobenzoate (CTP) and monomers were synthesized as previously described.[34-37]

4.2.2. Methods

Monomer structures and RAFT agent are shown in **Scheme 4-S1 in Appendix**. Average molecular weight (M_n) and polydispersity (M_w/M_n) were determined by gel permeation chromatography (GPC) using Pullulan standards (M_w = 5900–788 000 g mol^{-1}) at room temperature and a Viscotek model 250 dual detector [refractometer/viscometer in aqueous

eluents (0.5 M sodium acetate and 0.5 M acetic acid, for glyco-homopolymers) or in 10 mM lithium bromide *N*,*N*′-dimethylformamide (DMF) solution (for the thermally responsive polymers)] with flow rate of 1.0 mL/min. Bacterium–polymer interactions were studied with a QCM-D (Q-Sense, Sweden, E4 chamber) using gold-coated sensor chips (frequency: 4.95 MHz, 50 kHz; cut: AT; diameter: 14 mm; thickness: 0.3 mm; surface roughness <3 nm (RMS); electrode layer: 10–300 nm). The numbers of bacteria adhering to sensor surfaces were visualized by fluorescence microscopy (Microscope Axio Imager.M2, Carl Zeiss, Germany) with a wide-field fluorescence microscope excitation light source (X-cite 120Q, Lumen Dynamic, ON, Canada).

RAFT polymerization was chosen to prepare well-defined glycopolymers.[35, 37] In a typical polymerization of the homopolymers, 2-lactobionamidoethyl methacrylamide (LAEMA) (1 g, 2 mmol) was dissolved in 6 mL of distilled water in a 10 mL Schlenk tube with 1 mL of CTP (16 mg, 0. 057 mmol) and 4,4′-azobis (4-cyanovaleric acid) (ACVA) (8 mg, 0.032 mmol) in DMF stock solution. The tube was then sealed and degassed by purging it with nitrogen for 30 min. Polymerization was conducted in an oil bath (70 °C) for 24 h, followed by precipitation in acetone and subsequent washing with methanol to remove the unreacted monomers and residual RAFT agents. Polymerization was determined by Varian 500 ^{1}H NMR using D_2O. Polymer molecular weight and polydispersity were determined by aqueous gel permeation chromatography (GPC) (Viscotek GPC system) at room temperature with a flow rate of 1.0 mL/min.

3.2.2.1. One-Pot RAFT Synthesis of the Diblock Glycol-Copolymers

Diblock glycol-copolymers were prepared by one-pot RAFT synthesis in a water-DMF solution.[32] In a typical protocol on P(LAEMA-*b*-NIPAAm) synthesis, in a 10 mL Schlenk

tube, LAEMA (134.2 mg, 0.29 mmol) was dissolved in 2 mL of double distilled deionized water before the addition of CTP (20 mg, 0.072 mmol) and ACVA (10 mg, 0.040 mmol) in DMF stock solution (0.5 mL). After degassing under nitrogen atmosphere for 30 min, the flask was placed in a preheated oil bath (70 °C) for 4 h, followed by the addition of 14 mL of degassed NIPAAm (1.142 g, 10.10 mmol) and ACVA (10 mg, 0.040 mmol) in DMF. The mixture was continuously agitated at 70 °C for 24 h and then purified by dialysis against double distilled deionized water for 3 days to remove any unreacted monomers and RAFT agents (**Scheme 4-1**). After the polymers were obtained by freeze-drying, the conversion and composition of the copolymer were determined by Varian 500 ^{1}H NMR in D_2O. Polymer molecular weight and molecular weight distribution were determined by DMF GPC (Viscotek GPC system) at room temperature with a flow rate of 1.0 mL/min.[36]

3.2.2.2. Polymer Lower Critical Solution Temperature Measurements

Polymer lower critical solution temperatures (LCSTs) were determined from 50% transmittance of the 0.1 w/v% synthesized NIPAAm based polymers in aqueous solution at 500 nm with a heating rate of 0.5 °C/min with a UV–vis spectrometer.

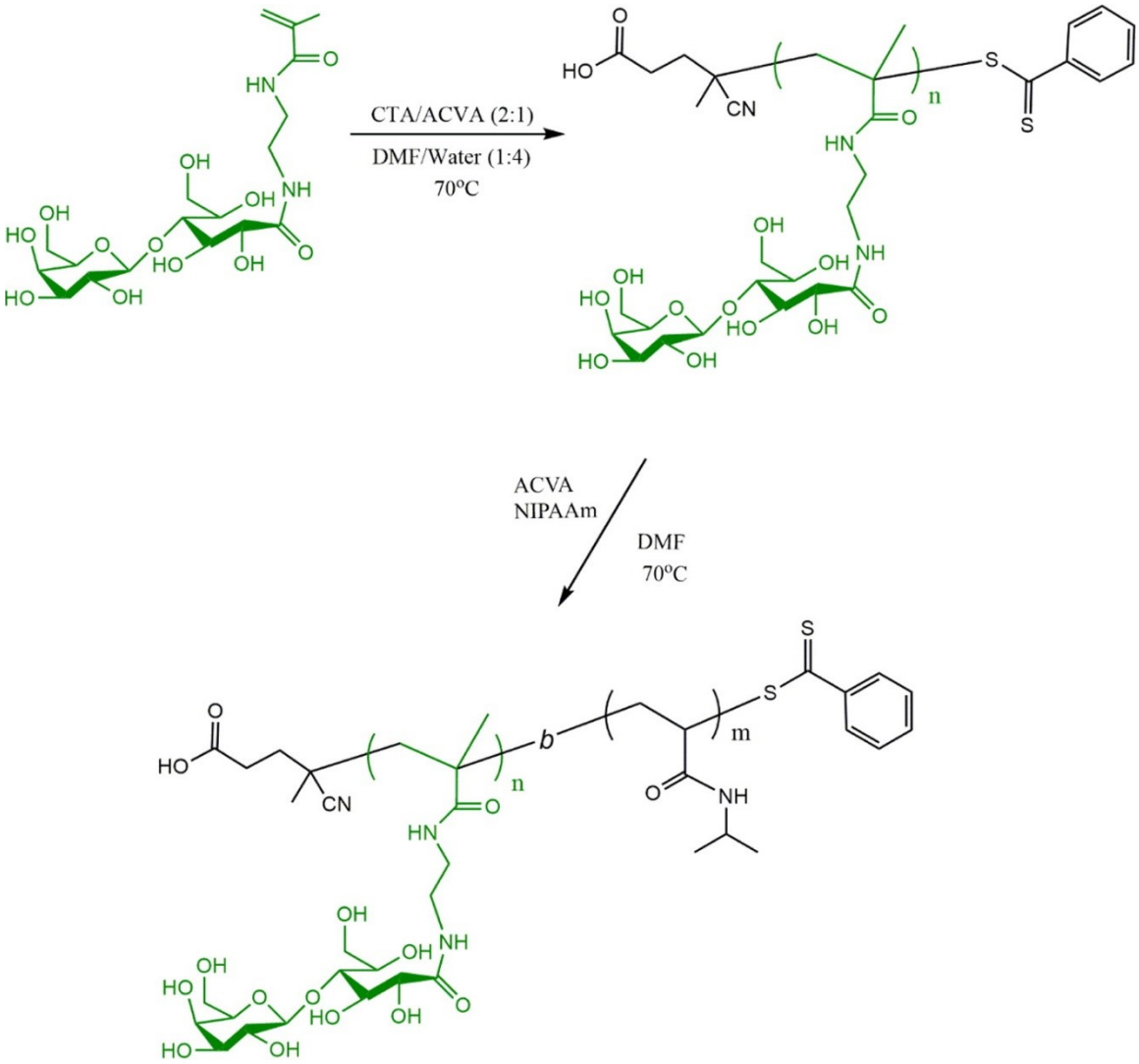

Scheme 4-1. One-Pot RAFT Synthesis of the Diblock Copolymer P(LAEMA-*b*-NIPAAm).

4.2.2.3. Bacterial Cultivation

P. aeruginosa PAO1 was streaked onto a Luria–Bertani (LB) agar plate and incubated at 37 °C overnight. A single colony was transferred into 5 mL of LB broth and grown overnight in a shaker incubator at 200 rpm and 37 °C. Stationary-phase hydrophobic bacterial cells with maximal lectin activity[38, 39] were harvested by centrifugation at 4000*g* and 4 °C for 5 min. After decanting the supernatant, the pellets were resuspended in a 10 mM $CaCl_2$ solution. The centrifugation (4000*g*, 5 min) and resuspension procedure was

repeated twice to remove traces of growth media and suspended extracellular polymeric substances from the solution.[40]

4.2.2.4. Studying the Bacteria–Polymer Interactions by QCM-D

Bacteria–polymer interactions were studied on a gold-coated QCM-D. Polymer aqueous solutions (1 mg/mL) were pumped into the sensor chambers at 20 °C with a flow rate of 50 μL/min to modify the gold-coated QCM-D sensor. When the frequency shifts were stable in the QCM-D (indicating that the polymer adsorption on the sensor surface was complete), the sensor surfaces were washed with DI water and then 10 mM $CaCl_2$ (0.15 mL/min) to remove weakly bound polymers from the surfaces. The bacterial suspension (10^7cells/mL) in 10 mM $CaCl_2$ was injected into the sensor chambers at 20 or 37 °C with a flow rate of 50 μL/min until the resonant frequencies of the sensors became stable.

Bacterial numbers on QCM-D sensor surfaces were counted with a fluorescent microscope (Microscope Axio Imager.M2, Carl Zeiss, Germany); for bacterial adhesion studied at 37 °C, temperature was controlled at 37 °C during the cell counting to avoid cell release from the thermal sensitive polymer surfaces.[41] All measurements were performed in duplicate with separately cultured bacteria.

After QCM-D measurement, bandwidths (Γ) were calculated using $\Gamma = Df/2$, where D is the dissipation shift measured by QCM-D and f is the frequency at each overtone (i.e., 5, 15, 25, 35, and 45 MHz at the fundamental frequency, third, fifth, seventh, and ninth overtone, respectively). The normalized shifts in frequency (Δf) and bandwidth ($\Delta\Gamma$) with the number of bacteria per unit area ($\Delta f/N_b$ and $\Delta\Gamma/N_b$) were then analyzed by small loading approximation. The small-loading approximation is an essential concept of QCM-D

analysis, which includes the well-known formalism of QCM data analysis for planar layer systems (i.e., the Sauerbrey equation). The relationship is given as

$$\frac{\Delta f^*}{N_b} = \frac{\Delta f + i\Delta\Gamma}{N_b} = \frac{f_F}{N_b \pi Z_q} f_{osc} \frac{m\omega(k + i\omega\zeta)}{m\omega^2 - (k + i\omega\zeta)'}$$

where f_F is the fundamental frequency (5 MHz), Z_q is the acoustic impedance of AT-cut quartz crystal (8.8×10^6 kg/m^2/s), k is the spring constant, and f_{osc} is the oscillator strength ($0 < f_{osc} < 1$). When bacterial cells interact with a sensor surface strongly ($k \gg m\omega^2$, $\Delta f^* = (-2f_F/Z_q)f_{osc}\Delta m$), they can move together with the resonator and can be termed as inertial loading in the Sauerbrey sense. For weak elastic bonding ($k \ll m\omega^2$), the frequency shift is positive and the equation can be rewritten as $\Delta f^* = (f_F/\pi Z_q)f_{osc}(k/\omega)$, describing elastic loading.

The circular relation between the shifts in bandwidth and frequency, $\Delta\Gamma/N_b$ and $\Delta f/N_b$, respectively, can be plotted on a polar diagram with radii proportional to the adhesive bond stiffness k:

$$2R \approx \frac{\Delta\Gamma(\omega = \omega_b)}{N_b} \approx \frac{f_F}{N_b \pi Z_q} f_{osc} \frac{m\omega_b(\omega_b^2 + i\omega_b\gamma)}{i\omega_b\gamma} \approx \frac{f_F}{N_b \pi Z_q} \frac{k}{\gamma'}$$

where γ is the introduced damping rate, as the ratio of the drag coefficient (ξ) and the mass of the particle (m), with the dimension of frequency.[24, 30, 31, 42, 43] The radius of the circles in polar diagrams representing bacterial adhesion on different surfaces were then calculated in MATLAB with the Taubin method.

4.3. Results and Discussions

4.3.1. Characterization of Thermally Responsive Diblock Copolymers

Glyco-homopolymers, NIPAAm homoPolymer and their corresponding thermally responsive diblock copolymers were synthesized by RAFT polymerization using dithiobenzoate as the RAFT agent. The RAFT process, which is applicable to a wide range of monomers under various conditions, enables one to control the polymer molecular weight and molecular weight distribution during the polymerization. Another advantage of RAFT polymerization is that the terminal dithioester groups can be used to directly interact with a gold surface[33] or can be reduced to thiol groups to introduce various functional groups.[44] RAFT polymerization was used here to have access to controlled telechelic polymer structures facilitating the interaction with the gold coated QCM-D surface.

Detailed characterization data of the synthesized polymers is shown in **Table 4-1**. The synthesized polymers showed relatively narrow molecular weight distributions. The copolymer compositions were determined by ^{1}H NMR (**Figure 4-S1 in Appendix**).

Table 4-1. Molecular Weight (M_n), Glycopolymer Content (φ), PDI (M_w/M_n), and Interactions with Bacterial Cells of Polymers Synthesized by RAFT

				bacterium–polymer interactions	
polymer[a]	φ (%)	M_n (GPC, g/mol)	M_w/M_n	20 °C	37 °C
P(GAPMA$_{39}$)	100	12 490	1.33	weak protein–carbohydrate interaction	weak protein–carbohydrate interaction
P(LAEMA$_{28}$)	100	13 338	1.30	strong protein–carbohydrate interaction	strong protein–carbohydrate interaction
P(NIPAAm$_{40}$)	0	4546	1.58	weak hydrophobic interaction	strong hydrophobic interaction
P(LAEMA$_2$-*b*-NIPAAm$_{40}$)	4	5656	1.31	weak hydrophobic interaction	strong protein–carbohydrate and hydrophobic interactions
P(GAPMA$_2$-*b*-NIPAAm$_{46}$)	4	6119	1.38	weak hydrophobic interaction	weak protein–carbohydrate and strong hydrophobic interactions

aP(GAPMA): glucose-derived glycopolymer; P(LAEMA): galactose-derived glycopolymer.

LCSTs of NIPAAm based polymers are shown in **Figure 4-1**. The LCST of the NIPAAm homopolymer is around 32 °C, which agrees with the results from other reports.[45-48] However, in the case of the diblock copolymers, the LCSTs were found to increase to around 36 °C (**Figure 4-1a**), which conflicts with previous reports.[49,50] The hydrophilic pendent carbohydrate residues in the polymer chains may play an important role in this observation. In the current study, the carbohydrate residues can be considered as the end functional group of the polymer and, therefore, would be expected to decrease intermolecular aggregation[51] and hence cause an increase in LCST of the diblock copolymers. Although the carbohydrate repeating units presented in P(LAEMA$_2$-*b*-

NIPAAm$_{40}$) and P(GAPMA$_2$-*b*-NIPAAm$_{46}$) were the same (**Table 4-1**), P(LAEMA$_2$-*b*-NIPAAm$_{40}$) shows a slightly higher LCST (**Figure 4-1a**). The LCST of poly(*N*-isopropylacrylamide) [P(NIPAAm)] has been reported to be inversely dependent on the molecular weight of the polymer;[52,53] therefore, the difference in LCST between P(LAEMA$_2$-*b*-NIPAAm$_{40}$) and P(GAPMA$_2$-*b*-NIPAAm$_{46}$) may be accounted for by the difference in molecular weight of the diblock copolymers (**Table 4-1**).

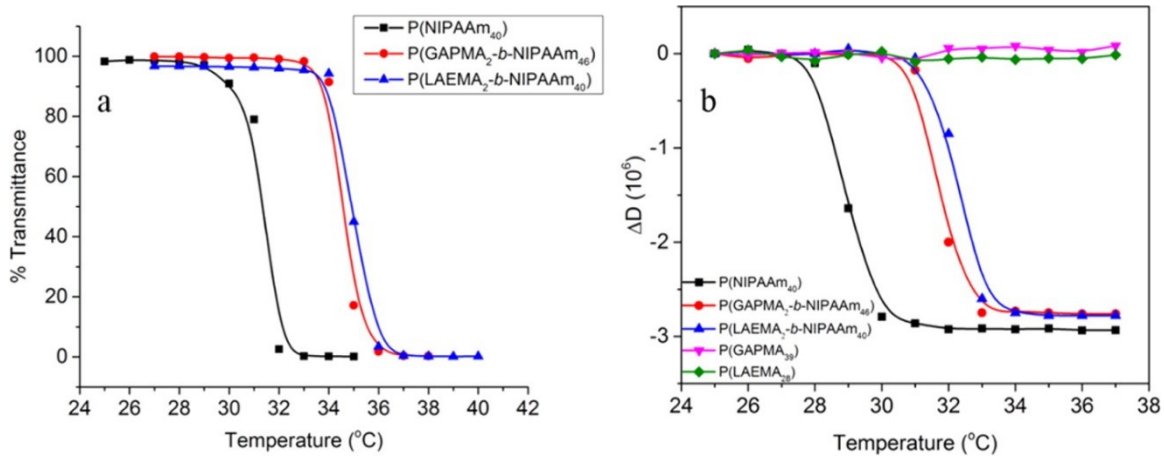

Figure 4-1. LCSTs of NIPAAm based polymers measured by (a) UV–vis and (b) QCM-D.

Although some studies claimed that, when the thermally responsive polymer was immobilized on a surface, its coil-to-globule transition temperature varied from its LCST in solution,[48] more recently, by measuring the thickness and contact angle changes of P(NIPAAm) brush in water as a function of temperature, Xue *et al.*[54] and Ko *et al.*[55] suggested that the polymer's coil-to-globule transition occurs at the temperature range of 23–32 °C and the polymer turns to its hydrophobic state at a temperature above the LCST. In this study, the P(NIPAAm) based polymers' coil-to-globule transition by QCM-D (**Figure 4-1b**) has been examined. The results showed that, at a temperature range between

28 and 34 °C, the thermally responsive polymers (P(NIPAAm$_{40}$), P(LAEMA$_2$-*b*-NIPAAm$_{40}$), and P(GAPMA$_2$-*b*-NIPAAm$_{46}$)) undergo coil-to-globule transition, which results in the dissipation decreases due to the dehydration of the polymer chains.[48] This result shows a good correlation with the LCSTs measured by UV–vis (**Figure 4-1a**) and indicates that the thermally responsive polymers are either completely hydrophilic or hydrophobic when comparing the bacterial adhesion at 20 and 37 °C, respectively.

4.3.2. Polymer Modification of Gold-Coated QCM-D Sensor Surfaces

The polymers synthesized by RAFT polymerization were directly deposited on gold-coated QCM-D surfaces at 20 °C due to the strong interactions of the dithioester end terminal groups on the gold surface.[33] The thickness and density of the polymer layer on the QCM-D sensor surface were calculated using the Sauerbrey function provided by QTools as shown in **Figure 4-2**. All polymers were successfully immobilized on gold-coated QCM-D surfaces and generated polymer films with the thickness in a range of 3 to 5 nm (**Figure 4-2a**), which is comparable to the result from other researchers.[56] Since the "grafting to" technique are used to anchor polymers on the gold-coated QCM-D sensor surface, the polymer film thickness is around half of the theoretical chain length values due to the polymers mushroom-like configuration at the sensor surface.[48] The polymers grafting density ranges from 0.02 to 0.09 nmol/cm^2 (**Figure 4-2b**). Compared to the results from Haddleton et al. that polymers with a dithio end group created less than 0.05 nmol/cm^2 surface coverage on a gold-coated QCM-D sensor surface,[33] the higher grafting density values that obtained in this study may be due to the shorter NIPAAm based polymers [P(NIPAAm$_{40}$), P(LAEMA$_2$-*b*-NIPAAm$_{40}$), and P(GAPMA$_2$-*b*-NIPAAm$_{46}$)] used. As expected, the glycopolymers [P(GAPMA$_{39}$) and P(LAEMA$_{28}$)] showed lower grafting

densities possibly due to their higher molecular weights and molecular crowding on the sensor surface.[28]

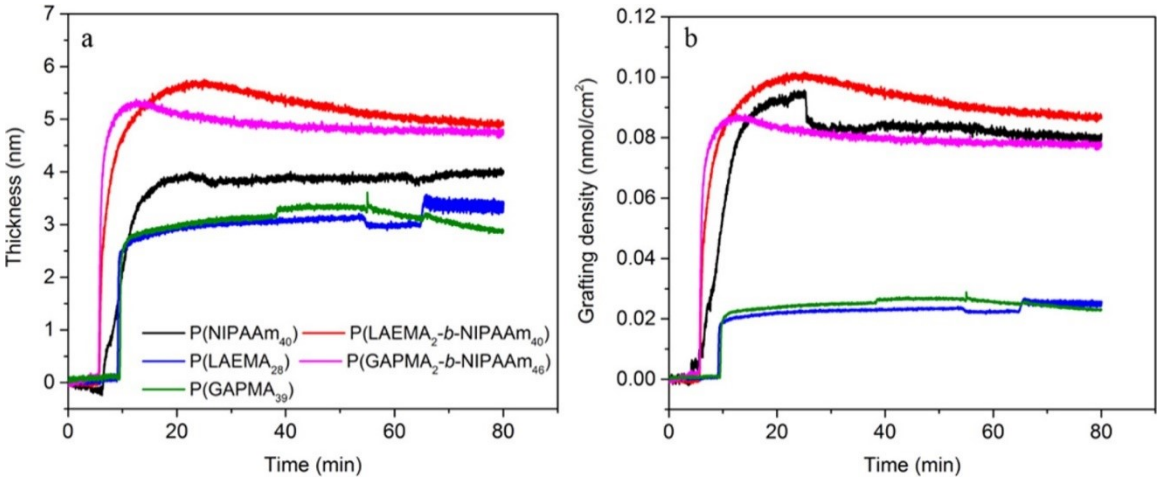

Figure 4-2. Thickness (a) and density (b) of polymer layers on QCM-D sensor surfaces.

4.3.3. *P. aeruginosa PAO1 Adhesion to QCM-D Sensor Surfaces Varied with Different Polymer Modifications*

Although *P. aeruginosa* PAO1 surface properties (e.g., LPS[57] and lectin[58] expression) may vary at different temperatures, and thereby affect bacterial adhesion,[59] previous studies suggested that *P. aeruginosa* adhesion on both hydrophilic (glass or poly(ethylene oxide) (PEO))[60] and hydrophobic (polystyrene)[61] surfaces can be barely affected within the temperature range of 20 and 37 °C. Therefore, in the present study, the effect of temperature in bacterial adhesion on thermally responsive polymers modified sensor surfaces is expected to be minimal.

The numbers of *P. aeruginosa* PAO1 adhesion to different polymer modified surfaces at 20 and 37 °C are shown in **Figure 4-3**. Compared to bacterial adhesion on glycopolymer modified surfaces, a significantly ($p < 0.05$) smaller amount of *P. aeruginosa* PAO1 is

observed from a carbohydrate-free P(NIPAAm$_{40}$) surface when temperature is controlled at 20 °C. Interestingly, although there are no glucose specific binding lectins present on the *P. aeruginosa* PAO1 membrane,[18,24] the bacteria can still interact with the P(GAPMA$_{39}$) surface and show a larger amount of cells adhered on the surface as compared to the galactose containing P(LAEMA$_{28}$) one. This observation might relate to the *P. aeruginosa* PAO1 cells interaction by their glucose transporters,[62,63] and the differences on bacterial cells adhesion on P(GAPMA$_{39}$) and P(LAEMA$_{28}$) surfaces might be explained by the "glycoside cluster effect".[64-67] On the other hand, an increase of the temperature from 20 to 37 °C seems to have negligible effect on *P. aeruginosa* PAO1 on P(LAEMA$_{28}$) and P(GAPMA$_{39}$) surfaces (p = 0.97, **Figure 4-3**); however, a significantly higher amount of bacterial cells could be found on the thermally responsive polymers surface [P(NIPAAm$_{40}$), P(LAEMA$_2$-*b*-NIPAAm$_{40}$), and P(GAPMA$_2$-*b*-NIPAAm$_{46}$)] as compared to the study performed at 20 °C (**Figure 4-3**). These observations can be explained as follows, at a temperature above the thermally responsive polymers LCST, the QCM-D surfaces become more hydrophobic, which would promote the bacterial adhesion.[41]

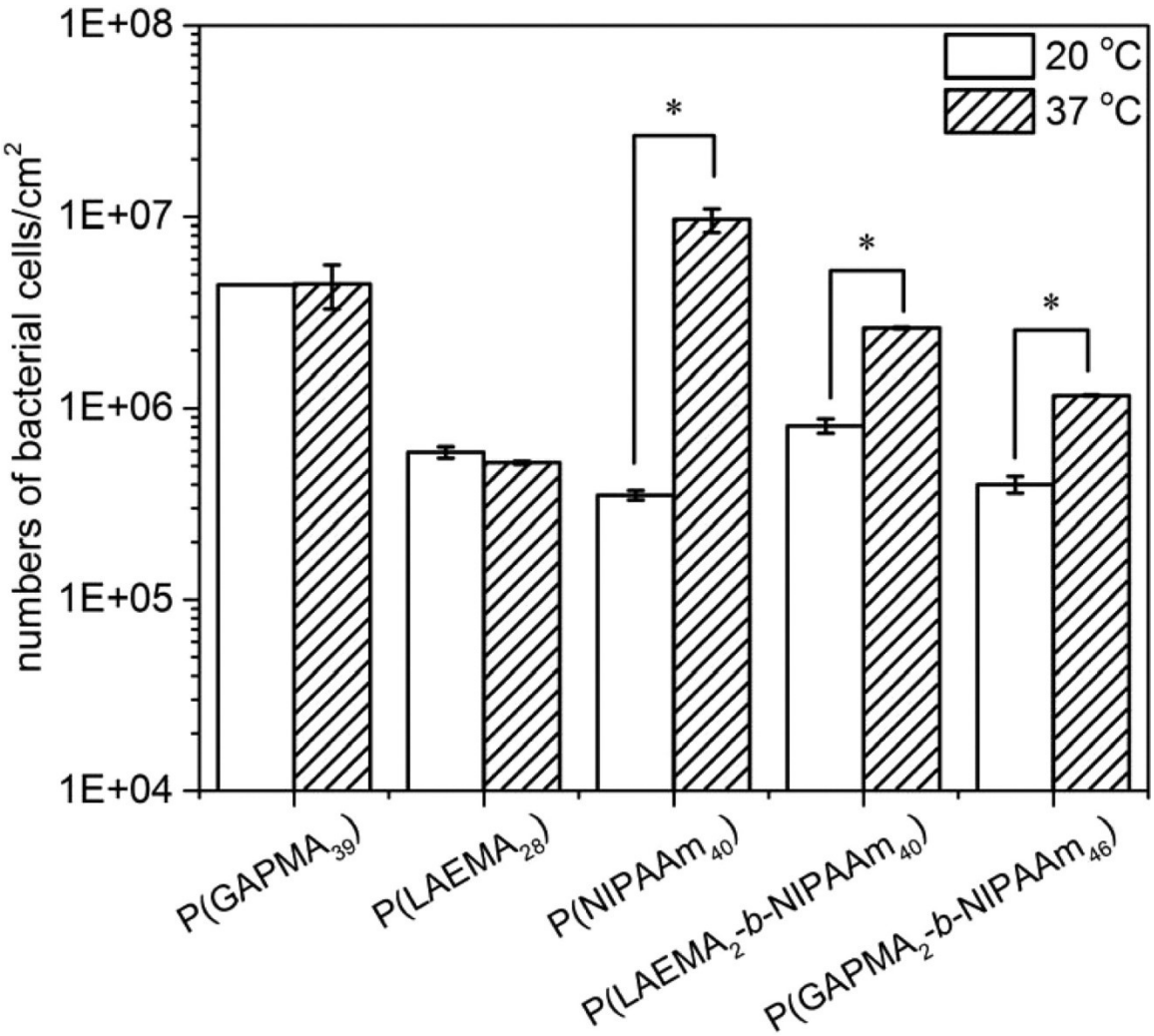

Figure 4-3. Numbers of *P. aeruginosa* PAO1 adhering to different polymer modified QCM-D surfaces at different temperatures. Values are presented as the mean ± SD ($n = 3$). The "asterisk" indicates significant differences ($p < 0.05$) on numbers of bacterial cells adhering on a surface at different temperatures.

Different bacterium–substratum interactions are also determined by QCM-D. At 20 and 37 °C, *P. aeruginosa* PAO1 adhesion to different polymer modified surfaces resulted in positive frequency shifts (**Figures 4-S2 and 4-S3 in Appendix**), which indicated that the bacteria linked elastically to the polymer surfaces.[13, 24, 30, 43] The frequency and bandwidth

shifts were normalized with numbers of bacteria (**Figure 4-3**) on each QCM-D sensor ($\Delta F/N_b$ and $\Delta\Gamma/N_b$, respectively), and the bacterium bond stiffness on different polymer surfaces were quantitatively analyzed by comparing the diameters of the circles in the polar diagrams (**Figure 4-4**).[30, 42]

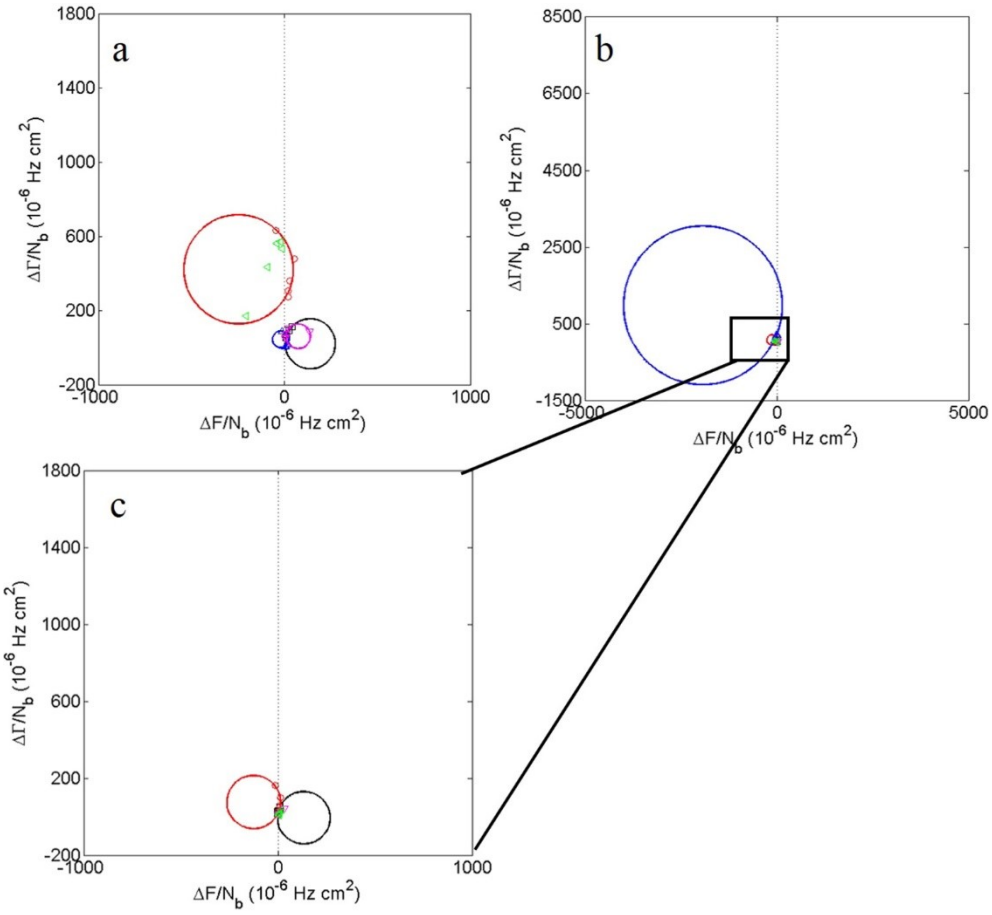

Figure 4-4. Polar diagrams of bandwidth and frequency shifts for (a) *P. aeruginosa* PAO1 adhesion to different polymer surfaces at 20 °C [$R_{P(LAEMA28)} > R_{P(GAPMA39)} > R_{P(LAEMA2\text{-}b\text{-}NIPAAm40)} > R_{P(NIPAAm40)}$], (b) *P. aeruginosa* PAO1 adhesion to different polymer surfaces at 37 °C [$R_{P(NIPAAm40)} \gg R_{P(GAPMA39)} \approx R_{P(LAEMA28)}$)], and (c) *P. aeruginosa* PAO1 adhesion to glycopolymers surfaces at 37 °C. [black: $P(GAPMA_{39})$; red: $P(LAEMA_{28})$; blue: $P(NIPAAm_{40})$; pink: $P(LAEMA_2\text{-}b\text{-}NIPAAm_{40})$; green: $P(GAPMA_2\text{-}b\text{-}NIPAAm_{46})$].

Figure 4-4 shows the polar diagrams of *P. aeruginosa* PAO1 adhering to different polymer surfaces at 20 and 37 °C. The largest radius ($R_{P(LAEMA28)}$ = 294.93 μHz cm^2) in the polar diagram for *P. aeruginosa* PAO1 adhering to a P(LAEMA$_{28}$) modified QCM-D sensor surface at 20 °C in **Figure 4-4a** indicates a high bacterium–polymer bond stiffness,[24, 30, 42] which is probably due to the specific ligand–receptor interactions between galactose moieties on the glycopolymer backbones[37] and lectin (PA-IL) moieties on the bacterial membranes.[18,24] Although higher numbers of *P. aeruginosa* PAO1 were observed on the glucose-derived P(GAPMA$_{39}$)[36] modified surface as compared to the galactose based glycopolymer [P(LAEMA$_{28}$)] surface (**Figure 4-3**), the bacterial adhesion on the P(GAPMA$_{39}$) surface was found to be less elastic and showed a smaller radius in the polar diagrams ($R_{P(GAPMA39)}$ = 135.48 μHz cm^2, **Figure 4-5a**) as compared to the bacterial adhesion event on the P(LAEMA$_{28}$) surface,[24] and this could be due to the fact that there are no glucose specific binding lectins on the *P. aeruginosa* PAO1 membrane.[17]

Interestingly, the radius for bacterial adhesion to the P(LAEMA$_2$-*b*-NIPAAm$_{40}$) modified surface ($R_{P(LAEMA2\text{-}b\text{-}NIPAAm40)}$ = 66.89 μHz cm^2) at 20 °C was found to be much smaller than $R_{P(LAEMA28)}$ but closer to that on the P(NIPAAm$_{40}$) modified surface ($R_{P(NIPAAm40)}$ = 45.29 μHz cm^2) (**Figure 4-4a**). On the basis of the "glycoside cluster effect" which implies that multivalent saccharide ligands can improve the binding affinity of carbohydrate–lectin interactions,[64-67] the above observation may be due to the number of galactose residues accessible on the P(LAEMA$_2$-*b*-NIPAAm$_{40}$) modified sensor surface. At 20 °C, P(LAEMA$_2$-*b*-NIPAAm$_{40}$) chains on the sensor surface are more hydrophilic, and hence, due to the random coil conformation of the chains, some of the carbohydrate residues may be buried within the polymer chains and may not be accessible on the surface to interact

with the *P. aeruginosa* PAO1 membrane (**Scheme 4-2**).[41, 49, 68, 69] Therefore, in this condition, *P. aeruginosa* PAO1 adhesion to P(LAEMA$_2$-*b*-NIPAAm$_{40}$) modified sensor surfaces was similar to that on P(NIPAAm$_{40}$) surfaces, providing the stiffness values presented in **Figure 4-4a**.

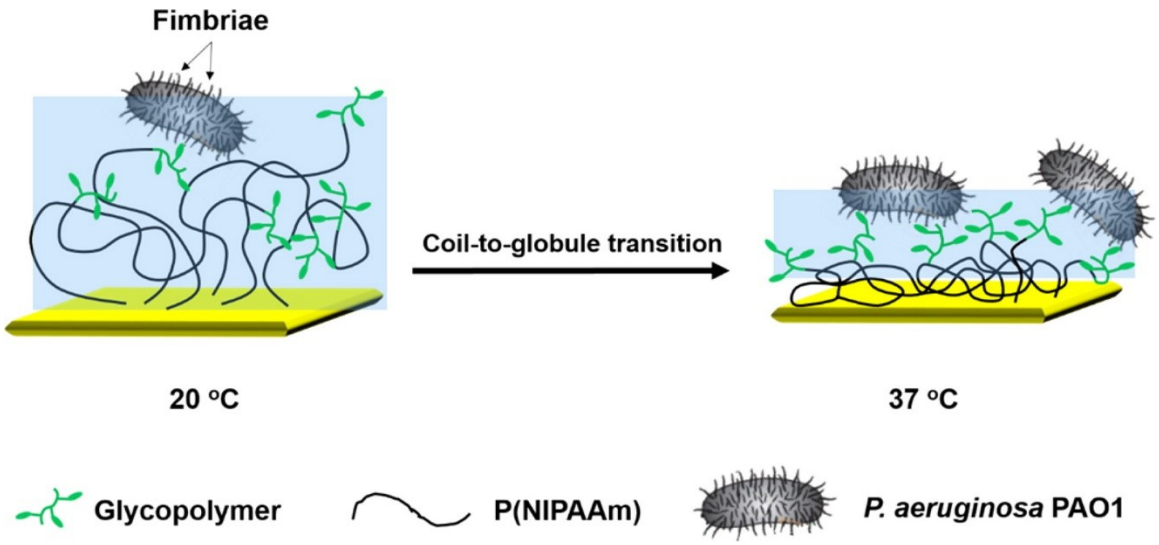

Scheme 4-2. Schematic Representation of *P. aeruginosa* PAO1 Adhesion on a Thermally Responsive P(LAEMA$_2$-*b*-NIPAAm$_{40}$) Modified QCM-D Sensor Surface at Different Temperatures.

At 37 °C, the $R_{P(GAPMA39)}$ value for bacterial adhesion to the P(GAPMA$_{39}$) modified surface is 136.49 μHz cm^2 (black circle, **Figure 4-4c**), which is close to the result obtained on the same surface at 20 °C (135.48 μHz cm^2, black circle in **Figure 4-4a**). Interestingly, for the P(LAEMA$_{28}$) modified surface, the $R_{P(LAEMA28)}$ value was reduced to 138.61 μHz cm^2 at 37 °C (pink circle, **Figure 4-4c**) as compared to the one obtained for bacterial adhesion on the same surface at 20 °C (294.93 μHz cm^2). This could be due to the decrease in binding affinity of the PA-IL to galactose residues as the temperature was increased from 20 to 37 °C.[50]

Both the numbers of *P. aeruginosa* PAO1 (Figures **4-3 and 4-5**) and the radii in polar diagrams ($R_{P(NIPAAm40)}$ = 2073.40 μHz cm^2, **Figure 4-4b**) for bacterial adhesion on the P(NIPAAm$_{40}$) surface were found to increase significantly at 37 °C. These results showed a stronger bacterium–substratum bond stiffness formed on the P(NIPAAm$_{40}$) modified surface at 37 °C indicative of the hydrophobic nature of the P(NIPAAM) where the temperature is above the LCST.[46,47] However, this may not be a valid explanation due to the aggregation of the *P. aeruginosa* PAO1 cells on the P(NIPAAm$_{40}$) modified surface at 37 °C making the cell counting difficult, and hence, the bond stiffness predicted in the polar diagrams may be incorrect (**Figure 4-5**). In addition, it was not possible to determine the bond stiffness involved in bacterial adhesion to P(LAEMA$_2$-*b*-NIPAAm$_{40}$) and P(GAPMA$_2$-*b*-NIPAAm$_{46}$) surfaces using the coupled resonance model, as the frequency shifts were positive at all overtones (Figure 4-S3 in Appendix) and no zero crossing frequencies could be observed from the polar diagrams (**Figure 4-4c**).[31] To address these issues and compare *P. aeruginosa* PAO1 adhesion to different polymer surfaces at 37 °C, $\Delta F/\Delta D$ values were instead used to cancel out the effect of bacterial numbers in the bacterium–substratum connection analysis. A higher $\Delta F/\Delta D$ value is usually associated with a stronger elastic connection.[13]

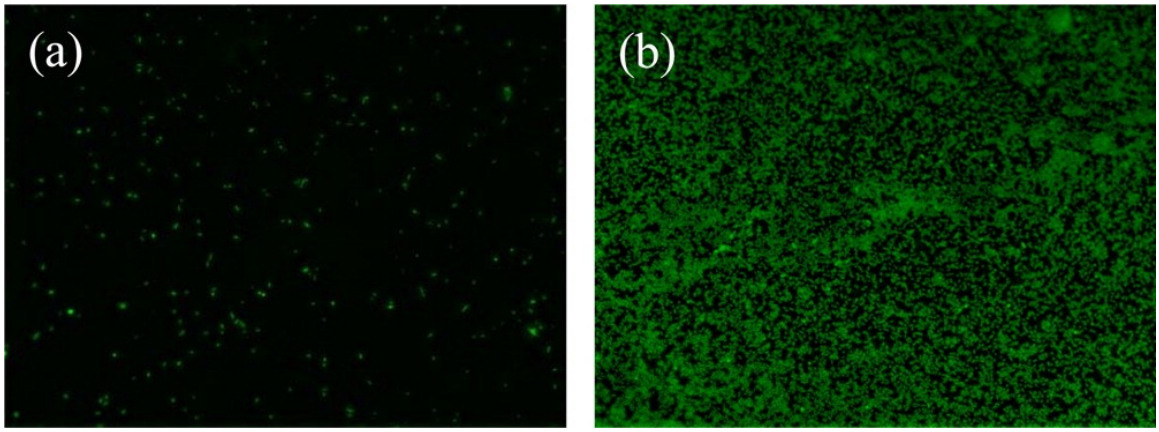

Figure 4-5. *P. aeruginosa* PAO1 adhesion to a P(NIPAAm$_{40}$) modified sensor surface at different temperatures (a: 20 °C; b: 37 °C).

The $\Delta F/\Delta D$ values of *P. aeruginosa* PAO1 adhesion to different polymer surfaces at 20 and 37 °C are shown in **Figure 4-6a and 4-6b**, respectively. The values for bacterial adhesion to different polymer surfaces at 20 °C (**Figure 4-6a**) and the P(LAEMA$_{28}$) surface at 37 °C (**Figure 4-6b**) showed good agreement with the results from the polar diagrams (**Figure 4-4a and 4-4c**). Interestingly, although bacterial adhesion to the P(GAPMA$_{39}$) modified surface showed a similar bond stiffness at different temperatures in the polar diagrams (**Figure 4-4a and 4-4c**), $\Delta F/\Delta D$ values calculated at different temperatures gave different results. At low overtones, $\Delta F/\Delta D$ values for bacterial adhesion to the P(GAPMA$_{39}$) surface were positive at 37 °C but became less positive at higher overtones ($n > 5$) (**Figure 4-6b**). This behavior may be due to the increasing flexibility of bacterium–polymer chains at higher temperature. Negative $\Delta F/\Delta D$ values at high overtones are due to the viscous takeover as this is the predominant factor in the viscoelastic bacterium–substratum connection.[13]

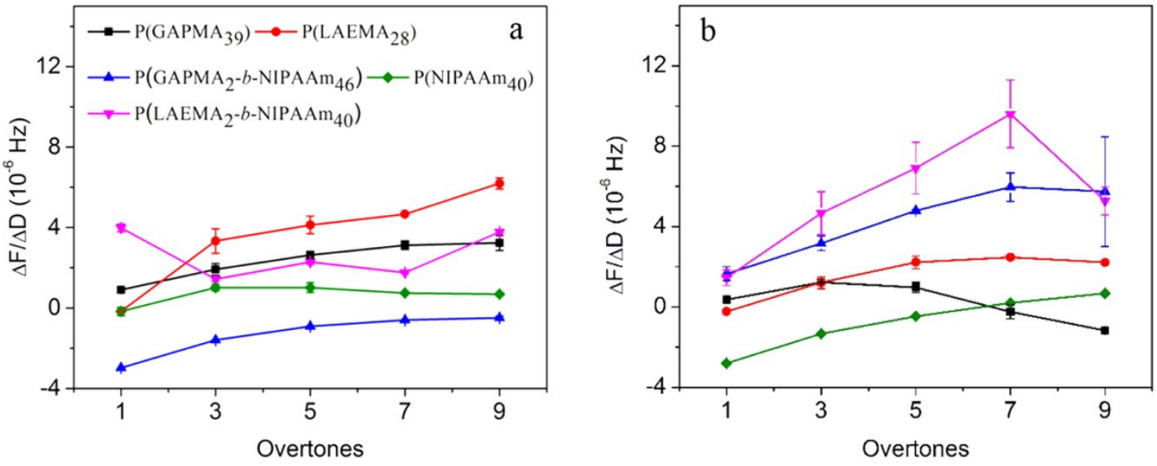

Figure 4-6. Δ*F*/ΔD values calculated at the end of *P. aeruginosa* PAO1 adhesion to different surfaces. (a) 20 °C; (b) 37 °C.

Interestingly, at 37 °C, although bacterial adhesion to the P(NIPAAm$_{40}$) modified surface showed the highest bond stiffness in the polar diagrams (**Figure 4-4b**), this result was not in agreement to the data shown in **Figure 4-6b**. The lowest Δ*F*/ΔD values obtained for *P. aeruginosa* PAO1 adhesion to the P(NIPAAm$_{40}$) modified surface at 37 °C suggested that the bacterium interacted weakly with the hydrophobic P(NIPAAm$_{40}$) surface. As bacterial cells aggregated on the P(NIPAAm$_{40}$) surface at 37 °C (**Figure 4-5**), an increase in dissipation was observed, possibly due to the large amount of water entrapped between bacterial cells or by viscous friction at the liquid gaps on bacterium–bacterium and bacterium–substratum interfaces.[13] The highest Δ*F*/ΔD values were observed when bacterial adhered on the P(LAEMA$_2$-*b*-NIPAAm$_{40}$) surface at 37 °C. Since the thermally responsive glycopolymer (P(LAEMA$_2$-*b*-NIPAAm$_{40}$)) turned to its hydrophobic state and exposed more carbohydrate residues (galactose) during the coil-to-globular transition at a temperature higher than its LCST, an enhanced *P. aeruginosa* PAO1 adhesion on the

P(LAEMA$_2$-*b*-NIPAAm$_{40}$) surface was noted to be possibly driven by both hydrophobic[14] and lectin–carbohydrate interactions (**Scheme 4-2**).[24]

To further illustrate the role of lectin–carbohydrate and hydrophobic interactions in bacterial adhesion on the surface, a competitive assay has been performed here, in which the interaction between galactophilic lectin (PA-IL) and galactose containing glycopolymers was competitively blocked by the addition of an excess of galactose containing compound (lactobionic acid) into the bacterial suspension. The $\Delta F/\Delta D$ values of *P. aeruginosa* PAO1 adhesion to different polymer surfaces in the presence of lactobionic acid at 20 and 37 °C are shown in **Figure 4-7a and 7b**, respectively.

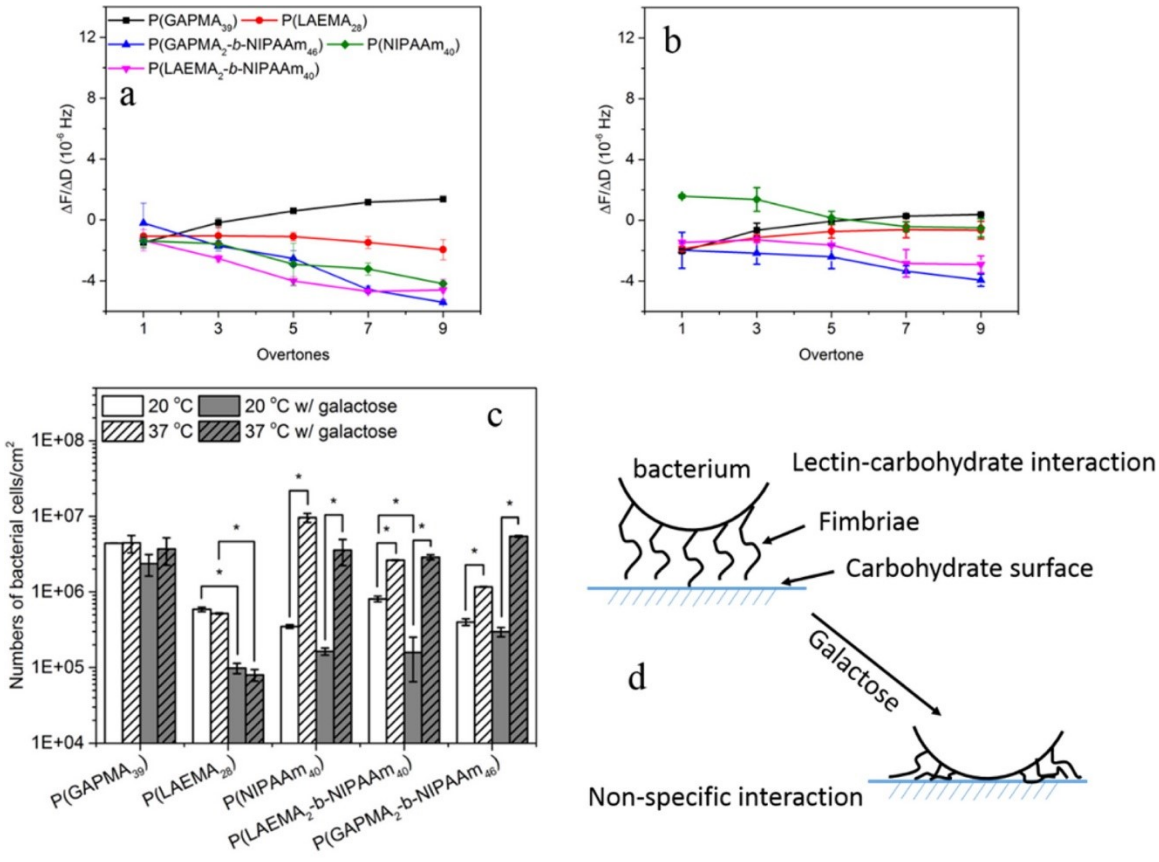

Figure 4-7. $\Delta F/\Delta D$ values calculated when *P. aeruginosa* PAO1 adheres to different surfaces in the presence of lactobionic acid. (a) 20 °C; (b) 37 °C. (c) Numbers of *P. aeruginosa* PAO1 adhering to different polymer modified QCM-D surfaces at different temperatures. The "asterisk" indicates significant differences ($p < 0.05$) on numbers of bacterial cells adhering on a surface at different temperatures. Values are presented as the mean ± SD ($n = 3$). (d) Schematic illustration of nonspecific and lectin–carbohydrate based bacterium–substratum interactions.

Compared to the bacterial adhesion to galactose containing glycopolymer surfaces [P(LAEMA$_{28}$) and P(LAEMA$_2$-*b*-NIPAAm$_{40}$)] at 20 °C (**Figure 4-6a**), the $\Delta F/\Delta$D values shifted to negative values when lactobionic acid was added in the bacterial suspension (**Figure 4-7a**), indicating contact between bacterium and carbohydrate substratum has changed from elastic to a weaker viscous connection (Figure 7d). These changes might relate to the blocking of the interaction between the bacterial galactophilic PA-IL and galactose containing glycopolymers, as the numbers of *P. aeruginosa* PAO1 on P(LAEMA$_{28}$) and P(LAEMA$_2$-*b*-NIPAAm$_{40}$) surfaces are reduced significantly in lactobionic acid solution at 20 °C (**Figures 4-7c and 4-S4 in Appendix**). On the other hand, compared to *P. aeruginosa* PAO1 adhesion on polymer surfaces in 10 mM Ca^{2+} (**Figures 4-3 and 4-6a**), neither bacterium–substratum interaction (**Figure 4-7a**) nor numbers of bacterial cells (**Figure 4-7c**) on P(GAPMA$_{39}$), P(GAPMA$_2$-*b*-NIPAAm$_{46}$), and P(NIPAAm$_{40}$) surfaces has been changed significantly in lactobionic acid solution. These observations might suggest that the addition of lactobionic acid only affects the lectin–carbohydrate interaction between *P. aeruginosa* PAO1 and galactose containing polymers.

At 37 °C, although the galactophilic PA-IL has been blocked by lactobionic acid, the numbers of *P. aeruginosa* PAO1 observed on the three thermally responsive polymer [P(NIPAAm$_{40}$), P(GAPMA$_2$-*b*-NIPAAm$_{46}$), and P(LAEMA$_2$-*b*-NIPAAm$_{40}$)] surfaces are close (**Figure 4-7c**). The above observations might be due to the increased hydrophobicity of the surface enhancing the bacterium–substratum affinity. On the other hand, similar to bacterial adhesion to the P(LAEMA$_{28}$) and P(LAEMA$_2$-*b*-NIPAAm$_{40}$) surface at 20 °C (**Figure 4-7a**), the $\Delta F/\Delta D$ shifted to negative values at 37 °C when lactobionic acid was introduced to the bacterial suspension (**Figure 4-7b**). Interestingly, although no galactose is present on P(NIPAAm$_{40}$) and P(GAPMA$_2$-*b*-NIPAAm$_{46}$), in lactobionic acid solution, the $\Delta F/\Delta D$ values also change their signs at 37 °C (**Figure 4-7b**) as compared to the results obtained in 10 mM Ca^{2+} (**Figure 4-6b**). These results showed a very good agreement to Marcus et al.'s study[13] in which the hydrophilic *P. aeruginosa* PAO1 adhered to a surface. Therefore, when the negatively charged lactobionic acid (pK_a = 3.8) is bound to the galactophilic PA-IL on the *P. aeruginosa* PAO1 membrane, the bacterial surface become more hydrophilic so that more water would appear on the bacterium–substratum interface, which may alter the bacterium–substratum interaction or increase the viscous friction to make the $\Delta F/\Delta D$ values closer to zero (**Figure 4-7b**).

4.4. Conclusions

Well-defined thermally responsive glycopolymers carrying galactose residues as pendant groups were successfully synthesized by the one-pot RAFT process and subsequently immobilized on gold-coated QCM-D sensor surfaces. Interactions between the polymers and *P. aeruginosa* PAO1 were studied by QCM-D at 20 and 37 °C and analyzed by a coupled resonance model. Although a significantly higher number of *P. aeruginosa* PAO1

adhered to a hydrophobic surface [P(NIPAAm$_{40}$)] at 37 °C than at 20 °C, the bond stiffness was much lower as compared to bacterial adhesion to glycopolymer homopolymers [P(LAEMA$_{28}$) and P(GAPMA$_{39}$)] and biomimetic cell surfaces [P(LAEMA$_2$-*b*-NIPAAm$_{40}$) and P(GAPMA$_2$-*b*-NIPAAm$_{46}$) modified sensor surfaces]. These results suggest that bacterial adhesion is regulated by specific lectin–carbohydrate interactions and is expected to be the dominant factor in pathogen infection.

4.5. References

1. M. B. Campa, Mauro Herman, Friedman, *Pseudomonas aeruginosa as an Opportunistic Pathogen*, Springer US, New York, 1993.

2. J. B. Lyczak, C. L. Cannon and G. B. Pier, *Microbes. Infect.* 2000, **2**, 1051-1060.

3. G. B. Pier, in *Goldman's Cecil Medicine (Twenty-Fourth Edition)*, W.B. Saunders, Philadelphia, 2012, pp. 1877-1881.

4. M. Larrosa, P. Truchado, J. C. Espín, F. A. Tomás-Barberán, A. Allende and M. T. García-Conesa, *Mol. Cell. Probes* 2012, **26**, 121-126.

5. P. Doig, T. Todd, P. A. Sastry, K. K. Lee, R. S. Hodges, W. Paranchych and R. T. Irvin, *Infect. Immun.* 1988, **56**, 1641-1646.

6. R. R. Maddikeri, S. Tosatti, M. Schuler, S. Chessari, M. Textor, R. G. Richards and L. G. Harris, *J. Biomed. Mater. Res. Part A.* 2008, **84A**, 425-435.

7. M. C. van Loosdrecht, J. Lyklema, W. Norde, G. Schraa and A. J. Zehnder, *Appl. Environ. Microbiol.* 1987, **53**, 1893-1897.

8. H. J. Busscher and A. H. Weerkamp, *FEMS Microbiol. Lett.* 1987, **46**, 165-173.

9. R. Bos, H. C. van der Mei and H. J. Busscher, *FEMS Microbiology Reviews*, 1999, **23**, 179-230.

10. R. J. Doyle, *Microb. Infect.*, 2000, **2**, 391-400.

11. G. M. Bruinsma, H. C. van der Mei and H. J. Busscher, *Biomaterials* 2001, **22**, 3217-3224.

12. A. G. Karakecili and M. Gumusderelioglu, *J. Biomater. Sci., Polym. Ed.* 2002, **13**, 185-196.

13. I. M. Marcus, M. Herzberg, S. L. Walker and V. Freger, *Langmuir* 2012, **28**, 6396-6402.

14. G. Hwang, J. Liang, S. Kang, M. Tong and Y. Liu, *BioChem. Eng. J.* 2013, **76**, 90-98.

15. G. Hwang, S. Kang, M. G. El-Din and Y. Liu, *Biofouling* 2012, **28**, 525-538.

16. N. Sharon, *FEBS Lett.* 1987, **217**, 145-157.

17. D. Tielker, S. Hacker, R. Loris, M. Strathmann, J. Wingender, S. Wilhelm, F. Rosenau and K.-E. Jaeger, *Microbiology*, 2005, **151**, 1313-1323.

18. S. P. Diggle, R. E. Stacey, C. Dodd, M. Cámara, P. Williams and K. Winzer, *Environ. Microbiol.* 2006, **8**, 1095-1104.

19. Z. Shen, M. Huang, C. Xiao, Y. Zhang, X. Zeng and P. G. Wang, *Anal. Chem.* 2007, **79**, 2312-2319.

20. G. B. Pier, *Int. J. Med. Microbiol.* 2007, **297**, 277-295.

21. M. J. Preston, J. M. Berk, L. D. Hazlett and R. S. Berk, *Infect. Immun.* 1991, **59**, 1984-1990.

22. Q. Lu, J. Wang, A. Faghihnejad, H. Zeng and Y. Liu, *Soft Matter* 2011, **7**, 9366-9379.

23. X.-L. Su and Y. Li, *Biosens. Bioelectron.* 2005, **21**, 840-848.

24. Y. Wang, R. Narain and Y. Liu, *Langmuir* 2014, **30**, 7377-7387.

25. H. Ghebeh, J. Gillis and M. Butler, *J. Biotechnol.* 2002, **95**, 39-48.

26. K. A. Krogfelt, H. Bergmans and P. Klemm, *Infect. Immun.* 1990, **58**, 1995-1998.

27. A. Pranzetti, S. Salaün, S. Mieszkin, M. E. Callow, J. A. Callow, J. A. Preece and P. M. Mendes, *Adv. Funct. Mater.* 2012, **22**, 3672-3681.

28. Y.-T. Tseng, H.-Y. Chang and C.-C. Huang, *Chem. Commun.* 2012, **48**, 8712-8714.

29. A. Razatos, Y.-L. Ong, M. M. Sharma and G. Georgiou, *Proceedings of the National Academy of Sciences of the United States of America*, 1998, **95**, 11059-11064.

30. A. L. J. Olsson, H. C. van der Mei, D. Johannsmann, H. J. Busscher and P. K. Sharma, *Anal. Chem.* 2012, **84**, 4504-4512.

31. A. L. J. Olsson, H. C. van der Mei, H. J. Busscher and P. K. Sharma, *Langmuir* 2010, **26**, 11113-11117.

32. I. Chaduc, W. Zhang, J. Rieger, M. Lansalot, F. D'Agosto and B. Charleux, *Macromol. Rapid Commun.* 2011, **32**, 1270-1276.

33. S. Slavin, A. H. Soeriyadi, L. Voorhaar, M. R. Whittaker, C. R. Becer, C. Boyer, T. P. Davis and D. M. Haddleton, *Soft Matter* 2011, **8**, 118-128.

34. M. Benaglia, E. Rizzardo, A. Alberti and M. and Guerra, *Macromolecules*, 2005, **38**, 3129-3140.

35. Z. Deng, H. Bouchékif, K. Babooram, A. Housni, N. Choytun and R. Narain, *J. Polym. Sci., Part A: Polym. Chem.* 2008, **46**, 4984-4996.

36. Z. Deng, M. Ahmed and R. Narain, *J. Polym. Sci., Part A: Polym. Chem.* 2009, **47**, 614-627.

37. Z. Deng, S. Li, X. Jiang and R. Narain, *Macromolecules*, 2009, **42**, 6393-6405.

38. A. H. Rickard, S. A. Leach, C. M. Buswell, N. J. High and P. S. Handley, *Appl. Environ. Microbiol.* 2000, **66**, 431-434.

39. S. P. Diggle, K. Winzer, S. R. Chhabra, K. E. Worrall, M. Cámara and P. Williams, *Mol. Microbiol.* 2003, **50**, 29-43.

40. X. Sun, C. Danumah, Y. Liu and Y. Boluk, *Chem. Eng. J.* 2012, **198-199**, 476-481.

41. M. Ebara, M. Yamato, T. Aoyagi, A. Kikuchi, K. Sakai and T. Okano, *Adv. Mater.* 2008, **20**, 3034-3038.

42. A. L. J. Olsson, N. Arun, J. S. Kanger, H. J. Busscher, I. E. Ivanov, T. A. Camesano, Y. Chen, D. Johannsmann, H. C. van der Mei and P. K. Sharma, *Soft Matter* 2012, **8**, 9870-9876.

43. I. Reviakine, D. Johannsmann and R. P. Richter, *Anal. Chem.* 2011, **83**, 8838-8848.

44. H. Willcock and R. K. O'Reilly, *Polym. Chem.* 2010, **1**, 149-157.

45. I. C. Barker, J. M. G. Cowie, T. N. Huckerby, D. A. Shaw, I. Soutar and L. Swanson, *Macromolecules*, 2003, **36**, 7765-7770.

46. E. S. Gil and S. M. Hudson, *Prog. Polym. Sci.* 2004, **29**, 1173-1222.

47. T. Hoare and R. Pelton, *Macromolecules*, 2007, **40**, 670-678.

48. G. Z. Zhang, *Macromolecules*, 2004, **37**, 6553-6557.

49. N. Idota, M. Ebara, Y. Kotsuchibashi, R. Narain and T. Aoyagi, *Sci. Technol. Adv. Mater.* 2012, **13**.

50. G. H. Chen and A. S. Hoffman, *Nature*, 1995, **373**, 49-52.

51. Q. Duan, Y. Miura, A. Narumi, X. Shen, S.-I. Sato, T. Satoh and T. Kakuchi, *J. Polym. Sci., Part A: Polym. Chem.* 2006, **44**, 1117-1124.

52. S. Furyk, Y. Zhang, D. Ortiz-Acosta, P. S. Cremer and D. E. Bergbreiter, *J. Polym. Sci., Part A: Polym. Chem.* 2006, **44**, 1492-1501.

53. Y. Xia, N. A. D. Burke and H. D. H. Stöver, *Macromolecules*, 2006, **39**, 2275-2283.

54. C. Xue, N. Yonet-Tanyeri, N. Brouette, M. Sferrazza, P. V. Braun and D. E. Leckband, *Langmuir* 2011, **27**, 8810-8818.

55. H. Ko, Z. Zhang, Y.-L. Chueh, E. Saiz and A. Javey, *Angew. Chem. Int. Ed.* 2010, **49**, 616-619.

56. F. Montagne, J. Polesel-Maris, R. Pugin and H. Heinzelmann, *Langmuir* 2008, **25**, 983-991.

57. S. A. Makin and T. J. Beveridge, *J. Bacteriol.* 1996, **178**, 3350-3352.

58. N. Gilboa-Garber and D. Sudakevitz, *FEMS Immunol. Med. Microbiol.* 1999, **25**, 365-369.

59. S. A. Makin and T. J. Beveridge, *Microbiology*, 1996, **142**, 299-307.

60. A. Roosjen, H. C. van der Mei, H. J. Busscher and W. Norde, *Langmuir* 2004, **20**, 10949-10955.

61. A. E. Zeraik and M. Nitschke, *Braz. arch. biol. technol.* 2012, **55**, 569-576.

62. G. Cioci, E. P. Mitchell, C. Gautier, M. Wimmerová, D. Sudakevitz, S. Pérez, N. Gilboa-Garber and A. Imberty, *FEBS Lett.* 2003, **555**, 297-301.

63. M. Ahmed and R. Narain, *Biomaterials* 2011, **32**, 5279-5290.

64. J. J. Lundquist and E. J. Toone, *Chem. Rev.* 2002, **102**, 555-578.

65. Y. C. Lee and R. T. Lee, *Acc. Chem. Res.* 1995, **28**, 321-327.

66. E. M. Munoz, J. Correa, E. Fernandez-Megia and R. Riguera, *J. Am. Chem. Soc.* 2009, **131**, 17765-17767.

67. Y. Wang, Y. Kotsuchibashi, K. Uto, M. Ebara, T. Aoyagi, Y. Liu and R. Narain, *Biomater. Sci.*, 2014, **3**, 152-162.

68. Y. Wang, Y. Kotsuchibashi, Y. Liu and R. Narain, *Langmuir* 2014, **30**, 2360-2368.

69. J. Hu and S. Liu, *Macromolecules*, 2010, **43**, 8315-8330.

70. G. Cioci, E.P. Mitchell, C. Gautier, M. Wimmerová, D. Sudakevitz, S. Pérez, N. Gilboa-Garber, A. Imberty, *FEBS Lett.* 2003, **555***,* 297-301.

71. M. Ahmed, and R. Narain, *Biomaterials* 2011, **32***,* 5279-5290.

Chapter 5. pH and Glucose Responsive Nanofibers for the Reversible Capture and Release of Lectin

The content of this chapter was published in *Biomat. Sci.* **2015**, 3, 152-162.

Chapter 5

5.1. Introduction

Over the past few decades, nanofibers of various polymers or inorganic materials with diameters ranging from a few tens of nanometers to a few micrometers have been produced by relatively simple and low-cost electrospinning techniques.[1] The obtained nanofibrous mats have shown great success in various fields, including tissue engineering,[2] drug delivery,[3] membrane filtration,[4,5] and sensors,[6,7] due to their extremely large surface area and high porosity.[1,5] Among the numerous electrospun materials, glycopolymers are believed to be one of the most attractive, not only because of the important roles that carbohydrate–protein interactions play in many biological processes,[8,9] but also due to the multiple copies of sugar residues attached to the polymer backbones that can enhance the binding affinity with proteins by the "glycoside cluster effect".[10]

However, the electrospun nanofibers based on the bulk glycopolymers remain a challenge, since most of the synthetic glycopolymers are water soluble, which leads to the instability of their nanofibers under aqueous conditions. Moreover, nanofibers made from glycopolymers (homopolymers) often suffer from lower efficacy towards molecular recognition processes due to the low availability of the sugar residues on the nanofiber surfaces.[11] To solve these problems, researchers have grafted sugar residues onto water-insoluble electrospun nanofibrous surfaces[12,13] or performed the copolymerization of sugar monomers with water insoluble monomers to obtain water insoluble copolymers which formed water insoluble electrospun nanofibrous mats after electrospinning.[11,14]

Recently, it was also noticed that the increased surface area on electrospun nanofibers can enhance the sensitivity of the stimuli-responsive materials to the external stimuli, and

therefore result in dynamically and reversibly tunable "smart" nanofibrous structures that can be potentially used for delivery of drugs or cells.[3,15] Boronic acids and their ester derivatives are a class of important stimuli-responsive materials, which can reversibly interact with diols at a pH value higher than their pK_a.[16,17] This unique property has made these materials attractive in a wide range of biomedical fields, such as controlled release of insulin,[18–20] capture and release of circulating tumor cells (CTCs),[21] glucose sensing,[22–24] and tissue engineering.[25] However, electrospun nanofibers containing boronic acids are not very common[26] due to the cost associated in making those nanofibers. A low cost version of boronic acid based photo-crosslinked nanofibers using a copolymer derived from 3-acrylamidophenylboronic acid (AAPBA) and 2-hydroxyethyl methacrylate (HEMA) and the subsequent modification of the nanofibers with glycopolymers allowed the selective binding of specific lectins has been proposed here.

5.2. Materials and Methods

5.2.1. Materials

All chemicals were purchased from Sigma-Aldrich Chemicals (Oakville, ON, Canada) and the organic solvents were from Wako Pure Chemical Industries, Ltd (Japan). The glycomonomers were synthesized as previously described.[27–30] The structures of the monomers and initiator (4,4′-azobis(4-cyanovaleric acid) (ACVA)) are shown in **Scheme 5-1.**

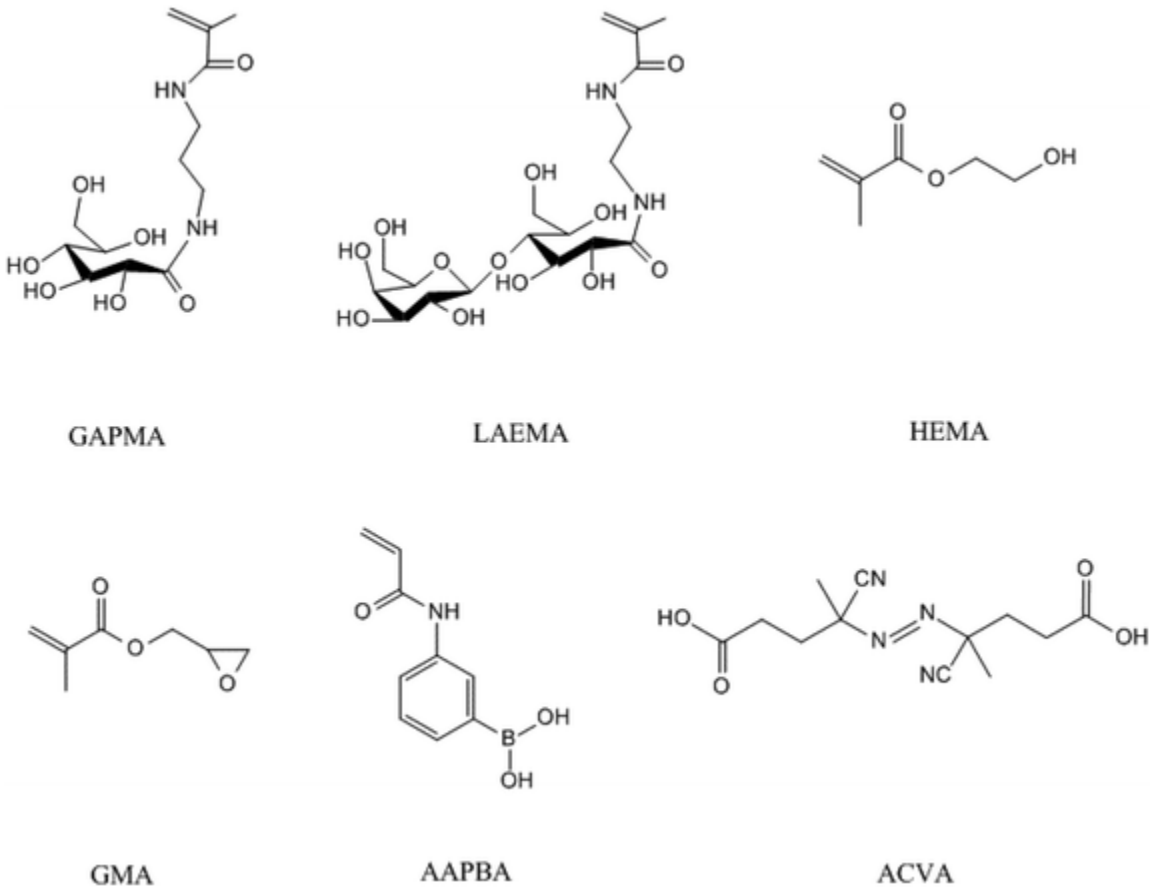

Scheme 5-1. Chemical structures of the monomers and ACVA.

5.2.2. Methods

The ^{1}H NMR spectra of the monomers and polymers were recorded on a Varian 500 MHz spectrometer using D_2O or DMSO-d_6 as the solvent. The number average molecular weight (M_n) and polydispersity (M_w/M_n) were determined using polystyrene standards (M_w = 2200–290 000 g mol^{-1}) at room temperature and a Viscotek model 250 dual detector (refractometer/viscometer) in DMF eluents (containing 10 mM LiBr) at a flow rate of 1.0 mL min^{-1}. The capture and release of FITC-labeled lectins (Vector Laboratories, USA) on glycopolymer modified boronic acid based nanofibers were studied by fluorescence microscopy (Microscope Axio Imager.M2, Carl Zeiss, Germany) with a wide-field

fluorescence microscope excitation light source (X-cite® 120Q, Lumen Dynamic, ON, Canada).

5.2.2.1. Synthesis of Glycopolymers.

The glycopolymers were synthesized by free radical polymerization using 4,4′-azobis(4-cyanovaleric acid) (ACVA) as the initiator. For a typical homopolymerization, a galactose containing monomer, 2-lactobionamidoethyl methacrylamide (LAEMA) (1 g, 2 mmol), was dissolved in 6 mL distilled water in a 10 mL Schlenk tube with 1 mL of ACVA (8 mg, 0.032 mmol) N,N′-dimethylformamide (DMF) stock solution. The tube was then sealed and degassed by purging it with nitrogen for 30 minutes. Polymerization was carried out in an oil bath (70 °C) for 24 hours followed by precipitation in acetone and subsequent washing with methanol to remove the monomers and the residual initiator. The molecular weights and polydispersity (PDI) of the synthesized glycopolymers were determined by gel permeation chromatography (GPC) at room temperature with a Viscotek model 250 dual detector (refractometer/viscometer in aqueous eluents (0.5 M sodium acetate and 0.5 M acetic acid)). The conversion of the polymer was calculated using a JNM-GSX300 ^{1}H NMR spectrometer (JEOL, Tokyo, Japan) with D_2O as the solvent.

5.2.2.2. Synthesis of the Photo-Crosslinkable Boronic Acid Based Polymer.

The photo-crosslinkable boronic acid based polymer was synthesized by free radical polymerization (**Scheme 5-2**, synthesis of GMA modified photo-crosslinkable P(HEMA-st-AAPBA)). The boronic acid groups in 3-acrylamidophenylboronic acid (AAPBA) (0.2558 g, 1.34 mmol) were first protected by stirring with diols (1,4-butanediol, 0.60 g (6.55 mmol)) in 10 mL DMF in the dark for 4 h. After that, the protected AAPBA DMF solution was transferred to a 10 mL Schlenk tube and mixed with 5 mL of ACVA (20 mg,

0.07 mmol) and 2-hydroxyethyl methacrylate (HEMA) (3.312 g, 25.45 mmol) DMF stock solution. The tube was then sealed and degassed by purging with nitrogen for 30 minutes. Polymerization was carried out in an oil bath at 70 °C for 24 hours and polymers were precipitated and purified by repeated washing with a large amount of diethyl ether. The conversion of the polymerization was determined using a JNM-GSX300 ^{1}H NMR spectrometer (JEOL, Tokyo, Japan) with DMSO-d_6 as the solvent and operated at 300 MHz. The polymer's molecular weight and polydispersity were determined by gel permeation chromatography (GPC) at 40 °C (DMF including 10 mM LiBr, 1 mL min^{-1}) with a TOSOH TSK-GEL a-2500 and a-4000 (Tosoh, Tokyo, Japan) and connected to an RI-2031 refractive index detector (JASCO International Co., Ltd, Tokyo, Japan).

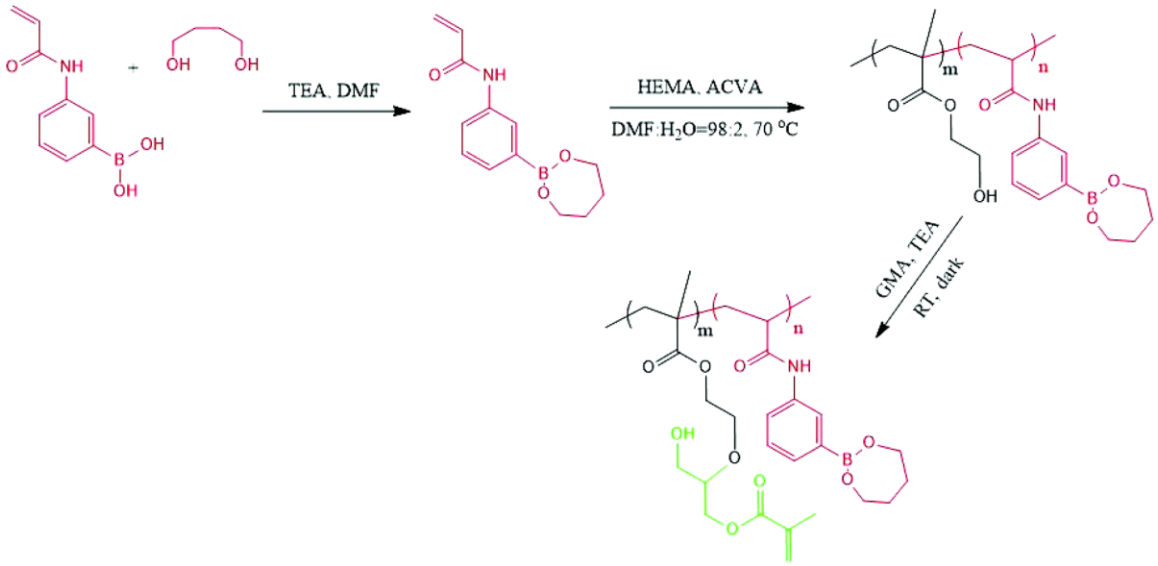

Scheme 5-2. Synthesis of GMA modified photo-crosslinkable P(HEMA-st-AAPBA).

To introduce the free double bonds onto P(HEMA-st-AAPBA) chains, 0.5 g of the polymer was dissolved in 20 mL DMF with an exceeding amount (1000×) of glycidyl methacrylate (GMA). After the addition of a small amount of triethylamine, the solution was left to stir

for 24 h in the dark, precipitated and purified by repeated washing with a large amount of diethyl ether. The conversion of the GMA modified P(HEMA-st-AAPBA) was again determined using a JNM-GSX300 ^{1}H NMR spectrometer (JEOL, Tokyo, Japan) with DMSO-d_6 as the solvent.

5.2.2.3. Electrospinning of Polymers and Photo-Crosslinking.

To make the electrospun P(HEMA-GMA-st-AAPBA) NFs easier to handle, in this study, the NFs are collected on glass slides. To do this, 0.3 g P(HEMA-GMA-st-AAPBA) and 30 mg photo-initiator (benzophenone) were dissolved in 3 mL of 1,1,1,3,3,3-hexafluoro-2-propanol (HFIP) and poured into a 5 mL plastic syringe equipped with a metal capillary needle (25 gauge). Glass slides with a diameter of 15 mm were placed on a ground aluminum foil, which was 19 cm away from the needle. The electrospinning process (Imoto IMC-19F5, Japan) was performed for 1 h at a polymer feed rate and at a DC voltage of 0.5 mL h^{-1} and 20 kV, respectively. The as-spun NFs were then photo-crosslinked by irradiation with nine UVA (350 nm) lamps in a Luzchem photoreactor for 30 min. The morphologies of the NFs were observed by SEM (Neoscope JCM-5000, JEOL, Japan) at an acceleration voltage of 10 kV.[3]

5.2.2.4. Lectin capture and release on the photo-crosslinked NF surface.

The interactions between glycopolymers and boronic acid containing nanofibers, as well as the nanofiber pH and glucose dual responsiveness were first evaluated using a fluorescence microscope (IX71, Olympus, Japan). To do this, the photo-crosslinked P(HEMA-st-AAPBA) nanofibers were placed in 24-well plates and loaded with 0.4 mL of 0.1 M HCl to deprotect the boronic acid groups. After 15 min, nanofibers were gently washed with PBS several times to remove the residual HCl. The nanofibers were then

incubated in 10 mg mL^{-1} FITC-glycopolymer (PLAEMA (with galactose pendent groups) or PGAPMA (with glucose pendent groups)) Tris-0.1 M buffer solution (pH 9.0) for 15 min, rinsed with Tris-0.1 M HCl buffer (pH 9.0) and observed using a fluorescence microscope. After that, the FITC-glycopolymer labeled nanofibers were incubated in 500 mg mL^{-1} glucose Tris-0.1 M buffer solution (pH 9.0) for 48 h, rinsed with pH 9.0 Tris-HCl buffer (0.1 M) three times and imaged using a fluorescence microscope again to evaluate the materials glucose responsiveness. Similarly, the materials' pH responsiveness was evaluated by observing the fluorescence after the acid (0.1 M HCl) treated FITC-glycopolymer modified nanofibers were rinsed with pH 9.0 Tris-HCl buffer (0.1 M) three times. The fluorescence images were obtained from three independent repeats and for each at least 5 different areas were recorded.

For lectin capture, the deprotected nanofibers were incubated in 10 mg mL^{-1} glycopolymer (PLAEMA (with galactose pendent groups) or PGAPMA (with glucose pendent groups)) Tris-0.1 M buffer solution (pH 9.0) for 15 min to make the glycopolymers deposit on nanofibers. The free glycopolymers were washed away from the nanofiber surfaces by rinsing with Tris-0.1 M HCl buffer (pH 9.0), followed by immersing the nanofibers in 100 μL FITC-lectin (Jacalin or ConA, 20 μL mL^{-1}) Tris-0.1 M HCl buffer solution (pH 9.0) for 15 min at room temperature. The nanofibers were washed again with pH 9.0 Tris-0.1 M HCl buffer several times before observing the florescence of the captured FITC-lectins in a fluorescence microscope.

For lectin release, the FITC-lectin/NF loaded 24-well plates were filled with 0.1 M HCl and incubated at room temperature in the dark for 15 min. The NFs were then rinsed with pH 9.0 Tris-0.1 M HCl buffer three times and imaged by fluorescence microscopy. At least

three lectin capture and release cycles were evaluated in the current study (**Scheme 5-3**, FITC-lectin capture and release on a photo-crosslinked polymer NF).

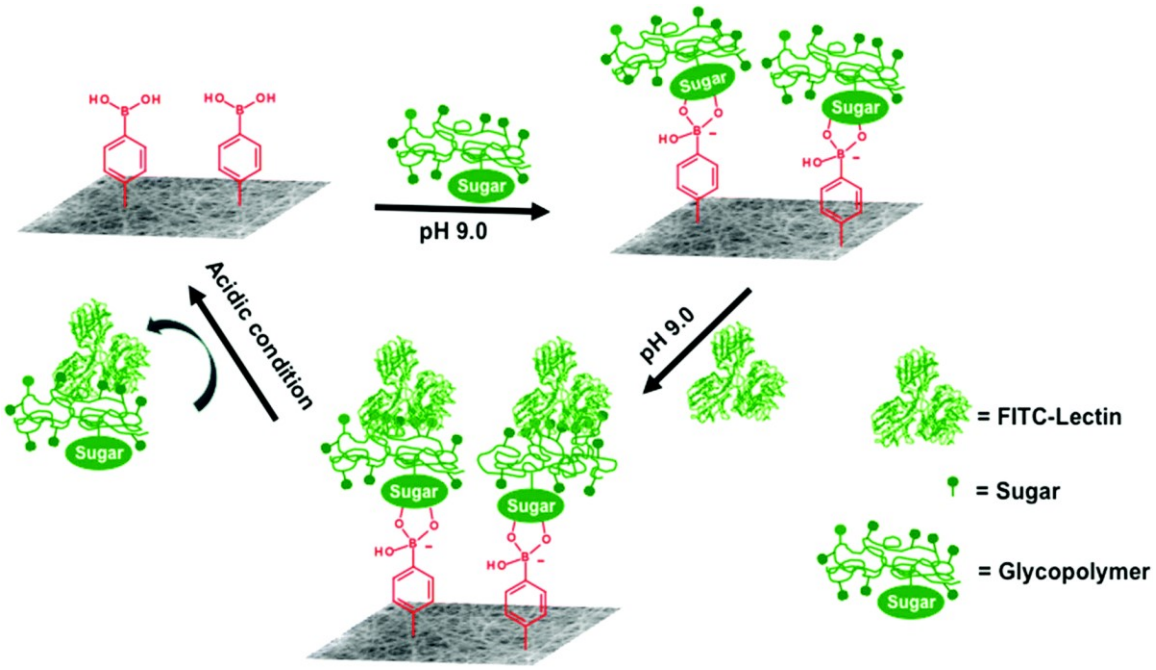

Scheme 5-3. FITC-lectin capture and release on a photo-crosslinked polymer NF.

The glycopolymer modification as well as lectin capture and release efficiencies on the NF surfaces were evaluated by the % fluorescence area value, which is determined as

$$\frac{\text{Fluorescent area (pixels)}}{\text{Total microscopy image area (pixels)}} \times 100\%$$

.

The fluorescence area was measured using ImageJ, whereas the total microscopy image area was always fixed as 1 443 520 pixels. The % fluorescence area values were obtained from three independent repeats.

5.3. Results and Discussions

5.3.1. Polymer Synthesis

3-Acrylamidophenylboronic acid (AAPBA) was first protected with 1,4-butanediol in the presence of triethylamine. The protected monomer was then copolymerized with 2-hydroxyethyl methacrylate (HEMA) via conventional free radical polymerization, and the molecular weight details are shown in **Table 5-1**. Since only 1,2-, 1,3-, and 1,4-diols can form a complex with boronic acids,[16] the adjacent hydroxyl groups in PHEMA should not have any interaction with boronic acids during the copolymerization.[31] The resulting copolymer was subsequently reacted with glycidyl methacrylate (GMA) so that free vinyl groups could be introduced onto the copolymers[32,33] (**Scheme 5-2**). The 1,4-butanediol protection on boronic acid is expected to prevent unnecessary reactions of the epoxy rings from GMA with the hydroxyl groups on boronic acid,[33] and additionally this could interfere with the complex formation between boronic acid and carbohydrates.

Table 5-1. GPC results of P(HEMA) and P(HEMA-st-AAPBA) synthesized by free radical polymerization.

	[a]N_{GMA}	M_n (Da)	M_w/M_n
$PHEMA_{321}$	64	50 100	1.98
Diol protected $P(HEMA_{760}\text{-}st\text{-}AAPBA_{38})$	69	108 200	1.64

a The number of GMA in each polymer (N_{GMA}) was calculated as N_{HEMA} × GMA mol%.

The ^{1}H NMR spectra of PHEMA and 1,4-butanediol protected P(HEMA-st-AAPBA) before and after the introduction of GMA are shown in **Figure 5-S1 in Appendix**. It was found that ~20 mol% of hydroxyl groups on the PHEMA homopolymer successfully reacted with GMA as evidenced from the =CH chemical shifts at δ = 5.5–6.5 (**Figure 5-**

S1a in Appendix). On the other hand, in Fig. S1b,† the proportion of phenyl groups in P(HEMA-st-AAPBA) was found to be around 5 mol%, which was identical to the amount of 1,4-butanediol present in polymers, indicating that all boronic acids had been successfully protected. However, from the ^{1}H NMR spectra of the GMA modified P(HEMA-st-AAPBA) (**Figure 5-S1b in Appendix**), only 10 mol% of the hydroxyl groups on copolymer chains had been successfully modified by the GMA molecules (based on the signal to noise in the spectra (**Figure 5-S1b in Appendix**), the actual proportion of the GMA in the polymer might be lower than 10 mol%). Although the amount of double bonds introduced onto polymers was relatively low in this study, according to the work of Aoyagi *et al.*,[3] 10 mol% of the photo-crosslinkable moiety present in electrospun nanofibers were high enough for photochemical crosslinking.

Similarly, for the glycopolymers synthesized by the conventional free radical polymerization, polymers' molecular weights and structures were characterized by GPC (**Table 5-2**) and NMR (**Figure 5-S1c in Appendix**), respectively. It was found that both glycopolymers (PLAEMA and PGAPMA) had been successfully synthesized by free radical polymerization. The polymers' molecular weights were found to be over 80 kDa with very wide molecular weight distribution (PDIs are over 4.0). Based on this information, the high molecular weight glycopolymers are capable of interacting on the boronic acid containing nanofiber surface by boronate–diol interactions,[19] while part of the carbohydrate residues on the polymer chains are still available to capture the lectins in aqueous medium.

Table 5-2. GPC results of PLAEMA and PGAPMA synthesized by free radical polymerization.

	M_n (Da)	M_w/M_n
$PLAEMA_{231}$	108 400	4.24
$PGAPMA_{270}$	86 400	4.38

5.3.2. Electrospinning and Photo-Crosslinking of the Nanofibers

The photo-crosslinkable P($HEMA_{760}$-st-$AAPBA_{38}$) nanofibers were fabricated by electrospinning under optimized conditions (**Figure 5-1a**). To ensure that UV light penetrates completely through the electrospun nanofibrous mats during the photo-crosslinking process, the thickness of the electrospun nanofibrous mats has been controlled by electrospinning the polymer solution for a short period (1 h)[34,35] at a low polymer concentration (10 wt%),[36] slow pumping rate (0.5 mL h^{-1}) and large needle-to-collector distance (19 mm).[1] As shown in **Figure 5-1**, nanofibers, with an average diameter of ~400 nm, were randomly distributed and formed a continuous fibrous structure on either aluminum foil (**Figure 5-1b**) or the glass surface (**Figure 5-1c**). Therefore, the morphology of the electrospun nanofibers is independent of the collector materials. On the other hand, the as-spun P($HEMA_{760}$-st-$AAPBA_{38}$) nanofibrous mats showed high porosity and therefore light can easily penetrate through, resulting in a bright background (**Figure 5-1c**). Therefore, the nanofibrous mats should be completely crosslinked during the photo-crosslinking process.

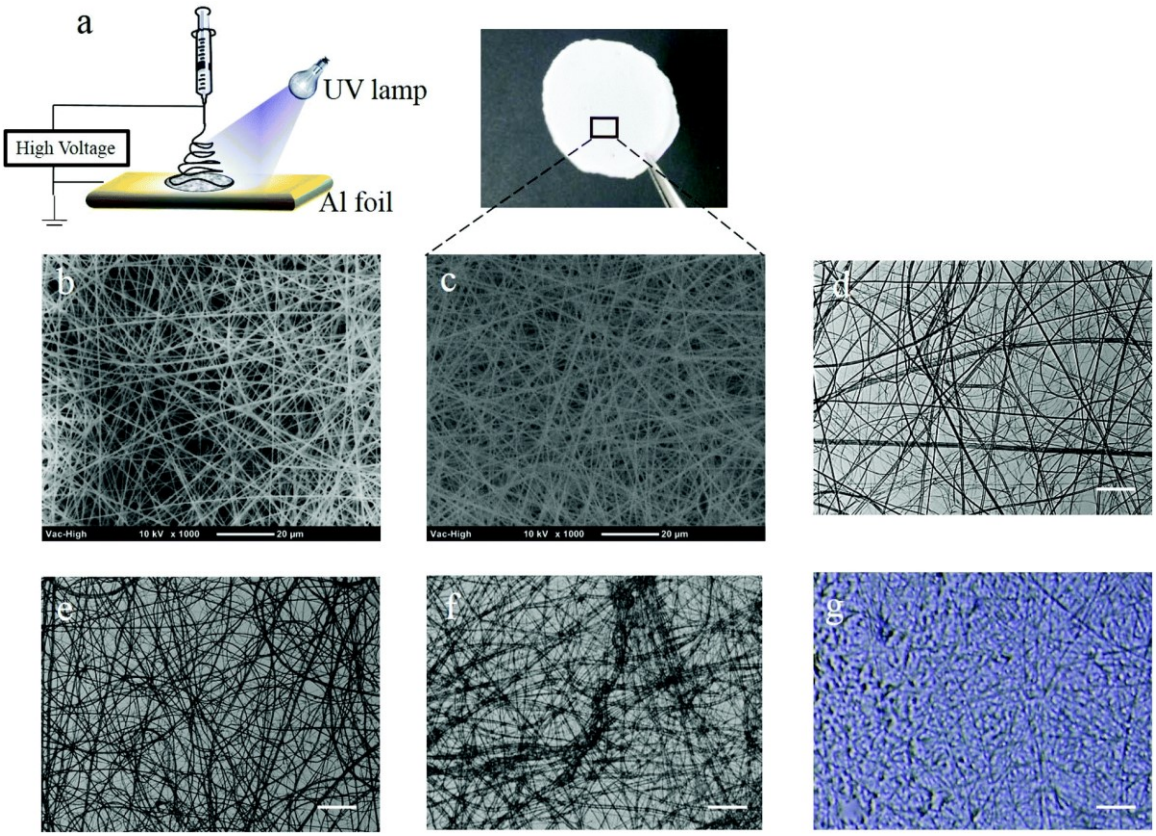

Figure 5-1. (a) Fabrication of photo-crosslinkable polymer nanofibers by electrospinning. SEM images of P(HEMA$_{760}$-st-AAPBA$_{38}$) nanofibers deposited on different substrates, (b) aluminum foil, (c) glass slides. (d) Optical microscopy images of the P(HEMA$_{760}$-st-AAPBA$_{38}$) nanofibers before photo-crosslinking, and photo-crosslinked P(HEMA$_{760}$-st-AAPBA$_{38}$) nanofibers after incubation in PBS (e) and pH 9.0 Tris-0.1 M HCl buffer (f) for 24 h. Optical microscopy images of the photo-crosslinked P(HEMA$_{321}$) nanofibers after incubation in pH 9.0 Tris-0.1 M HCl buffer for 24 h (g). Scale bar = 20 μm.

When irradiated with the UV light, the photoinitiator distributed on the surface or bulk of the nanofibers generated free radicals and chemically crosslinked the alkene groups on the P(HEMA$_{760}$-st-AAPBA$_{38}$) nanofibers (**Scheme 5-2**).[3] The photo-crosslinked nanofibers were water insoluble even after incubation in PBS buffer for 24 h (**Figure 5-1e**).

Interestingly, in pH 9.0 Tris-0.1 M HCl buffer, the nanofibers were found to be swollen (**Figure 5-1f**), which could be explained by the increasing water adsorption on nanofibers when boronic acids changed to the anionic ($B(OH)_3^-$) in the basic aqueous environment.[16,37]

The P($HEMA_{321}$) nanofibers were electrospun and crosslinked in a similar way to the P($HEMA_{760}$-st-$AAPBA_{38}$) nanofibers. Interestingly, after 24 h incubation in pH 9.0 Tris-0.1 M HCl buffer, the photo-crosslinked P($HEMA_{321}$) nanofibers were found to be extremely swollen (**Figure 5-1g**) possibly due to the adsorption and retention of a large amount of water.

5.3.3. pH and glucose dual responsiveness of the boronic acid containing nanofiber surface

Since the boronate–diol interaction only occurs under basic conditions,[16,19,37] the photo-crosslinked P($HEMA_{760}$-st-$AAPBA_{38}$) can be deprotected by incubation in a 24-well plate that is loaded with 0.4 mL of 0.1 M HCl. On the other hand, the binding affinity between the boronic acid and 1,4-diol is much weaker than 1,2 and 1,3-diols.[16,37] Therefore, in the present study, if there are residual 1,4-butanediol left on the nanofiber surface after the acid treatment, it should be completely replaced by the FITC-glycopolymers; images of the fluorescence signals uniformly distributed along the nanofibers are shown in **Figure 5-2**. During the HCl deprotection and FITC-glycopolymer modification, the chemical reactions should occur not only on the surface but also in the bulk of the nanofibrous mats as evidenced by the swelling (**Figure 5-1f**) and FITC staining (**Figure 5-2 and 5-3**) in the bulk of the mats.

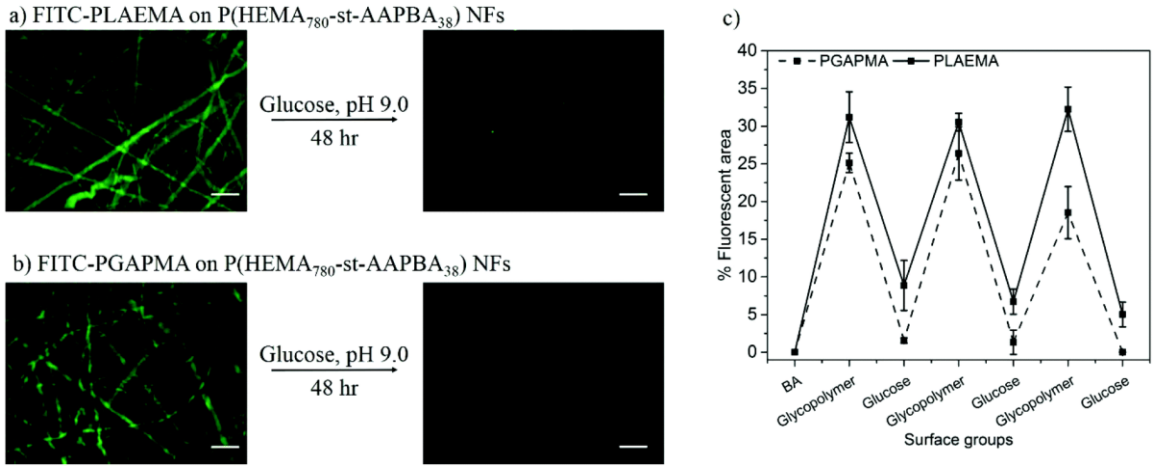

Figure 5-2. FITC-PLAEMA (a) and FITC-PGAPMA (b) modified photo-crosslinked P($HEMA_{760}$-st-$AAPBA_{38}$) nanofiber surfaces. Fluorescence could be removed after incubating glycopolymer modified NF in 500 mg mL^{-1} glucose solution (pH 9.0) for 48 h. (c) Reversible % fluorescence areas change when FITC-PLAEMA (solid line) and FITC-PGAPMA (dash line) modified NFs were incubated in 500 mg mL^{-1} glucose and 10 mg mL^{-1} FITC glycopolymer solutions (pH 9.0) for 48 h and 15 min, respectively. Scale bar = 20 μm.

The responsive nature of the resulting glycopolymer modified nanofiber to glucose was then studied. Immersion in glucose solution resulted in the displacement of the glycopolymer from the nanofiber surfaces, however long incubation time (48 h) was required for the complete displacement of the glycopolymers as shown in **Figure 5-2a and 2b**. Interestingly, compared to the FITC-PGAPMA modified NFs, the one modified with FITC-PLAEMA showed larger areas of fluorescence and some residual fluorescence could be spotted on the NF surface even after 48 h incubation at high glucose concentrations (**Figure 5-2c**). These observations could be explained by the higher association constant (pK_a) between galactose and boronic acids.[38]

The pH responsiveness of the photo-crosslinked P(HEMA$_{760}$-st-AAPBA$_{38}$) nanofibers was then studied as shown in **Figure 5-3**. Before fluorescence microscopy observations, the acid treated nanofibers were washed with Tris-0.1 M HCl buffer (pH 9.0) to prevent the fluorescence quenching under the acidic conditions.[39] The results clearly indicated that FITC-glycopolymers were able to adsorb on the boronic acid containing nanofiber surfaces under basic conditions (pH 9.0), whereas rapid dissociation of glycopolymers occurred when the nanofibers were rinsed with 0.1 M HCl.

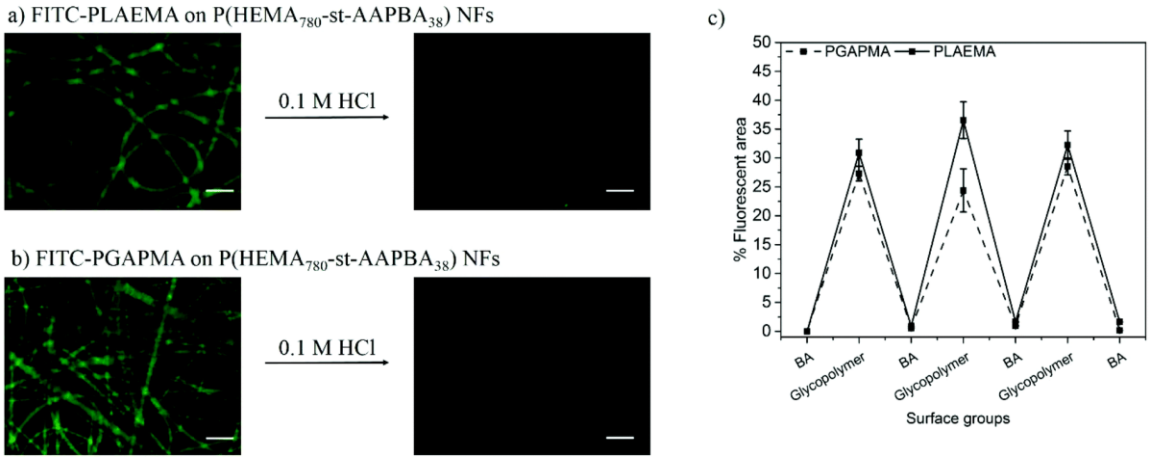

Figure 5-3. FITC-PLAEMA (a) and FITC-PGAPMA (b) modified photo-crosslinked P(HEMA760-st-AAPBA38) nanofiber surfaces. Fluorescence could be removed after rinsing the glycopolymer modified NFs with 0.1 M HCl. (c) Reversible % fluorescence areas change when FITC-PLAEMA (solid line) and FITC-PGAPMA (dash line) modified NFs were incubated in 10 mg mL−1 FITC glycopolymer solutions (pH 9.0) for 15 min, followed by rinsing with 0.1 M HCl. Scale bar = 20 μm.

5.3.4. Lectin Binding on Different Surfaces

The adsorption of FITC labeled lectins on photo-crosslinked nanofibrous membrane deposited glass slides was first studied by fluorescence microscopy. The glass slides were treated with an acidic solution to deprotect the boronic acid groups in the electrospun nanofibers. After rinsing with DI water and incubation with glycopolymers in Tris-0.1 M HCl buffer solution (pH 9.0) for 15 min, the resulting glycopolymer modified nanofibers were incubated with FITC labeled lectins in Tris-0.1 M HCl buffer solution (pH 9.0) for another 15 min and washed with Tris-0.1 M HCl buffer (pH 9.0) again to remove the free FITC-lectins. The results are shown in **Figure 5-4**.

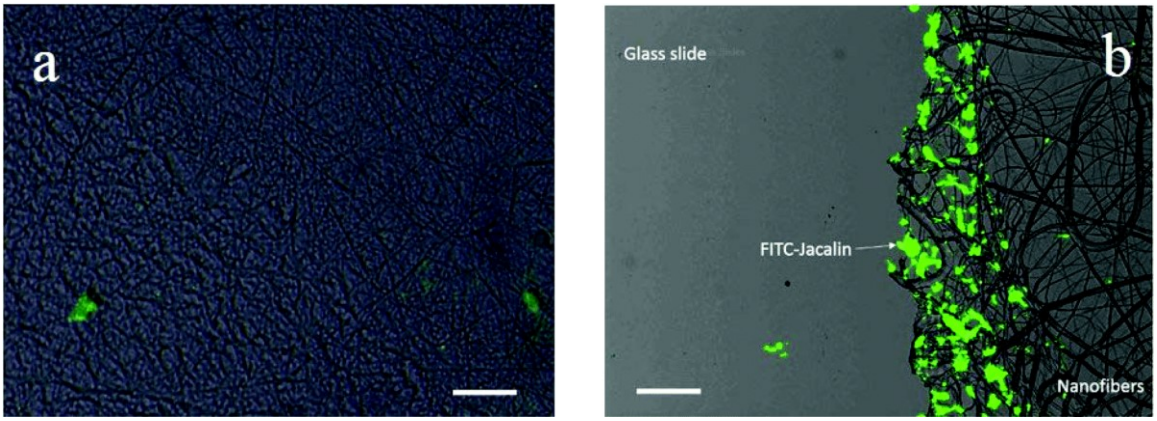

Figure 5-4. FITC-Jacalin adhered on photo-crosslinked (a) P(HEMA321) and (b) P(HEMA760-st-AAPBA38) nanofiber surfaces. At the edge of the nanofibrous mat on a glass slide, most of the FITC-Jacalin adsorbed on PLAEMA modified photo-crosslinked P(HEMA760-st-AAPBA38) nanofibers, whereas negligible FITC-Jacalin could be spotted on glass slides. Scale bar = 20 μm.

It was found that the FITC-Jacalin (galactose specific lectin) interaction on photo-crosslinked P($HEMA_{321}$) nanofiber (**Figure 5-4a**) surfaces was negligible as compared to

that on the PLAEMA modified photo-crosslinked P($HEMA_{780}$-st-$AAPBA_{38}$) nanofiber surface (**Figure 5-4**b). As compared to the results obtained by Wang et al. that no lectin adsorption could be observed on glycopolymer free nanofibers,[11] the results in the correct study might suggest that neither glycopolymers nor lectin can strongly adsorb on the photo-crosslinked P($HEMA_{321}$) homopolymer nanofibrous surfaces, whereas a significantly larger amount of FITC-Jacalin could be captured on the glycopolymer (PLAEMA) modified photo-crosslinked P($HEMA_{780}$-st-$AAPBA_{38}$) nanofiber surface through the lectin–carbohydrate interactions (**Figure 5-4**).

Incubation of the pristine and glycopolymer modified photo-crosslinked P($HEMA_{780}$-st-$AAPBA_{38}$) nanofibers in FITC-lectin Tris-0.1 M HCl buffer solutions (pH 9.0) for 15 min (**Figure 5-3**) showed that the lectins can only interact with the glycopolymer functionalized nanofiber surface, and not on the boronic acid modified nanofiber surface (**Figure 5-5a and 4-5e**). Nanofibers with PLAEMA (galactose containing glycopolymer) and PGAPMA (glucose containing polymer) modification can capture Jacalin (**Figure 5-5**b) and ConA (**Figure 5-5d**), respectively. No fluorescence signals could be observed when FITC-ConA was incubated with the PLAEMA modified photo-crosslinked P($HEMA_{780}$-st-$AAPBA_{38}$) nanofibers (**Figure 5-5c and 5-5e**). From these observations, the nanofibers could be used to selectively capture different lectins when the surface was functionalized with different glycopolymers.

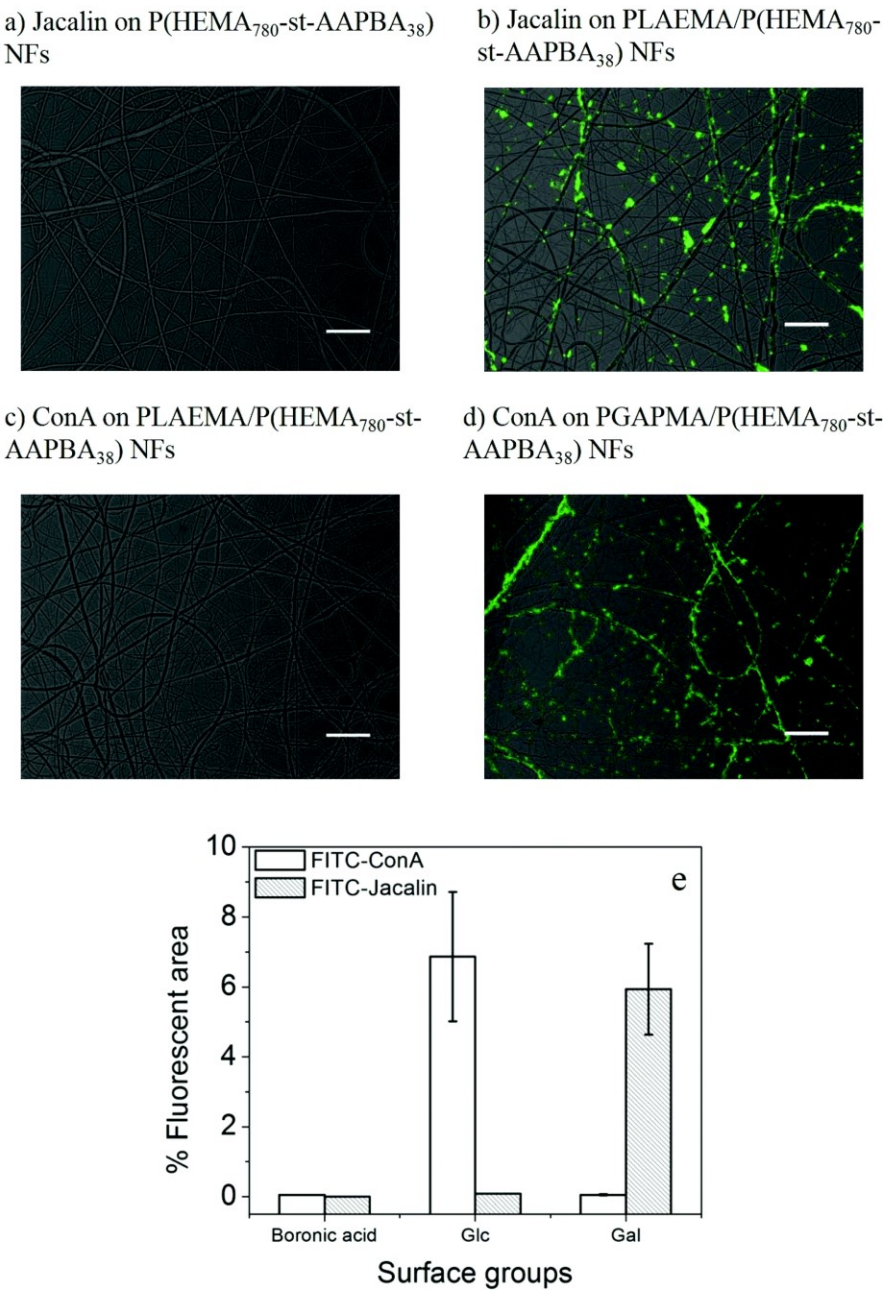

Figure 5-5. Fluorescence microscopy images for FITC-Jacalin adsorption on pristine (a) and PLAEMA modified photo-crosslinked P($HEMA_{780}$-st-$AAPBA_{38}$) nanofibers (b), and FITC-ConA on PLAEMA (c) and PGAPMA (d) modified photo-crosslinked P($HEMA_{780}$-st-$AAPBA_{38}$) nanofibers. Scale bar = 20 μm. (e) % Fluorescence areas of FITC-ConA or Jacalin on different nanofiber surfaces.

On the other hand, compared to the FITC-glycopolymer modified photo-crosslinked P(HEMA$_{780}$-st-AAPBA$_{38}$) nanofibers (**Figure 5-2c and 5-3c**), less fluorescence could be observed when FITC-lectins were captured on the glycopolymer modified P(HEMA$_{780}$-st-AAPBA$_{38}$) nanofiber surface (**Figure 5-5e**). These observations might be explained by the lower concentration of FITC-lectins (20 μL mL^{-1}) used for the lectin capture assay or the weaker affinity between carbohydrates and lectins in the aqueous environment.[40] Interestingly, unlike the FITC-glycopolymers that were uniformly distributed along the photo-crosslinked P(HEMA$_{780}$-st-AAPBA$_{38}$) nanofibers (**Figure 5-2 and 5-3**), FITC-lectins were found to be aggregated when adsorbed on the glycopolymers modified nanofibers surfaces (**Figure 5-5**). The latter case could be explained by the electrical double layer depression and the absolute zeta potential decrease of the proteins in the Tris-buffered saline.[41]

5.3.5. Reversible Capture and Release of Lectins on the Glycopolymer Modified Nanofiber Surface

The reversible capture and release of lectins on glycopolymers modified photo-crosslinked P(HEMA$_{780}$-st-AAPBA$_{38}$) nanofibers was studied (**Scheme 5-3**) and the results are shown in **Figure 5-6**. It was found that fluorescently labeled Jacalin and ConA could interact with PLAEMA (**Figure 5-6a**) and PGAPMA (**Figure 5-6b**) modified photo-crosslinked P(HEMA$_{780}$-st-AAPBA$_{38}$) nanofibers under basic conditions. After incubation with 0.1 M HCl for 15 min and rinsing with pH 9 buffer solution, no fluorescence was observed even after re-incubating the nanofibers with lectins (**Figure 5-6a and 5-6b**). Considering that a negligible amount of lectins could interact with pristine photo-crosslinked P(HEMA$_{780}$-st-

AAPBA$_{38}$) nanofibers (**Figure 5-5a**), these results suggest that the glycopolymers from the nanofiber surface were removed during the acid solution treatment.

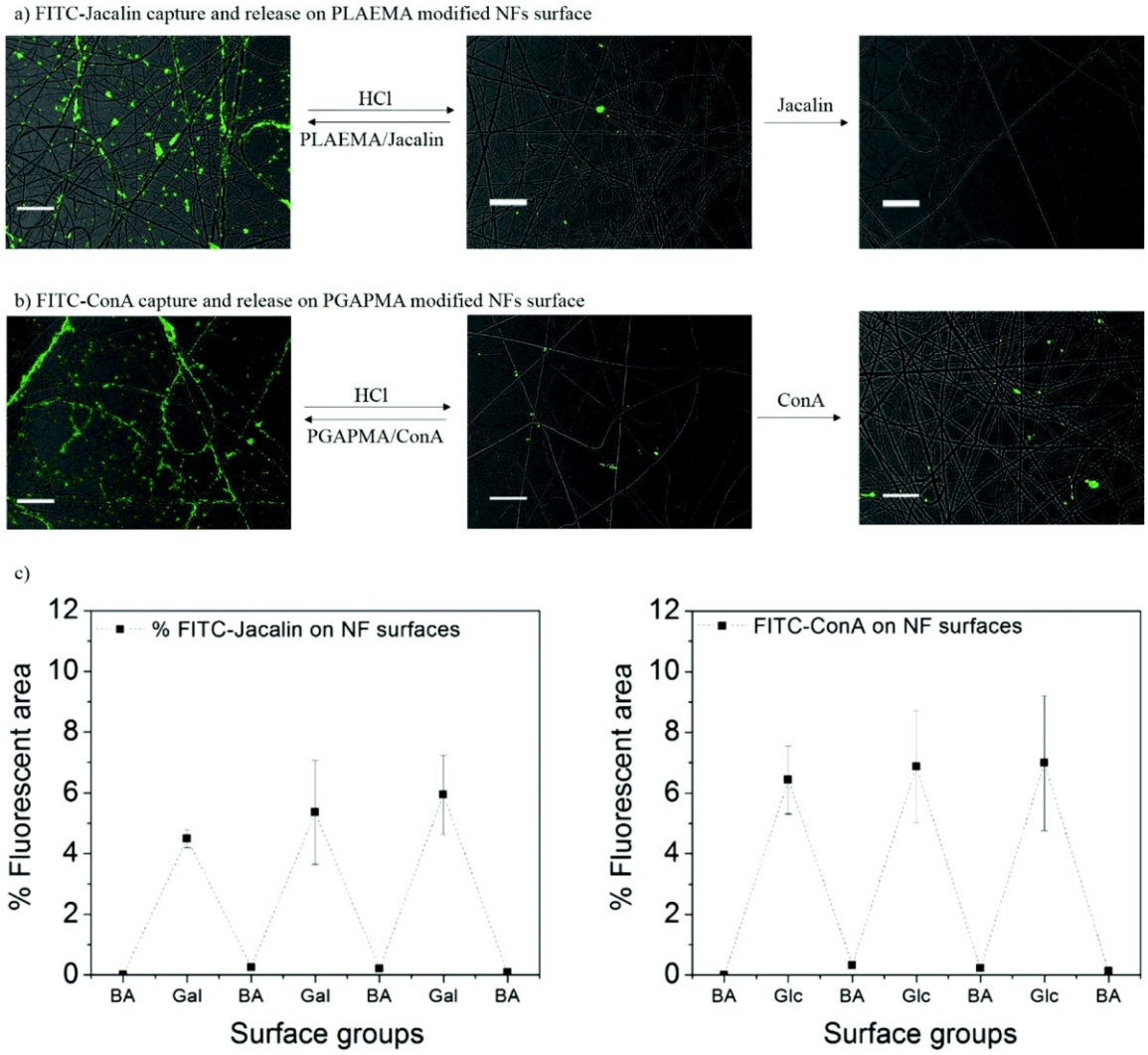

Figure 5-6. Fluorescence microscopy images for FITC-Jacalin (a) and FITC-ConA (b) reversibly captured and released from the photo-crosslinked P(HEMA$_{780}$-st-AAPBA$_{38}$) nanofibers. Scale bar = 20 μm. (c) % Fluorescence areas of FITC-ConA and FITC-Jacalin on the nanofiber surface in response to alternations of surface groups between carbohydrates and boronic acid.

Figure 5-6c shows the % fluorescence area changes on the photo-crosslinked P($HEMA_{780}$-st-$AAPBA_{38}$) nanofibers in response to alterations of surface groups between carbohydrates and boronic acid. When glycopolymer (PLAEMA) modified nanofibers were incubated with FITC-Jacalin for 15 min, the lectin was captured by the galactose groups on nanofibers and showed ~6% coverage with fluorescence signals in microscopy images (**Figure 5-6a and 5-6c**). Once the nanofibers were immersed in 0.1 M HCl for 15 min and rinsed with pH 9 buffer solution, the fluorescence areas were reduced to ~0%, indicating that PLAEMA and glycopolymer–lectin conjugates were removed from the nanofiber surface, and the surface groups were restored to boronic acids (**Figure 5-6a and 5-6c**). These observations could be repeated by alternatively incubating the photo-crosslinked PLAEMA modified P($HEMA_{780}$-st-$AAPBA_{38}$) nanofibers in FITC-Jacalin and acidic solutions (**Figure 5-6c**), suggesting that these materials could be used for reversible capture and release of Jacalin. The FITC-ConA capture and release on glucose containing glycopolymer (PGAPMA) modified nanofibers has also been evaluated. The results were similar to those for the FITC-Jacalin capture and release on PLAEMA modified nanofiber surface (**Figure 5-6c**), suggesting that using different glycopolymers to modify the nanofiber surface, the photo-crosslinked P($HEMA_{780}$-st-$AAPBA_{38}$) nanofibers could be used for reversible capture and release of various lectins. Moreover, the nanofiber fabricated in the present study could also be used for the reversible capture of virus or even bacteria from contaminated water. Compared to other platforms such as carbon nanotubes,[42] surfaces[43] and nanoparticles,[44,45] for pathogen capture/detection, these nanofibrous materials are easier to handle, reusable and less expensive.

5.4. Conclusions

This study presents the first example of using a boronic acid containing photochemically crosslinked polymer nanofiber membrane for the reversible capture and release of lectins. The pH and glucose dual responsive behavior, as well as the adsorption of lectins (FITC-Jacalin and FITC-ConA) on different surfaces (pristine, galactose and glucose containing polymer modified nanofibers) were studied by fluorescence microscopy. The FITC labeled glycopolymers could adsorb on the nanofiber surface under basic conditions (pH 9.0) and are released at either high glucose concentrations or under acidic conditions. FITC-Jacalin and FITC-ConA were successfully captured on the galactose and glucose containing polymer modified nanofiber surface, respectively, whereas no lectin adsorption can be observed on the pristine nanofibers. Immersion of the FITC-lectins conjugated nanofibers in acidic solution for 15 min resulted in the rapid release of both the lectins and the glycopolymers from the nanofiber surfaces. Therefore, such a type of nanofiber can find application in the quick removal of specific proteins or toxins in solution.

5.5. References

1. D. Li and Y. Xia, *Adv. Mater.* 2004, **16**, 1151-1170.

2. H. Yoshimoto, Y. M. Shin, H. Terai and J. P. Vacanti, *Biomaterials* 2003, **24**, 2077-2082.

3. Y.-J. Kim, M. Ebara and T. Aoyagi, *Angew. Chem. Int. Ed.* 2012, **51**, 10537-10541.

4. K. Namekawa, M. T. Schreiber, T. Aoyagi and M. Ebara, *Biomater Sci-Uk*, 2014, **2**, 674-679.

5. X. Wang, X. Chen, K. Yoon, D. Fang, B. S. Hsiao and B. Chu, *Environ. Sci. Technol.* 2005, **39**, 7684-7691.

6. J. Shin, S.-J. Choi, I. Lee, D.-Y. Youn, C. O. Park, J.-H. Lee, H. L. Tuller and I.-D. Kim, *Adv. Funct. Mater.* 2013, **23**, 2357-2367.

7. D.-J. Yang, I. Kamienchick, D. Y. Youn, A. Rothschild and I.-D. Kim, *Adv. Funct. Mater.* 2010, **20**, 4258-4264.

8. D. R. Bundle and N. M. Young, *Curr. Opin. Struct. Biol.* , 1992, **2**, 666-673.

9. N. Sharon, *FEBS Lett.* 1987, **217**, 145-157.

10. Y. C. Lee and R. T. Lee, *Acc. Chem. Res.* 1995, **28**, 321-327.

11. L. Wang, G. R. Williams, H.-l. Nie, J. Quan and L.-m. Zhu, *Polym. Chem.* 2014, **5**, 3009-3017.

12. S. Patel, K. Kurpinski, R. Quigley, H. Gao, B. S. Hsiao, M.-M. Poo and S. Li, *Nano Lett.* 2007, **7**, 2122-2128.

13. T. Uyar, R. Havelund, J. Hacaloglu, F. Besenbacher and P. Kingshott, *ACS Nano* 2010, **4**, 5121-5130.

14. Q. Yang, J. Wu, J.-J. Li, M.-X. Hu and Z.-K. Xu, *Macromol. Rapid Commun.* 2006, **27**, 1942-1948.

15. Y.-J. Kim, M. Ebara and T. Aoyagi, *Adv. Funct. Mater.* 2013, **23**, 5753-5761.

16. S. D. Bull, M. G. Davidson, J. M. H. van den Elsen, J. S. Fossey, A. T. A. Jenkins, Y.-B. Jiang, Y. Kubo, F. Marken, K. Sakurai, J. Zhao and T. D. James, *Acc. Chem. Res.* 2012, **46**, 312-326.

17. S. L. Wiskur, J. J. Lavigne, H. Ait-Haddou, V. Lynch, Y. H. Chiu, J. W. Canary and E. V. Anslyn, *Org. Lett.* 2001, **3**, 1311-1314.

18. Q. Guo, Z. Wu, X. Zhang, L. Sun and C. Li, *Soft Matter* 2014, **10**, 911-920.

19. Y. Kotsuchibashi, R. V. C. Agustin, J.-Y. Lu, D. G. Hall and R. Narain, *ACS Macro Letters* 2013, **2**, 260-264.

20. A. Matsumoto, K. Yamamoto, R. Yoshida, K. Kataoka, T. Aoyagi and Y. Miyahara, *Chem. Commun.* 2010, **46**, 2203-2205.

21. H. Liu, Y. Li, K. Sun, J. Fan, P. Zhang, J. Meng, S. Wang and L. Jiang, *J. Am. Chem. Soc.* 2013, **135**, 7603-7609.

22. T. Hoare and R. Pelton, *Macromolecules*, 2007, **40**, 670-678.

23. M. B. Lerner, N. Kybert, R. Mendoza, R. Villechenon, M. A. Bonilla Lopez and A. T. Charlie Johnson, *Appl. Phys. Lett.* 2013, **102**, -.

24. C. Zhang, M. D. Losego and P. V. Braun, *Chem. Mater.* 2013, **25**, 3239-3250.

25. T. Aoki, Y. Nagao, K. Sanui, N. Ogata, A. Kikuchi, Y. Sakurai, K. Kataoka and T. Okano, *J. Biomater. Sci., Polym. Ed.* 1997, **9**, 1-14.

26. E. Baştürk and M. V. Kahraman, *Polym. Compos.* 2012, **33**, 829-837.

27. M. Benaglia, E. Rizzardo, A. Alberti and M. and Guerra, *Macromolecules*, 2005, **38**, 3129-3140.

28. Z. Deng, H. Bouchékif, K. Babooram, A. Housni, N. Choytun and R. Narain, *J. Polym. Sci., Part A: Polym. Chem.* 2008, **46**, 4984-4996.

29. Z. Deng, M. Ahmed and R. Narain, *J. Polym. Sci., Part A: Polym. Chem.* 2009, **47**, 614-627.

30. Z. Deng, S. Li, X. Jiang and R. Narain, *Macromolecules*, 2009, **42**, 6393-6405.

31. Y.-J. Lee, S. A. Pruzinsky and P. V. Braun, *Langmuir* 2004, **20**, 3096-3106.

32. W. N. E. van Dijk-Wolthuis, O. Franssen, H. Talsma, M. J. van Steenbergen, J. J. Kettenes-van den Bosch and W. E. Hennink, *Macromolecules*, 1995, **28**, 6317-6322.

33. A. V. Reis, A. R. Fajardo, I. T. A. Schuquel, M. R. Guilherme, G. J. Vidotti, A. F. Rubira and E. C. Muniz, *J. Org. Chem.* 2009, **74**, 3750-3757.

34. G. Kim, H. Yoon and Y. Park, *Appl. Phys. A* 2010, **100**, 1197-1204.

35. J. Lee, Y. H. Jeong and D.-W. Cho, *Macromol. Mater. Eng.* 2014, n/a-n/a.

36. S. V. Fridrikh, J. H. Yu, M. P. Brenner and G. C. Rutledge, *Phys. Rev. Lett.* 2003, **90**, 144502.

37. D. G. Hall, in *Boronic Acids*, Wiley-VCH Verlag GmbH & Co. KGaA, 2006, pp. 1-99.

38. J. P. Lorand and J. O. Edwards, *J. Org. Chem.* 1959, **24**, 769-774.

39. D. Fangkai, M. Yunhao, Z. Fang, Y. Changmin and W. Shuizhu, *Nanotechnology*, 2013, **24**, 365101.

40. C. Ke, H. Destecroix, M. P. Crump and A. P. Davis, *Nat. Chem.* 2012, **4**, 718-723.

41. P. Attard, in *Adv. Chem. Phys.* John Wiley & Sons, Inc., 2007, pp. 1-159.

42. L. Gu, T. Elkin, X. Jiang, H. Li, Y. Lin, L. Qu, T.-R. J. Tzeng, R. Joseph and Y.-P. Sun, *Chem. Commun.* 2005, 874-876.

43. Q. Yang, M. Strathmann, A. Rumpf, G. Schaule and M. Ulbricht, *ACS Appl. Mat. Interfaces* 2010, **2**, 3555-3562.

44. G. Pasparakis and C. Alexander, *Angew. Chem. Int. Ed.* 2008, **47**, 4847-4850.

45. R. Ribeiro-Viana, M. Sánchez-Navarro, J. Luczkowiak, J. R. Koeppe, R. Delgado, J. Rojo and B. G. Davis, *Nat. Commun.* 2012, **3**, 1303.

Chapter 6. General Conclusions and Future Directions

Carbohydrate-protein interactions play significantly important roles in various biological events including cell adhesion, signalling, growth and differentiation. Understanding such interactions is crucial for the design of materials for various biomedical applications including drug/gene delivery, biosensing, pathogen inhibition, cell/protein isolation and controlling cell functions.

Operated based on the Sauerbrey equation that the oscillation frequency changes to the negative direction with the mass deposited on sensor surface, QCM-D is a simple, cost effective, high-resolution mass sensing technique that has been applied and showed great success on probing interactions at molecular levels. However, adsorbing large diameter colloidal objects (>1 μm), such as bacteria, to the surface of a QCM can lead positive frequency shifts. This is most likely due to a strong coupling between the adsorbed particles and the sensor surface during the point contacts. Here, the "coupled resonance model" is used to explain the positive frequency shifts observed when bacterial adhesion on glycopolymers modified QCM-D surface. Comparing to bacterial adhesion on a surface by non-specific interactions, one mediated by carbohydrate-protein interactions showed stronger bonding affinities, high selectivity, and calcium dependence if C-type lectins are presented on bacterial cell membrane (**Chapter 3**).

Further modification of the gold coated QCM-D sensor surface with RAFT polymerized thermally responsive glycopolymers bearing dithioester CTA terminal could generate a biomimetic host cell surface to probe the pathogen infection processes. When temperature was above the polymers LCST at 37 °C, the surface showed a slightly hydrophobicity with

the presence of hydrophilic carbohydrates to mimic glycoconjugates on host cell membrane. By comparing bacterial adhesion on the biomimetic PNIPAAm and glyco-homopolymers surfaces, one can conclude that although both hydrophobic and carbohydrate-protein interactions contribute to the pathogen infection process, the latter was found to play prominent role as bacterial cells can establish stronger bonding stiffness on a glycopolymer surface as compared to the one on a hydrophobic surface (**Chapter 4**).

After understanding of the fundamental principle of carbohydrate-protein interactions in bacterial adhesion, these carbohydrate containing polymers was used in the development of a cost-effective, highly selective device for lectin capture. To this end, in **Chapter 5**, pH and glucose dual responsive boronic acid containing polymer nanofibers with surface modification of glycopolymers have been developed for the reversible capture and release of lectins. Such device can be customized for capturing of different lectins by surface modifying of the materials with their corresponding glycopolymers. Moreover, due to the dynamic covalent bonds form between boronic acid derivatives and diols, the captured lectins can easily detach from the surface in acidic condition or in the presence of the competitive molecules (such as glucose). This unique property may allow the materials be used for tens or even hundreds of times. It is also import to note that the studies carried out in **Chapter 5** can be further improved with better experiment design. The glycopolymers modified materials can be potentially used for reversible capture and release of more complicated biological subjects, such as virus, bacteria, or even circulating tumor cells from human blood under the same principles.

Glycopolymers have shown enhanced binding affinity towards cell surface lectins through the “glycoside cluster effect”. However, the impact of the two-dimensional diffusion of

receptors within a fluid membrane bilayer on cellular signal transduction as well controlling of cell function due to the glycopolymer conjugation is still unclear. Studies of glycopolymers in this area may provide a greater pathogen inhibition efficacy, but also lead a new boulevard on the development of glycopolymer based macromolecular drugs.

Recently, polymers consisting of boronic acid and its derives, also known as “artificial lectins”, have attracted more and more research interests on the design of novel biomaterials due to their dynamic covalent interactions with diol containing molecules. Combination of these materials with glycopolymers may open a new window for the development of new classes of smart materials in various biomedical applications. For example, self-healing hydrogels based on glycopolymer-boronic acid dynamic crosslinking may be used for 3D printing/culturing of cells. Using their self-healing properties, epithelial cells can be introduced into another biodegradable hydrogel seeded with pluripotent stem cell and may eventually form capillary vessels for tissue engineering applications. Hydrogels or adhesives constructed by mixing of glycopolymers and boronate ester containing polymers can coagulate platelets at wound site and used as hemostatic materials. Cells cultured on the boronate ester containing polymers modified surface may form a single cell layer and released under certain stimulus (such as introducing of the diol competitors) for cell-sheet engineering application. Glyconanomaterials for gene/drug delivery can also be modified with boronic acid containing zwitterionic polymers to hind from the immune system during the blood circulating, while restore the materials endocytosis abilities when the zwitterionic protection layer is removed under acidic tumor site microenvironment.

Bibliography

L. L. Kiessling, J. E. Gestwicki and L. E. Strong, *Curr. Opin. Chem. Biol.* 2000, **4**, 696-703.

A. E. Smith and A. Helenius, *Science* 2004, **304**, 237-242.

U. Holmskov, S. Thiel and J. C. Jensenius, *Annu. Rev. Immunol.* 2003, **21**, 547-578.

E. Töpfer-Petersen, Hum. *Reprod. Update* 1999, **5**, 314-329.

K. Ohtsubo and J. D. Marth, *Cell* 2006, **126**, 855-867.

D. R. Bundle and N. M. Young, *Curr. Opin. Struct. Biol.*1992, **2**, 666-673.

Y. C. Lee and R. T. Lee, *Acc. Chem. Res.* 1995, **28**, 321-327.

B. Blanchard, A. Nurisso, E. Hollville, C. Tétaud, J. Wiels, M. Pokorná, M. Wimmerová, A. Varrot and A. Imberty, *J. Mol. Biol.* 2008, **383**, 837-853.

M. Meier, M. D. Bider, V. N. Malashkevich, M. Spiess and P. Burkhard, *J. Mol. Biol.* 2000, **300**, 857-865.

C. R. Bertozzi, Kiessling and L. L., *Science* 2001, **291**, 2357-2364.

C. W. Cairo, J. E. Gestwicki, M. Kanai and L. L. Kiessling, *J. Am. Chem. Soc.* 2002, **124**, 1615-1619.

J. E. Gestwicki, C. W. Cairo, L. E. Strong, K. A. Oetjen and L. L. Kiessling, *J. Am. Chem. Soc.* 2002, **124**, 14922-14933.

S. M. Dimick, S. C. Powell, S. A. McMahon, D. N. Moothoo, J. H. Naismith and E. J. Toone, *J. Am. Chem. Soc.* 1999, **121**, 10286-10296.

J. J. Lundquist and E. J. Toone, *Chem. Rev.* 2002, **102**, 555-578.

M. Mammen, S.-K. Choi and G. M. Whitesides, *Angew. Chem. Int. Ed.* 1998, **37**, 2754-2794.

W. Roy L, in Carbohydrates in Solution, American Chemical Society, 1973, vol. 117, pp. 242-255.

P. L. Nichols and E. Yanovsky, *J. Am. Chem. Soc.* 1944, **66**, 1625-1627.

R. H. Treadway and E. Yanovsky, *J. Am. Chem. Soc.* 1945, **67**, 1038-1039.

S.-K. Choi, M. Mammen and G. M. Whitesides, *J. Am. Chem. Soc.* 1997, **119**, 4103-4111.

E. J. Gordon, L. E. Strong and L. L. Kiessling, *Bioorgan. Med. Chem.* 1998, **6**, 1293-1299.

R. Roy, *Curr. Opin. Struct. Biol.* 1996, **6**, 692-702.

K. Matsuoka and S.-I. Nishimura, *Macromolecules* 1995, **28**, 2961-2968.

G. Descotes, J. Ramza, J.-M. Basset and S. Pagano, *Tetrahedron Lett.* 1994, **35**, 7379-7382.

M. Minoda, K. Yamaoka, K. Yamada, A. Takaragi and T. Miyamoto, *Macromolecular Symposia* 1995, **99**, 169-177.

K. Yamada, K. Yamaoka, M. Minoda and T. Miyamoto, *J. Polym. Sci., Part A: Polym. Chem.* 1997, **35**, 255-261.

S. Loykulnant, M. Hayashi and A. Hirao, *Macromolecules* 1998, **31**, 9121-9126.

C. Fraser and R. H. Grubbs, *Macromolecules* 1995, **28**, 7248-7255.

K. H. Mortell, M. Gingras and L. L. Kiessling, *J. Am. Chem. Soc.* 1994, **116**, 12053-12054.

M. Kato, M. Kamigaito, M. Sawamoto and T. Higashimura, *Macromolecules* 1995, **28**, 1721-1723.

J.-S. Wang and K. Matyjaszewski, *J. Am. Chem. Soc.* 1995, **117**, 5614-5615.

J. Chiefari, Y. K. Chong, F. Ercole, J. Krstina, J. Jeffery, T. P. T. Le, R. T. A. Mayadunne, G. F. Meijs, C. L. Moad, G. Moad, E. Rizzardo and S. H. Thang, *Macromolecules* 1998, 31, 5559-5562.

H. C. Kolb, M. G. Finn and K. B. Sharpless, *Angew. Chem. Int. Ed.* 2001, **40**, 2004-2021.

F. Pérez-Balderas, M. Ortega-Muñoz, J. Morales-Sanfrutos, F. Hernández-Mateo, F. G. Calvo-Flores, J. A. Calvo-Asín, J. Isac-García and F. Santoyo-González, *Org. Lett.* 2003, **5**, 1951-1954.

M. Buback, A. Feldermann, C. Barner-Kowollik and I. Lacík, *Macromolecules* 2001, **34**, 5439-5448.

G. Odian, Principle of Polymerization, 4th edn., Wiley, New York, 2004.

C. A. G. N. Montalbetti and V. Falque, *Tetrahedron*, 2005, **61**, 10827-10852.

S.-J. Richards, M. W. Jones, M. Hunaban, D. M. Haddleton and M. I. Gibson, *Angew. Chem. Int. Ed.* 2012, **51**, 7812-7816.

M. Ejaz, K. Ohno, Y. Tsujii and T. Fukuda, *Macromolecules* 2000, **33**, 2870-2874.

Y.-Z. Liang, Z.-C. Li, G.-Q. Chen and F.-M. Li, *Polym. Int.* 1999, **48**, 739-742.

Z.-C. Li, Y.-Z. Liang and F.-M. Li, *Chem. Commun.* 1999, 1557-1558.

J.-Q. Meng, F.-S. Du, Y.-S. Liu and Z.-C. Li, *J. Polym. Sci., Part A: Polym. Chem.* 2005, **43**, 752-762.

C.-M. Dong, X.-L. Sun, K. M. Faucher, R. P. Apkarian and E. L. Chaikof, *Biomacromolecules* 2004, **5**, 224-231.

V. Ladmiral, L. Monaghan, G. Mantovani and D. M. Haddleton, *Polymer* 2005, **46**, 8536-8545.

L.-C. You, F.-Z. Lu, Z.-C. Li, W. Zhang and F.-M. Li, *Macromolecules* 2003, **36**, 1-4.

S. Muthukrishnan, D. P. Erhard, H. Mori and A. H. E. Müller, *Macromolecules* 2006, **39**, 2743-2750.

S. Muthukrishnan, G. Jutz, X. André, H. Mori and A. H. E. Müller, *Macromolecules* 2005, **38**, 9-18.

S. Muthukrishnan, H. Mori and A. H. E. Müller, *Macromolecules* 2005, **38**, 3108-3119.

Y.-M. Chen and G. Wulff, Macromol. *Rapid Commun.* 2002, **23**, 59-63.

R. Narain and S. P. Armes, *Chem. Commun.* 2002, 2776-2777.

R. Narain and S. P. Armes, *Biomacromolecules* 2003, **4**, 1746-1758.

R. Narain and S. P. Armes, *Macromolecules* 2003, **36**, 4675-4678.

R. M. Broyer, G. M. Quaker and H. D. Maynard, *J. Am. Chem. Soc.* 2008, **130**, 1041-1047.

Y. Pan, C. Ma, W. Tong, C. Fan, Q. Zhang, W. Zhang, F. Tian, B. Peng, W. Qin and X. Qian, *Anal. Chem.* 2015, **87**, 656-662.

J. Lazar, H. Park, R. R. Rosencrantz, A. Böker, L. Elling and U. Schnakenberg, *Macromol. Rapid Commun.* 2015, **36**, 1472-1478.

J. Lee, E.-W. Lin, U. Y. Lau, J. L. Hedrick, E. Bat and H. D. Maynard, *Biomacromolecules* 2013, **14**, 2561-2569.

S. S. Gupta, K. S. Raja, E. Kaltgrad, E. Strable and M. G. Finn, *Chem. Commun.* 2005, 4315-4317.

S. Slavin, J. Burns, D. M. Haddleton and C. R. Becer, *Eur. Polym. J.* 2011, **47**, 435-446.

K. L. Heredia and H. D. Maynard, *Org. Biomol. Chem.* 2007, **5**, 45-53.

R. J. Mancini, J. Lee and H. D. Maynard, *J. Am. Chem. Soc.* 2012, **134**, 8474-8479.

V. Vázquez-Dorbatt and H. D. Maynard, *Biomacromolecules* 2006, **7**, 2297-2302.

N. V. Tsarevsky, T. Pintauer and K. Matyjaszewski, *Macromolecules* 2004, **37**, 9768-9778.

K. Matyjaszewski, W. Jakubowski, K. Min, W. Tang, J. Huang, W. A. Braunecker and N. V. Tsarevsky, *Proc. Natl. Acad. Sci.* 2006, **103**, 15309-15314.

W. Jakubowski and K. Matyjaszewski, *Angew. Chem. Int. Ed.* 2006, **45**, 4482-4486.

W. Jakubowski, K. Min and K. Matyjaszewski, *Macromolecules* 2006, **39**, 39-45.

V. Sciannamea, R. Jérôme and C. Detrembleur, *Chem. Rev.* 2008, **108**, 1104-1126.

M. R. Hill, R. N. Carmean and B. S. Sumerlin, *Macromolecules* 2015, **48**, 5459-5469.

M. Semsarilar and S. Perrier, *Nat. Chem.* 2010, **2**, 811-820.

J. Chiefari, R. T. A. Mayadunne, C. L. Moad, G. Moad, E. Rizzardo, A. Postma and S. H. Thang, *Macromolecules* 2003, **36**, 2273-2283.

S. J. Stace, G. Moad, C. M. Fellows and D. J. Keddie, *Polym. Chem.* 2015, **6**, 7119-7126.

Y. K. Chong, J. Krstina, T. P. T. Le, G. Moad, A. Postma, E. Rizzardo and S. H. Thang, *Macromolecules* 2003, **36**, 2256-2272.

C. L. McCormick and A. B. Lowe, *Acc. Chem. Res.* 2004, **37**, 312-325.

D. B. Thomas, A. J. Convertine, R. D. Hester, A. B. Lowe and C. L. McCormick, *Macromolecules* 2004, **37**, 1735-1741.

A. B. Lowe and C. L. McCormick, *Prog. Polym. Sci.* 2007, **32**, 283-351.

X.-L. Sun, W.-D. He, J. Li, L.-Y. Li, B.-Y. Zhang and T.-T. Pan, *J. Polym. Sci., Part A: Polym. Chem.* 2009, **47**, 6863-6872.

X.-L. Sun, W.-D. He, T.-T. Pan, Z.-L. Ding and Y.-J. Zhang, *Polymer* 2010, **51**, 110-114.

Y. K. Chong, T. P. T. Le, G. Moad, E. Rizzardo and S. H. Thang, *Macromolecules* 1999, **32**, 2071-2074.

Y. Mitsukami, M. S. Donovan, A. B. Lowe and C. L. McCormick, *Macromolecules* 2001, **34**, 2248-2256.

Y. Li, B. S. Lokitz and C. L. McCormick, *Macromolecules* 2006, **39**, 81-89.

Y. Li, B. S. Lokitz, S. P. Armes and C. L. McCormick, *Macromolecules* 2006, **39**, 2726-2728.

Bibliography

A. B. Lowe, B. S. Sumerlin, M. S. Donovan and C. L. McCormick, *J. Am. Chem. Soc.* 2002, **124**, 11562-11563.

A. J. Convertine, B. S. Lokitz, Y. Vasileva, L. J. Myrick, C. W. Scales, A. B. Lowe and C. L. McCormick, *Macromolecules* 2006, **39**, 1724-1730.

V. Ladmiral, M. Semsarilar, I. Canton and S. P. Armes, *J. Am. Chem. Soc.* 2013, **135**, 13574-13581.

X. Li and G. Chen, *Polym. Chem.* 2015, **6**, 1417-1430.

Y. Kotsuchibashi, M. Ebara, A. S. Hoffman, R. Narain and T. Aoyagi, *Polym. Chem.* 2015, **6**, 1693-1697.

Q. Zhang, P. Wilson, A. Anastasaki, R. McHale and D. M. Haddleton, *ACS Macro Letters* 2014, **3**, 491-495.

W. T. Liau, C. Bonduelle, M. Brochet, S. Lecommandoux and A. M. Kasko, *Biomacromolecules* 2015, **16**, 284-294.

M. Ahmed and R. Narain, *Biomaterials* 2013, **34**, 4368-4376.

M. Ahmed, M. Jawanda, K. Ishihara and R. Narain, *Biomaterials* 2012, **33**, 7858-7870.

M. Ahmed and R. Narain, *Biomaterials* 2011, **32**, 5279-5290.

M. Ahmed and R. Narain, *Biomaterials* 2012, **33**, 3990-4001.

M. Ahmed, B. F. L. Lai, J. N. Kizhakkedathu and R. Narain, *Bioconjugate Chem.* 2012, **23**, 1050-1058.

R. Narain, Y. Wang, M. Ahmed, B. F. L. Lai and J. N. Kizhakkedathu, *Biomacromolecules* 2015, **16**, 2990-2997.

S. Quan, Y. Wang, A. Zhou, P. Kumar and R. Narain, *Biomacromolecules* 2015, **16**, 1978-1986.

M. Ahmed, P. Wattanaarsakit and R. Narain, *Polym. Chem.* 2013, **4**, 3829-3836.

Y. Kotsuchibashi, R. V. C. Agustin, J.-Y. Lu, D. G. Hall and R. Narain, *ACS Macro Letters* 2013, **2**, 260-264.

M. Ahmed and R. Narain, *Mol. Pharm.* 2012, **9**, 3160-3170.

E. Bat, J. Lee, U. Y. Lau and H. D. Maynard, *Nat. Commun.* 2015, **6**.

J. Lu, W. Zhang, L. Yuan, W. Ma, X. Li, W. Lu, Y. Zhao and G. Chen, *Macromol. Biosci.* 2014, **14**, 340-346.

R. Narain, A. Housni, G. Gody, P. Boullanger, M.-T. Charreyre and T. Delair, *Langmuir* 2007, **23**, 12835-12841.

S. G. Spain, L. Albertin and N. R. Cameron, *Chem. Commun.* 2006, 4198-4200.

E. Rüde, O. Westphal, E. Hurwitz, S. Fuchs and M. Sela, *Immunochemistry* 1966, **3**, 137-151.

M. I. Gibson, G. J. Hunt and N. R. Cameron, *Org. Biomol. Chem.* 2007, **5**, 2756-2757.

J. R. Kramer and T. J. Deming, *J. Am. Chem. Soc.* 2010, **132**, 15068-15071.

J. R. Kramer and T. J. Deming, *Biomacromolecules* 2010, **11**, 3668-3672.

J. R. Kramer, A. R. Rodriguez, U.-J. Choe, D. T. Kamei and T. J. Deming, *Soft Matter* 2013, **9**, 3389-3395.

J. R. Kramer and T. J. Deming, *J. Am. Chem. Soc.* 2012, **134**, 4112-4115.

J. R. Kramer and T. J. Deming, *J. Am. Chem. Soc.* 2014, **136**, 5547-5550.

K.-S. Krannig, A. Doriti and H. Schlaad, *Macromolecules* 2014, **47**, 2536-2539.

Q. Zhang, A. Anastasaki, G.-Z. Li, A. J. Haddleton, P. Wilson and D. M. Haddleton, *Polym. Chem.* 2014, **5**, 3876-3883.

J. E. Moses and A. D. Moorhouse, *Chem. Soc. Rev.* 2007, **36**, 1249-1262.

R. K. Iha, K. L. Wooley, A. M. Nyström, D. J. Burke, M. J. Kade and C. J. Hawker, *Chem. Rev.* 2009, **109**, 5620-5686.

S. Hotha and S. Kashyap, *J. Org. Chem.* 2006, **71**, 364-367.

C. R. Becer, *Macromol. Rapid Commun.* 2012, **33**, 742-752.

Y. Miura, Y. Hoshino and H. Seto, *Chem. Rev.* 2015.

V. Ladmiral, G. Mantovani, G. J. Clarkson, S. Cauet, J. L. Irwin and D. M. Haddleton, *J. Am. Chem. Soc.* 2006, **128**, 4823-4830.

G. Chen, L. Tao, G. Mantovani, J. Geng, D. Nyström and D. M. Haddleton, *Macromolecules* 2007, **40**, 7513-7520.

C. R. Becer, M. I. Gibson, J. Geng, R. Ilyas, R. Wallis, D. A. Mitchell and D. M. Haddleton, *J. Am. Chem. Soc.* 2010, **132**, 15130-15132.

Bibliography

A. Anastasaki, V. Nikolaou, G. Nurumbetov, P. Wilson, K. Kempe, J. F. Quinn, T. P. Davis, M. R. Whittaker and D. M. Haddleton, *Chem. Rev.* 2015.

M. W. Jones, L. Otten, S. J. Richards, R. Lowery, D. J. Phillips, D. M. Haddleton and M. I. Gibson, *Chemical Science* 2014, **5**, 1611-1616.

C. R. Becer, K. Babiuch, D. Pilz, S. Hornig, T. Heinze, M. Gottschaldt and U. S. Schubert, *Macromolecules* 2009, **42**, 2387-2394.

J. M. Baskin, J. A. Prescher, S. T. Laughlin, N. J. Agard, P. V. Chang, I. A. Miller, A. Lo, J. A. Codelli and C. R. Bertozzi, *Proc. Natl. Acad. Sci.* 2007, **104**, 16793-16797.

J. A. Codelli, J. M. Baskin, N. J. Agard and C. R. Bertozzi, *J. Am. Chem. Soc.* 2008, **130**, 11486-11493.

E. M. Sletten and C. R. Bertozzi, *Org. Lett.* 2008, **10**, 3097-3099.

K. Godula, M. L. Umbel, D. Rabuka, Z. Botyanszki, C. R. Bertozzi and R. Parthasarathy, *J. Am. Chem. Soc.* 2009, **131**, 10263-10268.

K. Godula and C. R. Bertozzi, *J. Am. Chem. Soc.* 2010, **132**, 9963-9965.

K. Godula and C. R. Bertozzi, *J. Am. Chem. Soc.* 2012, **134**, 15732-15742.

M. J. Paszek, C. C. DuFort, O. Rossier, R. Bainer, J. K. Mouw, K. Godula, J. E. Hudak, J. N. Lakins, A. C. Wijekoon, L. Cassereau, M. G. Rubashkin, M. J. Magbanua, K. S. Thorn, M. W. Davidson, H. S. Rugo, J. W. Park, D. A. Hammer, G. Giannone, C. R. Bertozzi and V. M. Weaver, *Nature* 2014, advance online publication.

J. M. Gargano, T. Ngo, J. Y. Kim, D. W. K. Acheson and W. J. Lees, *J. Am. Chem. Soc.* 2001, **123**, 12909-12910.

B. D. Polizzotti and K. L. Kiick, *Biomacromolecules* 2005, **7**, 483-490.

K. Lin and A. M. Kasko, *Biomacromolecules* 2012, **14**, 350-357.

A. Spaltenstein and G. M. Whitesides, *J. Am. Chem. Soc.* 1991, **113**, 686-687.

R. Roy, F. O. Andersson, G. Harms, S. Kelm and R. Schauer, *Angewandte Chemie International Edition in English* 1992, **31**, 1478-1481.

M. Ogata, K. I. P. J. Hidari, W. Kozaki, T. Murata, J. Hiratake, E. Y. Park, T. Suzuki and T. Usui, *Biomacromolecules* 2009, **10**, 1894-1903.

T. Tanaka, H. Ishitani, Y. Miura, K. Oishi, T. Takahashi, T. Suzuki, S.-i. Shoda and Y. Kimura, *ACS Macro Letters* 2014, **3**, 1074-1078.

T. B. H. Geijtenbeek, D. S. Kwon, R. Torensma, S. J. van Vliet, G. C. F. van Duijnhoven, J. Middel, I. L. M. H. A. Cornelissen, H. S. L. M. Nottet, V. N. KewalRamani, D. R. Littman, C. G. Figdor and Y. van Kooyk, *Cell* 2000, **100**, 587-597.

C. P. Alvarez, F. Lasala, J. Carrillo, O. Muñiz, A. L. Corbí and R. Delgado, *J. Virol.* 2002, **76**, 6841-6844.

I. S. Ludwig, A. N. Lekkerkerker, E. Depla, F. Bosman, R. J. P. Musters, S. Depraetere, Y. van Kooyk and T. B. H. Geijtenbeek, *J. Virol.* 2004, **78**, 8322-8332.

N. Varga, I. Sutkeviciute, R. Ribeiro-Viana, A. Berzi, R. Ramdasi, A. Daghetti, G. Vettoretti, A. Amara, M. Clerici, J. Rojo, F. Fieschi and A. Bernardi, *Biomaterials* 2014, **35**, 4175-4184.

X. Wu, L. Su, G. Chen and M. Jiang, *Macromolecules* 2015, **48**, 3705-3712.

D. Appelhans, B. Klajnert-Maculewicz, A. Janaszewska, J. Lazniewska and B. Voit, *Chem. Soc. Rev.* 2015, **44**, 3968-3996.

Q. Zhang, J. Collins, A. Anastasaki, R. Wallis, D. A. Mitchell, C. R. Becer and D. M. Haddleton, *Angew. Chem. Int. Ed.* 2013, **52**, 4435-4439.

P. Thevenot, W. Hu and L. Tang, *Curr. Top. Med. Chem.* 2008, **8**, 270-280.

C. Leng, H.-C. Hung, S. Sun, D. Wang, Y. Li, S. Jiang and Z. Chen, *ACS Appl. Mat. Interfaces* 2015, **7**, 16881-16888.

S. Chen, L. Li, C. Zhao and J. Zheng, *Polymer* 2010, **51**, 5283-5293.

G. Cheng, Z. Zhang, S. Chen, J. D. Bryers and S. Jiang, *Biomaterials* 2007, **28**, 4192-4199.

M. Ukawa, H. Akita, T. Masuda, Y. Hayashi, T. Konno, K. Ishihara and H. Harashima, *Biomaterials* 2010, **31**, 6355-6362.

N. Saito, Y. Usui, K. Aoki, N. Narita, M. Shimizu, K. Hara, N. Ogiwara, K. Nakamura, N. Ishigaki, H. Kato, S. Taruta and M. Endo, *Chem. Soc. Rev.* 2009, **38**, 1897-1903.

B. C. Thompson, E. Murray and G. G. Wallace, *Adv. Mater.* 2015, n/a-n/a.

G. Jia, H. Wang, L. Yan, X. Wang, R. Pei, T. Yan, Y. Zhao and X. Guo, *Environ. Sci. Technol.* 2005, **39**, 1378-1383.

Bibliography

A. Magrez, S. Kasas, V. Salicio, N. Pasquier, J. W. Seo, M. Celio, S. Catsicas, B. Schwaller and L. Forró, *Nano Lett.* 2006, **6**, 1121-1125.

Y. Chen, A. Star and S. Vidal, *Chem. Soc. Rev.* 2013, **42**, 4532-4542.

X. Chen, U. C. Tam, J. L. Czlapinski, G. S. Lee, D. Rabuka, A. Zettl and C. R. Bertozzi*, J. Am. Chem. Soc.* 2006, **128**, 6292-6293.

P. Wu, X. Chen, N. Hu, U. C. Tam, O. Blixt, A. Zettl and C. R. Bertozzi, *Angew. Chem., Int. Ed.* 2008, **47**, 5022-5025.

K. Yu, B. F. L. Lai and J. N. Kizhakkedathu, *Adv. Healthcare Mater.* 2012, **1**, 199-213.

R. A. Worthylake and K. Burridge, *Curr. Opin. Cell Biol.* 2001, **13**, 569-577.

S. D. Rosen, *The American Journal of Pathology* 1999, **155**, 1013-1020.

S. D. Rosen, *Annu. Rev. Immunol.* 2004, **22**, 129-156.

P. Mowery, Z.-Q. Yang, E. J. Gordon, O. Dwir, A. G. Spencer, R. Alon and L. L. Kiessling, *Chem. Biol.* 2004, **11**, 725-732.

A. H. Courtney, N. R. Bennett, D. B. Zwick, J. Hudon and L. L. Kiessling, *ACS Chem. Biol.* 2014, **9**, 202-210.

J. R. Kramer, B. Onoa, C. Bustamante and C. R. Bertozzi, *Proc. Natl. Acad. Sci.* 2015, **112**, 12574-12579.

M. Malmqvist, *Nature* 1993, **361**, 186-187.

I. H. El-Sayed, X. Huang and M. A. El-Sayed, *Nano Lett.* 2005, **5**, 829-834.

X. Liu, Q. Zhang, Y. Tu, W. Zhao and H. Gai, *Anal. Chem.* 2013, **85**, 11851-11857.

Y. Zhang, S. Luo, Y. Tang, L. Yu, K.-Y. Hou, J.-P. Cheng, X. Zeng and P. G. Wang, *Anal. Chem.* 2006, **78**, 2001-2008.

M. Mayer and B. Meyer, *J. Am. Chem. Soc.* 2001, **123**, 6108-6117.

R. Kuhn, R. Frei and M. Christen, *Anal. Biochem.* 1994, 218, 131-135.

Y. C. Lee, *J. Biochem.* 1997, **121**, 818-825.

T. V. Ratto, K. C. Langry, R. E. Rudd, R. L. Balhorn, M. J. Allen and M. W. McElfresh, *Biophys. J.* 2004, **86**, 2430-2437.

X. Zeng, C. S. Andrade, M. L. Oliveira and X.-L. Sun, *Anal. BioAnal. Chem.* 2012, **402**, 3161-3176.

S. Slavin, A. H. Soeriyadi, L. Voorhaar, M. R. Whittaker, C. R. Becer, C. Boyer, T. P. Davis and D. M. Haddleton, *Soft Matter* 2012, **8**, 118-128.

Y. Chen, H. Vedala, G. P. Kotchey, A. Audfray, S. Cecioni, A. Imberty, S. Vidal and A. Star, *ACS Nano* 2011, **6**, 760-770.

X. Jiang, M. Ahmed, Z. Deng and R. Narain, Bioconjugate Chem. 2009, 20, 994-1001.

H. Uzawa, H. Ito, P. Neri, H. Mori and Y. Nishida, *ChemBioChem* 2007, **8**, 2117-2124.

T. Nagatsuka, H. Uzawa, K. Sato, S. Kondo, M. Izumi, K. Yokoyama, I. Ohsawa, Y. Seto, P. Neri, H. Mori, Y. Nishida, M. Saito and E. Tamiya, *ACS Appl. Mater. Interfaces* 2013, **5**, 4173-4180.

H. Uzawa, S. Kamiya, N. Minoura, H. Dohi, Y. Nishida, K. Taguchi, S.-i. Yokoyama, H. Mori, T. Shimizu and K. Kobayashi, *Biomacromolecules* 2002, **3**, 411-414.

C. L. Schofield, R. A. Field and D. A. Russell, *Anal. Chem.* 2007, **79**, 1356-1361.

M. J. Marin, A. Rashid, M. Rejzek, S. A. Fairhurst, S. A. Wharton, S. R. Martin, J. W. McCauley, T. Wileman, R. A. Field and D. A. Russell, *Org. Biomol. Chem.* 2013, **11**, 7101-7107.

Z. Shen, M. Huang, C. Xiao, Y. Zhang, X. Zeng and P. G. Wang, *Anal. Chem.* 2007, **79**, 2312-2319.

Y. Wang, R. Narain and Y. Liu, *Langmuir* 2014, **30**, 7377-7387.

Y. Wang, Y. Kotsuchibashi, Y. Liu and R. Narain, *ACS Appl. Mat. Interfaces* 2015, **7**, 1652-1661.

A. Mader, K. Gruber, R. Castelli, B. A. Hermann, P. H. Seeberger, J. O. Rädler and M. Leisner, *Nano Lett.* 2011, **12**, 420-423.

X. Gao, Y. Cui, R. M. Levenson, L. W. K. Chung and S. Nie, *Nat. Biotech.* 2004, **22**, 969-976.

R. Kikkeri, B. Lepenies, A. Adibekian, P. Laurino and P. H. Seeberger, *J. Am. Chem. Soc.* 2009, **131**, 2110-2112.

C.-T. Chen, Y. S. Munot, S. B. Salunke, Y.-C. Wang, R.-K. Lin, C.-C. Lin, C.-C. Chen and Y. H. Liu, *Adv. Funct. Mater.* 2008, **18**, 527-540.

L. Yang, X.-H. Peng, Y. A. Wang, X. Wang, Z. Cao, C. Ni, P. Karna, X. Zhang, W. C. Wood, X. Gao, S. Nie and H. Mao, *Clinical Cancer Research* 2009, **15**, 4722-4732.

S. I. van Kasteren, S. J. Campbell, S. Serres, D. C. Anthony, N. R. Sibson and B. G. Davis, *Proceedings of the National Academy of Sciences* 2009, **106**, 18-23.

M. K. Yu, Y. Y. Jeong, J. Park, S. Park, J. W. Kim, J. J. Min, K. Kim and S. Jon, *Angew. Chem., Int. Ed.* 2008, **47**, 5362-5365.

M. Kamat, K. El-Boubbou, D. C. Zhu, T. Lansdell, X. Lu, W. Li and X. Huang, *Bioconjugate Chem.* 2010, **21**, 2128-2135.

H. Hyun, K. Lee, K. H. Min, P. Jeon, K. Kim, S. Y. Jeong, I. C. Kwon, T. G. Park and M. Lee, *J. Controlled Release* 2013, **170**, 352-357.

K. Y. Choi, K. H. Min, H. Y. Yoon, K. Kim, J. H. Park, I. C. Kwon, K. Choi and S. Y. Jeong, *Biomaterials* 2011, **32**, 1880-1889.

K. S. Kim, W. Hur, S.-J. Park, S. W. Hong, J. E. Choi, E. J. Goh, S. K. Yoon and S. K. Hahn, *ACS Nano* 2010, **4**, 3005-3014.

S. Mura, J. Nicolas and P. Couvreur, *Nat. Mater.* 2013, **12**, 991-1003.

K. Cho, X. Wang, S. Nie, Z. Chen and D. M. Shin, Clin. Cancer Res., 2008, 14, 1310-1316.

Y. Wang, X. Zhang, P. Yu and C. Li, Int. *J. Pharm.* 2013, **441**, 170-180.

G. Chen, S. Amajjahe and M. H. Stenzel, *Chem. Commun.* 2009, 1198-1200.

L. Liu, J. Zhang, W. Lv, Y. Luo and X. Wang, *J. Polym. Sci., Part A: Polym. Chem.* 2010, **48**, 3350-3361.

M. Mahkam, *Drug Delivery* 2007, **14**, 147-153.

S. Vandewalle, S. Wallyn, S. Chattopadhyay, C. R. Becer and F. Du Prez, *Eur. Polym. J.* 2015, **69**, 490-498.

I. F. Tannock and D. Rotin, *Cancer Res.* 1989, **49**, 4373-4384.

A. Acharya, I. Das, D. Chandhok and T. Saha, Oxidative Medicine and Cellular Longevity, 2010, 3, 23-34.

Q. Guo, Z. Wu, X. Zhang, L. Sun and C. Li, *Soft Matter* 2014, **10**, 911-920.

E. Audebeau, E. K. Oikonomou, S. Norvez and I. Iliopoulos, *Polym. Chem.* 2014, **5**, 2273-2281.

M. Ahmed, Z. Deng and R. Narain, *ACS Appl. Mater. Interfaces* 2009, **1**, 1980-1987.

J.-T. Chen, M. Ahmed, Q. Liu and R. Narain, *J. Biomed. Mater. Research Part A* 2012, **100A**, 2342-2347.

R. Sunasee, P. Wattanaarsakit, M. Ahmed, F. B. Lollmahomed and R. Narain, *Bioconjugate Chem.* 2012, **23**, 1925-1933.

L. Xue, N. P. Ingle and T. M. Reineke, *Biomacromolecules* 2013.

A. Sizovs, L. Xue, Z. P. Tolstyka, N. P. Ingle, Y. Wu, M. Cortez and T. M. Reineke, *J. Am. Chem. Soc.* 2013, **135**, 15417-15424.

L. Xue, N. P. Ingle and T. M. Reineke, *Biomacromolecules* 2013, **14**, 3903-3915.

K. Anderson, A. Sizovs, M. Cortez, C. Waldron, D. M. Haddleton and T. M. Reineke, *Biomacromolecules* 2012, **13**, 2229-2239.

M. Tranter, Y. Liu, S. He, J. Gulick, X. Ren, J. Robbins, W. K. Jones and T. M. Reineke, *Mol. Ther.* 2012, **20**, 601-608.

E.-K. Lim, H.-O. Kim, E. Jang, J. Park, K. Lee, J.-S. Suh, Y.-M. Huh and S. Haam, *Biomaterials* 2011, **32**, 7941-7950.

I. Naokazu, E. Mitsuhiro, K. Yohei, N. Ravin and A. Takao, *Sci. Tech. Adv. Mater.* 2012, **13**, 064206.

Q. Meng, A. Haque, B. Hexig and T. Akaike, *Biomaterials* 2012, **33**, 1414-1427.

G. Simone, N. Malara, V. Trunzo, G. Perozziello, P. Neuzil, M. Francardi, L. Roveda, M. Renne, U. Prati, V. Mollace, A. Manz and E. Di Fabrizio, *Small* 2013, **9**, 2152-2161.

G. Simone, N. Malara, V. Trunzo, M. Renne, G. Perozziello, E. Di Fabrizio and A. Manz, *Mol. BioSyst.* 2014, **10**, 258-265.

H. Seto, Y. Ogata, T. Murakami, Y. Hoshino and Y. Miura, *ACS Appl. Mater. Interfaces* 2011, **4**, 411-417.

A.-F. Che, X.-J. Huang and Z.-K. Xu, *J. Membr. Sci.* 2011, **366**, 272-277.

Y.-C. Qian, N. Ren, X.-J. Huang, C. Chen, A.-G. Yu and Z.-K. Xu, *Macromol. Chem. Phys.* 2013, **214**, 1852-1858.

X.-Y. Ye, X.-J. Huang and Z.-K. Xu, *Colloids and Surfaces B: Biointerfaces* 2014, **115**, 340-348.

Y. Wang, Y. Kotsuchibashi, K. Uto, M. Ebara, T. Aoyagi, Y. Liu and R. Narain, *Biomater. Sci.* 2015, **3**, 152-162.

Bibliography

A. Fowler and M. Toner, *Ann. N.Y. Acad. Sci.* 2006, **1066**, 119-135.

G. M. Fahy, J. Saur and R. J. Williams, *Cryobiol.* 1990, **27**, 492-510.

J. A. Raymond, P. Wilson and A. L. DeVries, *Proc. Natl. Acad. Sci.* 1989, **86**, 881-885.

D. Gao and J. K. Critser, *ILAR Journal* 2000, **41**, 187-196.

M. I. Gibson, C. A. Barker, S. G. Spain, L. Albertin and N. R. Cameron, *Biomacromolecules* 2009, **10**, 328-333.

B. L. Wilkinson, R. S. Stone, C. J. Capicciotti, M. Thaysen-Andersen, J. M. Matthews, N. H. Packer, R. N. Ben and R. J. Payne, *Angew. Chem. Int. Ed.* 2012, **51**, 3606-3610.

R. C. Deller, M. Vatish, D. A. Mitchell and M. I. Gibson, *Nat. Commun.* 2014, **5**.

E. M. Pelegri-O'Day, E.-W. Lin and H. D. Maynard, *J. Am. Chem. Soc.* 2014, **136**, 14323-14332.

W. Yandi, S. Mieszkin, P. Martin-Tanchereau, M. E. Callow, J. A. Callow, L. Tyson, B. Liedberg and T. Ederth, *ACS Appl. Mat. Interfaces* 2014, **6**, 11448-11458.

J.-S. Gu, H.-Y. Yu, L. Huang, Z.-Q. Tang, W. Li, J. Zhou, M.-G. Yan and X.-W. Wei, *J. Membr. Sci.* 2009, **326**, 145-152.

Q. Shi, J.-Q. Meng, R.-S. Xu, X.-L. Du and Y.-F. Zhang, *J. Membr. Sci.* 2013, **444**, 50-59.

X. Dai and R. M. Hozalski, *Enviro. Sci. Tech.* 2003, **37**, 1037-1042.

L. Pang, U. Nowostawska, L. Weaver, G. Hoffman, A. Karmacharya, A. Skinner and N. Karki, *Environ. Sci. Tech.* 2012, **46**, 11779-11787.

T. Juhna, D. Birzniece, S. Larsson, D. Zulenkovs, A. Sharipo, N. F. Azevedo, F. Ménard-Szczebara, S. Castagnet, C. Féliers and C. W. Keevil, *Appl. Environ. Microbiol.* 2007, 73, 7456-7464.

N. J. Shikuma and M. G. Hadfield, *Biofouling* 2009, **26**, 39-46.

A. G. Gristina, *Science* 1987, **237**, 1588-1595.

V. Zijnge, M. B. M. van Leeuwen, J. E. Degener, F. Abbas, T. Thurnheer, R. Gmür and H. J. M. Harmsen, *PLoS ONE* 2010, **5**, e9321.

H. J. Busscher and A. H. Weerkamp, *FEMS Microbiol. Lett.* 1987, **46**, 165-173.

M. C. van Loosdrecht, J. Lyklema, W. Norde, G. Schraa and A. J. Zehnder, *Appl. Environ. Microbiol.* 1987, **53**, 1893-1897.

É. Kiss, J. Samu, A. Tóth and I. Bertóti, *Langmuir* 1996, **12**, 1651-1657.

Y. Sakagami, H. Yokoyama, H. Nishimura, Y. Ose and T. Tashima, *Appl. Environ. Microbiol.* 1989, **55**, 2036-2040.

D. Kiaei, A. S. Hoffman, T. A. Horbett and K. R. Lew, *J. Biomed. Mater. Res.* 1995, **29**, 729-739.

W. P. Johnson and B. E. Logan, *Water Res.* 1996, 30, 923-931.

G. Smit, M. H. Straver, B. J. Lugtenberg and J. W. Kijne, *Appl. Environ. Microbiol.* 1992, **58**, 3709-3714.

T. A. Camesano and B. E. Logan, *Environ. Sci. Technol.* 1998, **32**, 1699-1708.

M. C. M. Van Loosdrecht, W. Norde and A. J. B. Zehnder, *J. Biomater. Appl.* 1990, **5**, 91-106.

N. P. Boks, W. Norde, H. C. van der Mei and H. J. Busscher, *Microbiology* 2008, **154**, 3122-3133.

S. Bayoudh, A. Othmane, L. Mora and H. Ben Ouada, *Colloids Surf. B* 2009, **73**, 1-9.

N. Sharon, *FEBS Lett.* 1987, **217**, 145-157.

X.-Q. Mu and E. Bullitt, *Proc. Natl. Acad. Sci.* 2006, **103**, 9861-9866.

S. J. Hultgren, F. Lindberg, G. Magnusson, J. Kihlberg, J. M. Tennent and S. Normark, *Proc. Natl. Acad. Sci.* 1989, **86**, 4357-4361.

G. Cioci, E. P. Mitchell, C. Gautier, M. Wimmerová, D. Sudakevitz, S. Pérez, N. Gilboa-Garber and A. Imberty, *FEBS Lett.* 2003, **555**, 297-301.

N. Laurent, J. Voglmeir and S. L. Flitsch, *Chem. Commun.* 2008, **37**, 4400-4412.

X.-L. Su and Y. Li, *Biosens. Bioelectron.* 2005, **21**, 840-848.

Y.-T. Tseng, H.-Y. Chang and C.-C. Huang, *Chem. Commun.* 2012, **48**, 8712-8714.

C. Poitras and N. Tufenkji, *Biosens. Bioelectron.* 2009, **24**, 2137-2142.

Z. Shen, M. Huang, C. Xiao, Y. Zhang, X. Zeng and P. G. Wang, *Anal. Chem.* 2007, **79**, 2312-2319.

A. L. J. Olsson, H. C. van der Mei, H. J. Busscher and P. K. Sharma, *Langmuir* 2009, **25**, 1627-1632.

H. J. Busscher, W. Norde and H. C. van der Mei, *Appl. Environ. Microbiol.* 2008, **74**, 2559-2564.

H. C. van der Mei, M. Rustema-Abbing, J. de Vries and H. J. Busscher, *Appl. Environ. Microbiol.* 2008, **74**, 5511-5515.

Y. Gou, S.-J. Richards, D. M. Haddleton and M. I. Gibson, *Polym. Chem.* 2012, **3**, 1634-1640.

M. Huang, Z. Shen, Y. Zhang, X. Zeng and P. G. Wang, *Bioorg. Med. Chem. Lett.* 2007, **17**, 5379-5383.

Z. Deng, M. Ahmed and R. Narain, *J. Polym. Sci., Part A: Polym. Chem.* 2009, **47**, 614-627.

Z. Deng, H. Bouchékif, K. Babooram, A. Housni, N. Choytun and R. Narain, *J. Polym. Sci., Part A: Polym. Chem.* 2008, **46**, 4984-4996.

S. Slavin, A. H. Soeriyadi, L. Voorhaar, M. R. Whittaker, C. R. Becer, C. Boyer, T. P. Davis and D. M. Haddleton, *Soft Matter* 2011, **8**, 118-128.

S. M. Dimick, S. C. Powell, S. A. McMahon, D. N. Moothoo, J. H. Naismith and E. J. Toone, *J. Am. Chem. Soc.* 1999, **121**, 10286-10296.

M. Benaglia, E. Rizzardo, A. Alberti and M. and Guerra, *Macromolecules* 2005, **38**, 3129-3140.

Z. Deng, S. Li, X. Jiang and R. Narain, *Macromolecules* **2009**, 42, 6393-6405.

X. Sun, C. Danumah, Y. Liu and Y. Boluk, *Chem. Eng. J.* 2012, **198-199**, 476-481.

A. L. J. Olsson, H. C. van der Mei, H. J. Busscher and P. K. Sharma, *Langmuir* 2010, **26**, 11113-11117.

A. L. J. Olsson, H. C. van der Mei, D. Johannsmann, H. J. Busscher and P. K. Sharma, *Anal. Chem.* 2012, **84**, 4504-4512.

A. L. J. Olsson, N. Arun, J. S. Kanger, H. J. Busscher, I. E. Ivanov, T. A. Camesano, Y. Chen, D. Johannsmann, H. C. van der Mei and P. K. Sharma, *Soft Matter* 2012, **8**, 9870-9876.

I. Reviakine, D. Johannsmann and R. P. Richter, Anal. Chem. 2011, 83, 8838-8848.

J. C. Munro and C. W. Frank, *Polymer* 2003, **44**, 6335-6344.

S.-F. Chou, W.-L. Hsu, J.-M. Hwang and C.-Y. Chen, *Anal. Chim. Acta* 2002, **453**, 181-189.

H. Lis and N. Sharon, Lectins, Springer, 2007.

J. J. Lundquist and E. J. Toone, *Chem. Rev.* 2002, **102**, 555-578.

R. Karamanska, B. Mukhopadhyay, D. A. Russell and R. A. Field, *Chem. Commun.* 2005, 3334-3336.

M. Ahmed, B. F. L. Lai, J. N. Kizhakkedathu and R. Narain, *Bioconjugate Chem.* 2012, **23**, 1050-1058.

I. van Die, S. J. van Vliet, A. K. Nyame, R. D. Cummings, C. M. C. Bank, B. Appelmelk, T. B. H. Geijtenbeek and Y. van Kooyk, *Glycobiology* 2003, **13**, 471-478.

S. P. Diggle, R. E. Stacey, C. Dodd, M. Cámara, P. Williams and K. Winzer, *Environ. Microbiol.* 2006, **8**, 1095-1104.

D. Tielker, S. Hacker, R. Loris, M. Strathmann, J. Wingender, S. Wilhelm, F. Rosenau and K.-E. Jaeger, *Microbiology* 2005, **151**, 1313-1323.

A. L. J. Olsson, P. K. Sharma, H. C. van der Mei and H. J. Busscher, *Appl. Environ. Microbiol.* 2012, **78**, 99-102.

J. J. I. Ramos, I. Llarena and S. E. Moya, *J. Polym. Sci., Part A: Polym. Chem.* 2011, **49**, 2346-2352.

J. A. Lichter, M. T. Thompson, M. Delgadillo, T. Nishikawa, M. F. Rubner and K. J. Van Vliet, *Biomacromolecules* 2008, **9**, 1571-1578.

McLaughl.Sg, G. Szabo and G. Eisenman, *J. Gen. Physiol.* 1971, **58**, 667-&.

M. Ahmed and R. Narain, *Biomaterials* 2011, **32**, 5279-5290.

N. Kawasaki, T. Kawasaki and I. Yamashina, *J. Biochem.* 1989, **106**, 483-489.

Z. Barshavit, R. Goldman, I. Ofek, N. Sharon and D. Mirelman, *Infection and Immunit* 1980, **29**, 417-424.

B. Li and B. E. Logan, *Colloids Surf. B* 2004, **36**, 81-90.

I. M. Marcus, M. Herzberg, S. L. Walker and V. Freger, *Langmuir* 2012, **28**, 6396-6402.

M. B. Campa, Mauro Herman, Friedman, Pseudomonas aeruginosa as an Opportunistic Pathogen, Springer US, New York, 1993.

J. B. Lyczak, C. L. Cannon and G. B. Pier, *Microbes. Infect.* 2000, **2**, 1051-1060.

G. B. Pier, in Goldman's Cecil Medicine (Twenty-Fourth Edition), W.B. Saunders, Philadelphia, 2012, pp. 1877-1881.

M. Larrosa, P. Truchado, J. C. Espín, F. A. Tomás-Barberán, A. Allende and M. T. García-Conesa, *Mol. Cell. Probes* 2012, **26**, 121-126.

P. Doig, T. Todd, P. A. Sastry, K. K. Lee, R. S. Hodges, W. Paranchych and R. T. Irvin, *Infect. Immun.* 1988, **56**, 1641-1646.

R. R. Maddikeri, S. Tosatti, M. Schuler, S. Chessari, M. Textor, R. G. Richards and L. G. Harris, *J. Biomed. Mater. Res. Part A.* 2008, **84A**, 425-435.

M. C. van Loosdrecht, J. Lyklema, W. Norde, G. Schraa and A. J. Zehnder, *Appl. Environ. Microbiol.* 1987, **53**, 1893-1897.

H. J. Busscher and A. H. Weerkamp, *FEMS Microbiol. Lett.* 1987, **46**, 165-173.

R. Bos, H. C. van der Mei and H. J. Busscher, *FEMS Microbiology Reviews* 1999, **23**, 179-230.

R. J. Doyle, *Microb. Infect.* 2000, **2**, 391-400.

G. M. Bruinsma, H. C. van der Mei and H. J. Busscher, *Biomaterials* 2001, **22**, 3217-3224.

A. G. Karakecili and M. Gumusderelioglu, *J. Biomater. Sci., Polym. Ed.* 2002, **13**, 185-196.

G. Hwang, J. Liang, S. Kang, M. Tong and Y. Liu, *BioChem. Eng. J.* 2013, **76**, 90-98.

G. Hwang, S. Kang, M. G. El-Din and Y. Liu, *Biofouling* 2012, **28**, 525-538.

D. Tielker, S. Hacker, R. Loris, M. Strathmann, J. Wingender, S. Wilhelm, F. Rosenau and K.-E. Jaeger, *Microbiology* 2005, **151**, 1313-1323.

S. P. Diggle, R. E. Stacey, C. Dodd, M. Cámara, P. Williams and K. Winzer, *Environ. Microbiol.* 2006, **8**, 1095-1104.

Z. Shen, M. Huang, C. Xiao, Y. Zhang, X. Zeng and P. G. Wang, *Anal. Chem.* 2007, **79**, 2312-2319.

G. B. Pier, *Int. J. Med. Microbiol.* 2007, **297**, 277-295.

M. J. Preston, J. M. Berk, L. D. Hazlett and R. S. Berk, *Infect. Immun.* 1991, **59**, 1984-1990.

Q. Lu, J. Wang, A. Faghihnejad, H. Zeng and Y. Liu, *Soft Matter* 2011, **7**, 9366-9379.

X.-L. Su and Y. Li, *Biosens. Bioelectron.* 2005, **21**, 840-848.

Y. Wang, R. Narain and Y. Liu, *Langmuir* 2014, **30**, 7377-7387.

H. Ghebeh, J. Gillis and M. Butler, *J. Biotechnol.* 2002, **95**, 39-48.

K. A. Krogfelt, H. Bergmans and P. Klemm, *Infect. Immun.* 1990, **58**, 1995-1998.

A. Pranzetti, S. Salaün, S. Mieszkin, M. E. Callow, J. A. Callow, J. A. Preece and P. M. Mendes, *Adv. Funct. Mater.* 2012, **22**, 3672-3681.

Y.-T. Tseng, H.-Y. Chang and C.-C. Huang, *Chem. Commun.* 2012, **48**, 8712-8714.

I. Chaduc, W. Zhang, J. Rieger, M. Lansalot, F. D'Agosto and B. Charleux, *Macromol. Rapid Commun.* 2011, **32**, 1270-1276.

M. Benaglia, E. Rizzardo, A. Alberti and M. and Guerra, *Macromolecules* 2005, **38**, 3129-3140.

A. H. Rickard, S. A. Leach, C. M. Buswell, N. J. High and P. S. Handley, *Appl. Environ. Microbiol.* 2000, **66**, 431-434.

S. P. Diggle, K. Winzer, S. R. Chhabra, K. E. Worrall, M. Cámara and P. Williams, *Mol. Microbiol.* 2003, **50**, 29-43.

M. Ebara, M. Yamato, T. Aoyagi, A. Kikuchi, K. Sakai and T. Okano, *Adv. Mater.* 2008, **20**, 3034-3038.

I. Reviakine, D. Johannsmann and R. P. Richter, *Anal. Chem.* 2011, **83**, 8838-8848.

H. Willcock and R. K. O'Reilly, *Polym. Chem.* 2010, **1**, 149-157.

I. C. Barker, J. M. G. Cowie, T. N. Huckerby, D. A. Shaw, I. Soutar and L. Swanson, *Macromolecules* 2003, **36**, 7765-7770.

E. S. Gil and S. M. Hudson, *Prog. Polym. Sci.* 2004, **29**, 1173-1222.

T. Hoare and R. Pelton, *Macromolecules* 2007, **40**, 670-678.

G. Z. Zhang, *Macromolecules* 2004, **37**, 6553-6557.

G. H. Chen and A. S. Hoffman, *Nature*, 1995, **373**, 49-52.

Q. Duan, Y. Miura, A. Narumi, X. Shen, S.-I. Sato, T. Satoh and T. Kakuchi, *J. Polym. Sci., Part A: Polym. Chem.* 2006, **44**, 1117-1124.

S. Furyk, Y. Zhang, D. Ortiz-Acosta, P. S. Cremer and D. E. Bergbreiter, *J. Polym. Sci., Part A: Polym. Chem.* 2006, **44**, 1492-1501.

Y. Xia, N. A. D. Burke and H. D. H. Stöver, *Macromolecules* 2006, **39**, 2275-2283.

C. Xue, N. Yonet-Tanyeri, N. Brouette, M. Sferrazza, P. V. Braun and D. E. Leckband, *Langmuir* 2011, **27**, 8810-8818.

H. Ko, Z. Zhang, Y.-L. Chueh, E. Saiz and A. Javey, *Angew. Chem. Int. Ed.* 2010, **49**, 616-619.

F. Montagne, J. Polesel-Maris, R. Pugin and H. Heinzelmann, *Langmuir* 2008, **25**, 983-991.

S. A. Makin and T. J. Beveridge, *J. Bacteriol.* 1996, **178**, 3350-3352.

N. Gilboa-Garber and D. Sudakevitz, *FEMS Immunol. Med. Microbiol.* 1999, **25**, 365-369.

S. A. Makin and T. J. Beveridge, *Microbiology*, 1996, **142**, 299-307.

A. Roosjen, H. C. van der Mei, H. J. Busscher and W. Norde, *Langmuir* 2004, **20**, 10949-10955.

A. E. Zeraik and M. Nitschke, *Braz. arch. biol. technol.* 2012, **55**, 569-576.

G. Cioci, E. P. Mitchell, C. Gautier, M. Wimmerová, D. Sudakevitz, S. Pérez, N. Gilboa-Garber and A. Imberty, *FEBS Lett.* 2003, **555**, 297-301.

J. J. Lundquist and E. J. Toone, *Chem. Rev.* 2002, **102**, 555-578.

E. M. Munoz, J. Correa, E. Fernandez-Megia and R. Riguera, *J. Am. Chem. Soc.* 2009, **131**, 17765-17767.

Y. Wang, Y. Kotsuchibashi, Y. Liu and R. Narain, *Langmuir* 2014, **30**, 2360-2368.

J. Hu and S. Liu, *Macromolecules* 2010, **43**, 8315-8330.

G. Cioci, E.P. Mitchell, C. Gautier, M. Wimmerová, D. Sudakevitz, S. Pérez, N. Gilboa-Garber, A. Imberty, *FEBS Lett.* 2003, **555**, 297-301.

D. Li and Y. Xia, *Adv. Mater.* 2004, 16, 1151-1170.

H. Yoshimoto, Y. M. Shin, H. Terai and J. P. Vacanti, *Biomaterials* 2003, **24**, 2077-2082.

Y.-J. Kim, M. Ebara and T. Aoyagi, *Angew. Chem. Int. Ed.* 2012, **51**, 10537-10541.

K. Namekawa, M. T. Schreiber, T. Aoyagi and M. Ebara, *Biomater. Sci.* 2014, **2**, 674-679.

X. Wang, X. Chen, K. Yoon, D. Fang, B. S. Hsiao and B. Chu, *Environ. Sci. Technol.* 2005, **39**, 7684-7691.

J. Shin, S.-J. Choi, I. Lee, D.-Y. Youn, C. O. Park, J.-H. Lee, H. L. Tuller and I.-D. Kim, *Adv. Funct. Mater.* 2013, **23**, 2357-2367.

D.-J. Yang, I. Kamienchick, D. Y. Youn, A. Rothschild and I.-D. Kim, *Adv. Funct. Mater.* 2010, **20**, 4258-4264.

L. Wang, G. R. Williams, H.-l. Nie, J. Quan and L.-m. Zhu, *Polym. Chem.* 2014, **5**, 3009-3017.

S. Patel, K. Kurpinski, R. Quigley, H. Gao, B. S. Hsiao, M.-M. Poo and S. Li, *Nano Lett.* 2007, **7**, 2122-2128.

T. Uyar, R. Havelund, J. Hacaloglu, F. Besenbacher and P. Kingshott, *ACS Nano* 2010, **4**, 5121-5130.

Q. Yang, J. Wu, J.-J. Li, M.-X. Hu and Z.-K. Xu, *Macromol. Rapid Commun.* 2006, **27**, 1942-1948.

S. D. Bull, M. G. Davidson, J. M. H. van den Elsen, J. S. Fossey, A. T. A. Jenkins, Y.-B. Jiang, Y. Kubo, F. Marken, K. Sakurai, J. Zhao and T. D. James, *Acc. Chem. Res.* 2012, **46**, 312-326.

S. L. Wiskur, J. J. Lavigne, H. Ait-Haddou, V. Lynch, Y. H. Chiu, J. W. Canary and E. V. Anslyn, *Org. Lett.* 2001, **3**, 1311-1314.

Q. Guo, Z. Wu, X. Zhang, L. Sun and C. Li, *Soft Matter* 2014, **10**, 911-920.

A. Matsumoto, K. Yamamoto, R. Yoshida, K. Kataoka, T. Aoyagi and Y. Miyahara, *Chem. Commun.* 2010, **46**, 2203-2205.

H. Liu, Y. Li, K. Sun, J. Fan, P. Zhang, J. Meng, S. Wang and L. Jiang, *J. Am. Chem. Soc.* 2013, **135**, 7603-7609.

T. Hoare and R. Pelton, *Macromolecules* 2007, **40**, 670-678.

M. B. Lerner, N. Kybert, R. Mendoza, R. Villechenon, M. A. Bonilla Lopez and A. T. Charlie Johnson, *Appl. Phys. Lett.* 2013, **102**, -.

C. Zhang, M. D. Losego and P. V. Braun, *Chem. Mater.* 2013, 25, 3239-3250.

T. Aoki, Y. Nagao, K. Sanui, N. Ogata, A. Kikuchi, Y. Sakurai, K. Kataoka and T. Okano, *J. Biomater. Sci., Polym. Ed.* 1997, **9**, 1-14.

E. Baştürk and M. V. Kahraman, *Polym. Compos.* 2012, **33**, 829-837.

M. Benaglia, E. Rizzardo, A. Alberti and M. and Guerra, *Macromolecules* 2005, **38**, 3129-3140.

Z. Deng, M. Ahmed and R. Narain, *J. Polym. Sci., Part A: Polym. Chem.* 2009, **47**, 614-627.

Y.-J. Lee, S. A. Pruzinsky and P. V. Braun, *Langmuir* 2004, **20**, 3096-3106.

W. N. E. van Dijk-Wolthuis, O. Franssen, H. Talsma, M. J. van Steenbergen, J. J. Kettenes-van den Bosch and W. E. Hennink, *Macromolecules* 1995, **28**, 6317-6322.

A. V. Reis, A. R. Fajardo, I. T. A. Schuquel, M. R. Guilherme, G. J. Vidotti, A. F. Rubira and E. C. Muniz, *J. Org. Chem.* 2009, **74**, 3750-3757.

G. Kim, H. Yoon and Y. Park, *Appl. Phys. A* 2010, **100**, 1197-1204.

J. Lee, Y. H. Jeong and D.-W. Cho, *Macromol. Mater. Eng.* 2014, n/a-n/a.

S. V. Fridrikh, J. H. Yu, M. P. Brenner and G. C. Rutledge, *Phys. Rev. Lett.* 2003, **90**, 144502.

D. G. Hall, in Boronic Acids, Wiley-VCH Verlag GmbH & Co. KGaA, 2006, pp. 1-99.

J. P. Lorand and J. O. Edwards, *J. Org. Chem.* 1959, **24**, 769-774.

D. Fangkai, M. Yunhao, Z. Fang, Y. Changmin and W. Shuizhu, *Nanotechnology* 2013, **24**, 365101.

C. Ke, H. Destecroix, M. P. Crump and A. P. Davis, *Nat. Chem.* 2012, **4**, 718-723.

P. Attard, in Adv. Chem. Phys. John Wiley & Sons, Inc., 2007, pp. 1-159.

L. Gu, T. Elkin, X. Jiang, H. Li, Y. Lin, L. Qu, T.-R. J. Tzeng, R. Joseph and Y.-P. Sun, *Chem. Commun.* 2005, 874-876.

Q. Yang, M. Strathmann, A. Rumpf, G. Schaule and M. Ulbricht, *ACS Appl. Mat. Interfaces* 2010, **2**, 3555-3562.

G. Pasparakis and C. Alexander, *Angew. Chem. Int. Ed.* 2008, **47**, 4847-4850.

R. Ribeiro-Viana, M. Sánchez-Navarro, J. Luczkowiak, J. R. Koeppe, R. Delgado, J. Rojo and B. G. Davis, *Nat. Commun.* 2012, **3**, 1303.

Appendix

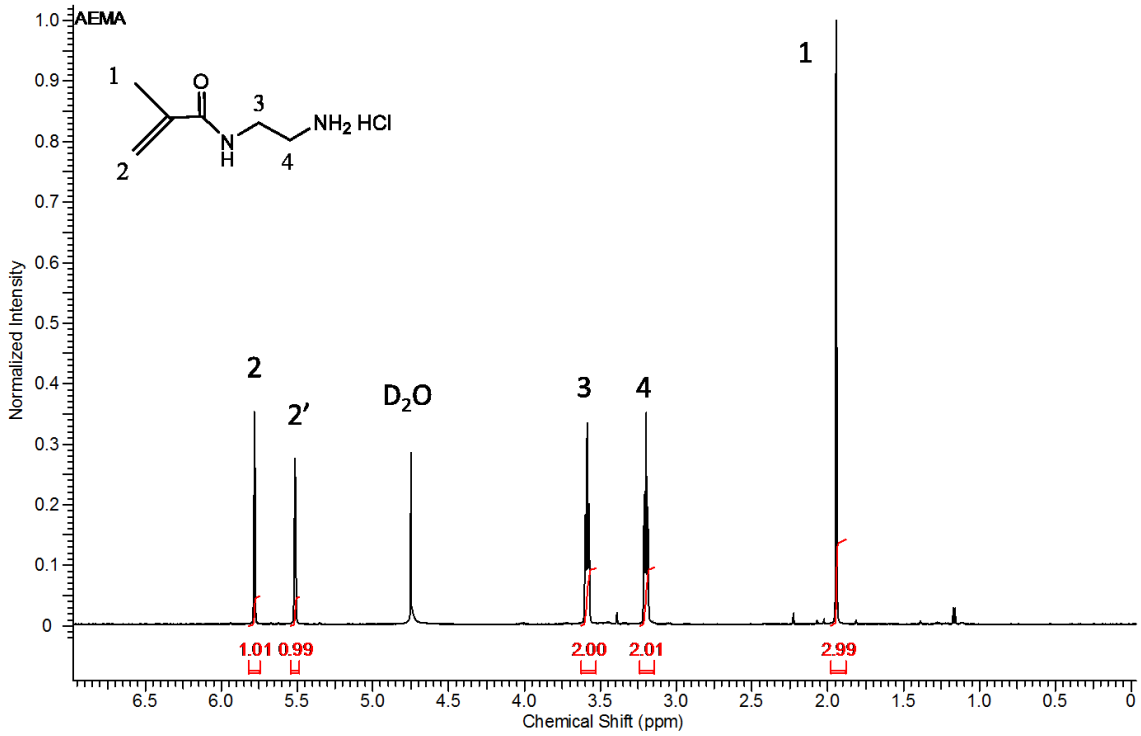

AEMA [1]HNMR spectrum.

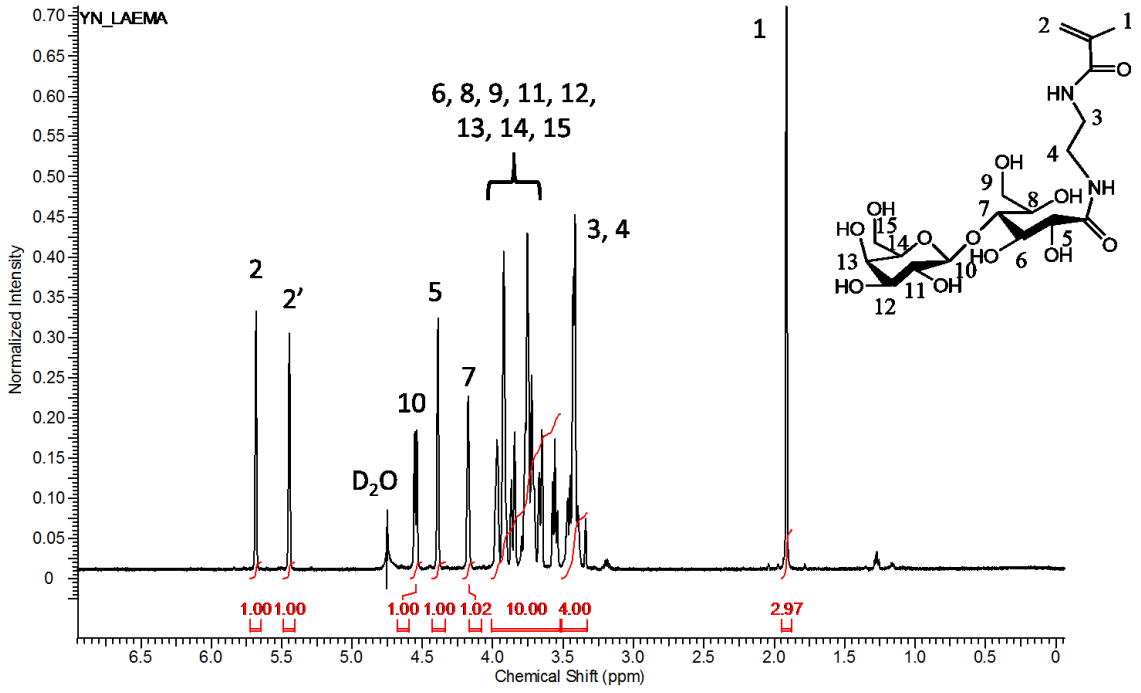

Appendix

LAEMA ^{1}HNMR spectrum.

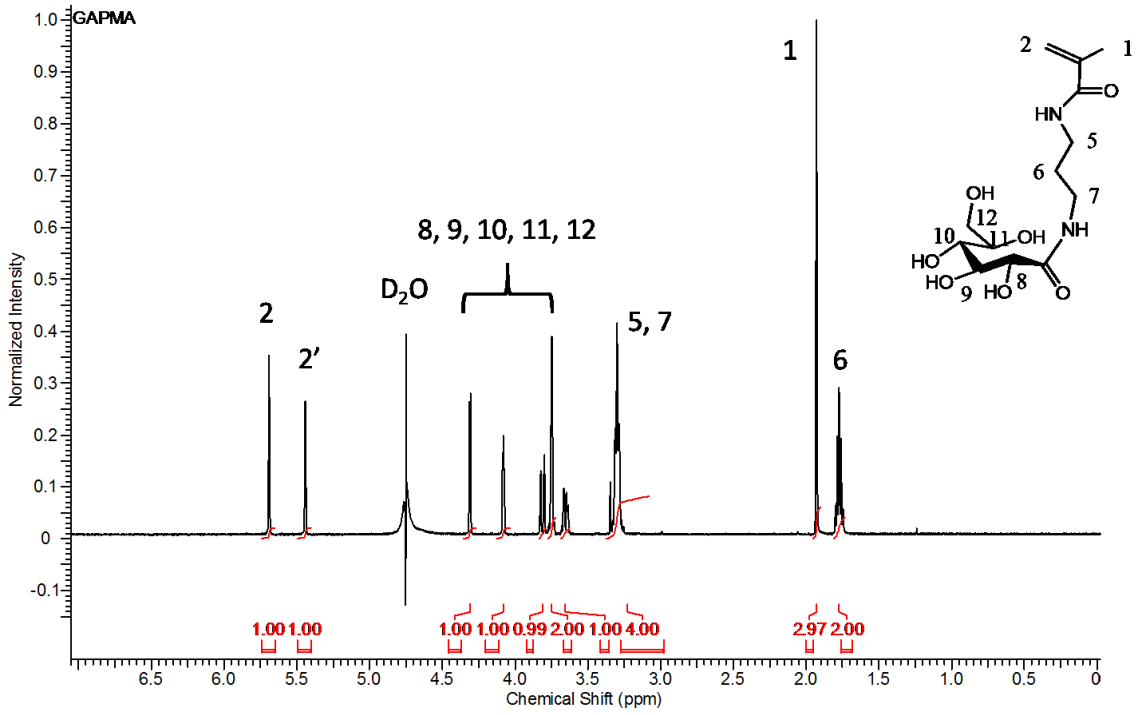

GAPMA ^{1}HNMR spectrum.

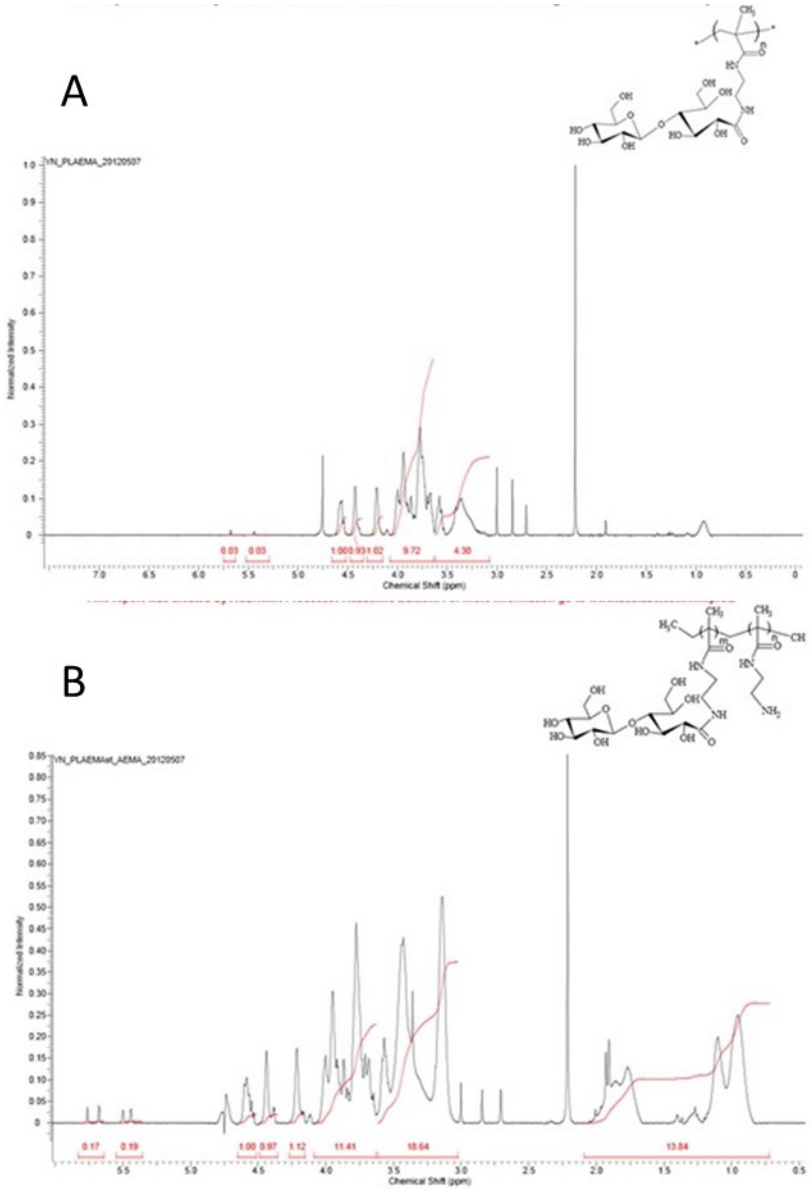

Figure 3-S1. 1H NMR spectra (D2O) for PLAEMA (A) and P(LAEMA-st-AEMA) (B).

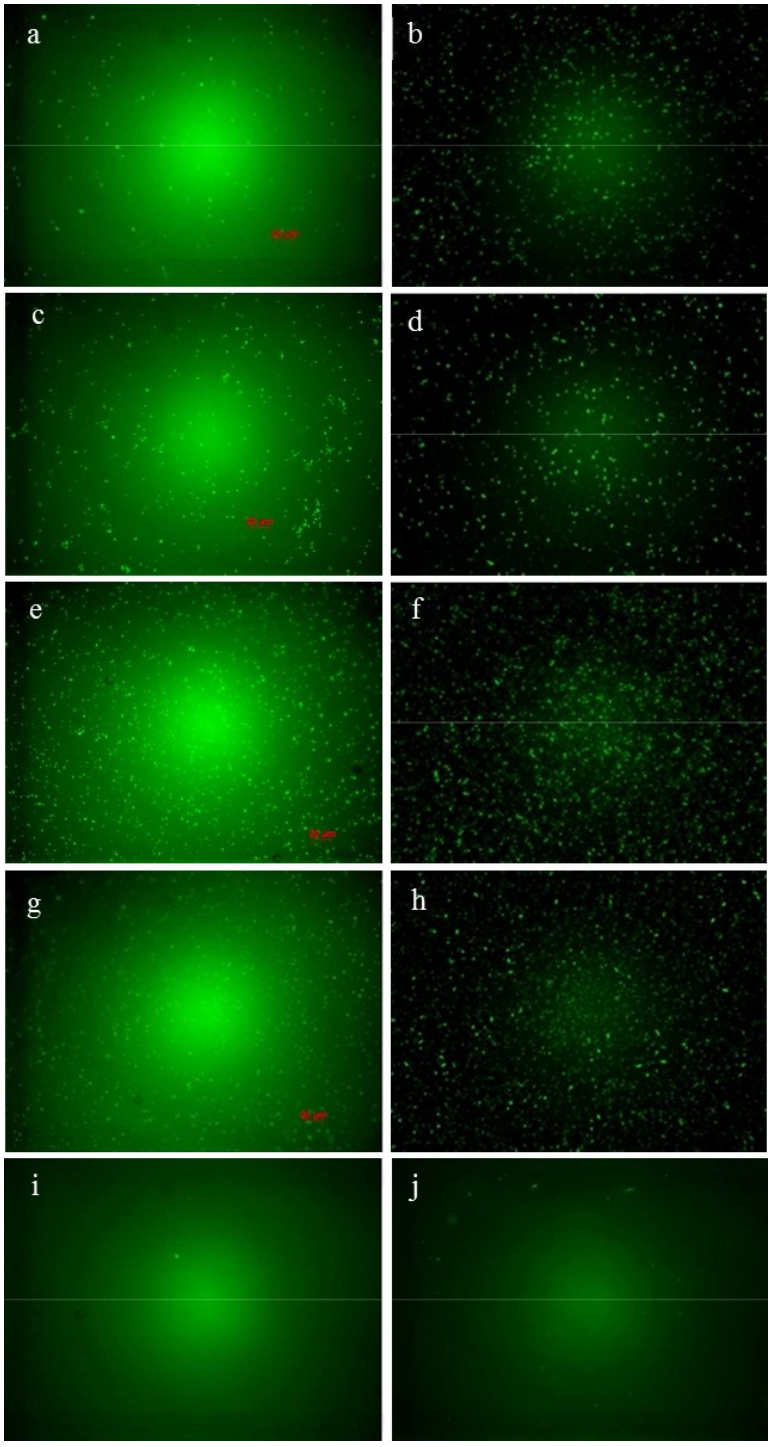

Figure 3-S2. PAO 1 adhesion on different polymers treated sensor surface (a, b: PGAPMA (Glc), c, d: PLAEMA (Gal), e, f: PAEMA (cationic), g, h: P(LAEMA-st- AEMA)

(cationic/Gal), i, j: PEG-SH) in different test media (a, c, e, g, i: in 10 mM NaCl, b, d, f, h, j: in 10 mM $CaCl_2$).

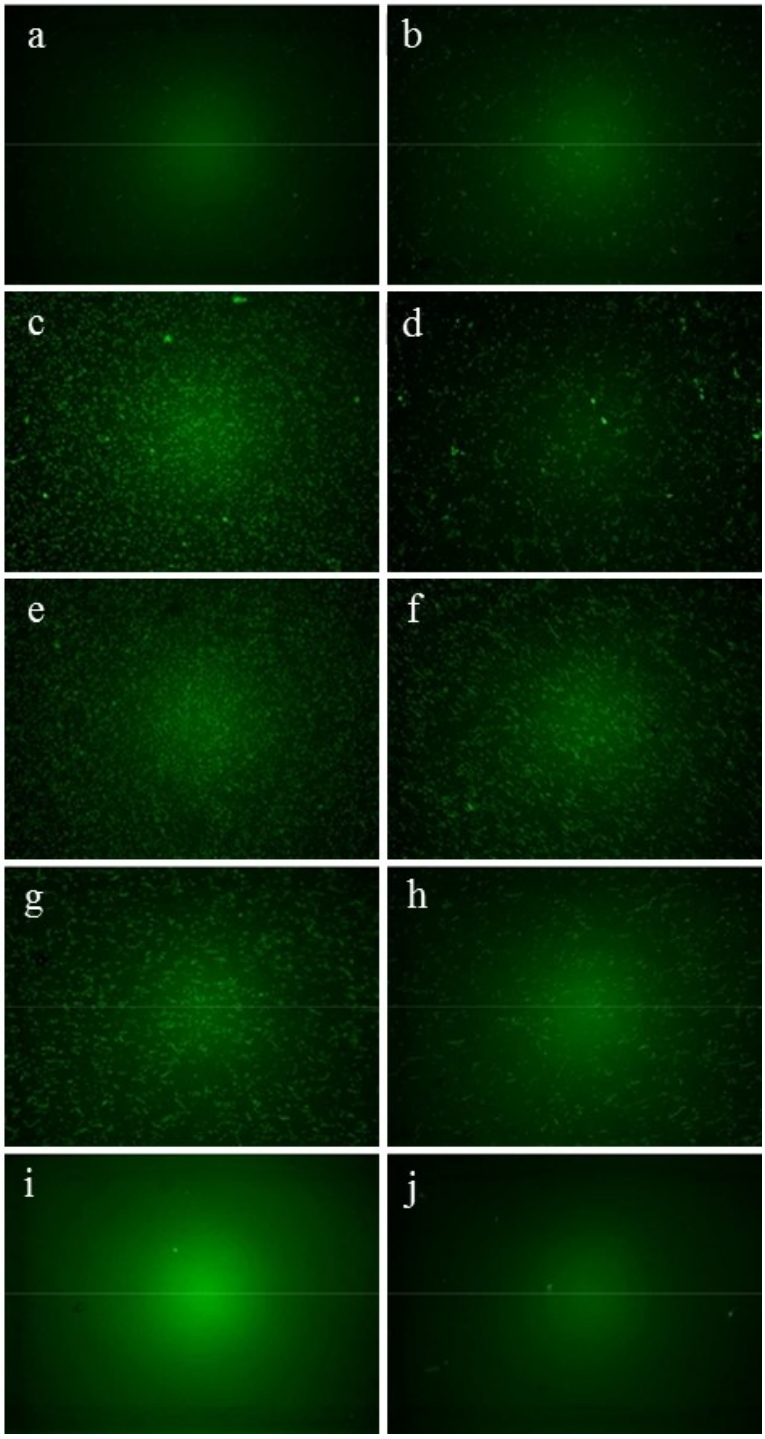

Figure 3- S3. *E. coli* K12 adhesion on different polymers treated sensor surface (a, b: PGAPMA (Glc), c, d: PLAEMA (Gal), e, f: PAEMA (cationic), g, h: P(LAEMA-st-AEMA) (cationic/Gal), i, j: PEG-SH) in different test media (a, c, e, g, i: in 10 mM NaCl, b, d, f, h, j: in 10 mM $CaCl_2$).

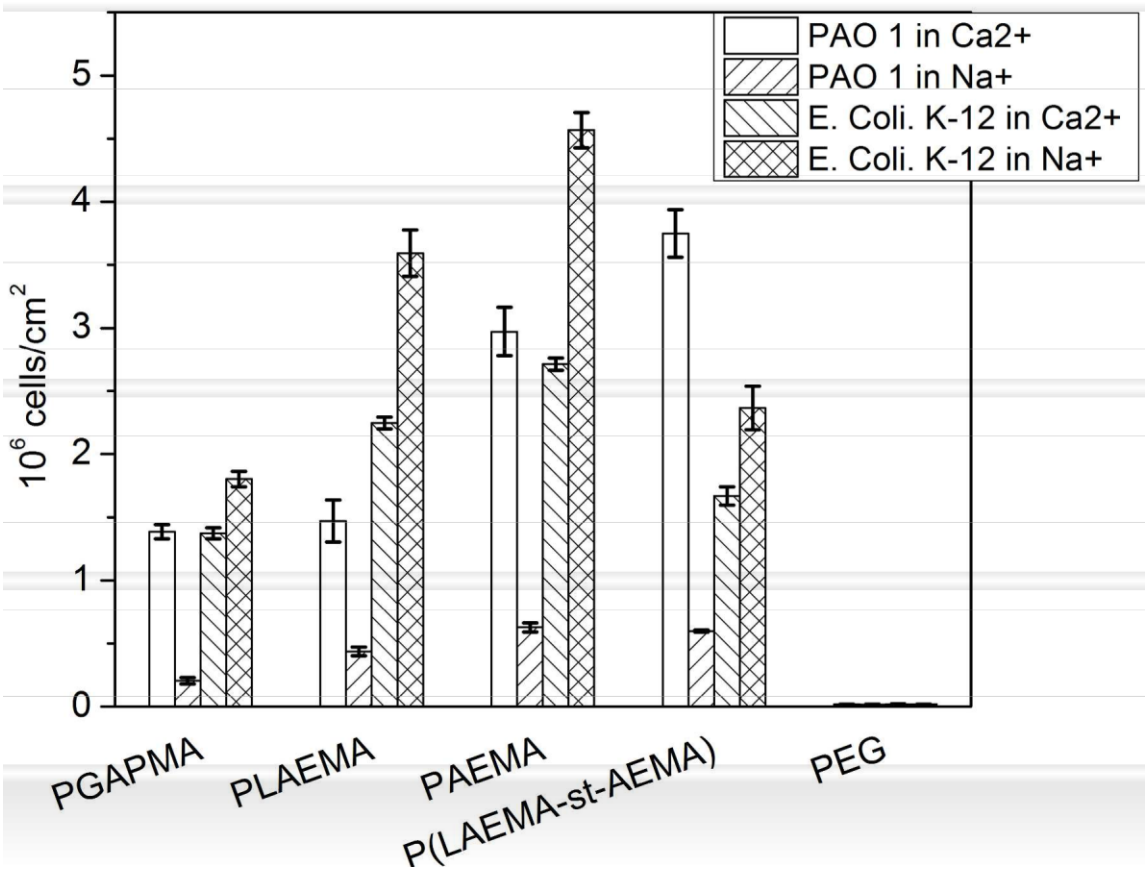

Figure 3- S4. Numbers of bacteria adhesion on different polymers surfaces at different conditions.

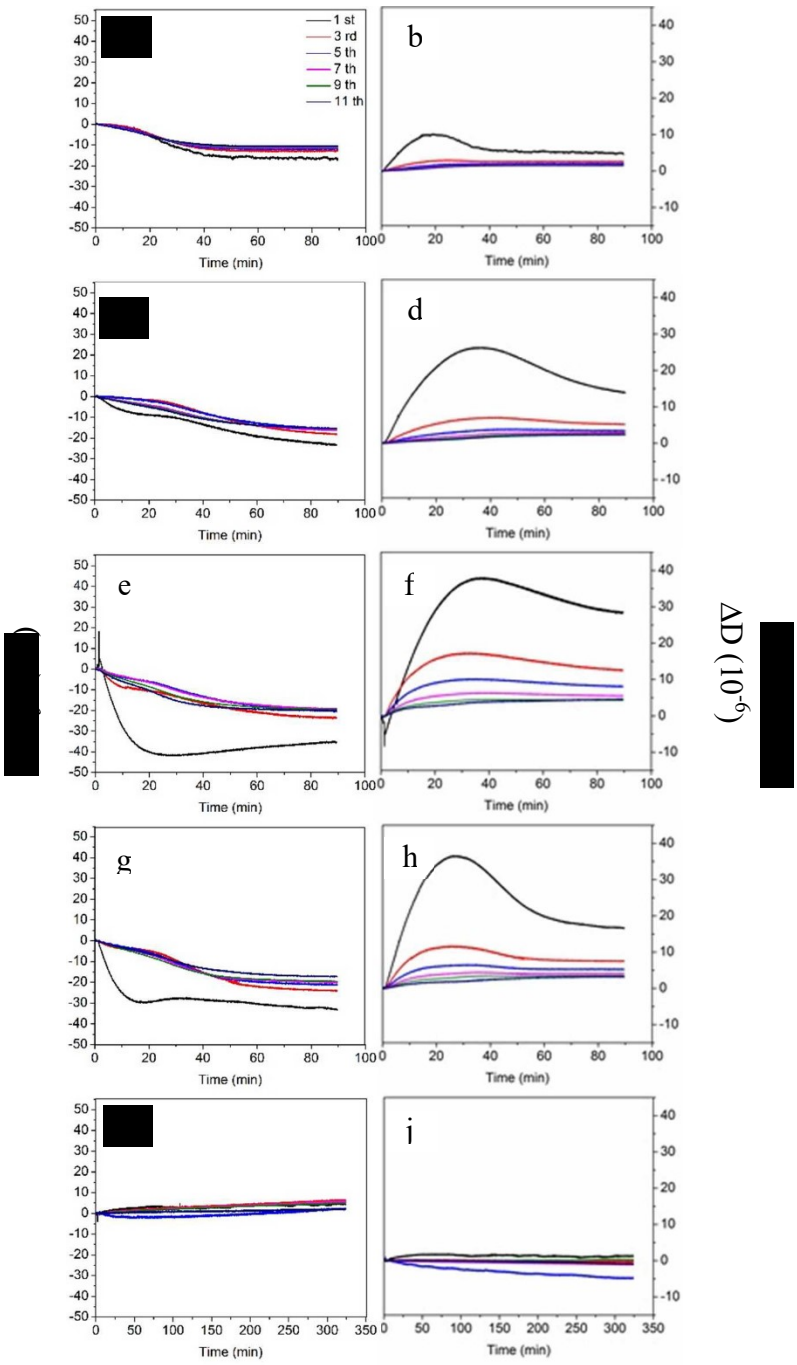

Figure 3-S5. Frequency (a, c, e, g, i) and dissipation (b, d, f, h, j) shifts of PAO 1 adhesion on different polymers treated QCM-D sensor surface (in 10 mM NaCl). (a, b): PGAPMA (Glc). (c, d): PLAEMA (Gal). (e, f): PAEMA (cationic). (g, h): P(LAEMA-st-AEMA) (cationic/Gal). (i, j): PEG-SH.

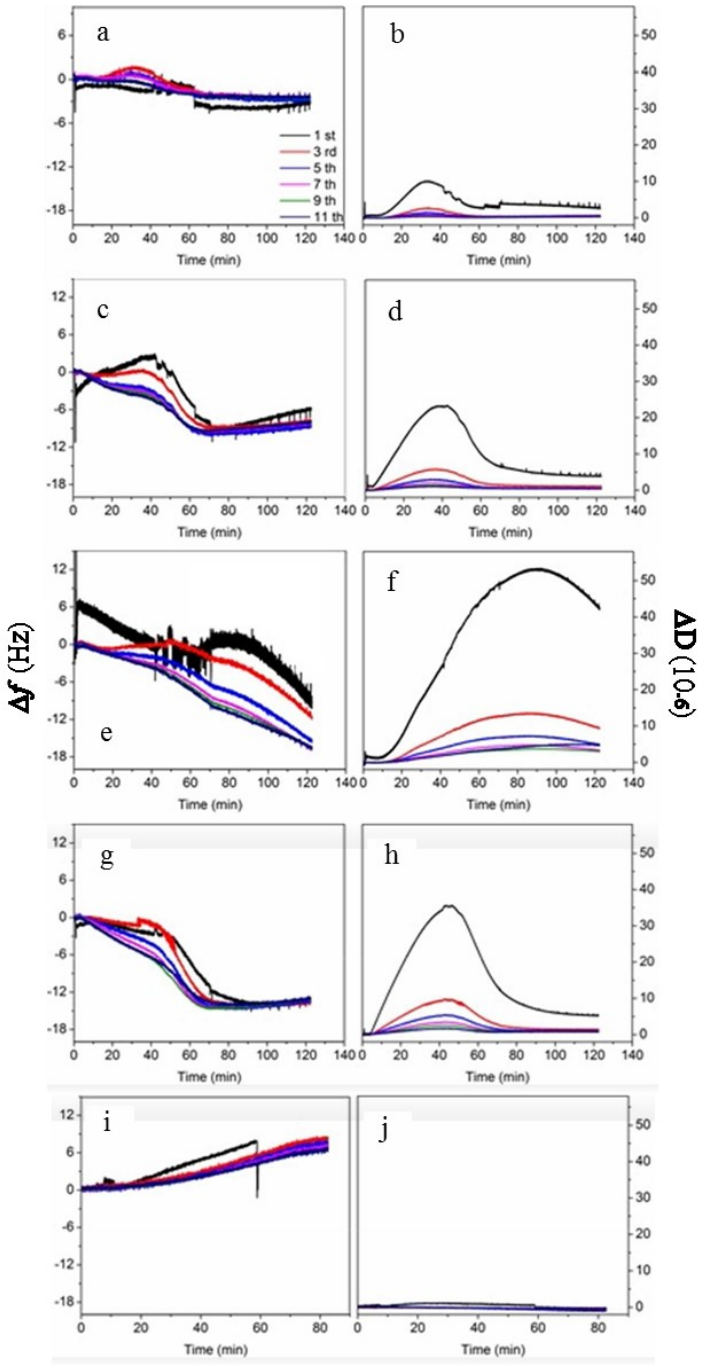

Figure 3-S6. Frequency (a, c, e, g, i) and dissipation (b, d, f, h, j) shifts of E. coli K-12 adhesion on different polymers treated QCM-D sensor surface (in 10 mM NaCl). (a, b):PGAPMA (Glc). (c, d): PLAEMA (Gal). (e, f): PAEMA (cationic). (g, h): P(LAEMA-st-AEMA) (cationic/Gal). (i, j): PEG-SH.

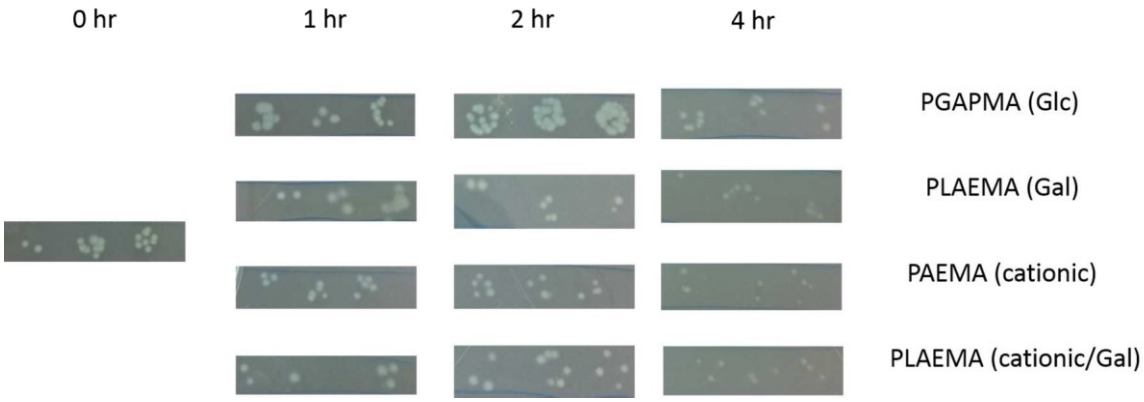

Figure 3-S7. Plate counting results for PAO1 adhesion on different polymer surfaces in 10 mM $CaCl_2$ at different time intervals.

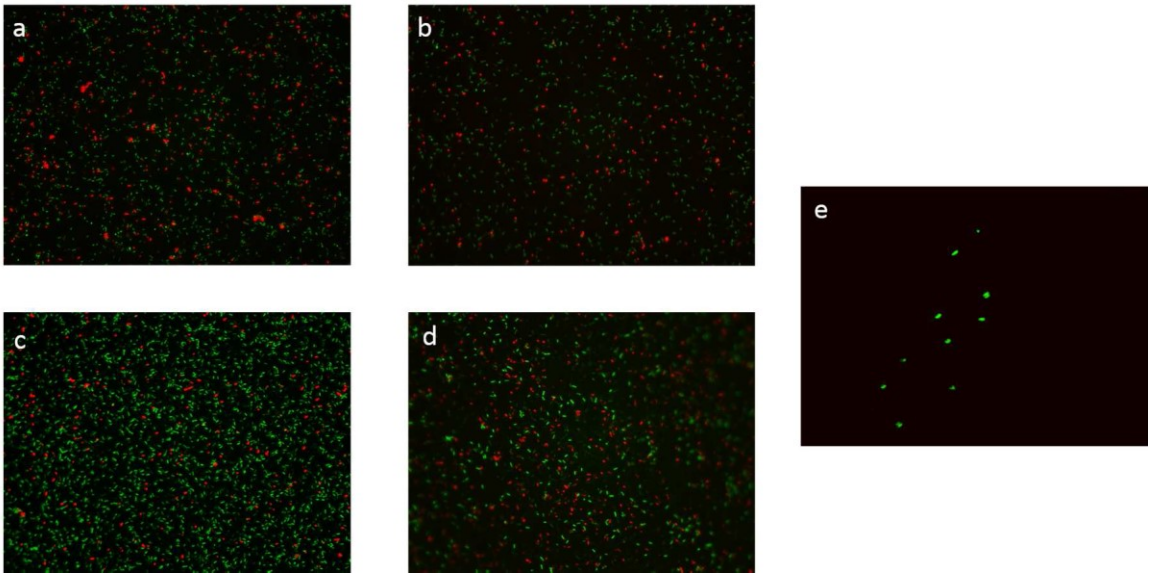

Figure 3-S8. PAO 1 viability observed by fluorescent microscope after 4 hr adhesion study on different polymers treated sensor surface (a,: PGAPMA (Glc), b: PLAEMA (Gal), c: PAEMA (cationic), d: P(LAEMA-st-AEMA) (cationic/Gal), e: PEG-SH). Green: SYTO 9, indicating live bacteria; red: propidium iodide, indicating dead bacteria.

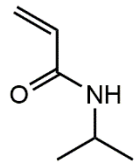

NIPAAm

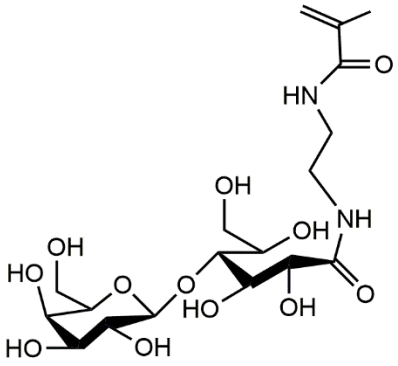

LAEMA

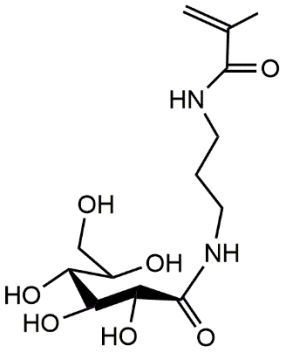

GAPMA

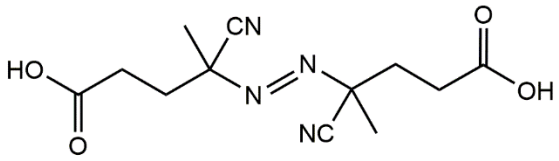

ACVA

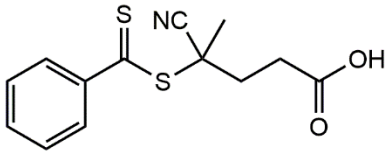

CTP

Scheme 4-S1. Chemical structures of the chain transfer agent (CTP), initiator (ACVA) and monomers used (NIPAAm, GAPMA and LAEMA).

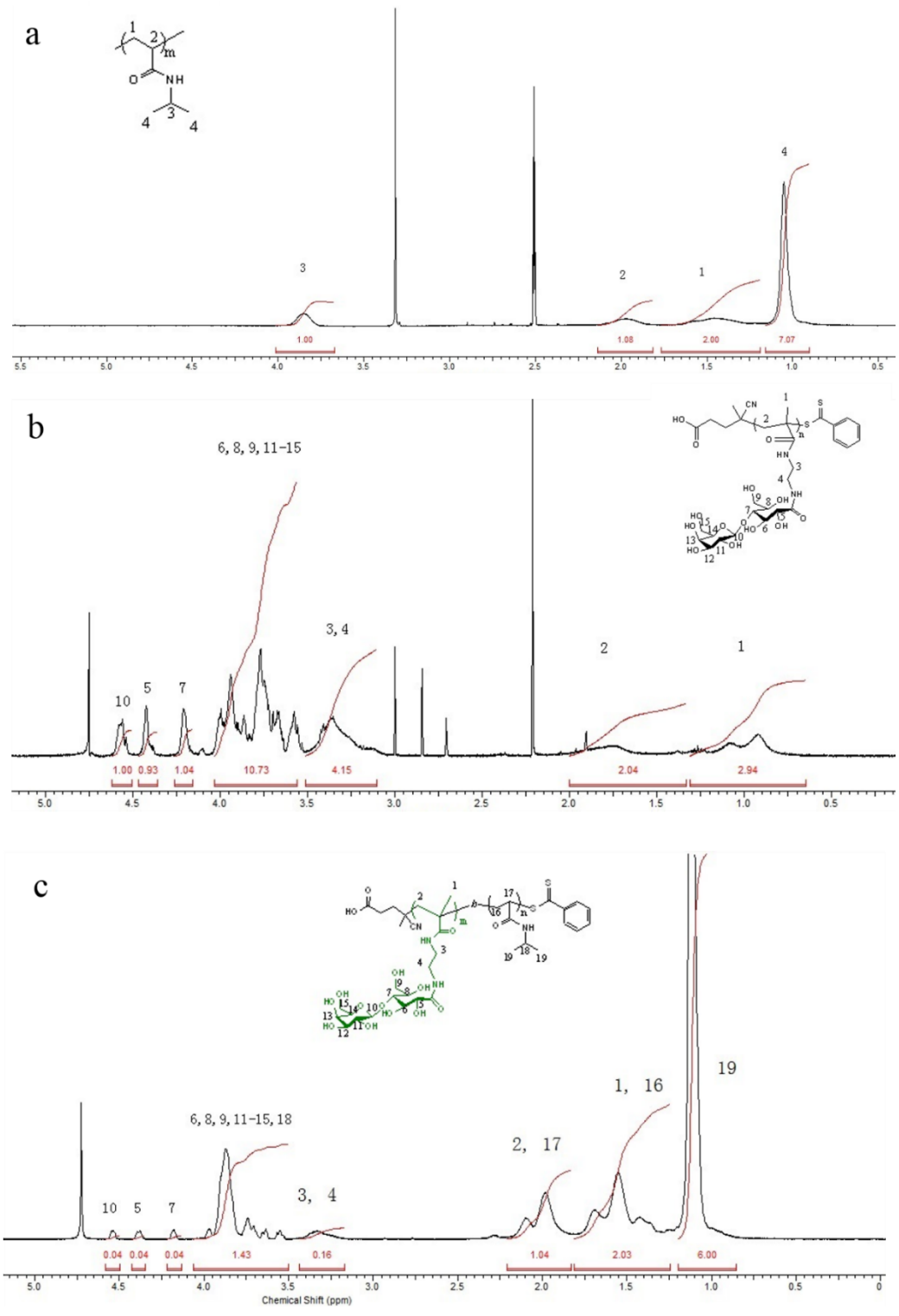

Figure 4-S1. ^{1}H NMR spectra (D_2O) for P(LAEMA$_{28}$) (a), P(NIPAAm$_{40}$) (b), and P(LAEMA$_2$-*b*-NIPAAm$_{40}$) (c).

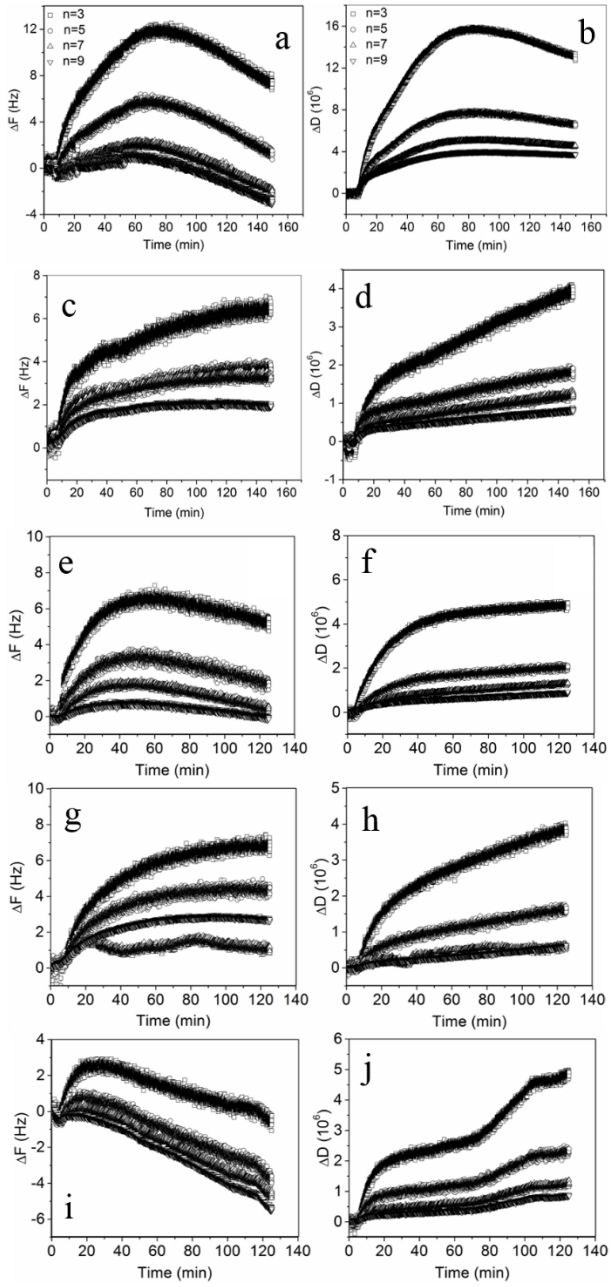

Figure 4-S2. Frequency [a. P(LAEMA$_{28}$), c. P(GAPMA$_{39}$), e. P(NIPAAm$_{40}$), g. P(LAEMA$_2$-*b*-NIPAAm$_{40}$), i. P(GAPMA$_2$-*b*-NIPAAm$_{46}$)] and dissipation [b. P(LAEMA$_{28}$), d. P(GAPMA$_{39}$), f. P(NIPAAm$_{40}$), h. P(LAEMA$_2$-*b*-NIPAAm$_{40}$), j. P(GAPMA$_2$-*b*-NIPAAm$_{46}$)] shifts during *P. aeruginosa* PAO1 adhesion on different polymers treated sensors at 20 ºC. (□ n=3, ○ n=5, Δ n=7, ∇ n=9).

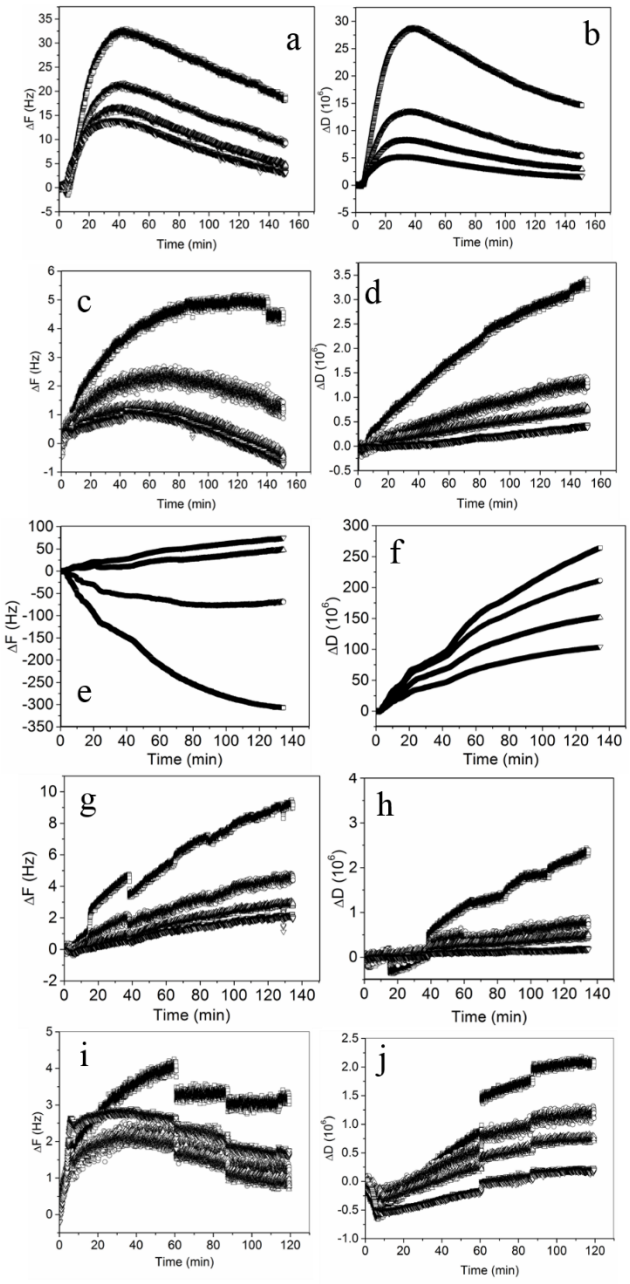

Figure 4-S3. Frequency [a. P(LAEMA$_{28}$), c. P(GAPMA$_{39}$), e. P(NIPAAm$_{40}$), g. P(LAEMA$_2$-*b*-NIPAAm$_{40}$), i. P(GAPMA$_2$-*b*-NIPAAm$_{46}$)] and dissipation [b. P(LAEMA$_{28}$), d. P(GAPMA$_{39}$), f. P(NIPAAm$_{40}$), h. P(LAEMA$_2$-*b*-NIPAAm$_{40}$), j. P(GAPMA$_2$-*b*-NIPAAm$_{46}$)] shifts during *P. aeruginosa* PAO1 adhesion on different polymers treated sensors at 37 ºC. (□ n=3, ○ n=5, Δ n=7, ∇ n=9).

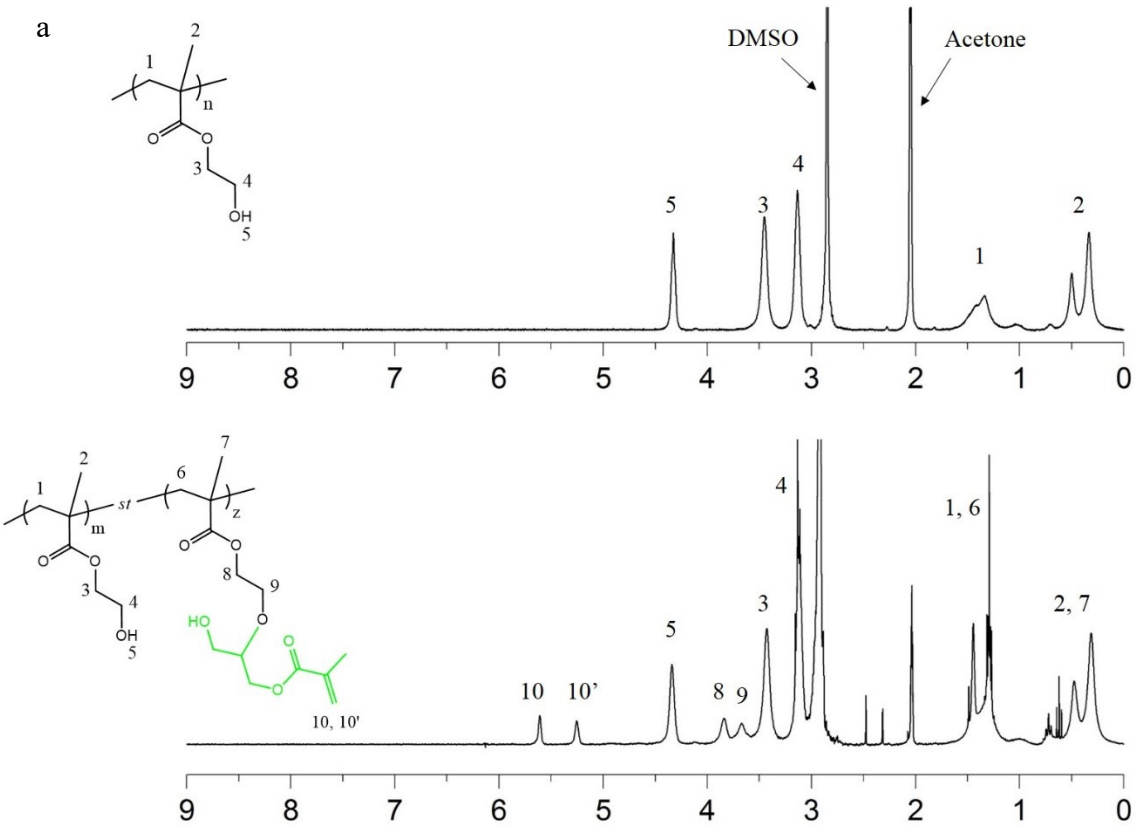
a
DMSO
Acetone
5
3
4
1
2
9
8
7
6
5
4
3
2
1
0
1, 6
2, 7
10
10'
8
9
10, 10'
HO
OH

b

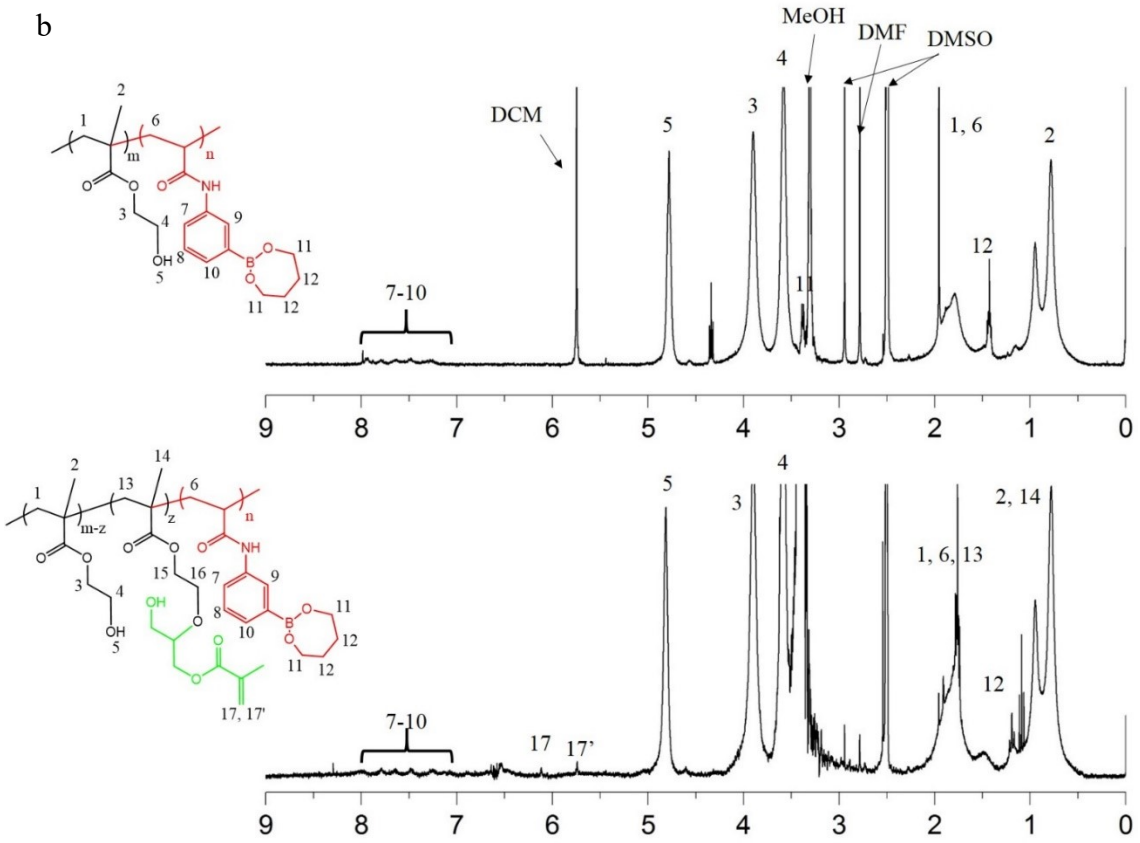

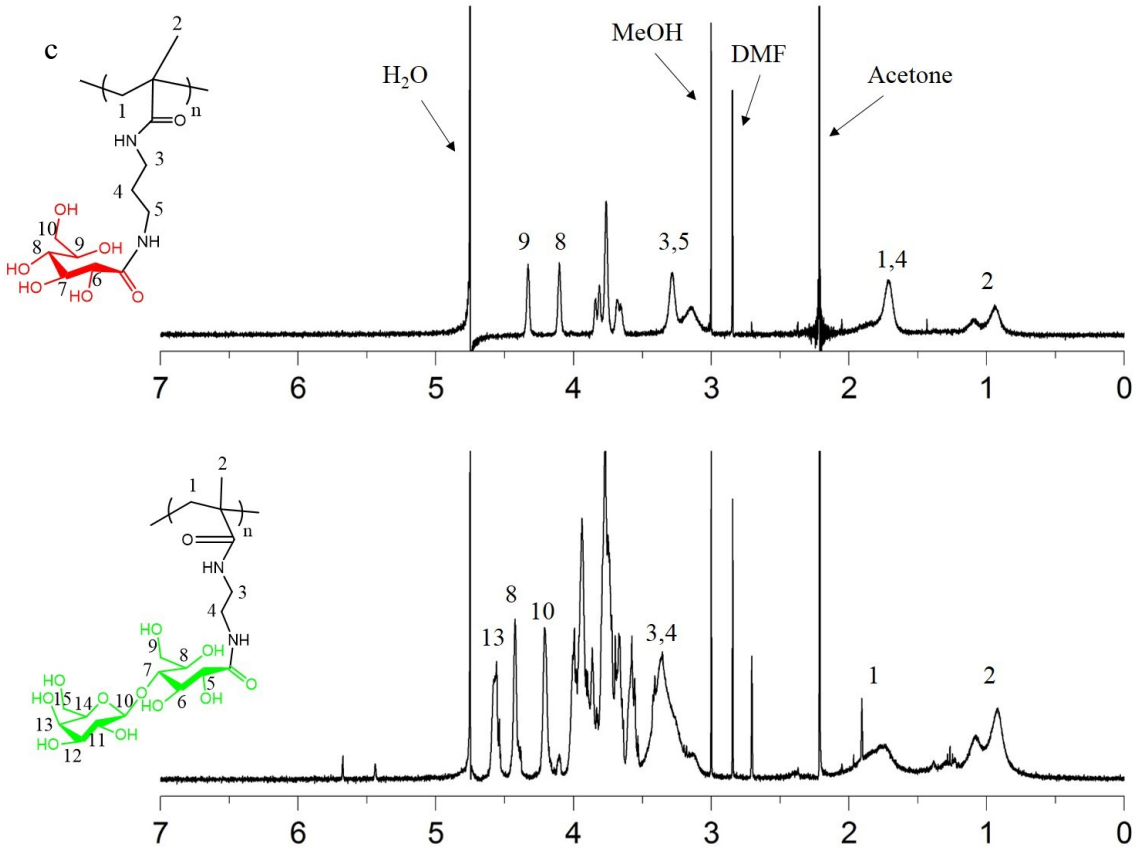

Figure 5-S1. ^{1}H NMR spectra of P(HEMA$_{321}$) (a) and 1,4-butanediol protected P(HEMA$_{780}$-st-AAPBA$_{38}$) before and after the introduction of GMA. (c) ^{1}H NMR spectra of PGAPMA and PLAEMA.